Head Office: Università degli Studi di Padova

Department: Biomedical Sciences

Ph.D. COURSE IN BIOMEDICAL SCIENCES

Neuromuscular plasticity with muscle disuse and sarcopenia

Thesis written with the financial contribution of the Italian Space Agency (ASI) (*MARS-PRE Project, n. DC-VUM-2017-006*), the Italian Ministry of Education, Universities and Research (MIUR) (PRIN projects *'NeuAge' n. 2017CBF8NJ_001* and *'InactivAge' n. 2020EM9A8X*) and Next Generation EU, in the context of the National Recovery and Resilience Plan, Investment PE8 – Project *Age-It: "Ageing Well in an Ageing Society*".

Coordinator: Prof. Fabio Di Lisa

Supervisor: Prof. Marco V. Narici

Co-Supervisor: Dr. Martino V. Franchi

Ph.D. student: Fabio Sarto

Syllabus

SUMMARY

Background: The neuromuscular system demonstrates an exceptional level of plasticity, enabling it to swiftly adapt to different environmental stimuli and other (patho)physiological scenarios that occur over an individual's lifespan. Motor units (MUs), the smallest functional components of the neuromuscular system, play a fundamental role in this remodelling. Certain conditions, such as exercise, fosters beneficial adaptive changes within the neuromuscular system. In contrast, other stimuli can trigger adverse effects, inducing muscle atrophy and impairing neuromuscular function. My PhD thesis focused on two detrimental conditions that negatively impact skeletal muscle: disuse and sarcopenia. Periods of muscle disuse, characterised by a combination of unloading and reduced neural activity, are commonly experienced throughout the lifespan due to injury, illness and surgery and can rapidly induce muscle wasting and weakness. Several models of muscle disuse have been developed and widely employed to investigate the effect of physical inactivity on different physiological systems. These models encompass bed rest, dry immersion, unilateral lower limb immobilisation and unilateral lower limb suspension (ULLS). Sarcopenia, the age-related loss of muscle mass and function, is a chronic condition widely spread among older adults, formally recognised as a disease. Sarcopenia significantly reduces individuals' quality of life and is associated with an increased risk of falls, functional decline, frailty, and ultimately death. Evidence suggests that both muscle disuse and sarcopenia have a key neurogenic component driven by the remodelling of the different MU components: the motoneuron, the neuromuscular junction (NMJ) and skeletal muscle fibres. However, little is known about how these maladaptations occur, particularly in humans. Understanding the neuromuscular alterations induced by disuse and sarcopenia represents a fundamental step for the development of effective countermeasures. Using an integrative physiological approach, I exploited musculoskeletal imaging, muscle function testing and electrophysiological and molecular approaches to comprehensively gain deeper insights into the mechanisms underpinning the neuromuscular changes triggered by disuse and sarcopenia in humans. In order to achieve this goal, I structured my PhD project along with two original research articles and one review article.

First Study: In this study (*Sarto F, Stashuk DW, Franchi M V et al. Effects of short-term unloading and active recovery on human motor unit properties, neuromuscular junction transmission and transcriptomic profile. J Physiol. 2022*; (Sarto *et al.*, 2022*b*)), 11 recreationally active young males (age: 22.1 (2.9) years) took part in a 10-day ULLS intervention. ULLS was followed by 21 days of active recovery based on resistance exercises (leg press and leg extension exercises) performed

three times per week. Our findings supported previous observations suggesting that short-term disuse is associated with muscle atrophy and weakness at the whole muscle level, NMJ molecular instability and initial signs of myofibre denervation. Moreover, we showed that NMJ function remains stable following the 10 days of ULLS, highlighting its functional resilience. Decreased MU firing rates and increased MU potential complexity were also observed following unloading, possibly due to increased axonal damage and alterations in skeletal muscle ion channels dynamics. Finally, the active recovery period effectively restored most of these neuromuscular changes.

Second Study – Literature review: Traditional severe disuse models, such as ULLS, provided essential advancement in understating the pathophysiological impact of extreme physical inactivity. However, they do not accurately reproduce the effects of a sedentary lifestyle, an authentic pandemic of modern society. My second PhD article (*Sarto F, Bottinelli R, Franchi M V et al. Pathophysiological mechanisms of reduced physical activity: insights from the human step reduction model and animal analogues. Acta Physiol. 2023;238(e13986)*; (Sarto et al., 2023)) is a narrative review focusing on an experimental paradigm that mimics better sedentarism: step reduction. This model consists in inducing an abrupt reduction in participants' daily steps, promoting sedentary behaviours. Analogues models of reduced physical activity have been proposed in rodents and are also discussed in the review. The existing body of literature unequivocally demonstrates that these interventions of reduced physical activity, even of brief duration, can induce remarkable alterations in skeletal muscle health and metabolic function. These changes encompass reductions in lean/muscle mass, muscle force, muscle protein synthesis, cardiorespiratory performance, endothelial function, and insulin sensitivity, while concurrently leading to increases in fat mass and inflammation. We provided a direct comparison of the pathophysiological impact of step reduction with other human models of disuse, confirming that step reduction can overall be considered a mild physical inactivity intervention. However, the alterations reported are consistent and should not be overlooked, particularly with regard to insulin sensitivity. Despite some mechanisms are not yet fully understood, we developed a conceptual framework aiming to illustrate the molecular pathways leading to muscle atrophy and insulin resistance in reduced physical activity scenarios. For the first time, we also linked the findings from time-use epidemiological research with those of the experimental step reduction studies, showing interesting similarities. Finally, methodological considerations, knowledge gaps and future directions for both animal and human models are also addressed in the review.

Third Study: My final PhD article (*Sarto F, Franchi M V, McPhee J et al. Motor units properties impairment, axonal damage, innervation profile alterations and neuromuscular junction instability with different stages of sarcopenia; in submission*) was focused on the investigation of the morphological, functional, electrophysiological and molecular alterations triggered by sarcopenia. In this cross-sectional study, we recruited 42 healthy young individuals (Y) (age: 25.8 (4.6) years; 57% females) and 88 older individuals (age: 75.9 (4.7) years; 55% females). According to the revised guidelines of the European Working Group on Sarcopenia in Older People (EWGSOP2), 39 older individuals were non-sarcopenic, 31 pre-sarcopenic and 18 sarcopenic. As expected, sarcopenic individuals displayed an overall greater impairment in different domains of muscle function and physical performance, accompanied by more pronounced muscle wasting. NMJ stability and transmission, MU potential properties, MUs number, axonal damage and innervation profile were impaired in aged compared to young individuals. However, none of these parameters was further exacerbated in sarcopenic individuals compared to non-sarcopenic counterparts. These observations prompt us to consider whether the conventional view, attributing primary sarcopenia to MU and NMJ degeneration, might benefit from further exploration. On the other hand, it appears that these neuromuscular alterations occur before the development of overt sarcopenia, as they are evident in non-sarcopenic older individuals.

Conclusion: Even short periods of muscle disuse are associated with initial signs of myofibre denervation, axonal damage, NMJ molecular instability, downregulation of skeletal muscle ion channels genes and alterations in MU potential properties. Whether similar are triggered by less severe forms of physical inactivity, such as step reduction, remains to be determined. Ageing is accompanied by MU and NMJ electrophysiological and molecular alterations that resemble those observed following periods of muscle disuse. NMJ transmission impairment, which showed resilience to short-term disuse, and MUs loss seem uniquely triggered by the ageing process. Sarcopenic individuals did not show exacerbated degeneration compared to non-sarcopenic older adults, despite displaying more profound muscle atrophy and greater impairments in muscle function and physical performance. These results suggest that MU loss and NMJ degeneration may precede sarcopenia. Overall, the findings of this dissertation contributed to advancing the present knowledge on the neuromuscular system plasticity with disuse and sarcopenia, providing a useful basis for the development of effective countermeasures in these scenarios.

1. INTRODUCTION

1.1. The motor unit (MU)

The motor unit (MU) is the smallest functional unit of the neuromuscular system. It is composed of a single α motoneuron and all of the innervated muscle fibres (Sherrington, 1925), linked by a chemical synapse called the neuromuscular junction (NMJ) (Davis *et al.*, 2022) (Figure 1). It is only thanks to the MUs that the brain can trigger the contraction of skeletal muscle and thereby control all the movements on which life depends, including swallowing and breathing. The MU acts as a neuromechanical transducer: it converts sensory and descending neural inputs from the central nervous system into forces to ultimately generate movements (Heckman & Enoka, 2012). Its role is fundamental, as every movement is accomplished by the fine-tuned activation of MU populations (Heckman & Enoka, 2012). MUs are heterogeneous (Kanning *et al.*, 2010), differing in size, composition and duration of force generated. Fine motor control is achieved through the recruitment of smaller MUs, involving fewer muscle fibres, while larger MUs with a greater number of muscle fibres are responsible for generating more force (Heckman & Enoka, 2004).

In the following paragraphs, I will describe the anatomy and physiology of the MU. This part does not aim to provide a comprehensive review of the topic; rather, it serves as an introductory overview to enhance understanding of the subsequent chapters.

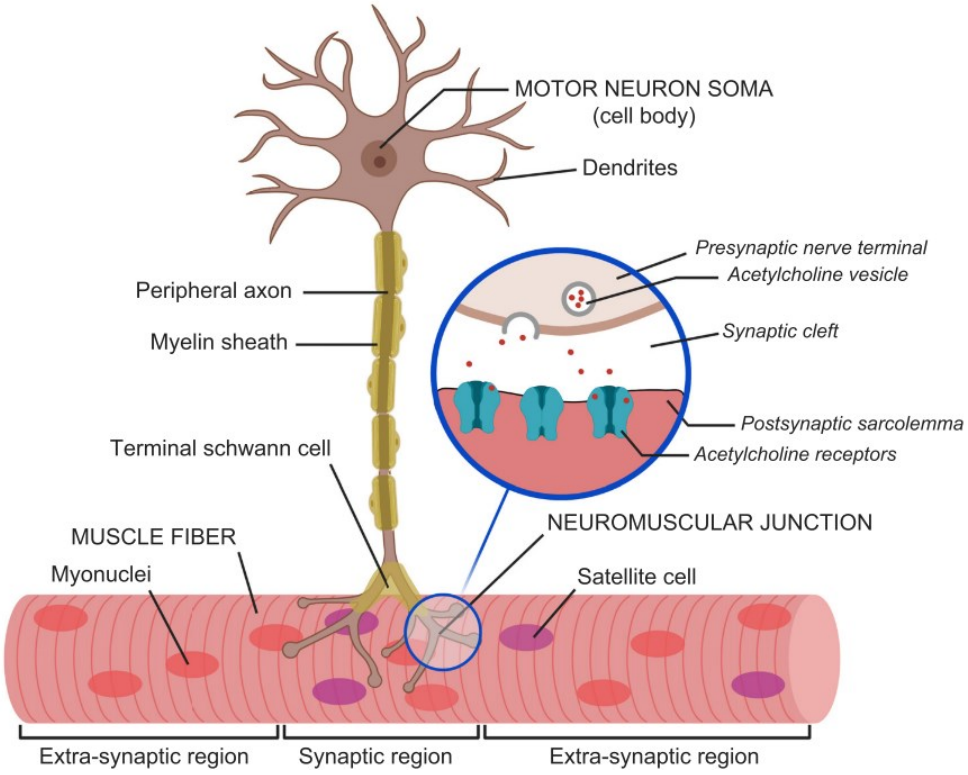

Figure 1: *Main components of the motor unit (Soendenbroe et al., 2021).*

1.1.1. Anatomy and physiology of the motor unit

1.1.1.a. The motoneuron

In the human body, an astounding number of over 120,000 motoneurons intricately connect and communicate with more than 100 million skeletal muscle fibres (Kanning *et al.*, 2010). Each motoneuron has its origin in either the ventral horn of the spinal cord or the brain stem. The group of motoneurons in the spinal cord innervating a single muscle is referred to as a motor pool or a motor nucleus (Heckman & Enoka, 2004, 2012). In transverse sections, the motor nuclei of proximal muscles generally exhibit ventral and lateral positioning, while the motor nuclei for distal muscles tend to be located relatively more dorsal and medial. Moreover, in terms of anterior and posterior muscles, the motor nuclei of anterior muscles are typically situated laterally compared to those of posterior muscles. The motoneuron is composed of three distinct regions (Figure 1), each with its predominant function (Heckman & Enoka, 2004):

- Dendrites: Motoneurons receive a substantial number of synapses, with up to 50,000 inputs, and the majority of these synaptic connections occur on the dendrites. Dendrites account for 95% of the cell surface area and their geometry is relevant for the integration of the synaptic inputs. While primarily responsible for conveying synaptic current to the soma in a passive system, motoneuron dendrites also possess potent voltage-sensitive currents that augment synaptic activity.
- Soma/Axon Initial Segment: The soma (cell body) and the initial segment of the axon play a crucial role in converting synaptic currents into trains of action potentials. This region hosts the nucleus and other organelles such as the endoplasmic reticulum and the mitochondria. The endoplasmic reticulum in this region produces proteins that maintain the functioning of the neuron. This region houses high densities of sodium (Na), potassium (K), and calcium (Ca) channels, which are instrumental in generating action potentials and regulating their firing rate (Rekling *et al.*, 2000).
- Axon: Serving as the link between the cell body and the muscle fibres, the axon is analogous to a cable. It is wrapped in myelin, which helps it to conduct electrical signals rapidly. Ranvier nodes, also known as myelin-sheath gaps, within the axon, possess elevated concentrations of Na and K channels, facilitating the rapid propagation of action potentials. As the axon enters the muscle, it extensively branches out to innervate the numerous muscle fibres under the control of the motoneuron.

1.1.1.a.i Channels and receptors of the motoneuron

As introduced above, the motoneuron acts as a molecular controller, with its properties mainly dependent on the receptors and ion channels that are inserted in its membrane. Four important types of channels are recognised in the motoneuron (Rekling *et al.*, 2000; Heckman & Enoka, 2004):

- Leak channels: These channels play a vital role in establishing the resting membrane potential of neurons, typically around -70 to -60 mV. Selectively permeable to K ions, leak channels also allow modest passage of other ions like Na and Cl. The resulting ion flux contributes to the maintenance of the resting membrane potential around -70 to -60 mV in motoneurons. Deviations from this potential indicate the involvement of other channels in generating the potential difference.
- Ionotropic synaptic channels: Also known as ligand-gated channels, these channels mediate a significant portion of the synaptic input to motoneurons upon binding of neurotransmitters to their receptors. Ionotropic synaptic channels can be excitatory or inhibitory. The primary excitatory neurotransmitter is glutamate, while glycine or GABA act as inhibitory neurotransmitters. Activation of these channels by neurotransmitters leads to membrane depolarisation in the case of excitatory channels and hyperpolarisation in inhibitory channels. Excitatory synaptic channels are nonselective, depolarising the membrane potential towards zero, resulting in excitatory post-synaptic potentials (EPSPs) and excitatory post-synaptic currents (EPSCs). Inhibitory channels are predominantly selective to chloride and potassium ions, with a reversal potential of around -80 mV. They generate hyperpolarising voltages or currents known as inhibitory post-synaptic potentials (IPSPs) or inhibitory post-synaptic currents (IPSCs).
- Voltage-gated channels: These channels are influenced by changes in the membrane voltage and are responsible for various electrical behaviours of neurons, including the generation of action potentials.
- Metabotropic receptors: In addition to ionotropic receptors, neurotransmitters can also bind to metabotropic receptors, initiating intracellular signalling pathways through G proteins. These pathways modulate the behaviour of voltage-sensitive channels, as well as influence leak channels and synaptic channels. Metabotropic receptors, often referred to as neuromodulatory receptors, exert their effects through second messenger cascades. Two

significant neurotransmitters with metabotropic actions in motoneurons are serotonin (5HT) and norepinephrine, both belonging to the monoamine class.

1.1.1.a.ii Motoneuron diversity

Adult motoneurons can be classified into functionally diverse classes and subtypes. One classification of motoneurons, based on the type of muscle fibre they innervate, involves the division into three classes: α, β and γ (Kanning *et al.*, 2010). Alpha motoneurons innervate extrafusal skeletal muscle fibres, initiating muscle contractions. Gamma motoneurons innervate intrafusal muscle fibres found within muscle spindles and contribute to complex functions in motor control. A third category, known as β motoneurons, has a less well-defined role and innervates both intrafusal and extrafusal muscle fibres. Reflecting their different functions, each class presents pronounced differences in size and form (Figure 2). First, γ motoneurons display distinct characteristics compared to α motoneurons. They are typically smaller in size, with an average soma diameter approximately half that of the smallest α motoneurons. Additionally, γ motoneurons have slower axon conduction velocities, reflecting their smaller axon calibre. In terms of dendritic morphology, the dendritic trees of α and γ motoneurons have similar lengths. However, the dendrites of γ motoneurons are less branched and exhibit overall simpler structural organization. Connectivity patterns within the spinal cord also differ between α and γ motoneurons. Gamma motoneurons lack direct monosynaptic input from proprioceptive sensory neurons (Ia input), whereas the majority of α motoneurons receive such direct Ia input, although there may be exceptions. Additionally, γ motoneurons have limited intraspinal axon collaterals, suggesting a lesser contribution to recurrent inhibition within the spinal cord.

Among the three classes, α motoneurons are the most abundant and can further be classified into subtypes based on the contractile properties of the MUs they form with target muscle fibres, including fast-twitch fatigable (FF), fast-twitch fatigue-resistant (FR), and slow-twitch fatigue-resistant (S) (Burke *et al.*, 1973). The differences between subtypes are not as sharply defined as those observed between α and γ motoneurons. However, a wide range of properties within the subtypes exists, including variations in size. On one end of the spectrum, type S motoneurons exhibit smaller cell bodies and axons, while at the other end, type FF motoneurons are larger with big-diameter, fast-conducting axons. The average membrane area of FF motoneurons is over 20% larger than that of S motoneurons, reflecting the presence of more axonal and dendritic branches, as well as an increased number of presynaptic neuromuscular terminals per motoneuron. These differences in size have biophysical implications for the recruitment order of MUs during graded stimulation.

Smaller S motoneurons have higher input resistance, requiring less synaptic activation to initiate action potentials. As a result, during muscle contraction, S motoneurons reach the threshold first, while the activation of large motoneurons occurs last. This recruitment pattern is called the "size principle" (Mendell, 2005). Consequently, during normal motor behaviour, fast MUs, which are stronger, are primarily engaged in short-lasting bouts of forceful contraction, such as during sprinting or jumping. In contrast, during postural tasks like standing, only S motoneurons are active. Firing rate is another distinguishing characteristic between FF and S motoneurons. S motoneurons exhibit repetitive firing, which can persist even in the absence of presynaptic excitatory drive. This persistent activity amplifies and prolongs synaptic input signals and ceases only upon the application of an inhibitory stimulus. This is partly due to the longer-lasting persistent inward currents (PIC) on the dendrites of S motoneurons compared to FF motoneurons (Heckman *et al.*, 2008). The duration of the post-spike after-hyperpolarization (AHP), largely shaped by a Ca^{2+}-dependent K+ current, is another physiological parameter that differs between α motoneuron subtypes (Eccles *et al.*, 1957). Fast motoneurons exhibit a shorter AHP compared to S motoneurons, allowing the firing frequency of each subtype to be matched to the contractile frequency of the target muscle fibre. While the characteristics of slow and fast muscle fibres are well-defined, less is known about the molecular differences between the corresponding motoneurons. Levels of succinate dehydrogenase and calcitonin gene-related peptides have been suggested to differ between fast and slow motoneurons, although these differences likely reflect variations in size rather than genetic distinctions. Finally, the synaptic vesicle protein SV2A has been reported to be restricted to slow neuromuscular synapses, although this distinction gradually emerges during the postnatal period (Kanning *et al.*, 2010).

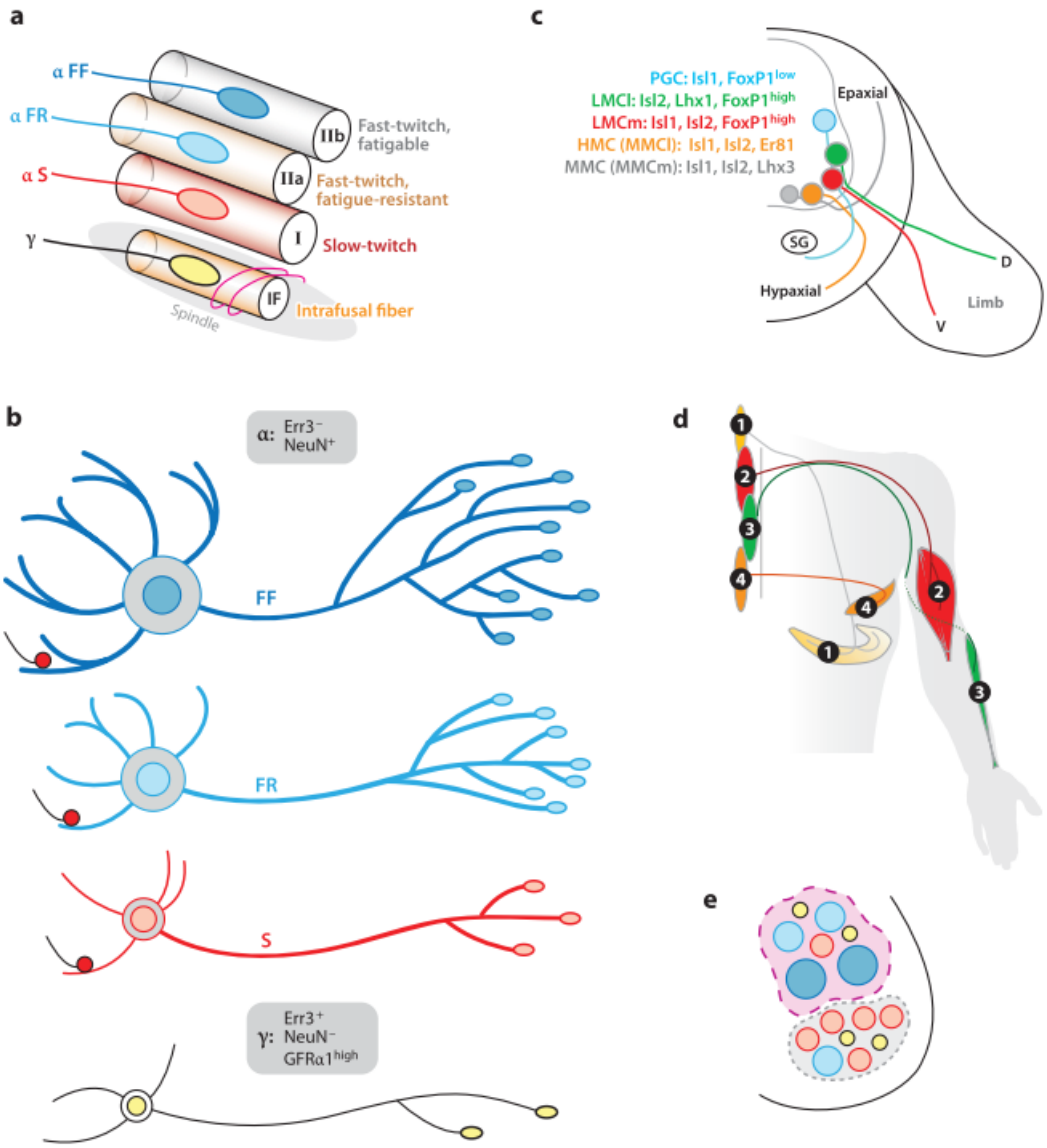

Figure 2: *Morphological features and spatial organization of motoneuron classes and subtypes (Kanning et al., 2010). (A) Distinct types of motor units in the skeletal muscle. (B) The dimension and complexity of α motoneurons diminish progressively from fast-twitch fatigable (FF), through fast-twitch fatigue-resistant (FR) to slow-twitch fatigue-resistant S motor units. (C) Motor columns in the embryonic spinal cord provide the basic framework for subsequent development of motor classes, subtypes, and pools. (D) Motor pools at later stages of development are spatially situated in the spinal cord according to their peripheral organization. (E) Motor pools contain multiple motoneuron classes and subtypes. PGC: preganglionic column; LMCm and LMCl: the medial and lateral subdivisions of the lateral motor column; HMC: hypaxial motor column; MMC: medial motor column.*

1.1.1.a.iii Force–frequency relation

The force-frequency relationship refers to the phenomenon by which the central nervous system regulates force production in muscle units by controlling the motoneurons firing rate (Heckman &

Enoka, 2004) (Figure 3). The force response to a single action potential is referred to as a muscle twitch. Typically, there is a one-to-one relationship between the action potentials discharged by a motoneuron and the twitches generated by the associated muscle fibres. As the rate of motoneuron discharge increases, the twitches occur closer together and begin to summate. While the summation of twitches increases with the discharge rate, there is an upper limit to the force capacity. This limit is reached when all the cross-bridges within the muscle fibres are cycling, attaching, and generating force simultaneously. This maximum force generated during continuous stimulation is known as a tetanic contraction.

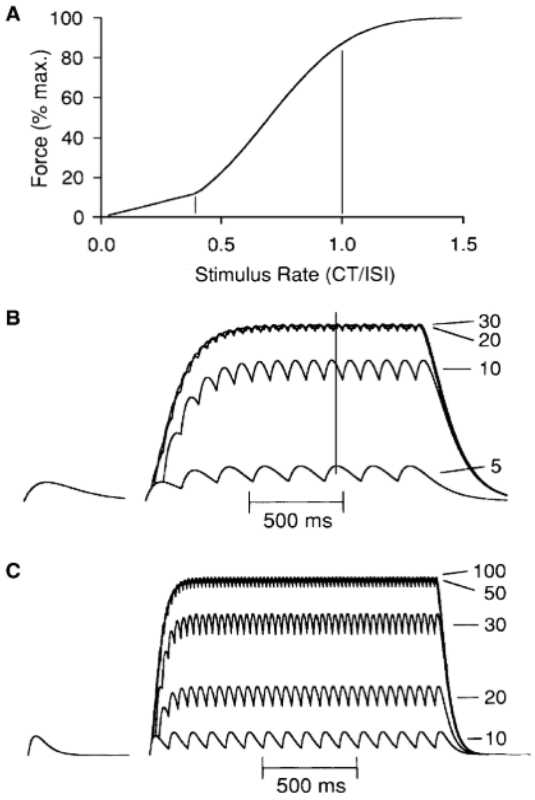

Figure 3: *Relationship between muscle force and activation frequency (Heckman & Enoka, 2004). (A) The force-frequency relation is approximately sigmoidal, showing how the force generated by the muscle varies with the frequency of stimulation. The y-axis represents the force normalized as a percentage of the maximum force. The x-axis in this graph normalizes the stimulation rate relative to the contraction speed of the motor unit, providing a measure of the relative stimulation rate. (B) Forces at four different stimulation rates for a slow-twitch fatigue-resistant motor unit. (C) Forces at five different stimulation rates for a fast-twitch fatigable unit.*

1.1.1.b. The neuromuscular junction (NMJ)

The NMJ is the highly specialised chemical synapse formed between an α motoneuron and its postsynaptic skeletal muscle fibres (Hughes *et al.*, 2006; Bloch-Gallego, 2015; Tintignac *et al.*, 2015; Li *et al.*, 2018; Pratt *et al.*, 2020*b*; Davis *et al.*, 2022). The organisation of the NMJ is tripartite and consists of the presynaptic nerve terminal, the postsynaptic membrane and the perisynaptic Schwann cells (Pratt *et al.*, 2020*b*; Davis *et al.*, 2022). However, some authors consider Schwann cells as part of the NMJ presynaptic terminal and the synaptic cleft as a separated NMJ component (Hughes *et al.*, 2006). The NMJ molecular architecture is complex (Figure 4) and will be illustrated below.

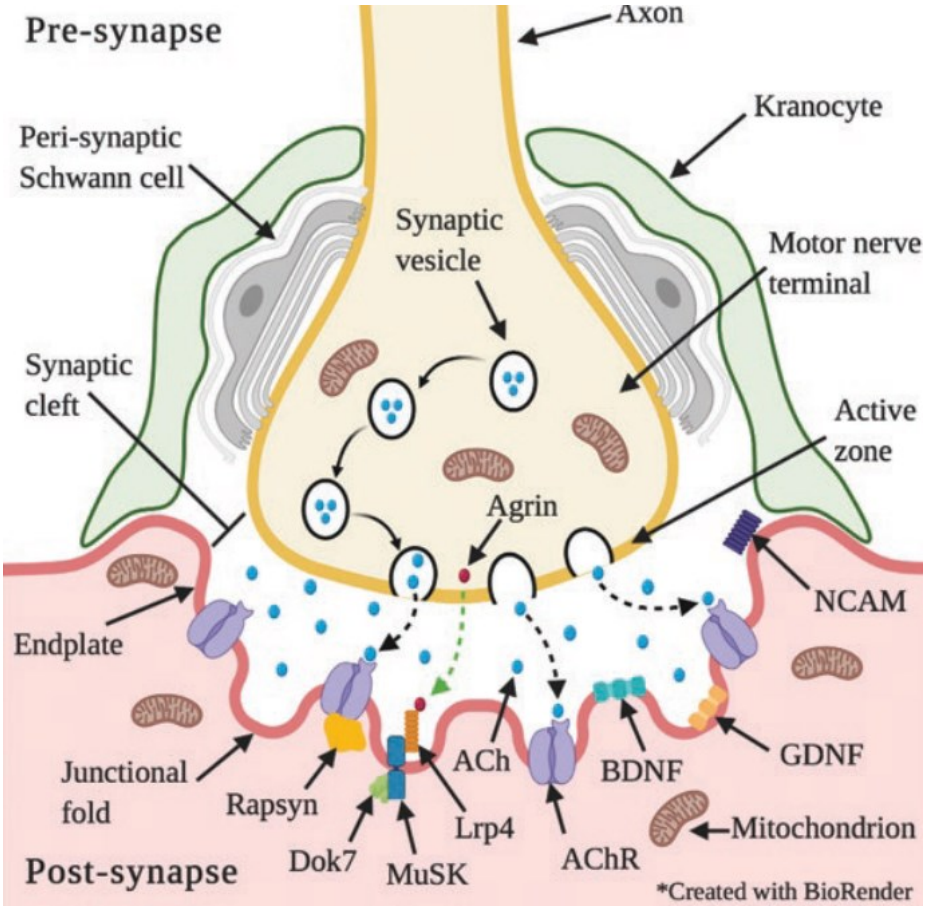

Figure 4: *Schematic representation of the neuromuscular junction architecture (Pratt et al., 2020b). ACh = acetylcholine; AChR = acetylcholine receptor; BDNF = brain-derived neurotrophic factor; Dok7 = docking protein downstream-of-tyrosine kinase 7; GDNF = glial cell line-derived neurotrophic factor; Lrp4 = low-density lipoprotein receptor-related protein 4; MuSK = muscle-specific tyrosine kinase NCAM = neural cell adhesion molecule.*

1.1.1.b.i Presynaptic region

The nerve terminal is characterised by the presence of synaptic vesicles, which play a central role in supporting synaptic function (Hughes *et al.*, 2006). These vesicles are precisely positioned across ACh receptor-rich synaptic folds and are closely associated with release sites known as active zones (Südhof, 2012). Calcium channels, primarily of the P/Q type (with some N-type channels), are activated upon the arrival of an action potential at the nerve terminal. Calcium influx triggers a significant rise in local calcium concentration, leading to the fusion of synaptic vesicle membranes with the plasma membrane of the nerve terminal (Südhof, 2004). Calcium micro domains created by individual calcium channels or the overlap of micro domains from neighbouring channels contribute to the localised internal calcium signal that promotes vesicle fusion. Functionally distinct pools of vesicles termed the readily releasable and reserve pools, have been identified and differ in their probability of fusion upon depolarisation. Vesicles within the readily releasable pool are dispersed throughout the vesicle cluster rather than being clustered in proximity to release sites.

The process of synaptic vesicle fusion involves conformational changes in multiple proteins present on both the vesicle and nerve terminal membranes (Hughes *et al.*, 2006). Docking and priming are the initial steps, where a synaptic core complex is formed, consisting of syntaxin-1, SNAP 25, and synaptobrevin. This complex brings the vesicle membrane close to the nerve terminal membrane, creating an intermediate state capable of forming a fusion pore. Munc18-1 regulates synaptic vesicle fusion by dissociating from syntaxin and allowing the core complex to form, while synaptophysin dissociates from synaptobrevin (Südhof, 2004). The calcium signal for membrane fusion is mediated by synaptotagmins, which reside on the synaptic vesicle membrane. Synaptotagmins bind to the SNARE protein complex and, as the local calcium concentration rises, translocate to the plasma membrane, leading to membrane insertion. The binding of synaptotagmin induces mechanical stress, destabilizing the core complex and resulting in the opening of a fusion pore for the release of vesicle contents.

Synaptic vesicle membrane recycling occurs through several processes. One involves the complete fusion of the vesicle membrane with the plasma membrane, followed by clathrin-dependent endocytosis and subsequent recycling of membrane components. Clathrin-coated vesicles shed their coats and enter the interior of the nerve terminal, where vesicle membranes fuse with endosomes. New vesicles bud from the endosomes and actively transport ACh to reload synaptic vesicles, which then translocate back to the active zone either through diffusion or cytoskeletal transport. Rapid recycling mechanisms, such as the "kiss-and-run" and "kiss-and-stay" processes,

have also been observed, where fused vesicle membranes are rapidly endocytosed and recycled either independently of endosomes or near the active zone. These fast recycling mechanisms are more prevalent in highly active central nervous system nerve terminals and may not be as prominent in the majority of NMJs.

Mitochondria are abundantly present in nerve terminals and serve prominent roles (Hughes *et al.*, 2006). In addition to their role in energy production for synaptic release, neurotransmitter synthesis, and ion and ACh transport, mitochondria also participate in intracellular calcium buffering. During repetitive action potentials, cytosolic calcium in nerve terminals rapidly increases and is then further regulated by calcium uptake into mitochondria. Blockade of calcium uptake from mitochondria results in a rapid and sustained increase in cytosolic calcium. Post-tetanic potentiation, the enhancement of synaptic transmission after high-frequency stimulation, is also mediated by slow release over minutes, which involves mitochondrial calcium release.

1.1.1.b.ii Synaptic cleft

The space between the presynaptic and postsynaptic membranes, where ACh diffuses, is divided into the primary cleft, bounded by the presynaptic membrane and the basement membrane, and the secondary clefts, spaces between the junctional folds of the postsynaptic membrane. The central region of the synaptic cleft is occupied by the synaptic basement membrane, also known as the basal lamina. In addition to its well-known mechanical role, the basal lamina is a crucial player in NMJ innervation, development, and regeneration, influencing the architecture and physiological functions of the presynaptic and postsynaptic membranes (Sanes, 2003). The basal lamina consists of various components, including laminins, collagen IV, heparan sulfate proteoglycans, and nidogen-2. Laminins and collagen IV are primarily deposited by the muscle, while a synaptic proteoglycan called agrin is deposited by the nerve.

1.1.1.b.iii Postsynaptic region

The mammalian postsynaptic muscle membrane is characterised by deep infoldings called secondary synaptic folds, where ACh receptors are anchored (Hughes *et al.*, 2006). These folds contain a cytoskeletal matrix composed of proteins similar to those found in the extrasynaptic sarcolemma. The ACh receptors are connected to the sarcolemma through α- and β-dystroglycans, which are part of a larger family of proteins called the dystroglycan complex. α-Dystroglycan is located extracellularly and binds to β-dystroglycan, which spans the sarcolemma, effectively linking

the basal lamina to the intracellular cytoskeleton. Rapsyn anchors β-dystroglycan to the NMJ, and β-dystroglycan binds to utrophin, a protein homologous to dystrophin, at the NMJ. Utrophin is localised with AChRs at the crests of postsynaptic junctional folds, while dystrophin is found with sodium channels in the troughs of junctional folds. The Na channels, along with ankyrin, the sarcoglycan complex, dystrobrevins, and dystroglycan complex, are densely present in the secondary folds. Utrophin and dystrobrevin also interact with α1 syntrophin and α2 syntrophin, which are associated with nitric oxide synthase. Rapsyn is associated with the cytoplasmic extensions of ACh receptors and plays a crucial role in the formation of ACh receptors clusters.

The ACh receptors have been extensively studied as a model for ligand-gated ion channel neurotransmitter receptors (Karlin, 2002). It consists of two α subunits and single β, δ, and ε subunits in the mature mammalian NMJ, while the γ subunit replaces the ε subunit in the fetal ACh receptor. The extracellular portions of the subunits form a large extracellular vestibule surrounding the channel orifice, while the intracellular orifice of the ion channel is surrounded by a smaller vestibule. Post-translational modifications, including phosphorylation, can modify the properties of the ACh receptors. During muscle development, the fetal ACh receptor is expressed along the entire fibre surface, contributing to spontaneous muscle contraction necessary for normal muscle maturation. Adult and fetal ACh receptors differ in their electrophysiological characteristics, with adult channels having shorter mean open times and larger single-channel conductance. Upon innervation, fetal ACh receptor is downregulated, and the adult receptor is expressed at the synapse. Denervated muscles re-express the fetal ACh receptors throughout the muscle fibre (Soendenbroe *et al.*, 2021), potentially leading to the development of spontaneous action potentials.

1.1.1.b.iv Schwann cells

Schwann cells are another essential element of the NMJ. There are three types of Schwann cells: myelinating and non-myelinating Schwann cells, which cover the motor axons with and without myelin, respectively, and perisynaptic Schwann cells (also known as teloglia Schwann cells), which do not enclose axons but instead envelop the nerve terminal and the adjacent muscle surface in close proximity to the synapse while covering the synaptic cleft (Li *et al.*, 2018). In mice, NMJs initially have one perisynaptic Schwann cell covering them, and this number increases to 3-5 in adults (Hughes *et al.*, 2006). They originate from neural crest cells and migrate alongside the growth cones of motoneuron axons. Schwann cells are critical in several aspects of NMJ function and

formation, including modulation of synaptic transmission, nerve terminal growth and maintenance, axonal sprouting, and nerve regeneration (Hughes *et al.*, 2006; Darabid *et al.*, 2014; Li *et al.*, 2018; Davis *et al.*, 2022).

The initial genetic evidence highlighting the crucial role of Schwann cells in NMJ formation emerged from studies conducted on Nrg1 and ErbB mutant mice (Darabid *et al.*, 2014). Notably, ErbB2 mutant mice, which lack Schwann cells, still exhibit motor nerve projection to muscle fibres, but the development of nerve terminals is impaired and eventually leads to retraction. ErbB2 mutation primarily affects the structure of junctional folds but does not influence synapse-specific transcription. In support of these findings, Schwann cell ablation experiments revealed their impact on nerve terminal growth, ACh receptor clusters, and neuromuscular transmission when at different stages of NMJ formation and maturation (Li *et al.*, 2018).

Perisynaptic Schwann cells lack electrical excitability but possess the ability to sense ACh, ATP, and nerve trophic factors. Upon sensing these signals, these cells elevate their intracellular calcium levels, which subsequently regulate neuromuscular transmission through a G protein-coupled receptor pathway (Darabid *et al.*, 2014).

In the process of NMJ regeneration following nerve injury, Schwann cells play a critical role. In cases of minor nerve injury, regenerating axons can retrace their original paths along Schwann cell tubes to reach their initial targets. This specificity is lost when nerves are completely severed. Following nerve section, Schwann cells become activated and extend into the synaptic cleft to envelop fragments of nerve terminals. Additionally, NMJs denervation prompts Schwann cells to sprout into adjacent intact NMJs, forming bridges. These bridges guide regenerating axons from intact NMJs to injured synapses, preventing the loss of ACh receptors and facilitating the formation of new ACh receptor clusters.

Finally, Schwann cells have the potential to promote synaptogenesis through the release of synaptogenic factors or by indirectly regulating motoneurons. Agrin, released by Schwann cells, is implicated in target selection and synapse formation by regenerating axons. TGF-β1 has been shown to enhance synapse formation in cultured systems (Shi *et al.*, 2012). Following nerve injury, Schwann cells produce a plethora of factors including GDNF, artemin, BNDF, nerve growth factor, leukemia inhibitory factor, cytokines, and chemokines (Li *et al.*, 2018). These factors play a crucial role in promoting motoneuron survival and facilitating axonal regeneration.

1.1.1.b.v The NMJ safety factor

The transmission of electric signals through the NMJ is an extremely reliable process. This reliability results from the release of more quanta of ACh than are necessary to initiate an action potential. The term safety factor, or safety margin, is the phenomenon that describes this excess (Wood & Slater, 2001). In other words, the NMJ safety factor is an expression of how much greater an effect the nerve has on the muscle fibre than is required to generate an action potential. Many different approaches have been applied to assess the NMJ safety factor, as reviewed elsewhere (Wood & Slater, 2001). The safety factor of neuromuscular transmission is influenced by many features of the pre and postsynaptic NMJ components, including the nerve terminal size, the density and distribution of ACh receptor and voltage-gated sodium channels, ACh esterase activity and organisation of postsynaptic folds. Various species employ different strategies to achieve a safety factor at their NMJs. Some rely on a high quantal content, while others depend on extensive postsynaptic amplification, facilitated by the presence of folds and VGSCs within these junctions, such as humans. The safety factor is a phenomenon essential for normal function of the body and its reduction is associated with a number of pathological conditions, such as myasthenia gravis and Miller–Fischer and Lambert-Eaton myasthenic syndromes. This phenomenon could arise due to either a decrease in transmitter release or a disruption in the efficacy of the transmitted signal.

1.1.1.c. Skeletal muscle fibre

1.1.1.c.i The sarcomere

Skeletal muscle fibres, also known as myofibres, are cylindrical cells constituting the skeletal muscle tissue. These fibres possess a length varying from 2-3 cm up to 50 cm, with an average of 10 cm in men, and a thickness ranging from 10 to 100 μm. At the ultrastructural level, skeletal muscle fibres display the essential components found in typical cells, namely the membrane known as sarcolemma, the cytoplasm referred to as sarcoplasm and nuclei situated at the periphery (Frontera & Ochala, 2015).

The sarcomere is the basic contractile unit of the skeletal muscle. The sarcomere exhibits a sophisticated structure, comprising two main sets of protein filaments that alternate with each other. These filaments include the thin filaments consisting of α-actin and associated proteins, as well as the thick filaments composed of myosin and associated proteins. It was originally believed that both filaments were parallel, but recent evidence showed that muscle cells contain highly connected myofibrillar networks via sarcomere branching (Willingham *et al.*, 2020) (Figure 5).

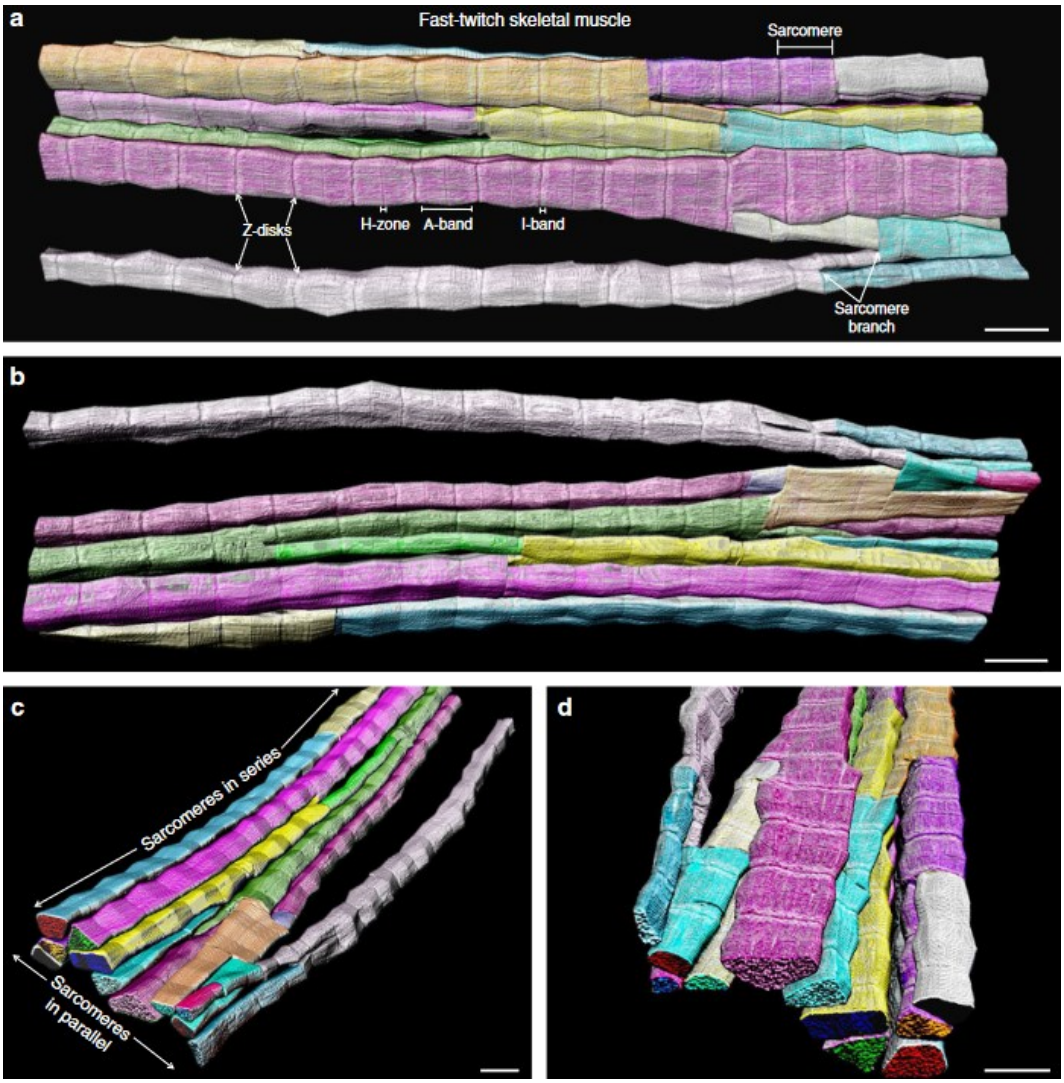

Figure 5: *Three-dimensional rendering of directly connected sarcomeres within the myofibrillar matrix of a fast-twitch muscle (Willingham et al., 2020).*

The sarcomere demarcation is defined by the Z-lines or Z-disks, thin dark disks distinguished by their high protein density. Each Z-line divides a lighter I-band, which extends between adjacent sarcomeres and exhibits weak birefringence due to its composition primarily of actin and its associated proteins (thin filaments). Positioned at the centre of the sarcomere is the dark and densely electron-dense A-band, predominantly comprised of thick filaments. Within the A-band, there is a lighter H-zone, and the M-line bisects this H-zone. The thin filaments are laterally arranged and connected at the Z-disk, while the M-band serves as an interconnection for the thick filaments. Other proteins, including myosin binding proteins (MyBPs) C and H, titin, and M-line proteins (myomesin, obscurine, creatin-kinases), are associated with myosin to form the thick filaments. Titin, an elastic protein, spans the length of the thick filament, connecting it to the Z-disk and

assisting in its stabilisation and alignment, regulating structural integrity of the sarcomere (Nishikawa, 2020). This ensures equal forces are developed in both halves of the A-band and also allows titin to function as a dynamic spring in active muscle. MyBPC interacts with titin and is present as transverse stripes within the A-band. Similar to thick filaments, thin filaments are associated with proteins that facilitate contraction. Troponin and tropomyosin are the most important proteins in this regard. Troponin, composed of three domains (TNN-I, TNN-C, and TNN-T), binds to actin, calcium, and tropomyosin, respectively. Tropomyosin stabilises actin and positions the troponin molecule on the filament, making it sensitive to calcium levels (Dominguez, 2011). Nebulin acts as a molecular template for thin filaments and seems to contribute to the generation of force during muscle contractions (Ottenheijm & Granzier, 2010), while tropomodulin serves as a capping protein for the pointed end of actin, contributing to the composition of the thin filament network. α-Actinin, a key structural component, connects the barbed ends of each actin filament to those of the adjacent sarcomere, while also linking titin molecules from opposing halves of the sarcomere (Henderson *et al.*, 2017). Several other proteins, including myozenins, myotilin, myopalladin, myopodin, γ-filamin, γ-actin, muscle LIM protein (MLP), desmin, and NRIP proteins, are also present within the Z-line and contribute to its structure. The proteins mentioned earlier, along with many others, collectively contribute to the formation of the structural support system known as the cytoskeleton within the muscle sarcomere. The cytoskeleton encompasses not only the sarcomeric structural and regulatory proteins but also includes other components (Henderson *et al.*, 2017): (i) the intermediate filaments: these proteins link the sarcomeres to other organelles, such as mitochondria or nuclei, providing additional structural support and organization; (ii) the costameres: these structures connect the sarcomere to the sarcolemma via the Z-disc and M-band, establishing a mechanical linkage between the contractile apparatus and the cell membrane and (iii) proteins at the myotendinous junction: this junction is where the force generated by muscle contractions is transmitted to the tendons, enabling movement and locomotion. The coordinated action of all these cytoskeletal assemblies is essential for the proper functioning of muscle contractions, ensuring efficient force generation, and transmission throughout the muscle fibres (Henderson *et al.*, 2017).

Besides myofibrils structures, skeletal muscle contains different types of organelles, including the transverse tubular system (T-tubule), the sarcoplasmic reticulum, and a network of mitochondria (Frontera & Ochala, 2015). The T-tubule system consists of invaginations of the sarcolemma (and plays a crucial role in transmitting nerve action potentials into the interior of the cell. This network

of tubules is in contact with the extracellular space, ensuring the uniform spread of excitation throughout the fibre. The sarcoplasmic reticulum is responsible for the storage, release, and reuptake of calcium ions during muscle activation. Calcium is stored in the terminal cisternae, which are located in close proximity to the T-tubule system. Two cisternae on either side of the T-tubule form a structure known as the triad. Two types of proteins within the sarcoplasmic reticulum contribute to maintaining calcium homeostasis: the sarco/endoplasmic reticulum Ca^{2+}-ATPase (SERCA) and calsequestrin. SERCA is responsible for the reuptake of calcium into the cisternae after muscle activation, while calsequestrin binds calcium loosely within the sarcoplasmic reticulum. Mitochondria are present throughout the muscle fibre in a three-dimensional network, rather than as isolated organelles (Dahl *et al.*, 2015; Katti *et al.*, 2022). They generate the energy required for muscle contractions when oxygen is available in the muscle fibre. Some mitochondria are located closer to the sarcolemma, reducing the diffusion distance for oxygen supplied by the capillaries. These cellular elements collectively contribute to the proper functioning of muscle fibres, ensuring the conduction of nerve signals, calcium regulation, and energy production for muscle actions (Frontera & Ochala, 2015). Moreover, recent evidence showed that the location and orientation of mitochondria within muscle cells influence sarcomere structure and myofilament interactions (Katti *et al.*, 2022) (Figure 6).

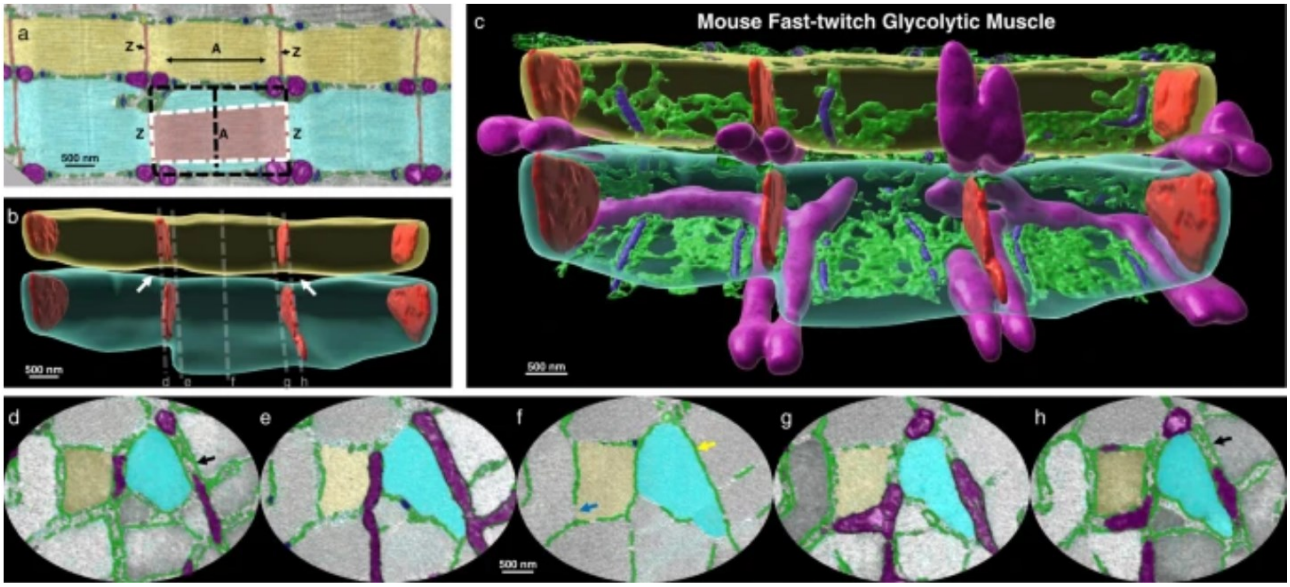

Figure 6: *Intrasarcomere cross-sectional area (CSA) heterogeneity due to the location and orientation of mitochondria. Upon close inspection of a mouse fast-twitch glycolytic muscle using focused ion beam scanning electron microscopy (FIB-SEM), sarcomeres CSA varies along different regions of its length. Specifically, CSA is smaller near the ends of the sarcomere, closer to the Z-disks, compared to the centre of the sarcomere within the A-band. Further analysis through 3D rendering of the sarcomeres reveals the presence of significant gaps between the parallel sarcomeres near the Z-disks. These gaps corresponded to regions where mitochondria were arranged in a perpendicular alignment. Adapted from (Katti et al., 2022).*

1.1.1.c.ii Heterogeneity of skeletal muscle fibres

Mammalian skeletal muscles are heterogeneous. According to one of the most common classifications based on their contractile performance and metabolism, myofibres can be divided into three categories: (i) slow, fatigue-resistant fibres with low mechanical power output and very active aerobic metabolism, (ii) fast and quickly fatigable fibres with high mechanical power output and predominant glycolytic metabolism and (iii) fast intermediate fibres which combine high power output and resistance to fatigue (Blaauw *et al.*, 2013). A second common classification is based on the pH lability of actomyosin ATPase staining, where fibres can be classified as type I, IIA, IIB and IIX. Indeed, myofibres are primarily composed of a single myosin heavy chain isoform (MyHC) which, together with the myosin light chains, forms the myosin proteins in the sarcomeres. MyHC represents a major determinant of fibre contractile performance and the most abundant proteins in myofibres (about 50% of their whole protein complement). In addition, MyHC can be easily detected via specific antibodies or gel electrophoresis. Accordingly, this histochemical approach represents the most accepted classification: muscle fibres classified as type I, IIA, IIB, and IIX are composed of MyHC-I, MyHC-2A, MyHC-2B, and MyHC-2X isoforms, respectively (Schiaffino &

Reggiani, 2011). Specifically, human skeletal muscles mostly express MyHC-1 MyHC-2A and MyHC-2X. Despite in some fibres a single MyHC isoform is expressed, differently, in a significant number of them two or more MyHC isoforms are co-expressed, often referred to as hybrid or mixed fibres. It is important to highlight that slow and fast fibres differ in several aspects, including contractile apparatuses structure, contraction and relaxation processes, metabolism and kinetic parameters, as reviewed in detail elsewhere (Schiaffino & Reggiani, 2011).

1.1.1.c.iii Excitation–contraction coupling

Excitation-contraction coupling is a coordinated process that involves two essential steps for force generation in muscle: the transmission of a nerve stimulus to the triad and the subsequent release of calcium from the sarcoplasmic reticulum, as well as the interaction between actin and myosin to form cross-bridges (Frontera & Ochala, 2015). The action potential arriving at the muscle fibre membrane is conducted through the T-tubule system, which extends into the interior of the muscle cell. At the triad, where the T-tubule is near the terminal cisternae of the sarcoplasmic reticulum, which stores calcium, a voltage sensor subunit of the dihydropyridine receptors on the T-tubule opens, allowing an inward calcium current. This calcium influx triggers the opening of the ryanodine receptors in the terminal cisternae, leading to the release of a large amount of calcium into the sarcoplasm. The released calcium binds to the regulatory protein troponin C on the thin actin myofilament, initiating a series of molecular events that displace tropomyosin, which normally blocks the active sites on actin. This exposure of the active site enables the myosin head to bind with actin (Figure 7). ATP and the ATPase located in the myosin head facilitate the detachment of myosin from actin, breaking the cross-bridge formed during a previous contraction, and the formation of a new cross-bridge. The detailed structure of the myosin head (Rayment *et al.*, 1993), greatly contributed to our understanding of the mechanics and physiology of this process.

The sliding filament theory, proposed in 1954 and still widely accepted with some modifications, explains the fundamental mechanism by which a muscle fibre generates force (Huxley & Hanson, 1954; Huxley & Niedergerke, 1954) (Figure 7). The force generated by individual actin-myosin cross-bridges is transmitted both longitudinally and laterally within the muscle fibre. The transmission of force to the Z-disk of the sarcomeres in series is particularly important. Ultimately, the force is propagated to the myotendinous junction, tendons, and joints, resulting in movement. The process leading to force generation begins when ATP becomes available to an existing actin-myosin cross-bridge. ATP binds to its binding site on the myosin head, and the ATPase in the myosin head

hydrolyses ATP, resulting in the detachment of the cross-bridge. The myosin head then swings over and binds to a new actin molecule. The release of inorganic phosphate (Pi) triggers a power stroke, during which myosin pushes the actin filament. Force is generated during this power stroke. At the end of the power stroke, ADP is released, and myosin remains bound to actin in a rigor state.

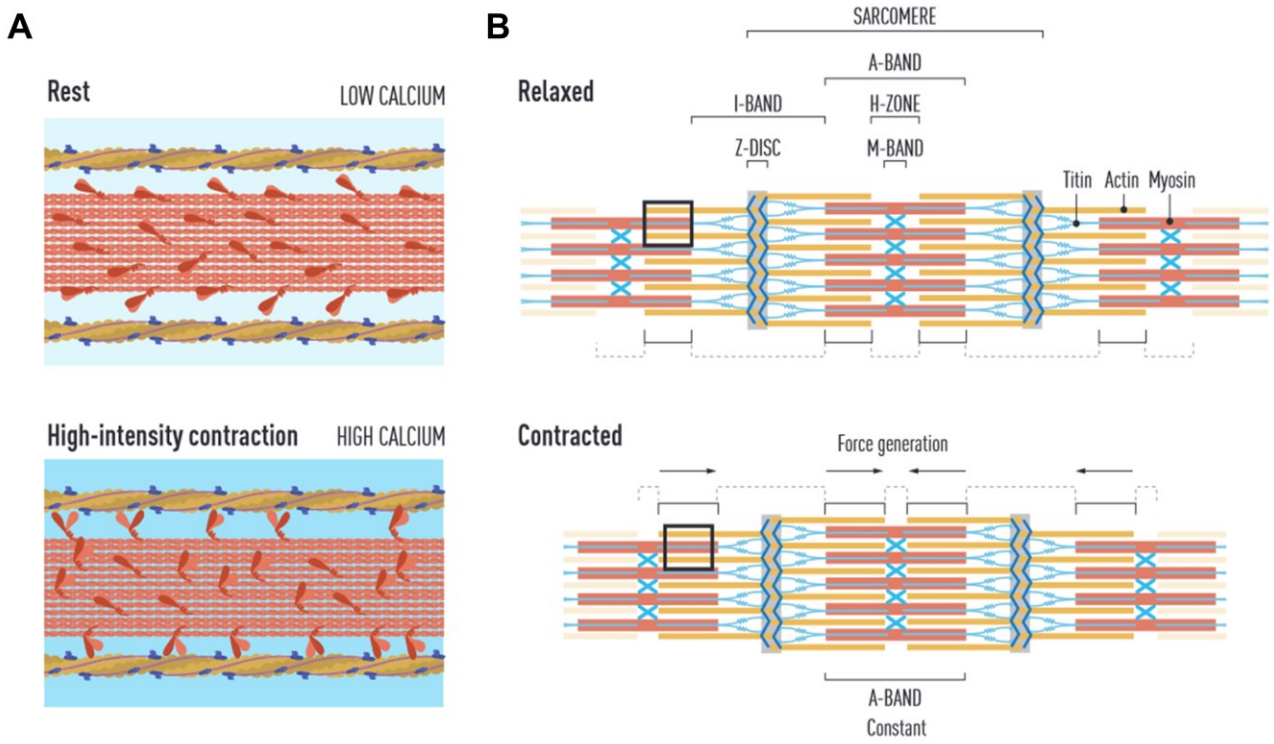

Figure 7: *The sarcomere structure in relaxed and contracted states. (A) Schematic representation of myosin activation during the excitation-contraction coupling. (B) The sliding filament theory. Adapted from (Smith et al., 2023).*

1.1.1.c.iv Length-tension and force-velocity relationships

During various types of muscle contractions (isometric, concentric, and eccentric contractions) the total active force generated by sarcomeres is influenced by several fundamental biomechanical properties of the musculoskeletal system (Frontera & Ochala, 2015). To this extent, the length-tension and force-velocity relationships are two essential aspects to consider.

The sarcomere length-tension relationship demonstrates that the force developed during an isometric contraction is critically dependent on the sarcomere length upon activation. At sarcomere lengths longer or shorter than the optimal length, the force generated after muscle activation is reduced because the overlap between actin and myosin, which is necessary for the formation of cross-bridges, is suboptimal. Differences exist between the models of length-tension relationship in vitro (Walker & Schrodt, 1974) (Figure 8) and in vivo (Herzog *et al.*, 1992). Indeed, this latter shows

that at longer sarcomere lengths, although the theoretical active tension that can be developed is reduced, the total tension achievable is increased. This is due to the generation of passive force related to sarcomeres and, thus, muscle stretch.

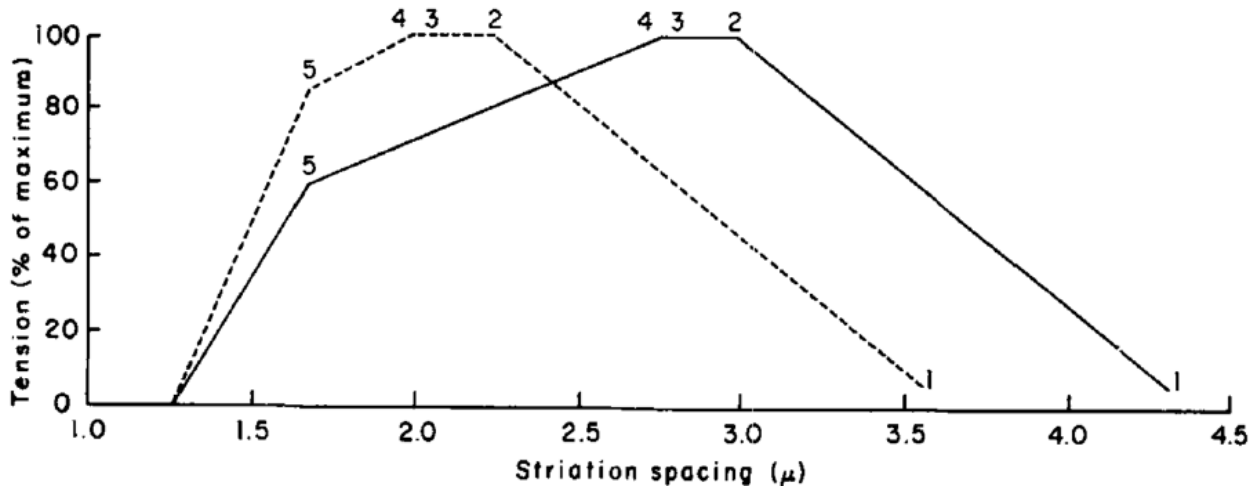

Figure 8: *Representation of the in vitro length-tension (L-T) relationship (Walker & Schrodt, 1974). Dashed line: frog muscle; continuous line: human muscle.*

During dynamic contractions, whether concentric (muscle shortening) or eccentric (muscle lengthening), the force developed also depends on the velocity of the movement, as described by the force-velocity curve (Wilkie, 1949; Bottinelli *et al.*, 1996) (Figure 9). In concentric muscle actions, an increase in movement velocity leads to a decrease in force. Similarly, performing muscle actions against high loads can only be achieved at relatively slower velocities. In contrast, during eccentric muscle actions, an increase in velocity results in higher force (Frontera & Ochala, 2015). It is worth noting that during eccentric contractions, the muscle force substantially increases during the stretch phase. Some of this additional force dissipates when the stretch stops, but a significant portion of the force remains, exceeding the isometric force at the stretched length. This residual force, known as residual force enhancement, persists until the muscle returns to its initial length or is deactivated.

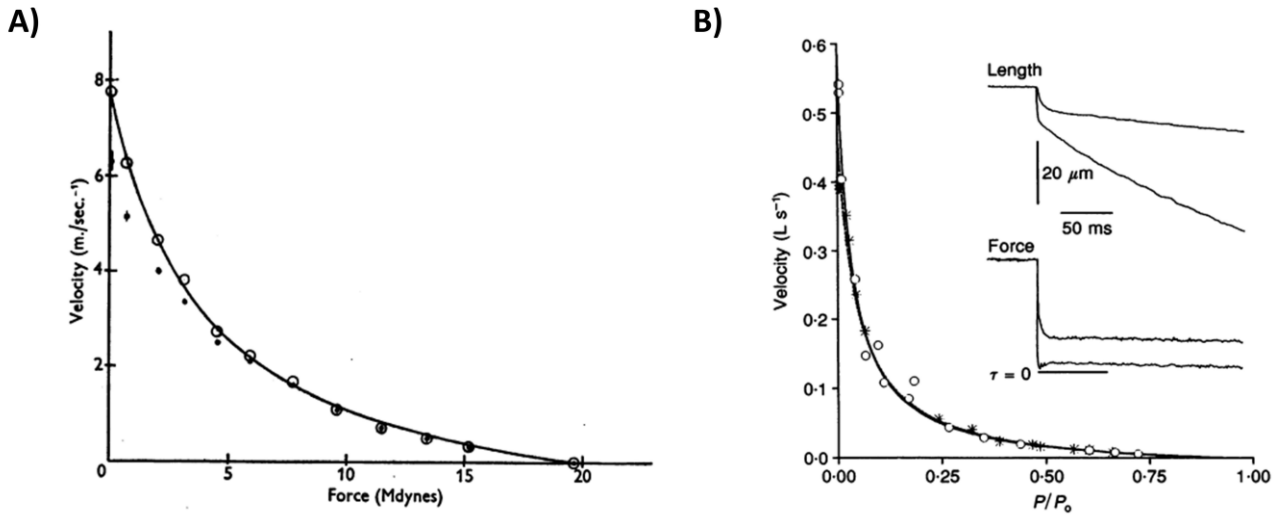

Figure 9: *Representation of the force-velocity (F-V) relationship at whole muscle (A) (Wilkie, 1949) and single fibres (B) (Bottinelli et al., 1996) level in humans.*

1.2. Neuromuscular plasticity

After this description of the anatomy and physiology of the neuromuscular system, it is now crucial to introduce a core concept of my thesis: neuromuscular plasticity. This term refers to the ability of the constitutive elements of the neuromuscular system, the MUs, to undergo structural and functional adaptive changes in response to different stimuli. This phenomenon represents an important evolutionary achievement as it improves survival under altered environmental conditions across the lifespan (Blaauw *et al.*, 2013). John Eccles's group, after introducing the term "plasticity" in this scenario for the first time in the late '50s (Eccles, 1958), performed the nerve cross-union experiment, considered a landmark study for the genesis of the concept of neuromuscular plasticity (Buller *et al.*, 1960). In this study, the authors showed that when an acutely denervated slow-twitch muscle (the soleus) of the cat was reinnervated by a nerve normally supplying a fast-twitch muscle (the flexor digitorum longus) turned to a faster phenotype (Buller *et al.*, 1960). Conversely, implantation of the nerve typically innervating the soleus converted the flexor digitorum longus muscles to slow. These experiments proved the remarkable malleability of skeletal muscle and highlighted that its regulation relies on neural control. Since this pioneering experiment, it has become well-established that skeletal muscle shows adaptive remodelling in response to various physiological and pathophysiological scenarios. Some specific stimuli can promote positive adaptive changes in the neuromuscular system. One such stimulus is exercise and in particular resistance training, known to support skeletal muscle health and hypertrophy, as for instance highlighted by the extreme case of increased muscle mass in bodybuilders (Monti *et al.*, 2020*b*). Conversely, other conditions can have opposite effects, leading to muscle atrophy and neuromuscular dysfunction. My PhD work is focused on thoroughly investigating the alterations of the neuromuscular system to muscle disuse and sarcopenia, two detrimental conditions that will be presented and discussed in detail in the next paragraphs.

1.2.1. Neuromuscular plasticity with muscle disuse

Changes in mechanical load unveil the highly plastic nature of the skeletal muscle. Muscle disuse has been defined as 'a combination of unloading and reduced neural activity' (Bodine, 2013), 'an expansive label for the low mechanical load or mechanical unloading of muscle' (Brooks & Myburgh, 2014), 'a reduction of load and number of action potentials delivered by motoneurons' (Reggiani, 2015), and 'decreased skeletal muscle contractile activity' (Nunes *et al.*, 2022). Periods of muscle disuse are commonly experienced across the lifespan following musculoskeletal injury, disease and surgery and have a profound impact on skeletal muscle health. Indeed, even short periods of disuse lead to a severe loss of muscle mass and function (Narici & De Boer, 2011; Campbell *et al.*, 2019; Di Girolamo *et al.*, 2021; Hardy *et al.*, 2022; Preobrazenski *et al.*, 2023). Episodic disuse is now recognised as a pivotal event contributing to age-related loss of muscle size and weakness (Wall *et al.*, 2013; Nunes *et al.*, 2022) (Figure 10). Understanding the mechanisms behind muscle disuse-induced atrophy and weakness is crucial for developing effective strategies to mitigate its adverse effects. Despite its relevance, there is still much that remains unknown about the intricate processes involved in muscle disuse-induced changes, including the exact cascade of molecular events. The exploration of these aspects has prompted the proposition of various experimental animal and human models. In the upcoming paragraph, I will delve into these models and examine how they have contributed to our understanding of muscle disuse.

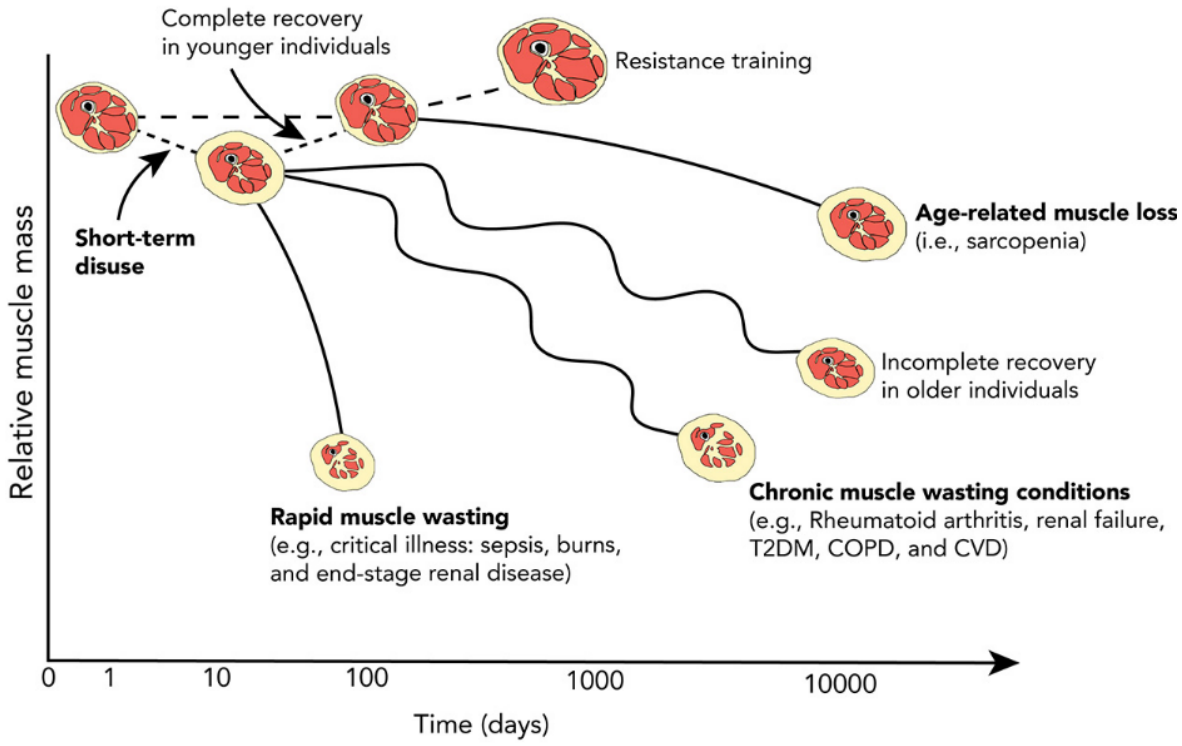

Figure 10: *The timeline of skeletal muscle atrophy is graphically depicted, highlighting various underlying causes (Nunes et al., 2022). Nonlinear lines accentuate the significance of periodic disuse as a catalyst for accelerated muscle loss in both aging and disease states. CVD: cardiovascular diseases; COPD: chronic obstructive pulmonary disease; T2DM: type 2 diabetes.*

1.2.1.a. Experimental models of disuse & physical inactivity

1.2.1.a.i Animal models

Hindlimb suspension

The hindlimb suspension method involves suspending an animal by its hindlimbs in order to simulate the effects of weightlessness or reduced gravity (Morey-Holton & Globus, 2002). Since the National Aeronautics and Space Administration (NASA) Ames Research Center approved this model, it has been used extensively in spaceflight and disuse research. Model testing started in 1975, but the first paper describing it was published in 1979 (Morey, 1979), quickly followed by another publication (Musacchia *et al.*, 1980). In these first experiments, a body harness was employed to unload hindlimbs, with a rotating beam that allowed the head-down animal to move in an arc. These pioneering studies paved the way for many other investigations, however, the harness system and degree of mobility varied significantly between laboratories, leading to differential muscle changes in response to the intervention (Morey-Holton & Globus, 2002). The angle between the torso and the floor of the cage was quickly addressed as an important factor. A 30° angle was recommended, as it applies 50% of rats body weight to their forelimbs (Hargens *et al.*, 1984). This is particularly relevant as this condition has to be maintained for using forelimbs as an internal control. The concept of using a tail harness to induce hindlimbs suspension was introduced by Russian researchers employing a tail cast (L'in & Novikov, 1980), then rapidly substituted by a traction tape. Traction tape can be applied to an anaesthetised animal, allowing the tail to grow without restriction and appears to be less stressful to animals than whole-body harnesses. For these reasons, the use of tail traction in the hindlimb unloading model has become the gold standard approach (Morey-Holton & Globus, 2002). Hindlimb unloading has been shown to induce similar, although not always identical, physiological changes in many systems compared to spaceflight (e.g. Tischler *et al.*, 1993).

Limb immobilisation

Following musculoskeletal traumatic injury, the injured area often needs to be immobilised to prevent secondary damage. This experimental model is used to mimic these scenarios, elucidating the adaptations that occur in skeletal muscle during prolonged immobilisation. Limb immobilisation

as an animal model of muscle disuse has been widely applied in different species, including rats (Fischbach & Robbins, 1969; Booth & Kelso, 1973), cats (Tabary *et al.*, 1972), rabbits (Herbert & Balnave, 1993) and lesser bush babies (*Galago senegalensis*) (Edgerton *et al.*, 1975). It has long been recognised that the length of the muscle at specific fixed positions is a very important factor influencing muscle atrophy (Booth, 1982; Goldspink, 1985). For instance, according to the findings of a seminal study conducted in mice, it has been observed that muscles immobilised in either a stretched or shortened position undergo a compensatory adaptation through sarcomere addition or subtraction, respectively, to their constituent muscle fibres (Williams & Goldspink, 1971). Limb immobilisation is one of the oldest and most employed disuse models and permitted the study of many fundamentals problems concerning mechanisms of muscle atrophy.

Wheel-lock & Cage reduction

Wheel-lock and cage reduction models represent animal analogues of the human step reduction model (see below). Both models are typically classified as models of reduced physical activity rather than muscle disuse, as the inactivity stimulus they induce is mild. In the wheel-lock model, rodents are given access to running wheels and allowed to voluntarily engage in running for an extended period (typically 3-6 weeks). Subsequently, the wheels are locked, inducing the cessation of the animals habitual activity and promoting sedentary behaviours (Kump & Booth, 2005*a*, 2005*b*). The cage reduction model is implemented by altering the size and features of rodents home cages, thereby intentionally diminishing their voluntary ambulatory activity. In Chapter 4, the reader will find a narrative review (Sarto *et al.*, 2023) that offers a detailed and updated description of these models.

Models of complete disuse

Other extreme models inducing complete muscle disuse are commonly employed in animal research and include denervation, spinal cord injury/transection, tenotomy and synaptic blockade via toxin application. The first three models are based on the section of a nerve (Midrio, 2006), the spinal cord (Cho *et al.*, 2016) or a tendon (Pachter & Spielholz, 1990), respectively, leading to permanent disuse of muscle(s) distal to the lesion. In the fourth one, a toxin (often tetrodotoxin) is injected to block nerve impulse conduction (Pestronk & Drachman, 1978). All these models are considered very severe and changes observed at skeletal muscle levels are generally much more rapid compared to other traditional disuse models.

1.2.1.a.ii Human models

Bed rest

Bed rest represents an extreme model of physical inactivity. Participants are asked to lie without the possibility of standing up or leaving the bed, typically moving only the upper limbs. The first human bed rest study was conducted in 1929 (Cuthbertson, 1929). This study reported a rapid loss of nitrogen, sulphur, phosphorus and calcium within one/two days from the onset of bed rest. The first investigation with a major impact employing this model was the seminal Dallas bed rest study (Saltin *et al.*, 1968), showing remarkable decreases in VO_2 max, maximal total heart volume, maximal stroke volume, and maximal cardiac output following a 20 day-intervention. In alternative to conventional horizontal bed rest, the head-down bed rest has also been developed and frequently employed as an analogue of spaceflight to mimic microgravity in many experimental studies (Pavy-Le Traon *et al.*, 2007; Narici & De Boer, 2011; Watenpaugh, 2016). This experimental paradigm was born in the early 1970s from observations of cosmonauts returning from space complaining of sleeping issues due to the sensation of slipping off the foot of the bed. This sensation generally improved by raising the foot of the bed until it was felt horizontal by the cosmonauts. Russian researchers posited that the head-down position on Earth was closer to what is experienced in space and tested different conditions, concluding that –6° was the best compromise (Atkov & Bednenko, 1992). One advantage of bed rest studies is the high level of standardisation possible, allowing for full monitoring of volunteers conditions, diet and compliance. Moreover, bed rest studies are clinically relevant to conditions that require forced bed rest to heal the primary disorder. The main drawbacks of the bed rest model are the expense of conducting these experiments and the potential health risks for the participants. Indeed, during bed rest, symptoms such as musculoskeletal complaints, signs of anxiety and depression, vertigo, nausea, reduced appetite and gastroesophageal reflux can be occasionally experienced. Participants in bed rest studies can potentially be exposed to an increased risk of renal calculi, urinary tract infections and deep vein thrombosis.

Dry immersion

In order to better comprehend the impact of microgravity on human physiology, other various experimental models have been explored. In the early 1960s, some studies tested the physiological impact of immersion to assess its capacity to mimic the effects of weightlessness (Beckman *et al.*, 1961; Graveline *et al.*, 1961). The drawback of this method is its duration, which cannot exceed 6–

12 hours, due to the deleterious cutaneous effects of prolonged water immersion (Navasiolava *et al.*, 2011; Watenpaugh, 2016). The dry immersion model was devised at the beginning of the '70s by two scientists from the Institute of Biomedical Problems (Russia) (Shulzhenko & Vil-Vilyams, 1975, 1976). With this method, participants are immersed up to the neck level in a water pool (originally 2m long, 1m wide, and 1m deep; nowadays generally 2.2m x 1.1m x 0.85m) and kept dry thanks to a special waterproof and highly elastic fabric, enabling a condition similar to zero gravity via floatation (Navasiolava *et al.*, 2011; Tomilovskaya *et al.*, 2019). As reviewed elsewhere (Tomilovskaya *et al.*, 2019), dry immersion and head-down bed rest induce similar physiological effects, however, the time course and the magnitude of these changes are largely different. For instance, muscle fibre atrophy with 21-day dry immersion (15-18%) is similar to what observed only after 60 days of bed rest (Shenkman *et al.*, 1997). Skeletal muscle alterations with dry immersion are dramatically rapid, with alterations such as in muscle innervation profile (Demangel *et al.*, 2017) and mitochondrial respiration (Popov *et al.*, 2023) observed as early as 3 days into the intervention. This model is considered the gold standard for mimicking the effects of spaceflight, as all three conditions of weightlessness are reproduced with this model: physical inactivity, support withdrawal and elimination of the vertical vascular gradient (Navasiolava *et al.*, 2011; Tomilovskaya *et al.*, 2019). However, it has to be considered that this model has a very strong on volunteers health impacting different physiological systems and that in the initial stages of dry immersion, abdominal and back pain, sleep issues, loss of appetite and constipation (Tomilovskaya *et al.*, 2019).

Unilateral lower limb suspension

The unilateral lower limb suspension model (ULLS) was introduced at the Karolinska Institute (Sweden) to investigate the impact of a period of disuse/unloading on skeletal muscle function in humans (Berg *et al.*, 1991). Two primary versions of ULLS have been proposed. In the original one (Berg *et al.*, 1991), participants were asked to walk with crutches and were equipped with a shoe having an elevated sole (50 mm). Moreover, to keep one lower limb slightly flexed and prevent ground contact when walking, a harness sling was worn across the shoulder and attached to the shoe. Differently, in the modified protocol (Ploutz-Snyder *et al.*, 1995), the harness sling was omitted and a higher sole (100 mm) was employed. In this way, the unloaded leg is allowed to swing freely. NASA has recognized ULLS as an important model to simulate microgravity (Tesch *et al.*, 2016*a*). Indeed, during spaceflight, the lower limb is unloaded but free to move through a wide range of motions (Hackney & Ploutz-Snyder, 2012). Employing this model several studies showed marked

unloading-induced impairment of muscle morphology and function, as well as alterations of skeletal and circulatory systems, as reviewed elsewhere (Hackney & Ploutz-Snyder, 2012; Tesch *et al.*, 2016*a*). ULLS is probably the most cost-effective method to study unloading, with no or limited systemic effects and without major restrictions on volunteers private or social life. One of the most evident issues of the ULLS interventions is that volunteers' compliance cannot be fully monitored. Moreover, the original method was associated with a greater risk (∼2.7%) of deep vein thrombosis (Bleeker *et al.*, 2004).

Limb immobilisation

Similarly to ULLS, limb immobilisation induces disuse at a local muscle level. However, this model is generally considered a more extreme disuse stimulus compared to ULLS, as a cast or brace is used to abolish the movement of one limb. For instance, the estimated median daily decrease in knee extensor strength is expected to be $-2.0\%\cdot day^{-1}$ for unilateral lower limb immobilisation and $-1.0\%\cdot day^{-1}$ for ULLS (Campbell *et al.*, 2019). The use of limb immobilisation as a disuse model in humans became prominent in the '80s (White *et al.*, 1984; Davies *et al.*, 1987), following earlier observations of immobilisation-induced muscle atrophy in conditions of musculoskeletal injuries (Patel *et al.*, 1969; Sargeant *et al.*, 1977). While essentially sharing with ULLS most of its pros and cons, it has to be considered that limb immobilisation is the only disuse model that can be applied also to upper limbs. This is of particular interest, as upper and lower limbs may be differently affected by disuse (Campbell *et al.*, 2019).

Step reduction

More recently, an additional physical inactivity model, termed step reduction, has been proposed (Olsen *et al.*, 2008; Thyfault & Krogh-Madsen, 2011). Step reduction involves inducing a decrease in participants' usual daily step count (typically measured using a pedometer and/or an accelerometer) to a lower maximum step limit, ranging from approximately 750 to 4500 steps per day (Oikawa *et al.*, 2019*b*). Step reduction is generally considered a model of reduced physical activity rather than muscle disuse, as participants are still exposed to loading stimuli. For a detailed and updated description of this model, the reader is referred to a narrative review that I recently published (Sarto *et al.*, 2023), entirely reported in this dissertation in Chapter 4.

1.2.1.b. MU remodelling with muscle disuse

As mentioned above, at whole muscle level, disuse leads to a rapid and marked decrease in muscle mass and force (Narici & De Boer, 2011; Campbell *et al.*, 2019; Di Girolamo *et al.*, 2021; Hardy *et al.*, 2022; Preobrazenski *et al.*, 2023). Interestingly, the reported loss of muscle function largely exceeds that of muscle size, suggesting an impairment in the intrinsic capacity of muscle force production (Marusic *et al.*, 2021). Although a clear and exhaustive explanation of why this disuse-induced loss of specific force is still lacking, there is growing evidence that motoneuron dysfunction, NMJ instability and early denervation processes may play a role in this loss of specific force (Demangel *et al.*, 2017; Monti *et al.*, 2021). In the following paragraphs, the impact of muscle disuse on the different MU components is discussed. I decided to focus mainly on the findings from studies employing the most conventional and established animal (hindlimb suspension and cast immobilisation) and human (bed rest and unilateral lower limb suspension/immobilisation) disuse models (Figure 11), as closer to real-life scenarios (i.e. more similar to conditions of forced inactivity due to injuries, surgeries etc.).

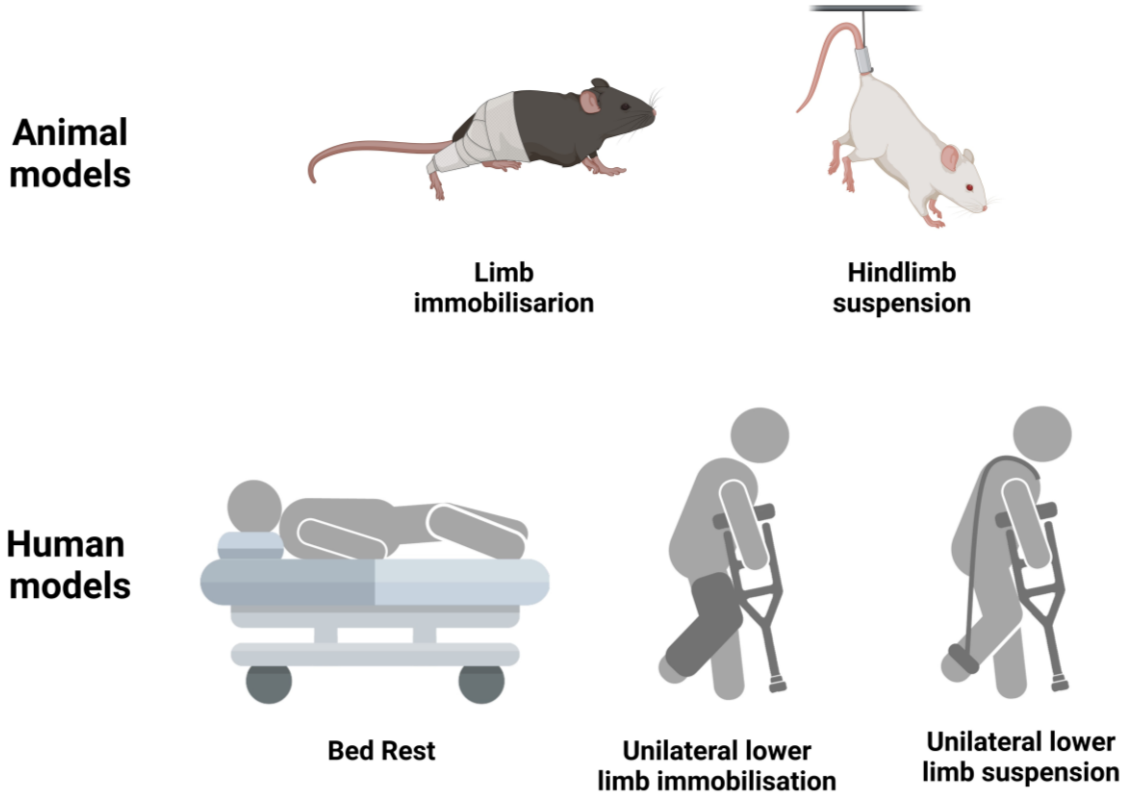

Figure 11: *Graphical representation of the main animal and human models of muscle disuse. Adapted from* (Sarto *et al.*, 2022*c*).

1.2.1.b.i. Effects of disuse on the motoneuron

There is some evidence that motoneurons are affected by muscle disuse. Hindlimb-suspended rats exhibited motoneuron soma (De-Doncker *et al.*, 2006) and nerve fibre diameter (Canu *et al.*, 2009) atrophy. Similarly, the growth-related increase in the cell body size of large-sized alpha motoneurons in neonatal rats is slowed down when hindlimb unloading is applied (Nagatomo *et al.*, 2009). Unloading is also accompanied by reductions in myelin thickness (Canu *et al.*, 2009) and marked myelin damage (Islamov *et al.*, 2015), axonal swelling and irregular spacing of the nodes of Ranvier (Malathi & Batmanabane, 1983). These structural alterations may have functional implications, leading to motoneuron hypoexcitability (Gardiner, 2006; Banzrai *et al.*, 2016). Indeed, in suspended rats, motoneurons become less excitable for the generation of single spikes, as indicated by elevated rheobase, and require more excitation to produce rhythmic trains of impulses (i.e. right shift of the frequency-current relationships) (Cormery *et al.*, 2005). Moreover, reductions in motoneuron conduction velocity have been observed in rats following hindlimb suspension (Canu *et al.*, 2003, 2009) and in cats following limb immobilisation (Robinson *et al.*, 1991). A modeling study showed that these reductions in motoneuron excitability could potentially be explained by reduced persistent Na^+ currents along with parameters related to current leakage (Banzrai *et al.*, 2016). This dysfunction of the motoneuron ion channels could be mediated by inactivity-induced decreased expression of neurotrophins, altering the gene expression of ion channel subunits via their specific tyrosine kinase receptors (Gardiner, 2006). In support of this view, skeletal muscle from hindlimb-unloaded rats showed a decrease in GDNF in the soleus and gastrocnemius (Wehrwein *et al.*, 2002). Finally, the increased H-reflex amplitude observed in disuse scenarios (De-Doncker *et al.*, 2006; Islamov *et al.*, 2011), reflecting increased reflex excitability, may suggest changes in presynaptic inhibition of Ia afferents (Lundbye-Jensen & Nielsen, 2008). Retrograde axonal transport was also found to be significantly decreased during the first week of simulated hypogravity (Islamov *et al.*, 2011). However, these processes of motoneuron degeneration seem to occur without affecting its oxidative capacity (Ishihara *et al.*, 1997). Moreover, no signs of apoptosis in motoneurons are observed with hindlimb suspension (Islamov *et al.*, 2008, 2011), potentially due to the activation of compensatory neuroprotective mechanisms, such as increased expression of heat shock proteins (Islamov *et al.*, 2011).

Motoneuron alterations in human models of disuse

One study suggested that 2 to 4 months bed rest is associated with decreases in nerve conduction velocity (Ruegg *et al.*, 2003), potentially explained by a reduction in myelin sheath diameter and/or changes in membrane properties at the nodes of Ranvier. Another shorter bed rest (10 days) did not observe these changes in nerve conduction velocity but detected some signs of nerve dysfunction, suggested by decreased F wave amplitude (Manganotti *et al.*, 2021). In agreement with animal studies, increased H-reflex amplitude was observed in different human disuse models (Duchateau, 1995; Lundbye-Jensen & Nielsen, 2008; Seynnes *et al.*, 2010). Evidence of initial disuse-induced denervation processes is observable at myofibre level (see Paragraph 1.2.1.b.iii.) and obtained by other electrophysiological analyses. Indeed, a 2-week immobilisation study showed an increased number of MU potential turns, indicative of increased MU potential complexity (Inns *et al.*, 2022). This parameter is generally elevated in conditions of denervation, suggesting early signs of altered innervation pattern could occur with limb immobilisation. However, in accordance with the evidence from animal models where no motoneuron apoptosis is observed, these processes seem to occur in the absence of MU loss (Attias *et al.*, 2020; Zeppelin *et al.*, 2023). Finally, motoneuron firing rates, one of the fundamental properties of muscle force production, were found to decrease across different intensities both in small hand muscles (adductor pollicis and the first dorsal interosseous) (Duchateau & Hainaut, 1990; Seki *et al.*, 2001, 2007), in the muscles of the triceps surae (Divjak *et al.*, 2022) and vastus lateralis (Inns *et al.*, 2022).

1.2.1.b.ii. Effects of disuse on the NMJ

NMJ undergoes remarkable dynamic remodelling in conditions of muscle disuse (Wilson & Deschenes, 2005). Researchers from the University of Southern California showed already in the ‘80s relevant NMJ morphological changes evaluated by electron microscopy in the soleus muscle after only 5 days of limb immobilisation (Fahim & Robbins, 1986; Fahim, 1989). These consisted of nerve terminals sprouting and disruption (Fahim & Robbins, 1986; Fahim, 1989) and alterations of post-synaptic fold structure (Fahim, 1989), this latter reported previously by other authors (Pachter & Eberstein, 1984). Changes in endplate dimension following muscle disuse (Malathi & Batmanabane, 1983; Deschenes *et al.*, 2006; Chibalin *et al.*, 2018) and increased fragmentation (Kravtsova *et al.*, 2019) were detected by other studies. Expansion of ACh vesicle and receptor dimensions (old rats only) (Deschenes & Wilson, 2003), increased density of the ACh receptors distribution (Chibalin *et al.*, 2018) and changes in extrajunctional ACh sensitivity (Fischbach &

Robbins, 1971) were also observed in response to hindlimb unloading/immobilisation. Moreover, changes in the expression of Homer proteins, essential for binding and coupling the actions of multiple proteins involved in NMJ regulation, have been observed with spaceflight and hindlimb suspension (Blottner *et al.*, 2022). Alterations in the NMJ presynaptic component have also been reported with disuse. Of particular interest, one recent study observed decrements in active zone staining, as measured by Bassoon, and presynaptic calcium channel expression following 2 weeks of unloading (Deschenes *et al.*, 2021). It is noteworthy to highlight that NMJ remodelling in animal models occurs extremely rapidly, with early changes detectable already in an acute phase 6-12h following disuse (Chibalin *et al.*, 2018). Overall, these findings observed with hindlimb suspension or immobilisation are similar to those reported following complete disuse (denervation, tenotomy and tetrodotoxin-induced muscle disuse) (Pestronk *et al.*, 1976; Brown & Ironton, 1977; Pestronk & Drachman, 1978; Eldridge *et al.*, 1981; Labovitz *et al.*, 1984; Pachter & Spielholz, 1990). Interestingly, it has been hypothesised that exacerbated deficits in skeletal muscle recovery following disuse in ageing may be associated due to NMJ instability and denervation (Baehr *et al.*, 2016).

The scientific literature has devoted comparatively less attention to exploring the disuse-induced alterations in NMJ transmission. In a pioneering study, the size and frequency of spontaneously released quanta of the transmitter were unchanged following immobilisation periods ranging from 3 to 42 days (Robbins & Fischbach, 1971). The mean quantum content released in response to single shocks was either normal or increased, while during prolonged tetani of the nerve, higher quanta content was observed during low-frequency physiological stimulations (Robbins & Fischbach, 1971). Two additional studies reported changes in neurotransmitter handling with tetrodotoxin-induced muscle disuse, showing increased ACh quantal release in disused muscle (Snider & Harris, 1979; Tsujimoto & Kuno, 1988). The physiological significance of these changes with muscle disuse remains largely unexplored, although they could be interpreted as a compensatory mechanism for the altered NMJ morphology.

NMJ alterations in human models of disuse

Very little is known regarding NMJ plasticity in human models of disuse. Our recent bed rest project was one of the first studies to specifically investigate this aspect (Monti *et al.*, 2021). In this investigation, we showed increases in C-terminal agrin fragment concentration, a well-established biomarker of NMJ instability (Monti *et al.*, 2023*a*), following 10 days of bed rest. This finding was accompanied by changes in the expression of selected genes involved in NMJ regulation (Monti *et*

al., 2021). Among these, HOMER2, known to regulate the expression of synaptic genes, was downregulated in agreement with a previous 60-day bed rest study (Salanova *et al.*, 2011). Impact of muscle disuse on human NMJ function remains controversial. One investigation based on small sample size (n = 6; aged 21 to 48 years) found increased jitter in the soleus following 28-day cast immobilisation (Grana *et al.*, 1996). Differently, another study observed no differences in jiggle in the vastus lateralis in response to 2 weeks of knee bracing (Inns *et al.*, 2022). Thus, the duration of the period of disuse may play a crucial role.

1.2.1.b.iii. Effects of disuse on skeletal muscle fibres

Disuse is known to promote a slow-to-fast fibre-type shift (Blaauw *et al.*, 2013; Vikne *et al.*, 2020). However, this is generally observable in immunohistochemical sections only during relatively long periods of disuse. Differently, modifications are observable at mRNA level already following short-term disuse, as we for instance shown in a 10-day bed rest study (Monti *et al.*, 2021). This change in muscle phenotype is paralleled by progressive myofibre atrophy, both in animal and human models (Bodine, 2013). Among human models, dry immersion and limb immobilisation are the ones inducing the most profound and rapid changes, with declines fibre CSA already detectable after 3 (Demangel *et al.*, 2017) and 4 (Suetta *et al.*, 2012) days of intervention, respectively. In humans, muscle atrophy seems mainly due to reduced protein synthesis rather than increased protein breakdown (Crossland *et al.*, 2019; Nunes *et al.*, 2022), while in rodents both processes seem to occur (Bodine, 2013; Crossland *et al.*, 2019). In animal models is generally well established that type I fibres are more susceptible to disuse atrophy (Bodine, 2013). This seems to be confirmed in human spaceflight (Fitts *et al.*, 2007) and bed rest (Brocca *et al.*, 2012), although results are often conflicting (e.g. Hvid *et al.*, 2010). Human studies failing to detect differential atrophy have generally been short-term (less than 14 days) (Bodine, 2013). Muscle fibre contractile properties are also impaired, with decreases in both absolute force (P_0) and specific force (P_0/CSA) generally reported (Widrick *et al.*, 1998, 2002; Trappe *et al.*, 2008; Hvid *et al.*, 2011; Brocca *et al.*, 2015). Despite changes in these classic parameters were not always observed with short-term disuse, when assessing the tension development in response to caffeine-induced Ca^{2+} release we recently observed an impaired with 10 days of bed rest (Monti *et al.*, 2021). Changes in muscle fibre unloaded shortening velocity (V_0) in response to muscle disuse are more controversial with studies reporting increases with spaceflight and bed rest (Widrick *et al.*, 2001, 2002) and others decrease or no alterations with ULLS (Widrick *et al.*, 2002; Brocca *et al.*, 2015). Signs of initial and early stages of myofibre denervation in

response to disuse have been shown in several studies by increases in neural cell adhesion molecule (NCAM) positive fibre, as reported with hindlimb suspension (Deschenes & Wilson, 2003; Deschenes *et al.*, 2018), dry immersion (Demangel *et al.*, 2017) and bed rest (Arentson-Lantz *et al.*, 2016; Monti *et al.*, 2021).

1.2.2 Neuromuscular plasticity with sarcopenia

1.2.2.a. Sarcopenia

Ageing is known to be accompanied by a chronic, inevitable and progressive reduction in muscle mass and strength. This phenomenon represents a concern for mankind since early Greek and Roman history, with observations regarding the loss of flesh and vigour with old age already reported by Aristotle, Galen of Pergamon and Cicero (Narici & Maffulli, 2010). The term sarcopenia was introduced by Irwin H. Rosenberg in 1989 and originally refers to the loss of muscle mass associated with ageing: from the Greek *sarx* (flesh) and *penia* (loss) (Rosenberg, 1997). Sarcopenia is an intrinsic component of the ageing process but it can be further accelerated by several factors including inflammation, physical inactivity, malnutrition and chronic diseases (Dennison *et al.*, 2017; Tieland *et al.*, 2018; Coletta & Phillips, 2023). A condition of sarcopenia impairs physical performance and the ability to carry out activities of daily living (Mitchell *et al.*, 2012; Hunter *et al.*, 2016; Tieland *et al.*, 2018), lowers individuals' quality of life and is associated with adverse outcomes, including increased risk of falls and fractures, chronic diseases, cognitive impairment and mortality (Cruz-Jentoft *et al.*, 2019). Besides this enormous health cost, sarcopenia also represents a heavy burden on the healthcare system (Norman & Otten, 2019). In 2016, sarcopenia was officially recognised as a disease receiving an International Classification of Diseases, Tenth Revision, Clinical Modification (ICD-10-CM) code (Anker *et al.*, 2016). This represented an important step similar to the much earlier recognition of osteoporosis as a disease. Consequently, sarcopenia is no longer solely of interest to scientists, but there is increasing interest in the diagnosis and treatment of this condition in clinical practice (Coletta & Phillips, 2023). Recently, some authors proposed that there is a lack of evidence to support essential diagnostic aspects of sarcopenia and that its inclusion in the international classification of diseases could lead to overdiagnosis (Haase *et al.*, 2022). However, it should be considered that sarcopenia is associated with a greater risk of falls and fractures (Cruz-Jentoft *et al.*, 2019), greater length of hospital stay and postoperative complications (Norman & Otten, 2019), polypharmacy (Prokopidis *et al.*, 2023) and that prescription of resistance training for sarcopenic individuals requires specific attention (Coelho-Júnior *et al.*, 2022). Thus, diagnosing sarcopenia seems an essential step for the recognition of this condition and the investigation of adequate countermeasures.

1.2.2.a.i. Operational definitions of sarcopenia

From the original genesis of the term sarcopenia (Rosenberg, 1997), several operational definitions have been proposed by different international working groups (Figure 12). After some cross-sectional studies that based their definitions exclusively on low appendicular lean mass (ALM)/height^2 determined by dual-energy X-ray absorptiometry (DEXA) (Baumgartner *et al.*, 1998; Delmonico *et al.*, 2007), the first attempt toward a consensus was made by a Special Interest Group within the European Society for Clinical Nutrition and Metabolism (ESPEN) (Muscaritoli *et al.*, 2010). Sarcopenia was defined as the loss of muscle mass and strength associated with ageing and the diagnostic criteria proposed were the combined presence of (i) low muscle mass, i.e. reductions ≥2 standard deviations below the mean measured in young adults of the same sex and ethnicity; and (ii) low gait speed, i.e. walking speed <0.8 m/s (Muscaritoli *et al.*, 2010). The European Working Group on Sarcopenia in Older People (EWGSOP) introduced another algorithm for sarcopenia diagnosis, recommending a combination of low muscle mass and either low muscle function or poor physical performance (Cruz-Jentoft *et al.*, 2010). Differently from the ESPEN Special Interest Group, they also provided possible diagnostic thresholds and described tools for muscle mass assessment (Cruz-Jentoft *et al.*, 2010). In 2011, two new operational definitions were proposed by the International Working Group on Sarcopenia (IWGS) (Fielding *et al.*, 2011) and the Society for Sarcopenia, Cachexia, and Wasting Disorders (SCWD) (Morley *et al.*, 2011). For both working groups, a sarcopenic individual was defined as a person with muscle loss and low gait speed (≤1.0 m/s). For the SCWD a 6 minutes walking test could be used as an alternative to low gait speed to evaluate limited mobility and 400 meters were set as the cut-off (Morley *et al.*, 2011). The Foundation for the National Institutes of Health (FNIH), as most of the previous definitions, proposed to evaluate muscle strength by handgrip dynamometry, but proposed the novelty to normalise ALM to body mass index (Studenski *et al.*, 2014). The Asian Working Group for Sarcopenia (AWGS) (Chen *et al.*, 2014) agreed with the EWGSOP that sarcopenia should be described as low muscle mass plus low muscle strength and/or low physical performance and provided cut-offs relevant for Asian populations, which were later revised in 2019 (Chen *et al.*, 2020). In the same year, a revised consensus of the EWGSOP (EWGSOP2) was issued, giving greater emphasis on muscle strength assessment that comes to the forefront, with low muscle mass used only to confirm the sarcopenia diagnosis (Cruz-Jentoft *et al.*, 2019). Detection of low physical performance was used to identify the severity of sarcopenia. To evaluate muscle strength, besides handgrip assessment, the authors proposed to employ the chair-to-stand test (Cruz-Jentoft *et al.*, 2019). Finally, the EWGSOP2 was

the first working group to recommend using a self-report questionnaire, the SARC-F (Malmstrom *et al.*, 2016), for sarcopenia risk screening (see Paragraph 1.2.2.a.v. for further information). Although the EWGSOP2 is the most widely cited definition nowadays (Cruz-Jentoft & Sayer, 2019), several studies expressed concerns regarding this revised approach, reporting lower sarcopenia prevalence (i.e. increased risk of underdiagnosis) (e.g. Van Ancum *et al.*, 2020; Petermann-Rocha *et al.*, 2022) and worse predictive validity for unfavourable outcomes (e.g. Fernandes *et al.*, 2022). For this reason, a recent work proposed new modified thresholds for handgrip strength in the EWGSOP2 classification (Westbury *et al.*, 2023). The Sarcopenia Definitions and Outcomes Consortium (SDOC) was the first to not include measurements of muscle mass in the diagnosis of sarcopenia, which is instead determined solely by handgrip strength and gait speed (Bhasin *et al.*, 2020). Finally, in 2023, the Australian and New Zealand Society for Sarcopenia and Frailty Research (ANZSSFR) Task Force endorsed the EWGSOP2 definition in Australia and New Zealand (Zanker *et al.*, 2023). An African consensus on sarcopenia definition is still missing, despite the mounting interest from African researchers on sarcopenia and other ageing syndromes (Essomba *et al.*, 2020). Although considerable attention has been given to reaching a consensus worldwide (Sayer & Cruz-Jentoft, 2022; Barazzoni *et al.*, 2023), the operational definition of sarcopenia is still evolving and elusive, complicating the diagnosis/patient identification and prescription of preventive interventions for this disease (Coletta & Phillips, 2023), as well as the study of its predictive validity for adverse outcomes (Stuck *et al.*, 2022).

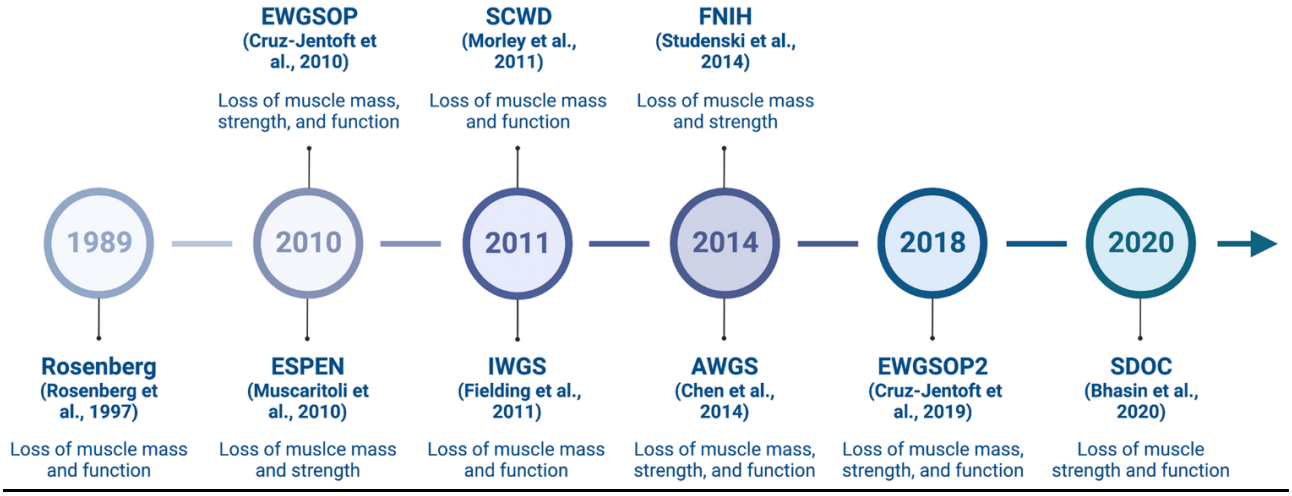

Figure 12: *Chronological timeline of the evolution of the definition of sarcopenia (Coletta & Phillips, 2023). ESPEN: European Society for Clinical Nutrition and Metabolism; EWGSOP: European Working Group on Sarcopenia in Older People; IWGS: International Working Group on Sarcopenia; SCWD: Society for Sarcopenia, Cachexia, and Wasting Disorders; AWGS: Asian Working Group for Sarcopenia; FNIH: Foundation for the National Institutes of Health; SDOC: Sarcopenia Definitions and Outcomes Consortium.*

1.2.2.a.ii. Epidemiology of sarcopenia

Due to its evolving definition, the study of sarcopenia prevalence is also challenging and dependent on the classification employed. Indeed, all the available systematic reviews and meta-analyses on the topic highlighted a large variability and poor agreement between different classifications (Shafiee *et al.*, 2017; Mayhew *et al.*, 2019; Papadopoulou *et al.*, 2020; Do Nascimento *et al.*, 2021; Petermann-Rocha *et al.*, 2022). Based on the most updated one (Petermann-Rocha *et al.*, 2022), the global prevalence of sarcopenia for individuals older than 60 years varies between 10% and 27%, with the prevalence of severe sarcopenia ranging from 2% to 9%. The prevalence for each classification considered is the following: EWGSOP: 22% (95% CI: 20–25%); EWGSOP2: 10% (2–17%); AWGS: 15% (13–27%); IWGS: 14% (9–18%) and FNIH: 11% (9–14%). These estimate rates increase when using bioelectrical impedance analysis for the evaluation of lean mass instead of DEXA, as was reported in previous meta-analyses (Shafiee *et al.*, 2017; Mayhew *et al.*, 2019; Do Nascimento *et al.*, 2021). Classifications using muscle mass as a single criterion (e.g. Baumgartner *et al.*, 1998) lead to the highest sarcopenia prevalence: 27% (23–31%). Despite a recent study showed that sarcopenia seems to have a common transcriptional profile across ethnicities (Migliavacca *et al.*, 2019), the prevalence of sarcopenia differs by country (Petermann-Rocha *et al.*, 2022) (Figure 13). The prevalence of sarcopenia is higher in men compared with women employing the EWGSOP2 (11% vs 2%) and muscle mass (35% vs 27%) classifications, but not using others (Petermann-Rocha *et al.*,

2022). Moreover, prevalence of sarcopenia increases steeply with age (Cruz-Jentoft *et al.*, 2014; Dennison *et al.*, 2017). Finally, the prevalence of sarcopenia is influenced by the studied population. For instance, a recent meta-analysis found a progressive increase in sarcopenia prevalence considering community, hospitalised and nursing home older adults (Papadopoulou *et al.*, 2020). Moreover, sarcopenia prevalence is generally higher in pathological conditions (defined as secondary sarcopenia), reaching 66% in patients with unresectable esophageal cancer (Yuan & Larsson, 2023).

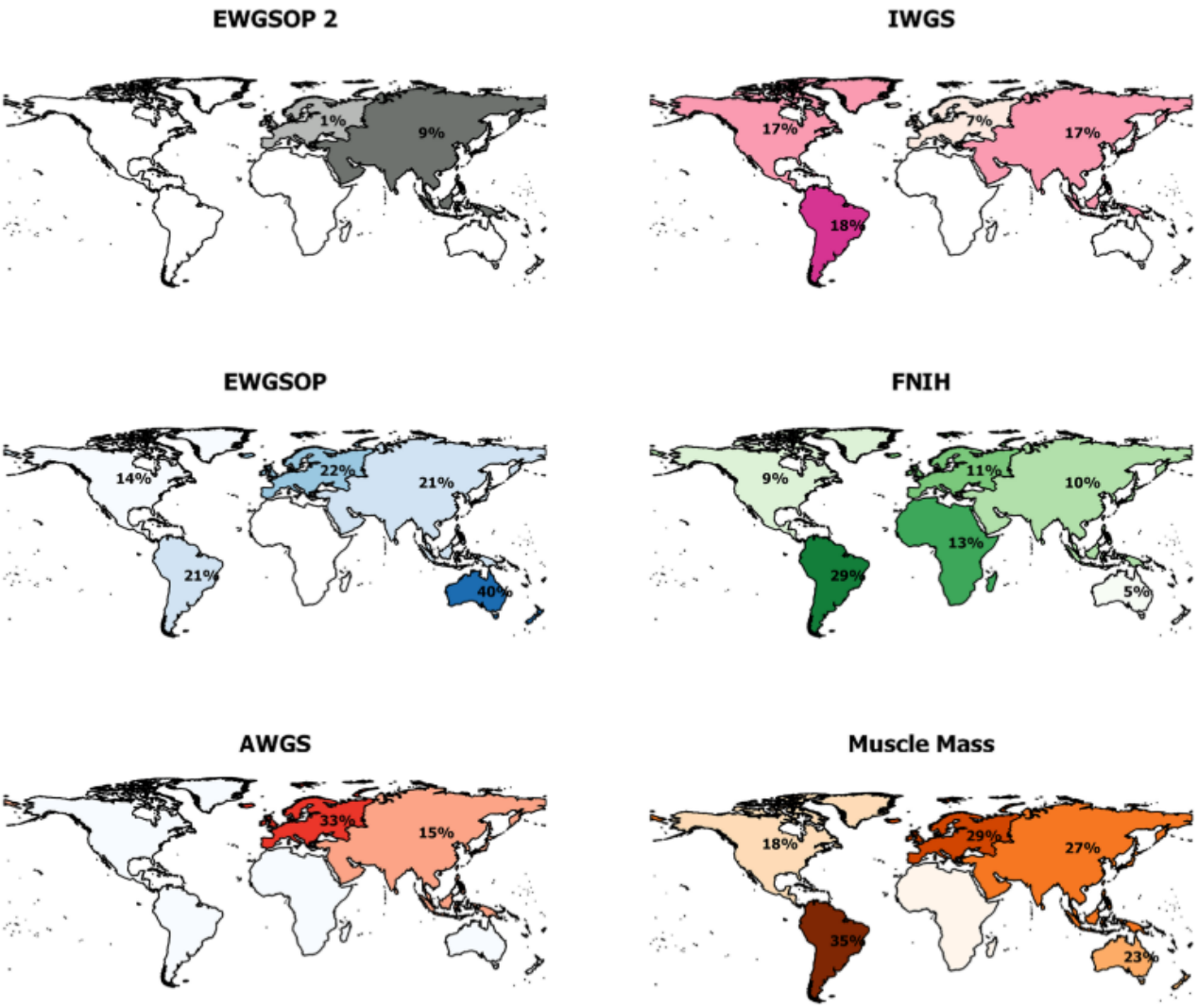

Figure 13: *The prevalence of sarcopenia categorized by classification and region (Petermann-Rocha et al., 2022). EWGSOP: European Working Group on Sarcopenia in Older People; IWGS: International Working Group on Sarcopenia; AWGS: Asian Working Group for Sarcopenia; FNIH: Foundation for the National Institutes of Health.*

Numerous intrinsic, lifestyle, pharmacological and psychosocial risk factors for sarcopenia are recognised in the literature (Dennison *et al.*, 2017; Tieland *et al.*, 2018; Yuan & Larsson, 2023).

Among internal risk factors, the presence of comorbidities and increased age are considered among the most impactful risk factors and have indeed a relevant impact on sarcopenia prevalence (see above). Although genetic architecture underlying a full-blown sarcopenia condition considering both muscle mass and strength remains largely unclear, genetic factors are overall recognised to play an important role (Pratt *et al.*, 2020*a*; Liu *et al.*, 2022). For instance, a seminal twin study showed that about 34–47% of the variation in physical performance in elderly Danish women could be attributed to genetic factors (Christensen *et al.*, 2000). Moreover, a large-scale study detected 15 susceptibility loci linked with low muscle strength in older adults (Jones *et al.*, 2021*b*); suggesting that muscle weakness is heritable to a certain extent. Interestingly, there is also evidence that small birth weight is associated with lower grip strength in older age (Dodds *et al.*, 2012), suggesting that sarcopenia might have its origins in early life (Cruz-Jentoft & Sayer, 2019).

Altered body composition may represent another risk factor for sarcopenia. After normalisation for measures of muscle mass, a higher body mass index is associated with an increased risk of sarcopenia, similarly to what observed for visceral fat area (Yuan & Larsson, 2023). Fat accumulation can lead to an increase in adipokines and inflammation that may adversely affect muscle quality (Dennison *et al.*, 2017).

Several lifestyle-associated factors contribute to sarcopenia. Physical inactivity and malnutrition are considered among the most important. Low number of daily steps (Iwasaka *et al.*, 2023), levels of moderate-vigorous physical activity (Mijnarends *et al.*, 2016; Sánchez-Sánchez *et al.*, 2019) and protein intake (Jyväkorpi *et al.*, 2020; Petermann-Rocha *et al.*, 2020) are indeed generally reported to be associated with an increased sarcopenia risk. In addition, some minerals have been shown to contribute to the maintenance of optimal muscle function and metabolism. In particular, low magnesium, selenium, calcium and phosphorus intake are associated with an increased prevalence of sarcopenia (van Dronkelaar *et al.*, 2018). Although vitamin D is important for skeletal muscle health (Tieland *et al.*, 2018; Dzik & Kaczor, 2019), whether its low intake represents a risk factor for sarcopenia remains controversial, with studies reporting associations (Visser *et al.*, 2003; Luo *et al.*, 2021) and other contrary results (Yu *et al.*, 2014; Tay *et al.*, 2015). Smoking as an isolated factor may contribute to the development of sarcopenia (Steffl *et al.*, 2015), potentially exacerbating NMJ degeneration and mitochondrial dysfunction (Thome *et al.*, 2022). Insufficient sleep quantity also seems to be associated with an increased sarcopenia risk (Pourmotabbed *et al.*, 2020; Li *et al.*, 2023). The condition of polypharmacy and increased number of medications in individuals with sarcopenia (Prokopidis *et al.*, 2023) is considered a risk factor for muscle wasting and reduced physical

performance in the context of sarcopenia, as reported for instance in the BASE-II study (König *et al.*, 2018). Indeed, some medications commonly used in older people such as beta blockers and non-steroidal anti-inflammatory drugs can disrupt electrolyte, hormonal, and acid-base homeostasis, while others such as statins, glucocorticoids and antidepressants may directly impair skeletal muscle health (König *et al.*, 2018; Prokopidis *et al.*, 2023). This polypharmacy condition can also have an impact on other risk factors, affecting body composition and leading to malnutrition and physical inactivity due to drug-induced nausea or diarrhoea and orthostatic hypotension, respectively (König *et al.*, 2018; Prokopidis *et al.*, 2023).

Finally, some psychosocial factors such as low socioeconomic status, self-efficacy, fear of falling and depression may, directly and indirectly, influence the age-related loss of muscle mass and strength, as reviewed elsewhere (Tieland *et al.*, 2018)

1.2.2.a.iii. Impact of different definitions on sarcopenia prevalence: an example from our cohort

Intrigued by the different sarcopenia definitions, I tested their impact on sarcopenia prevalence in our NeuAge cohort, consisting of 88 older adults aged >70 years old (see Chapter 5 for further information). I compared some of the official definitions of sarcopenia presented above and in addition, as EWGSOP (Cruz-Jentoft *et al.*, 2010, 2019) supports the use of cut-off based on regional normative populations and, in a research setting, the assessment of knee extensors isometric force, I added also two EWGSOP2 adaptations, based on handgrip and chair to stand cut-offs obtained from Italian population reference values (Landi *et al.*, 2020) ($EWGSOP2_{ITA}$) and on the database of maximum voluntary contractions of our laboratory ($EWGSOP2_{MVC}$), respectively. In both cases, ≥2 standard deviations from the young reference population were employed as a criterion to determine the cut-offs (Cruz-Jentoft *et al.*, 2019). Each participant was assigned to the corresponding group using a custom Python (v.3.9) script, developed together with my colleague Mr. Giacomo Valli. As presented in Table 1, the distribution of the participants largely varies among the different classes of sarcopenia depending on the classification employed. In particular, the number of individuals with sarcopenia ranges between 2 in the SDOC and FNIH classifications to 23 in the $EWGSOP2_{ITA}$.

Classification	NS	LMM	LMF	S
EWGSOP1	74	11	12	3
EWGSOP2	47	30	5	6
$EWGSOP2_{ITA}$	23	12	29	23
$EWGSOP2_{MVC}$	44	23	10	11
$EWGSOP\ 2_{WESTBURY}$	39	28	13	18
SDOC	62	/	24	2
$SDOC_{WESTBURY}$	62	/	12	14
IWGS	72	0	/	4
FNIH	54	31	1	2

Table 1: Distribution among different stages of sarcopenia in our NeuAge cohort (N=88) according to different sarcopenia definitions. NS: non-sarcopenic; LMM: low muscle mass; LMF: low muscle function; S: sarcopenic.

1.2.2.a.iv. Diagnosis

Irrespective of the definition, sarcopenia diagnosis is based on the measurements of a combination of muscle mass, muscle strength and physical performance.

Muscle mass

DEXA is the most commonly employed and recommended device for the evaluation of muscle mass in the context of sarcopenia. DEXA is a widely accessible tool that gives other important information for clinical practice (bone mineral density and fat mass) and regional cut-offs for ALM are available (Cruz-Jentoft *et al.*, 2019; Chen *et al.*, 2020). However, DEXA has the substantial drawback that does not measure muscle mass per se, but instead provides an assessment of lean mass that includes other non-relevant tissue components, such as connective tissue and water. It is also important to note that DEXA seems to underestimate the age-related loss of muscle mass, in comparison to the gold standard magnetic resonance imaging. Thus, DEXA may lead to an under-representation of the stage of muscle wasting in older individuals (Fuchs *et al.*, 2023). The use of bioelectrical impedance analysis as a cheap and portable alternative to DEXA is supported by some of the official sarcopenia guidelines (Cruz-Jentoft *et al.*, 2019; Chen *et al.*, 2020), despite it can provide only an estimation of lean mass based on whole-body electrical conductivity and it is well known to be less accurate than DEXA (Dent *et al.*, 2018).

Magnetic resonance imaging and computed tomography scans are considered the gold standard for muscle mass assessment (Mitsiopoulos *et al.*, 1998). Both techniques have the advantage of enabling the evaluation of the size of single muscles, although it could be argued which muscle(s) should be considered in the context of sarcopenia evaluation, as age-related muscle atrophy is muscle group-specific (Naruse *et al.*, 2023). However, the use of these devices in the context of sarcopenia is limited due to costs, limited availability in research and primary care settings and the requirement of highly specialized personnel for both scan acquisition and analysis (Coletta & Phillips, 2023). Moreover, a substantial and under-recognised issue is the absence of large datasets of population reference values (Perkisas *et al.*, 2018) that limit the application of these techniques to obtain cut-offs relevant to define a "low muscle mass" condition in sarcopenia diagnosis.

Ultrasound is another promising tool for assessing sarcopenia, given its affordability, reliability, validity, and good agreement with DEXA, magnetic resonance imaging and computed tomography (Ticinesi *et al.*, 2017; Perkisas *et al.*, 2018). However, the specific training needed, its operator-dependent nature (Sarto *et al.*, 2021*b*) and potential differences in the extended-field-of-view algorithms across devices represent drawbacks of this technique that complicate its implementation in a clinical setting.

Finally, there is increasing research interest in deuterium (D)-labelled creatine (D_3-creatine) assessment for the estimation of muscle mass in sarcopenia diagnosis (Coletta & Phillips, 2023). This technique is based on the concept that creatine is almost exclusively stored within skeletal muscle (∼95%) and excess circulating creatine is converted to creatinine and excreted in the urine. However, further refinement is needed to make this methodology of practical use (Cruz-Jentoft *et al.*, 2019).

Muscle strength

Handgrip is the most widely used tool for the assessment of muscle strength. It is inexpensive, has minimal risk, is simple to perform for patients and is a good predictor of poor health outcomes (Cruz-Jentoft *et al.*, 2019). Handgrip is the preferred choice of all the available sarcopenia guidelines and standardised procedures are available in the literature (Roberts *et al.*, 2011). However, it may be argued that handgrip strength cannot be assumed as a proxy for overall muscle strength (Yeung *et al.*, 2018) and that lower limb muscles undergo more pronounced age-related changes compared to upper limbs muscles and have a stronger impact on mobility and fall-related injuries (Larsson *et al.*, 2019). To overcome this issue, the assessment of knee extensors strength by isometric

dynamometry could represent a reliable solution, although at the moment EWGSOP2 supports its application only for special cases (e.g. hand disability) and for research studies (Cruz-Jentoft *et al.*, 2019). The EWGSOP2 proposed to use the five times chair-to-stand measure of strength (Cruz-Jentoft *et al.*, 2019). However, this test should be considered a physical performance measure rather than a measure of muscle function (Alcazar *et al.*, 2022). Moreover, the cut-off proposed by EWGSOP2 (>15 s) (Cruz-Jentoft *et al.*, 2019) is not based on their recommendation of setting cut-off points at ≥2 standard deviations from the young reference population.

Physical performance

Physical performance evaluation is generally proposed to evaluate the severity of sarcopenia and/or in alternative or combination of muscle strength assessment (Cruz-Jentoft *et al.*, 2019; Bhasin *et al.*, 2020; Chen *et al.*, 2020). Gait speed over 4 or 8 meters is the most commonly employed test, with cut-off values set at ≤0.8 (Muscaritoli *et al.*, 2010; Cruz-Jentoft *et al.*, 2019; Bhasin *et al.*, 2020) or ≤1 m/s (Fielding *et al.*, 2011; Morley *et al.*, 2011; Chen *et al.*, 2020; Westbury *et al.*, 2023). The Short Physical Performance Battery (SPPB), the time-up and go and the 400-meter walking test represent other alternatives supported by EWGSOP2 (Cruz-Jentoft *et al.*, 2019).

1.2.2.a.v. Screening, prevention and management

A case-finding approach for sarcopenia is recommended in clinical practice, as most cases of sarcopenia go undiagnosed. The SARC-F (Malmstrom *et al.*, 2016) is the most commonly recommended screening tool, supported by both EWGSOP2 (Cruz-Jentoft *et al.*, 2019) and AWGS2 (Chen *et al.*, 2020). The SARC-F consists of a questionnaire assessing five components: patient perception of his/her limitations in strength, walking, rising from a chair, climbing stairs and fall history (Malmstrom *et al.*, 2016). Each component receives a score from 0 (no limitation) to 2 (maximum limitation), with scores ≥4 used to proceed with further assessment for sarcopenia diagnosis. Calf circumference is also another simple and recommended case-finding method (Chen *et al.*, 2020). The combination of SARC-F and calf circumference is called SARC-CalF and has shown improved sensitivity compared to SARC-F alone (Barbosa-Silva *et al.*, 2016).

The preventive and management strategies for sarcopenia to date consist essentially in modifying the recognised risk factors (see Paragraph 1.2.2.a.ii. in advanced age (Cruz-Jentoft & Sayer, 2019). These include mainly recommendations for increasing physical activity levels, in particular strength training practice, and daily protein intake (Dent *et al.*, 2018, 2021; Shen *et al.*, 2023).

1.2.2.b. Age-related MU remodelling

Sarcopenia has a complex and multifactorial aetiology and its pathophysiological mechanisms are far from being entirely elucidated. However, mounting evidence suggests that motoneuron and NMJ degeneration, muscle fibre denervation and loss of MUs may play a pivotal role in muscle wasting and weakness in old age (Tintignac *et al.*, 2015; Piasecki *et al.*, 2016*b*; Rudolf *et al.*, 2016; Rygiel *et al.*, 2016; Hepple & Rice, 2016; Hunter *et al.*, 2016; Willadt *et al.*, 2018; Taetzsch *et al.*, 2019; Larsson *et al.*, 2019; Pratt *et al.*, 2020*b*; Badawi & Nishimune, 2020; Allen *et al.*, 2021; Soendenbroe *et al.*, 2021; Delbono *et al.*, 2021; Moreira-Pais *et al.*, 2022; Deschenes *et al.*, 2022; Jones *et al.*, 2022; Arnold & Clark, 2023; Clark, 2023). In the following paragraphs, the impact of ageing on the different components of the neuromuscular system is discussed. However, some considerations should be made. First, there is a substantial paucity of human studies investigating these aspects that diagnosed sarcopenia using official guidelines. Moreover, the evolving and elusive definition of sarcopenia makes the comparison between these few studies very challenging. Similarly, although several animal models of sarcopenia have been developed (Christian & Benian, 2020), at present, there are no diagnostic criteria for the determination of sarcopenia in animal models (Xie *et al.*, 2021). In addition, employing some of these models sarcopenia advancement may differ from the natural progression observed in humans (Xie *et al.*, 2021). Hence, most of the evidence that will be presented here is essentially based on the comparison between young and old individuals or young and old animals, without a determination of a diagnosed sarcopenia status. When available, evidence of differences between sarcopenic and non-sarcopenic older adults will be discussed.

1.2.2.b.i. Age-related effects on the motoneuron

During ageing, our neuromuscular system undergoes a chronic remodelling, consisting of cycles of motoneuron loss and muscle fibre reinnervation via collateral sprouting (Hepple & Rice, 2016) (Figure 14). In support of this view, there is evidence of age-related declines in myelinated neurons in peripheral nerves and ventral roots across different species (Larsson *et al.*, 2019). Moreover, the direct count of the motoneuron cell bodies in the lumbosacral cord shows a progressive decline from the age of 60, with losses of ∼30% from specimens aged around 75 (Kawamura *et al.*, 1977; Tomlinson & Irving, 1977). Findings from in vivo electrophysiological studies using the MU number estimate method support these anatomical observations in humans (Piasecki *et al.*, 2016*b*). Age-related structural alterations of the motoneuron have been reported, including Wallerian

degeneration, myelin sheet abnormalities, myelin ovoids, infolded loops of myelin, macrophages overloaded with myelin debris, and myelin reduplication (Larsson *et al.*, 2019). These structural changes have a profound impact on the motoneuron functional capacity leading to a decreased rate of axonal transport, speed of nerve regeneration and axonal conduction velocity (Larsson *et al.*, 2019). The largest and fastest conducting neurons appear to be more vulnerable, particularly in their distal region (the NMJ presynaptic component). Evidence obtained from human electromyographical studies highlights declines in motoneuron firing rates of older adults in different muscle groups, especially at higher contraction intensities (Orssatto *et al.*, 2022). Apart from motoneuron structural changes, reduced firing rate can be due to changes in neuromodulation on motoneuron excitability, as suggested by recent evidence showing decreases in estimates of persistent inward currents with ageing (Hassan *et al.*, 2021; Orssatto *et al.*, 2021).

The drivers of progressive motoneuron damage and death during ageing are complex and multifactorial. At a molecular level, recent evidence showed that low-grade inflammation, apoptosis, changes in extracellular matrix components and aberrant microglia activation are predominant mechanisms occurring in the aged spinal cord in mice (Piekarz *et al.*, 2020; Castro *et al.*, 2023). Moreover, leveraging single-nucleus RNAseq analysis, upregulation of neurodegeneration-associated genes was observed in human motoneurons of seven adult and old donors (50–80 years old) when compared to a dataset of human embryonic spinal cord (Yadav *et al.*, 2023). Recent evidence also suggests that loss of excitatory synapses may be responsible for the compromised function of aged motoneurons in animals and humans (Castro *et al.*, 2023). DNA damage and modifications accumulating throughout life are considered other important contributing factors, possibly deriving from mitochondrial dysfunction (Alway *et al.*, 2017). Reactive oxygen species accumulation and posttranslational modifications such as nonenzymatic glycation are also likely to be involved (Larsson *et al.*, 2019). Finally, age-related impairment of microcirculation and vascular permeability of the spinal cord may contribute to motoneuron damage and loss (Larsson *et al.*, 2019; Piekarz *et al.*, 2020).

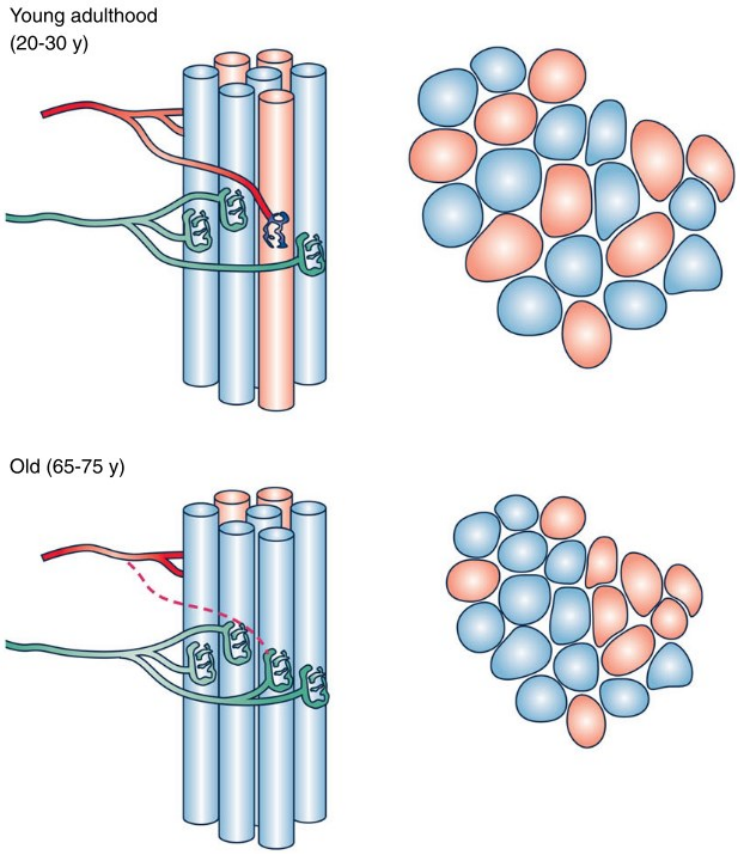

Figure 14: *Cycles of denervation and reinnervation in aged skeletal muscle, leading to fibre type grouping. Adapted from (Hepple & Rice, 2016).*

Motoneuron and human sarcopenia

Evidence of motoneuron damage and loss in the specific context of diagnosed human sarcopenia is scant. In a well-conducted investigation in a large cohort of older adults, Pratt et al. assessed plasma levels of neurofilament light chain, a circulating biomarker of axonal damage (Pratt *et al.*, 2022). Sarcopenia was diagnosed according to EWGSOP2 with modified cut-off points relevant to the study population. Neurofilament light chain concentration was associated with grip strength and lean mass evaluated by DEXA and was elevated in sarcopenic individuals compared with non-sarcopenic participants (Pratt *et al.*, 2022). Although these findings are interesting and showed the pertinence of circulating neurofilament light chain levels as a biomarker of sarcopenia, it has to be considered that neurofilaments are expressed in all types of neurons, thus they are not specific for motoneurons and may also reflect a central nervous system impairment (Khalil *et al.*, 2018). To this extent, it is interesting to highlight that in our recent study, we did not observe decreases in this biomarker following a two-year exercise intervention in sarcopenic individuals according to the original EWGSOP guidelines (Monti *et al.*, 2023*b*). Using the electrophysiological MU number

estimate technique, fewer MUs in sarcopenic compared to non-sarcopenic individuals in the vastus lateralis but not tibialis anterior were observed (Piasecki *et al.*, 2018*b*). While MU potential area was significantly elevated in non-sarcopenic and pre-sarcopenic individuals compared to young controls, no such difference was observed in sarcopenic subjects. This finding was suggested to reflect a failure to expand MU size in response to a decline in MU number in sarcopenic individuals (Piasecki *et al.*, 2018*b*). However, this study was conducted only in male individuals and used a sarcopenia definition exclusively based on low muscle mass, evaluated by magnetic resonance imaging. Thus, the generalisability of these findings should be interpreted with caution. In contrast, another investigation did not observe changes in estimated MU numbers across different stages of sarcopenia (pre-sarcopenia vs sarcopenia vs severe sarcopenia, according to EWGSOP) (Gilmore *et al.*, 2017), although the small sample size of this work should be considered.

1.2.2.b.ii. Age-related effects on the NMJ

Morphological adaptations

There is consistent evidence that ageing is associated with NMJ remodelling. At the presynaptic level, the number, length and complexity of nerve terminal branches are remarkably increased in old rodents (Pratt *et al.*, 2020*b*; Deschenes *et al.*, 2022). This adaptive response has been considered an attempt to enhance the communication between the pre and postsynaptic components of the NMJ (Gonzalez-Freire *et al.*, 2014) and was also confirmed in humans by pioneering studies conducted with autopsy samples (Arizono *et al.*, 1984; Oda, 1984) and biopsy obtained from the external intercostal muscle of patients during thoracotomy (Wokke *et al.*, 1990). However, this evidence has been challenged by a recent study, showing that NMJ morphology was stable throughout the lifespan in samples obtained from amputated lower limbs, despite increases in axon diameter and nerve terminal area (Jones *et al.*, 2017). The expansion of the nerve terminal network is accompanied by a decrease in the total number of ACh vesicles and reduced expression of active zones (Pratt *et al.*, 2020*b*; Deschenes *et al.*, 2022) with specific degradation of some of their key components such as Bassoon, Piccolo, and voltage-gated calcium channels (Nishimune *et al.*, 2014). A possible explanation for the active zone alterations is the impaired axonal transport observed during ageing (see Paragraph 1.2.2.b.i.). Considerable age-related remodelling is also observable at the NMJ postsynaptic component. Endplate size is generally increased during ageing and accompanied by a degeneration of the complex network of junctional folds (Pratt *et al.*, 2020*b*) and greater dispersion of ACh receptors (Deschenes *et al.*, 2022), a phenomenon called “endplate

fragmentation". Whether this NMJ fragmentation represents a sign of degeneration or regeneration (i.e. a compensatory mechanism) is still debated in the scientific community (Slater, 2020*a*). The Agrin-Lrp4-MuSK-Dok7 pathway is considered one of the predominant molecular mechanisms regulating these processes (Tintignac *et al.*, 2015; Larsson *et al.*, 2019; Moreira-Pais *et al.*, 2022). For instance, knockout of MuSK (Hesser *et al.*, 2006) and overexpression of neurotrypsin leading to excessive agrin cleavage (Bütikofer *et al.*, 2011) resulted in NMJ fragmentation and a muscle phenotype typically observed in advanced age. Conversely, injection of neurotrypsin-resistant agrin rescues many facets of the sarcopenic phenotype (Hettwer *et al.*, 2014). Abnormalities of the mitochondria within the NMJ can also occur with ageing, further contributing to NMJ degeneration (Rygiel *et al.*, 2016; Anagnostou & Hepple, 2020). Indeed, presynaptic mitochondria have been reported to be swollen, larger, virtually devoid of cristae, and with ruptured membranes in old rats (Garcia *et al.*, 2013). Perisynaptic Schwann cells also undergo age-related deterioration. It is estimated that 80% of aged NMJ are no longer wrapped by perisynaptic Schwann cells (Deschenes *et al.*, 2022). Those still visible at NMJ are unusually thin and exhibit disorganised branching invading the synaptic cleft (Pratt *et al.*, 2020*b*). Since kranocytes, fibroblast-like cells covering the perisynaptic Schwann cells and the endplate, are early responders following denervation, it has been speculated their alterations could play a role in NMJ degeneration in the context of ageing and sarcopenia (Pratt *et al.*, 2020*b*).

Functional alterations

Besides morphological remodelling, ageing also triggers adaptations to the NMJ physiological function (Arnold & Clark, 2023). Briefly, the general view is that ageing leads to a greater amount of ACh released with a single impulse (quantal content) and of ACh stored in a single vesicle (quantal size) (Willadt *et al.*, 2018; Deschenes *et al.*, 2022). While upon initial consideration, such age-related increase in quantal content and size may appear to substantiate the NMJ safety factor and enhance cholinergic transmission, however, it is important to recall the concurrent age-induced reduction in ACh vesicles and receptors availability. Indeed, although increased quantities of ACh may be released in old age, the marked deterioration in ACh vesicles and ACh receptors availability during ageing, coupled with the aforementioned decline in neuromuscular transmission stamina is likely to provoke a decline in safety factor nonetheless. Moreover, it has to be considered that this evaluation reflects the presynaptic NMJ function only and postsynaptic mechanism for NMJ transmission failure could still occur (Arnold & Clark, 2023). In support of this view, it has been

shown that post-synaptic calcium signalling regulates presynaptic ACh release in a feedback control system (Ouanounou *et al.*, 2016). Thus, it has been postulated that the enhanced endplate response that has been noted in these isolated synaptic recording studies in aged rodents may represent a presynaptic compensation in response to NMJ failure to trigger action potentials identified by these channels at postsynaptic level (Arnold & Clark, 2023).

Apart from these experiments based on neurotransmitter handling, the impact of ageing on NMJ function has been evaluated electrophysiological by single-fibre electromyography (Sanders *et al.*, 2019). The two most commonly evaluated parameters to assess NMJ transmission using this technique are jiggle and jitter, reflecting the shape variability (Stålberg & Sonoo, 1994) and temporal variability (Piasecki *et al.*, 2021) in consecutive MU action potentials. In particular, jitter assessment is particularly employed in clinical settings and is considered a proxy for the NMJ safety factor (Juel, 2012). Jiggle values were found to be increased in the tibialis anterior and vastus lateralis in older men compared with young controls (Hourigan *et al.*, 2015; Piasecki *et al.*, 2016*c*). Similarly, databases of human jitter values in different muscle groups show progressive increases with ageing (Gilchrist, 1992). These human observations have been also confirmed in rats (Chung *et al.*, 2018; Chugh *et al.*, 2020; Padilla *et al.*, 2021). Significant correlations between NMJ transmission and muscle strength and mass were also reported (Padilla *et al.*, 2021), highlighting that NMJ dysfunction may represent a potential mechanism for age-related muscle loss and weakness.

Some specific NMJ structures are functionally impaired, contributing to the overall NMJ transmission impairment. For instance, the regulatory ability of perisynaptic Schwann cells is also significantly decreased, with a particular impact on the structural integrity of the postsynaptic region (Pratt *et al.*, 2020*b*). In addition, the postsynaptic voltage-gated sodium channels show slower activation and inactivation kinetics (Davis *et al.*, 2022).

Whether these NMJ functional alterations are linked to changes in NMJ structure is still unclear (Willadt *et al.*, 2018; Slater, 2020*a*). For instance, in one of the few studies that tried to directly compare NMJ morphology, evaluated through the number of ACh receptors fragments, and features of NMJ transmission, no correlation was found in mice (Willadt *et al.*, 2016). This aspect should be further investigated in future studies.

NMJ and human sarcopenia

Data regarding NMJ alterations with human sarcopenia are limited. Different studies reported increased concentration of circulating CAF in sarcopenic individuals compared to age-matched non-

sarcopenic controls, as reviewed elsewhere (Monti *et al.*, 2023*a*). Agrin is a proteoglycan involved in the stabilisation of the synaptic structure, which is cleaved by neurotrypsin, releasing the soluble CAF into circulation (Bütikofer *et al.*, 2011). Thus, higher circulating concentrations of CAF observed in sarcopenic individuals are indicative of increased NMJ instability (Monti *et al.*, 2023*a*). In contrast with this view, a recent transcriptomic investigation conducted in three cohorts of different ethnicities observed no changes in pathways involved in NMJ regulation and processes of denervation in vastus lateralis muscle biopsies of sarcopenic individuals compared to controls (Migliavacca *et al.*, 2019). The only studies investigating NMJ transmission reported increased near fibre jiggle and jitter in individuals with severe sarcopenia compared to pre-sarcopenic (Gilmore *et al.*, 2017). In any case, it is still not understood whether NMJ changes should be considered the cause or the consequence of human sarcopenia (Tintignac *et al.*, 2015).

1.2.2.b.iii Age-related effects on skeletal muscle fibres

The age-related loss of motoneurons is paralleled by muscle fibre loss (Lexell *et al.*, 1988). Ageing is also associated with a fast-to-slow fibre-type shift (Schiaffino & Reggiani, 2011) and increased frequency of hybrid fibre types (Delbono *et al.*, 2021), accompanied by fibre type grouping due to collateral reinnervation (Hepple & Rice, 2016; Larsson *et al.*, 2019). Marked skeletal muscle fibre atrophy during ageing is evident in type II fibres, while type I fibres are generally well-preserved (Narici & Maffulli, 2010; Grosicki *et al.*, 2022). In the only study comparing non-sarcopenic and sarcopenic individuals diagnosed with EWGSOP guidelines, the latter group exhibited ∼15% smaller fibres, although this trend was not significant, likely due to the low number of sarcopenic included (N=5) (Patel *et al.*, 2015). When considering single fibre mechanical properties, age-related decrements in contractile function (primarily absolute force and power) were reported in type II but not I fibres (Grosicki *et al.*, 2022). Although mechanisms underlying the higher susceptibility of type II fibres with ageing are still largely unknown, recent findings obtained from single fibre proteomics revealed enhanced glycolytic pathway and protein turnover in aged type I fibre (Murgia *et al.*, 2017). Evidence of denervation is recognisable also at myofibre level and can be identified by the expression of several markers, including NCAM, developmental myosins, nestin, sodium channel Nav 1.5 and the presence of small, angulated fibres (Soendenbroe *et al.*, 2021).

2. AIM OF THE PHD PROJECT & STUDIES INCLUDED

Despite the above-presented literature, the neuromuscular alterations induced by muscle disuse and sarcopenia are still far from being fully understood, particularly in humans. My PhD project aimed to gain a deeper understanding of these alterations, with a particular focus on NMJ and MU potential properties. I adopted an integrative physiological approach, encompassing in vivo imaging techniques, muscle function testing, state-of-the-art intramuscular electromyographic recording and molecular analysis from muscle and blood samples. This comprehensive approach enabled me to interrogate the mechanisms underlying the neuromuscular maladaptations triggered by disuse and sarcopenia. The thesis is based on two original research articles and one review article.

My first PhD study was published in the Journal of Physiology in 2022 (*Sarto F, Stashuk DW, Franchi M V et al. Effects of short-term unloading and active recovery on human motor unit properties, neuromuscular junction transmission and transcriptomic profile. J Physiol. 2022. doi:10.1113/JP283381*; (Sarto *et al.*, 2022*b*)). We performed a longitudinal investigation, part of a bigger project aiming to detect early biomarkers of neuromuscular degeneration after short-term unloading. As explained in Chapter 1.2.1., very little is known about NMJ alterations in human models of disuse. Similarly, disuse-induced changes in MU properties were investigated previously in humans only in small hand muscles (Duchateau & Hainaut, 1990; Seki *et al.*, 2007). In this study, we performed 10-day ULLS, to investigate the electrophysiological and molecular alterations triggered by unloading. We also studied the recovery of these properties with 21-day retraining based on resistance exercises. Our findings indicated that human NMJs undergo molecular destabilisation without compromising their function following ULLS, showcasing the remarkable resilience of NMJ transmission stability. Disuse also induced changes in MU potential properties, likely due to alterations in skeletal muscle ion channel dynamics and early signs of axonal damage and myofibre denervation. Encouragingly, the active recovery intervention efficiently reinstated neuromuscular integrity and function to their original baseline levels.
I coordinated the organisation of the ULLS campaign from which this article stems. I was also co-author of two additional articles from the same research campaign, published in 2023 (Sirago *et al.*, 2023; Valli *et al.*, 2023). Other four articles are in preparation.

These works, together with previous involvement in the bed rest campaign MARSPRE2019 conducted in Izola (Slovenia) (Monti *et al.*, 2021; Sarto *et al.*, 2021*a*; Franchi *et al.*, 2022*a*), enhanced

my understanding of the morphological, functional, electrophysiological and molecular alterations in extreme human models of muscle disuse. However, periods of bed rest and immobilisation occur arguably less frequently than periods of reduced physical activity and models closer to real-life conditions are needed e to mimic the deleterious effects of a sedentary lifestyle. My interest was quickly piqued by this topic and an in-depth literature search led to **my second PhD article** (*Sarto F, Bottinelli R, Franchi M V et al. Pathophysiological mechanisms of reduced physical activity: insights from the human step reduction model and animal analogues. Acta Physiol. 2023;238(e13986). doi:10.1111/apha.13986;* (Sarto *et al.*, 2023)), a narrative review on step reduction, a model that consists of a decrease in participants' regular daily steps to a lower level. We explored analogous models of reduced physical activity in rodents, which can serve as a basis for human investigations. The existing evidence demonstrates that even short periods of reduced physical activity can result in significant changes in skeletal muscle health and metabolic function. Specifically, reductions in lean/muscle mass, muscle function, muscle protein synthesis, cardiorespiratory fitness, endothelial function, and insulin sensitivity have been observed, along with an increase in fat mass and inflammation. I dedicated particular effort to find novel angles for this review: a direct comparison of step reduction with human extreme models of disuse and a conceptual framework aiming to untangle the mechanisms underlying muscle atrophy and insulin resistance in the specific context of reduced ambulatory activity were indeed also provided. Moreover, we compared the step reduction findings with those of 'theoretical' epidemiological studies. Finally, the review also encompasses thoroughly methodological considerations, knowledge gaps and future directions for both animal and human models.

The current lack of step reduction studies focusing on the assessment of neuromuscular integrity and function prompts me to organise a step reduction investigation during the last few months of my PhD. Ten young volunteers (age: 21.4 (2.95) years; 6 females) took part in this study and were asked to reduce their daily steps to 1500 for 14 days. Physical activity levels and the number of daily steps were assessed at baseline for 7 days and during the intervention with an accelerometer and a step counter. Before and after the step reduction period, we collected knee extensors ultrasound scans, simultaneous intramuscular and high-density electromyography recordings from the vastus lateralis, blood samples and muscle biopsies. Data analysis for this project is currently ongoing.

My third PhD study (*Sarto F, Franchi M V, McPhee J et al. Motor units properties impairment, axonal damage, innervation profile alterations and neuromuscular junction instability with different stages*

of sarcopenia; in submission) was a cross-sectional investigation conducted in a large cohort of young and older adults. Considering the paucity of data on the mechanisms driving primary human sarcopenia, this study aimed to comprehensively investigate the neuromuscular alterations with this condition. Older individuals were grouped into non-sarcopenic, pre-sarcopenic and sarcopenic, according to the revised guidelines of the European Working Group on Sarcopenia in Older People (EWGSOP2). We fully characterised their muscle functional and morphological impairment and, as expected, sarcopenic individuals showed an exacerbated profile compared to non-sarcopenic and pre-sarcopenic participants. However, upon investigation of several electrophysiological and molecular biomarkers of MU and NMJ degeneration, sarcopenic individuals did not overall exhibit a more profound impairment. Thus, these findings raise the question of whether the conventional perspective, which considers alterations in MUs and NMJs among the prime culprits of sarcopenia, could potentially gain from further exploration. Moreover, the observed neuromuscular alterations seem to originate before the diagnosis of sarcopenia, highlighting the importance of early prevention.

These three articles are entirely reported in the next chapters. In addition to the studies included in the thesis, during my PhD I made contributions to several other published original, review and commentary articles in the field of neuromuscular physiology. The following is a brief mention of these studies:

1. **Sarto F**, Valli G, Monti E. Motor units alterations with muscle disuse: what is new? J Physiol. 2022. 600(22):4811-4813. DOI: 10.1113/JP283868

Scientific significance: In this journal club commentary article (Sarto *et al.*, 2022*c*), we briefly summarised the new findings in the field of MUs alterations with muscle disuse. Particular focus was given to a recent investigation (Inns *et al.*, 2022), that similarly to my second PhD study (Sarto *et al.*, 2022*b*), found some changes in MU potential properties analysed by intramuscular electromyography in response to 15 days of unilateral lower limb immobilisation.

Role in this research: I conceived the idea for the article and drafted the manuscript.

2. **Sarto F**, Spörri J, Fitze DP, Quinlan JI, Narici M V, Franchi M V. Implementing Ultrasound Imaging for the Assessment of Muscle and Tendon Properties in Elite Sports: Practical Aspects,

Methodological Considerations and Future Directions. *Sport Med*. 2021;51(6):1151–1170. https://doi.org/10.1007/s40279-021-01436-7

Scientific significance: In this narrative review (Sarto *et al.*, 2021*b*), we (i) presented the main ultrasound measures and field of applications in the context of elite sports; (ii)) discussed, from a methodological perspective, the strengths and shortcomings of ultrasound imaging for the assessment of muscle and tendon properties; and (iii) provided future directions for research and application.

Role in this research: I performed the literature search and drafted the manuscript.

3. **Sarto F**, Monti E, Simunič B, Pišot R, Narici M V., Franchi M V. Changes in Biceps Femoris Long Head Fascicle Length after 10-day Bed Rest Assessed with Different Ultrasound Methods. *Med Sci Sport Exerc*. 2021;(9):1–9. DOI: 10.1249/MSS.0000000000002614

Scientific significance: In this study (Sarto *et al.*, 2021*a*), we aimed to investigate whether the methodological limitations of biceps femoris long head fascicle length extrapolation, observed in some previous cross-sectional studies, may also affect the assessment of fascicle length changes in a longitudinal study design. Thus, in a short-term disuse scenario, we showed that different ultrasound methods lead to different results in the assessment of biceps femoris long head fascicle length changes. We recommend the implementation of panoramic scans or the use of the manual linear extrapolation method.

Role in this research: I assisted in the data collection, performed the data analysis and drafted the paper.

4. **Sarto F**, Pizzichemi M, Chiossi F, Bisiacchi P, Franchi M V, Narici M V, Monti E, Paoli A, Marcolin G. Physical active lifestyle promotes static and dynamic balance performance in young and older adults. Front Physiology. 2022. 13:986881. DOI 10.3389/fphys.2022.986881

Scientific significance: In this cross-sectional study (Sarto *et al.*, 2022*a*), we compared static and dynamic balance among sedentary and active young and older participants. We observed that the active older and sedentary young individuals presented similar balance, while the sedentary older adults exhibited poorer performance on both static and dynamic balance tasks than all other groups. Hence, we concluded that a physically active lifestyle promotes balance preservation.

Role in this research: I performed the data collection and data analysis and drafted the manuscript.

5. Valli G, **Sarto F**, Casolo A, Del Vecchio A, Franchi M V, Narici M V, De Vito G. Lower limb suspension induces threshold-specific alterations of motor units properties that are reversed by active recovery. J Sport Heal Sci. 2023. S2095-2546(23)00059-5. DOI: 10.1016/j.jshs.2023.06.004

Scientific significance: In this longitudinal study from our ULLS campaign (Valli *et al.*, 2023), we exploited high-density electromyography to noninvasively study changes in neural control following a period of muscle disuse. Our findings showed ULLS altered the firing rate of lower- but not of higher- threshold MUs, suggesting a preferential impact of disuse on motoneurons with a lower depolarisation threshold. The 21-day retraining based on resistance exercise was effective in restoring these alterations.

Role in this research: I was responsible for recruiting the participants, planning the experiments and calendar, assisting in data collection and contributing to manuscript revision.

6. Monti E, **Sarto F**, Sartori R, Zanchettin G, Löfler S, Kern H, Narici M V, Zampieri S. C-terminal agrin fragment as a biomarker of muscle wasting and weakness: a narrative review. J Cachexia Sarcopenia Muscle. 2023. 14(2):730-744. DOI: 10.1002/jcsm.13189

Scientific significance: This narrative review (Monti *et al.*, 2023*a*) summarised and critically discussed the studies measuring CAF concentration in young and both healthy and diseased older individuals, cross-sectionally and in response to inactivity and physical exercise. We also provided possible explanations behind the discrepancies observed in the literature, thoroughly examining several methodological aspects.

Role in this research: I designed the figures and assisted in the literature search and manuscript revision.

7. Franchi M V*.,* **Sarto F**, Simunič B, Pišot R, Narici M V. Early Changes of Hamstrings Morphology and Contractile Properties During 10 Days of Complete Inactivity. Med Sci Sport Exerc. 2022; 54(8):1346–1354. DOI: 10.1249/MSS.0000000000002922

Scientific significance: With this study (Franchi *et al.*, 2022*a*), we investigated hamstrings morphological and contractile properties changes following a 10-day bed rest intervention. Despite being a nonpostural muscle group, hamstrings exhibited moderate muscle atrophy, accompanied by alterations in biceps femoris long head architecture and impairment in contractile properties assessed by tensiomyography.

Role in this research: I assisted in the data collection, performed the data analysis and drafted the paper.

8. Franchi M V, Badiali F, **Sarto F**, Müller P**,** Müller N, Rehfeld K, Monti E, Hökelmann A, Narici M V. Neuromuscular Aging: A Case for the Neuroprotective Effects of Dancing. *Gerontology*. 2022. 69(1):73-81. DOI: 10.1159/000524843

Scientific significance: With this two-experiment study (Franchi *et al.*, 2022*b*), we reported that active elderly practicing dance presented a lower CAF serum concentration compared to their moderately active peers. We also showed that 6 months of either dance or general fitness training differentially influence CAF concentration. Indeed, the dance protocol reduced the concentration of this biomarker, while general fitness did not. We concluded that physical activities involving fine motricity and coordination such as dance better preserve the NMJ in ageing.

Role in this research: I performed the statistical analysis, designed the figures and drafted the manuscript.

9. Monti E, Tagliaferri S, Zampieri S, **Sarto F**, Sirago G, Franchi M V, Ticinesi A, Longobucco Y, Adorni E, Lauretani F, Von Haehling S, Marzetti E, Calvani A, Bernabei R, Cesari M, Maggio M, Narici M V. Effects of a 2-year exercise training on neuromuscular system health in older individuals with low muscle function. J Cachexia Sarcopenia Muscle. 2023. 14(2):794-804. DOI: 10.1002/jcsm.13173

Scientific significance: In this 2-year longitudinal study (Monti *et al.*, 2023*b*), we showed that a mixed aerobic, strength and balance training was effective for preventing the age-induced raises in CAF concentration and preserving muscle architecture (pennation angle and fascicle length) in sarcopenic older individuals.

Role in this research: I analysed the ultrasound images and revised the manuscript.

10. Ritsche P, Wirth P, Cronin N, **Sarto F**, Narici M V, Faude O, Franchi M V. DeepACSA: Automatic Segmentation of Cross-sectional Area in Ultrasound Images of Lower Limb Muscles Using Deep Learning. Med Sci Sport Exerc. 2022;54(12):2188-2195. DOI: 10.1249/MSS.0000000000003010

Scientific significance: In this study (Ritsche *et al.*, 2022), we introduced an open-source deep-learning approach to automatically analyse cross-sectional ultrasound images: DeepACSA. This tool provides a fast and objective segmentation, comparable with manual analysis.

Role in this research: I helped with the data collection of ultrasound images and revised the manuscript.

11. Sirago G, Candia J, Franchi M V, **Sarto F**, Monti E, Toniolo L, Reggiani C, Giacomello E, Zampieri S, Hartnell L M, De Vito G, Sandri M, Ferrucci L, Narici M V. Upregulation of Sarcolemmal Hemichannels and Inflammatory Transcripts with Neuromuscular Junction Instability during Lower Limb Unloading in Humans. Biology (Basel). 2023;12:431. https://doi.org/10.3390/biology12030431
Scientific significance: In this ULLS longitudinal investigation (Sirago *et al.*, 2023), we showed that short-term (10 days) unloading is accompanied by sarcolemmal hemichannels upregulation and increased transcriptional signatures of muscle inflammation and denervation.
Role in this research: I was responsible for recruiting the participants, planning the experiments and calendar and participating in manuscript revision.

12. Marcolin G, Franchi M V, Monti E, Pizzichemi M, **Sarto F**, Sirago G, Paoli A, Maggio M, Zampieri S, Narici M V. Active older dancers have lower C-terminal Agrin fragment concentration and better balance and gait performance than sedentary peers. *Exp Gerontol*. 2021;153(111469). https://doi.org/10.1016/j.exger.2021.111469
Scientific significance: In this cross-sectional study (Marcolin *et al.*, 2021), we compared active elderly practicing dance to healthy sedentary peers. We observed no differences in their muscle mass and strength; however, active dancers presented lower serum CAF concentration. We suggest that activities involving fine motricity and coordination, such as dance, may have a neuroprotective effect.
Role in this research: I assisted in data collection and drafted the introduction of the paper.

13. Monti E, Reggiani C, Franchi M V, Toniolo L, Sandri M, Armani A, Giacomello E, **Sarto F,** Sirago G, Murgia M, Nogara L, Marcucci L, Ciciliot S, Šimunic B, Pišot R, Narici M V. Neuromuscular junction instability and altered intracellular calcium handling as early determinants of force loss during unloading in humans. *J Physiol*. 2021;599:3037–3061. doi: 10.1113/JP281365.
Scientific significance: In this longitudinal study, we performed a 10-day bed rest. We used an integrated in vivo and ex vivo approach to assess changes in muscle mass, force, and activation capacity, as well as NMJ stability and single fibre contractility. For the first time, we report that short-term unloading is sufficient to activate NMJ destabilisation or remodelling pathways,

accompanied by signs of altered innervation pattern. Additionally, we show that single muscle fibres present reduced contractility, likely due to sarcoplasmic reticulum calcium handling impairments.
Role in this research: I assisted in the data collection of muscle function testing and ultrasound. Moreover, I analysed the MRI images and contributed to the revision of the manuscript.

3. Effects of short-term unloading and active recovery on human motor unit properties, neuromuscular junction transmission and transcriptomic profile

Fabio Sarto[1], Daniel W. Stashuk[2], Martino V. Franchi[1,3], Elena Monti[1], Sandra Zampieri[1,3,4], Giacomo Valli[1], Giuseppe Sirago[1], Julián Candia[5], Lisa M. Hartnell[5], Matteo Paganini[1], Jamie S. McPhee[6], Giuseppe De Vito[1,3], Luigi Ferrucci[5], Carlo Reggiani[1,7] and Marco V. Narici[1,3,7]

[1] Department of Biomedical Sciences, University of Padova, Padova, Italy

[2] Department of Systems Design Engineering, University of Waterloo, Ontario, Canada

[3] CIR-MYO Myology Center, University of Padova, Padova, Italy

[4] Department of Surgery, Oncology, and Gastroenterology, University of Padova, Padova, Italy

[5] Longitudinal Studies Section, Translational Gerontology Branch, National Institute of Aging, National Institutes of Health, Baltimore, MD 21224, USA

[6] Department of Sport and Exercise Sciences, Manchester Metropolitan University Institute of Sport, Manchester M1 7EL, United Kingdom

[7] Science and Research Center Koper, Institute for Kinesiology Research, Koper, Slovenia

Corresponding authors

Mr. Fabio Sarto, Department of Biomedical Sciences, University of Padova, Padova, Italy, 35131, Italy - Email: fabio.sarto.2@phd.unipd.it – ORCID: https://orcid.org/0000-0001-8572-5147

Prof. Marco V. Narici: Department of Biomedical Sciences, CIR-MYO Myology Centre, University of Padova, Padova, 35131, Italy - Email: marco.narici@unipd.it - ORCID: https://orcid.org/0000-0003-0167-1845

The article has been published in the *Journal of Physiology* and can be found at https://doi.org/10.1113/JP283381

Key points

- We used integrative electrophysiological and molecular approaches to comprehensively investigate changes in neuromuscular integrity and function after a 10-day unilateral lower limb suspension (ULLS), followed by 21 days of active recovery (AR) in young healthy men, with a particular focus on neuromuscular junction (NMJ) and motor unit potential (MUP) properties alterations.
- After 10-day ULLS, we found significant NMJ molecular alterations in absence of NMJ transmission stability impairment. These findings suggest that human NMJ is functionally resilient against insults and stresses induced by short-term disuse at least at relatively low contraction intensities, at which low-threshold, slow-type MUs are recruited.
- Intramuscular electromyography revealed that unloading caused increased MUP complexity and decreased motor unit firing rates, and these alterations could be related to the observed changes in skeletal muscle ion channel pool and initial and partial signs of fibre denervation and axonal damage.
- The AR period restored these neuromuscular changes.

Running title: Electrophysiological alterations with unloading

Keywords

C-terminal agrin fragment; Disuse; Intramuscular electromyography; Motor units; NFM jitter; NFM jiggle

Abstract

Electrophysiological alterations of the neuromuscular junction (NMJ) and motor unit potential (MUP) with unloading are poorly studied. We aimed to investigate these aspects and the underlying molecular mechanisms with short-term unloading and active recovery (AR). Eleven healthy males underwent a 10-day unilateral lower limb suspension (ULLS) period, followed by 21-day AR based on resistance exercise. Quadriceps femoris (QF) cross-sectional area (CSA) and isometric maximum voluntary contraction (MVC) were evaluated. Intramuscular electromyographic recordings were obtained during 10% and 25% MVC isometric contractions from the vastus lateralis (VL). Biomarkers of NMJ molecular instability (serum c-terminal agrin fragment, CAF), axonal damage (neurofilament light chain) and denervation status were assessed from blood samples and VL biopsies. NMJ and ion channels transcriptomic profiles were investigated by RNA-sequencing. QF CSA and MVC decreased with ULLS. Increased CAF and altered NMJ transcriptome with unloading suggested the emergence of NMJ molecular instability, which was not associated with impaired NMJ transmission stability. Instead, increased MUP complexity and decreased motor unit firing rates were found after ULLS. Downregulation of ion channel gene expression was found together with increased neurofilament light chain concentration and partial denervation. The AR period restored most of these neuromuscular alterations. In conclusion, the human NMJ is destabilized at the molecular level but shows functional resilience to a 10-day unloading period at least at relatively low contraction intensities. However, MUP properties are altered by ULLS, possibly due to alterations in ion channel dynamics and initial axonal damage and denervation. These changes are fully reversed by 21-day AR.

Graphical Abstract

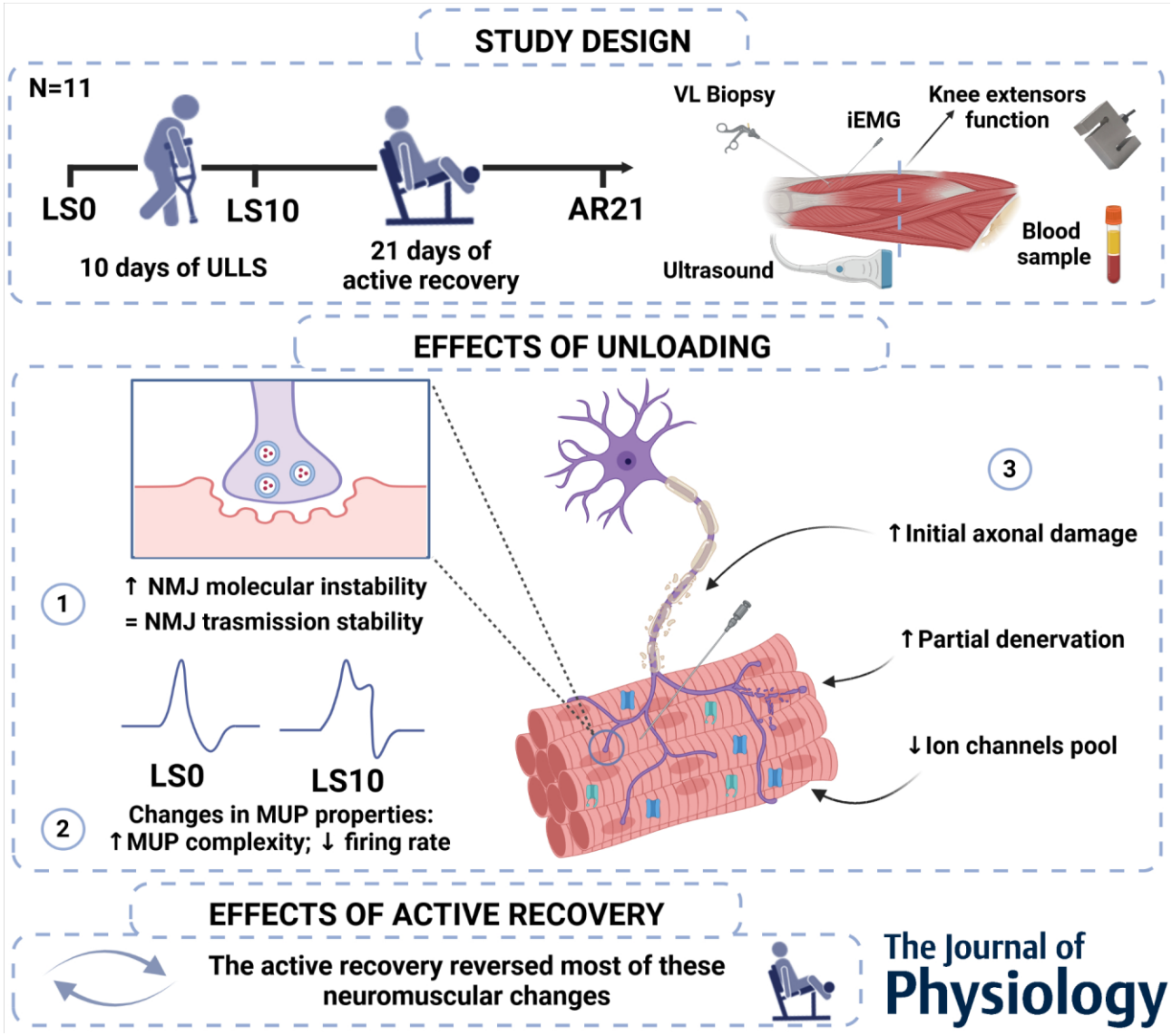

INTRODUCTION

The neuromuscular junction (NMJ) is a highly specialised synapse in the peripheral nervous system enabling electrical transmission between a motor neuron terminal and its post-synaptic skeletal muscle fibre. NMJ maintenance and dynamic remodelling are essentially shaped by neuromuscular activity (Wilson & Deschenes, 2005; Bloch-Gallego, 2015). Physical exercise is well known to maintain NMJ integrity both at its pre- and post-synaptic components, via the action of different neurotrophins, as reported mostly in animal works (Nishimune *et al.*, 2014). Conversely, seminal studies conducted in animal models have shown NMJ alterations in response to both total disuse (induced by denervation or synaptic blockade via toxin application) (Pestronk *et al.*, 1976; Brown & Ironton, 1977; Pestronk & Drachman, 1978; Eldridge *et al.*, 1981; Labovitz *et al.*, 1984) and partial disuse (muscle unloading, such as hindlimb suspension) (Pachter & Eberstein, 1984; Fahim & Robbins, 1986; Fahim, 1989; Deschenes & Wilson, 2003). In particular, previous works reported changes in endplate size (Pestronk & Drachman, 1978; Eldridge *et al.*, 1981; Labovitz *et al.*, 1984; Deschenes & Wilson, 2003), post-synaptic fold structure (Labovitz *et al.*, 1984; Fahim, 1989), subcellular active zones (Deschenes *et al.*, 2021), acetylcholine (ACh) receptor distribution (i.e., increased expression of extra-synaptic ACh receptors) and density (Pestronk *et al.*, 1976; Pestronk & Drachman, 1978; Eldridge *et al.*, 1981) and nerve terminal sprouting (Pestronk *et al.*, 1976; Pestronk & Drachman, 1978; Eldridge *et al.*, 1981; Fahim & Robbins, 1986). While it is still unclear whether some of these NMJ alterations are reflective of signs of impairment or compensatory mechanisms (Slater, 2020*b*), it is evident that animal NMJs exhibit remarkable remodelling in response to chronic disuse or decreased neuromuscular activity (Wilson & Deschenes, 2005). However, direct translation of these findings obtained in murine models to humans is complex. NMJ structure varies according to phylum and species, thus animal and human NMJs have different morphology (Wood & Slater, 2001; Hughes *et al.*, 2006). For instance, human NMJs are generally smaller and more “fragmented” than those in mice (Slater, 1992; Jones *et al.*, 2017) and recent evidence revealed the existence of specific cellular and molecular features in human NMJs (Jones *et al.*, 2017). In addition, the presence of NMJ structures in muscle biopsies obtained with conventional sampling procedures in humans is generally low (Aubertin-Leheudre *et al.*, 2019), making the direct observation of their morphology challenging, particularly for longitudinal studies. For this reason, human NMJ stability is generally assessed indirectly by employing biomarkers of muscle denervation and/or systemic biomarkers of NMJ health (Soendenbroe *et al.*, 2021).

It has been recently suggested that human NMJs may also be affected by disuse/unloading (Monti *et al.*, 2021). An early and partial sign of fibre denervation was reported by two studies, after 3 days of dry immersion (an extreme model of unloading) in healthy males (Demangel *et al.*, 2017) and 14 days of bed rest in middle-aged men and women (Arentson-Lantz *et al.*, 2016), respectively. Moreover, our research group recently observed greater NMJ molecular instability (inferred from increased serum C-terminal agrin fragment concentration; CAF) and changes in the expression of some selected genes involved in the NMJ regulation after 10 days of bed rest (Monti *et al.*, 2021). These findings seem particularly relevant from a physiological and clinical perspective as NMJ alterations, together with an altered intracellular calcium handling, may represent an early determinant of force loss during periods of unloading, commonly experienced after injury, surgery and illness (Monti *et al.*, 2021). While there is convincing evidence that NMJs are affected by disuse/unloading from a morphological and molecular perspective, whether NMJ transmission stability (i.e., NMJ function) becomes impaired is, at present, poorly understood. In this scenario, intramuscular electromyography (iEMG), and more specifically 'near-fibre (NF) electromyography', represents a unique opportunity to study *in vivo* human NMJ transmission stability, together with an evaluation of motor units potential (MUP) properties (size, spatial distribution) and motor unit (MU) firing rates (Sanders *et al.*, 2019; Piasecki *et al.*, 2021).

Hence, we aimed to investigate the neuromuscular changes in response to a short period of unloading (employing the unilateral lower limb suspension (ULLS) model) and active recovery (AR) in humans with a particular focus on NMJ alterations and MUP characteristics. Our hypotheses were that (i) 10-day ULLS, would be sufficient to cause NMJ molecular alterations, possibly resulting in NMJ transmission stability impairment, and increased MUP complexity and decreased MU firing rates, in association with loss of muscle function and (ii) 21-day AR would counteract these neuromuscular changes.

MATERIALS AND METHODS

Ethical approval

The present study was conducted in accordance with the standards set by the latest revision of the Declaration of Helsinki, and was approved by the Ethics Committee of the Department of Biomedical Sciences of the University of Padova (Italy) with reference number HEC-DSB/01-18. Participants were informed about all the experimental procedures through an interview and an information

sheet. Volunteers signed a written consent form and were allowed to drop out of the study at any stage.

Participants and experimental protocol

Twelve recreationally active young adults (age: 22.1 (2.9) years; height: 1.78 (0.03) m; body mass (72.1) kg) took part in this study. We decided to recruit only male individuals because ULLS can be associated with an increased risk of deep venous thrombosis (Bleeker *et al.*, 2004) which is generally more common in young females. The sample size was defined using a priori power analysis calculations (see the statistical analysis section for further details). Inclusion criteria were 18-35 years of age, body mass index comprised between 20 and 28 kg m^{-2} and involvement in recreational physical activities (1-3 times/week). Exclusion criteria were sedentary and very active (>3 training/week) individuals, smokers, history of deep venous thrombosis and acute or chronic musculoskeletal, metabolic and cardiovascular disorders. The protocol included one day of familiarization with the experimental procedure and measurements at baseline (LS0), after 10 days of ULLS (LS10) and 21 days of AR based on resistance exercise (AR21). The duration of the AR phase was based on previous observations that full recovery of muscle function after a two-week lower limb immobilisation required a retraining period lasting twice as long (4 weeks) as the unloading phase (Suetta *et al.*, 2009). An intermediate measurement of MVC was performed after 10 days of AR (AR10) to verify how much force had been recovered with respect to baseline values. Final measurements were performed 3 days after the last training session of the AR phase to avoid potential muscle fatigue. Participants were asked to maintain their habitual diet period throughout the entire intervention period and refrain from coffee and alcohol intake and any form of exercise during the 24 hours preceding the data collection at each time point. Each participant performed all the tests at the same time of the day to minimise possible influences of circadian variations.

Unilateral lower limb suspension (ULLS)

The ULLS model, originally described by Berg et al. (Berg *et al.*, 1991), was applied for 10 days. The non-dominant leg of the participants was fitted with a shoe having an elevated sole (50 mm), while the dominant leg was suspended and kept at a slightly flexed position (∼15/20 degrees of knee flexion) using straps. Volunteers were asked to walk with crutches during the whole ULLS period and to refrain from loading the suspended leg in any way. A familiarization session, in which the participants practiced carrying out daily tasks while performing ULLS (Tesch *et al.*, 2016*a*), was

completed. Participants were recommended to wear elastic compression socks on the suspended leg during ULLS and to perform passive, range of motion, non-weight-bearing exercises of the ankle, as precautionary measures to prevent deep venous thrombosis (Bleeker *et al.*, 2004). Moreover, an ultrasound-Doppler examination was performed after 5 days of ULLS. Compliance of the participants was evaluated through daily calls and messages and by comparing calves temperature and circumference after 5 and 10 days of ULLS, as previously suggested (Tesch *et al.*, 2016*a*).

Active recovery

After the ULLS period, participants took part in a 21-day AR program based on resistance exercise. The training program started 3/4 days after the LS10 measurements in order to grant a period of recovery from the damage induced by the muscle biopsy sampling. Participants trained 3 times per week with training sessions separated by at least 24h. The AR program consisted of 10 repetitions of unilateral leg press and leg extension exercises for 3 sets at 70% of one-repetition maximum (1RM). The 1RM was estimated indirectly since the participants were not previously involved in resistance exercise and underwent 10 days of unloading. Briefly, 4-6RM (i.e., the heaviest load that they could lift and lower under control in the range between 4 and 6 repetitions) was assessed and the 1RM was subsequently estimated using a previously proposed formula (Brzycki, 1993), verifying that the resulting value was within the range indicated by the National Strength and Conditioning Association (NSCA) training load chart (Beachle & Earle, 1994). The 1RM was reassessed at the first training session of each week and the load employed during the training was adjusted accordingly. Both exercises were executed from full knee extension (0 degrees) to ∼90 degrees limb flexion. Sets were separated by a 2-min rest. The time under tension was set at ∼2 seconds both in the concentric and eccentric phases.

In-vivo muscle structure and function

Muscle size measurements

Muscle cross-sectional area (CSA) of the quadriceps femoris was evaluated using extended-field-of-view ultrasonography imaging (Mylab70, Esaote, Genoa, Italy). A 47 mm, 7.5 MHz linear array transducer was used to collect images at different muscle length percentages. Three different regions of interest were detected at 30%, 50% (CSA50) and 70% of femur length (measured as the distance between the great trochanter and the mid-patellar point), where 0% represents the mid-patellar point (distal part) and 100% the greater trochanter (proximal part). The transducer was

moved slowly in the transversal plane from the medial border of the vastus medialis to the lateral borders of the vastus lateralis, keeping the pressure on the skin as constant as possible. An adjustable guide was used in each acquisition in order to keep the same transverse path (Monti *et al.*, 2020*a*). A generous amount of transmission gel was applied to improve the acoustic contact. Two scans were obtained for each site and the image with the best quality was analysed. CSA measures were obtained by tracing the contours of the quadriceps and vastus lateralis using ImageJ software (1.52v; National Institutes of Health, Bethesda, MD). Quadriceps and vastus lateralis CSA_{mean} were computed by averaging the values at 30%, 50% and 70% femur length of each subject.

Quadriceps force, rapid force production and activation capacity

Procedures regarding the *in-vivo* muscle function assessment have been described in detail previously (Monti *et al.*, 2021). Briefly, quadriceps force was evaluated during an isometric contraction at 90 degrees of knee flexion using a custom-made knee dynamometer equipped with a load cell. Participants were instructed to push as strongly and as fast as they could for ∼4s. Visual feedback and loud vocal encouragement were provided. Three trials were recorded, separated by 1-minute rest. The force signal was sampled at 1000 Hz using Labchart software (v.8.13, ADInstruments). The maximum force value reached during these trials was considered the maximum voluntary contraction (MVC). This value was then divided for quadriceps CSA50 to obtain the specific force (force/CSA; N/cm^2). The capacity for rapid force production was evaluated using its time constant (the time required to reach 63% of MVC; TTP63%). Activation capacity, defined as the ability to voluntarily recruit MUs, was evaluated using the interpolated twitch technique. During the MVC procedures, two electrical stimulations (Digitimer DS7AH, Digitimer Ltd, Welwyn Garden, Hertfordshire, UK) were applied in the proximal and distal region of quadriceps during the MVC plateau, and one approximately one second after the end of the contraction. Activation capacity was calculated as previously described (Monti *et al.*, 2021). All the analyses were performed with a custom MATLAB script (version R2021b; TheMathWorks, Natick, MA, USA).

Intramuscular electromyography (iEMG)

Identification of the motor point

The vastus lateralis motor point was detected as the location at which the largest muscle twitch was evoked in response to low-intensity percutaneous electrical stimulation using a pen electrode (Botter *et al.*, 2011). Since vastus lateralis usually presents three different motor points (Botter *et*

al., 2011), the central one, located around the mid-thigh, was targeted. Stimulations were induced using a Digitimer DS7AH (Digitimer Ltd, Welwyn Garden, Hertfordshire, UK) with an electrical current set at 16 mA (400V; pulse width: 50 µs). Once the motor point was identified, the current was reduced to 8-10 mA to verify that it was the most sensitive (i.e., largest twitch) point for stimulation.

Intramuscular electromyography procedures

The iEMG signals were recorded using a concentric needle electrode with a diameter of 0.46 mm and a recording area of 0.07 mm^2 (S53153; Teca Elite, Natus Medical Incorporated., USA). The iEMG signal was sampled at 40 kHz using the Labchart software (v.8.13, ADInstruments). The iEMG procedures were based on previous works (Piasecki *et al.*, 2016*c*; Jones *et al.*, 2021*a*). The needle was inserted diagonally (∼60 degrees) in the vastus lateralis muscle at the motor point. At each new location (see below), participants were asked to perform a very low-intensity contraction (∼5% MVC) and the needle position was slightly adjusted to ensure that the iEMG signal had adequate sharpness (Piasecki *et al.*, 2016*c*; Jones *et al.*, 2021*a*). Using an ultrasound device (Mylab70, Esaote, Genoa, Italy), we measured muscle and subcutaneous fat thickness in this location in order to avoid inserting the needle beyond the vastus lateralis deep aponeurosis (Jones *et al.*, 2021*a*). Afterward, participants were asked to perform submaximal isometric contractions at 10% and 25% MVC. Visual feedback was provided. Each contraction lasted 20s, with 30s of rest between contractions. Care was taken to maintain a constant needle position during recording. Needle position was slightly changed after each pair of 10% and 25% contractions by twisting the needle 180 degrees or extracting it by ∼2-3mm. Recordings were performed at three different depths and two different rotations. A total of 12 contractions (six at 10% and six at 25% MVC) were collected.

Intramuscular electromyography decomposition and MUP analysis

DQEMG software was employed to automatically extract MUP trains, representing the electrophysiological activity of individual sampled MUs, from the recorded iEMG signals and perform all subsequent quantitative analyses (Stashuk, 1999*a*). MUP trains that contained fewer than 35 MUPs or MUPs with signal-to-noise ratios <15 and/or non-physiological shapes were excluded. All extracted MUP trains were reviewed by a trained operator (FS) and markers, relative to MUP onset, end, positive peak and negative peaks were adjusted, where appropriate. MUP duration was expressed as the time between the onset and end markers. MUP size was evaluated

as MUP area within the MUP duration. MUP complexity was assessed as the number of turns (i.e., a change in MUP direction of at least 20 μV) (Piasecki *et al.*, 2016*c*). The mean inter-discharge interval (IDI_{mean}) of the MU firing pattern was also estimated.

Near fibre electromyography and NMJ transmission stability evaluation

NF electromyography is based on the electrophysiological assessment of individual muscle fibre potentials (MFPs) generated by fibres located near the electrode recording surface (Sanders *et al.*, 2019; Piasecki *et al.*, 2021). Near-fibre MUPs (NF MUPs) are generated by band-pass filtering MUPs using a second-order low-pass differentiator (Stashuk, 1999*b*). Compared to near fibres, contributions from (i.e., MFPs generated by) distant fibres will be of lower amplitude and frequency content. Therefore, by band-pass filtering MUPs, it is possible to focus on the activity of NFs (i.e., those in close proximity, within ∼350 μm, to the needle electrode) (Piasecki *et al.*, 2021). All NF MUP trains were visually inspected and NF MUPs containing contaminating MFP components (i.e., activity generated by other MUs) were manually excluded. Only NF MUPs trains with signal-to-noise ratios >15, >34 NF MUPs and having a NF count (see below) of at least 1 were included. The following parameters were evaluated (Piasecki *et al.*, 2021): (i) NF MUP duration and (ii) NF Count, the number of fibre contributions detected within the NF MUP duration. NMJ transmission stability was evaluated using (iii) NF MUP jiggle and (iv) NF MUP segment jitter which represent the shape variability (i.e., mean absolute consecutive amplitude differences) and temporal variability (i.e., mean absolute consecutive temporal differences) in consecutive NF MUPs, respectively (Stålberg & Sonoo, 1994; Piasecki *et al.*, 2021).

Muscle Biopsy

In each participant, a vastus lateralis muscle biopsy (∼150 mg) was collected using a Weil–Blakesley conchotome (Gebrüder Zepf Medizintechnik GmbH & Co. KG, Dürbheim, Germany). Since our intention was to relate the changes in iEMG measures to biopsy outcomes, each biopsy was performed at ∼2 cm from the central motor point, similarly to Aubertin-Leheudre et al. (Aubertin-Leheudre *et al.*, 2019). A distance of ∼2/3 cm between the three biopsies sites was maintained to avoid effects of pre-sampling (for further details we refer the reader to the open peer review history in the Supporting Information section). Two ml of lidocaine (2%) were injected in the area of the sampling and a small incision of muscle and fascia was performed. Muscle samples were divided

into two different parts. The first part for mRNA analysis was frozen in liquid nitrogen and stored at −80°C. The second part used for immunohistochemical analysis was included in optimal cutting temperature (OCT) compound and frozen in isopentane, then stored at −80°C. Cryosections were cut with a manual cryostat (Leica CM1850), producing 10 µm thick sections.

Immunohistochemistry

Detection and quantification of denervated and regenerating myofibres were performed by neural cell adhesion molecule (NCAM) and neonatal myosin immunolabelling, respectively, as described: serial cryosections were fixed in pre-chilled methanol at -20°C (NCAM staining only), washed in PBS and then blocked in 10% FBS/PBS (both for NCAM and neonatal myosin heavy chain staining). The same cryosections were then labelled (1 hour at room temperature) using rabbit polyclonal antibody directed either against NCAM (Chemicon, Millipore, cat. n. AB5032, Milan, Italy) or against laminin (Sigma-Aldrich, cat. N. L9393, MO, USA) 1:200 and 1:100 diluted, respectively, in 2% goat serum in PBS. Sections were then rinsed in PBS (3x5 min), blocked in 10% goat serum in PBS (10 min at room temperature) and then incubated with goat anti-rabbit IgG Alexa Fluor 594 red fluorescent dye (Thermo Fisher Scientific, A-11012, MA, USA) 1:500 diluted in PBS (1 hour at room temperature). After washes, sections stained for NCAM were coverslipped using ProLong™ Diamond Antifade Mountant with DAPI dye (Thermo Fisher Scientific, D1306, MA, USA). The sections devoted to neonatal heavy chain staining were washed in PBS (2x5), incubated using mouse monoclonal antibody directed against developmental (embryonic and neonatal)-myosin heavy chain (Novocastra, NCL-MHCd, RRID:AB_563901) and 1:10 diluted in PBS. Finally, after rinsing 3x5 min in PBS and blocking in 10% goat serum (20 min), sections were incubated with goat anti-mouse IgG Alexa Fluor 488 green fluorescent dye (Thermo Fisher Scientific, A-11001, MA, USA) 1:500 diluted in PBS (1 hour at room temperature). After washes, sections were coverslipped using ProLong™ Diamond Antifade Mountant with DAPI dye (Thermo Fisher Scientific, D1306, MA, USA) and observed under a Zeiss microscope (objective 20x) connected to a Leica DC 300F camera. Serial cryosections belonging to a regenerating rat muscle were used as positive controls, while negative controls were performed by omitting the primary antibodies from sample incubations. NCAM and neonatal myosin-positive fibres were counted on captured images, using ImageJ software (1.52v; National Institutes of Health, Bethesda, MD) and expressed as the number of positive myofibres per total number of myofibres detected in the biopsy area by laminin staining (approximately 400 muscle fibres). NCAM evaluation was performed only at LS0 and LS10 since this was part of a parallel investigation focused only on the unloading period. Analyses were performed blinded to time point.

ATPase staining

To evaluate muscle fibre type distribution, conventional techniques were used to stain serial cross-sections for myofibrillar ATPases, as previously described (Carraro *et al.*, 1985). After pre-incubation at pH 4.35, slow-twitch muscle fibres (those possessing a higher ATPase activity) were visualized as dark, while fast-type fibre (or those possessing a low ATPase activity) were lightly stained. To overcome the distortion of obliquely cut or kinked muscle fibres, commonly observed in human muscle biopsies, muscle fibre minimum Feret diameter was manually measured over all the visible fibres (about 200 to 400 in each section) using ImageJ software (1.52v; National Institutes of Health, Bethesda, MD). Mean, standard deviation and distribution of the diameters were assessed. The variability of muscle fibres diameters was expressed, per each participant and time-point, as the coefficient of variation (CV; standard deviation/mean of all the muscle fibres visible on the biopsy section). Fibre type percentage was measured by manually counting all the dark and light observable fibres over the whole biopsy in each section. Fibre type grouping for the quantification of large and very large fibre type clusters (>10 or >20 fibres, respectively) was evaluated using the method of "enclosed fibre" (fibre entirely surrounded by fibres of the same histochemical type) (Jennekens *et al.*, 1971). Longitudinally oriented muscle fibres were not considered for analyses. Analyses were performed blinded for time point.

RNA extraction, sequencing and transcriptomic analysis

RNA-Seq was employed to study changes in the expression of genes known to be involved in NMJ and skeletal muscle ion channels regulation. The RNA was extracted from ~10/15 mg of the muscle tissues by REPROCELL (USA) using a Norgen Animal Tissue RNA Purification Kit #257 (Norgen Biotek Corp, Ontario, CA). The RNA integrity score (RIN) average was 9.21 (range: 7.90-9.86). The concentration of extracted RNA ranged from 34 ng/ul to 166 ng/ul per sample. RNA-Seq was performed at the Frederick National Laboratory for Cancer Research Sequencing Facility, NIH. The libraries were made using the TruSeq Stranded Total RNA Library Prep protocol from Illumina. This protocol involves the removal of ribosomal RNA (rRNA) using biotinylated, target-specific oligos combined with Ribo-Zero rRNA removal beads. The RNA was fragmented pieces and the cleaved RNA fragments were copied into first-strand cDNA using reverse transcriptase and random primers, followed by second-strand cDNA synthesis using DNA Polymerase I and RNase H. The resulting double-strand cDNA was used as the input to a standard Illumina library prep with end-repair,

adapter ligation and PCR amplification being performed to provide a library ready for sequencing. Samples were sequenced on NovaSeq 6000 on S4 flowcell using paired-end sequencing with read length of 100bps. The sequencing quality of the reads was assessed using FastQC (v. 0.11.5; https://www.bioinformatics.babraham.ac.uk/projects/fastqc/), Preseq (v. 2.0.3) (Daley & Smith, 2013), Picard tools (v. 2.17.11; https://broadinstitute.github.io/picard/) and RSeQC (v. 2.6.4) (Wang *et al.*, 2012). The samples had 295 to 419 million pass filter reads (average: 367 million reads per sample) with more than 90% of bases above the quality score of Q30. In addition, Kraken (v. 1.1) (Wood & Salzberg, 2014) was used as a quality-control step to assess microbial taxonomic composition. Reads were trimmed using Cutadapt (v. 1.18) (Martin, 2011) to remove sequencing adapters prior to mapping to the human reference genome hg38 using STAR (v. 2.7.0f) (Dobin *et al.*, 2013) in two-pass mode. Expression levels were quantified using RSEM (v. 1.3.0) (Li & Dewey, 2011) with GENCODE annotation (v. 21) (Harrow *et al.*, 2012). In order to filter out low expressed genes, filterByExpr() from package edgeR (v. 3.32.1) (Robinson *et al.*, 2010) was used, resulting in 20,555 genes that passed the filter. Subsequently, quantile normalization was performed using the voom algorithm (Law *et al.*, 2014) from the Limma R package (v. 3.46.0) (Smyth, 2004), followed by empirical Bayes smoothing of standard errors to assess case-vs-control differentially expressed genes adjusted for subject ID (paired analysis). Based on p-values derived from this analysis, all measured genes were ordered by -log10(p-value); this ordered list of genes was analysed to assess enrichment of a pre-selected set of pathways associated with NMJs and ion channels in skeletal muscle. Gene set enrichment analysis (GSEA) was performed using package fgsea (v. 1.20.0) (Korotkevich *et al.*, 2021). A customized implementation in R was developed in-house to add robustness to the GSEA analysis; since GSEA's enrichment estimates (and statistical significance) are stochastic, our software embeds GSEA in a Monte Carlo algorithm that performs 1000 iterations and chooses significant pathways based on the total statistical ensemble. Leading edge genes shown in Figure 5 were those selected by GSEA in more than 80% of the iterations.

Blood sampling and circulating biomarkers evaluation

Blood samples were obtained from the medial cubital vein in Gel Clot Activator tubes (368969, BD Diagnostic, Oxford UK) before the *in-vivo* muscle function evaluation and were then centrifuged (CN45, Eurotek, Orma, Milan, Italy) at 3000 rpm for 10 min to separate serum from the other blood components. Samples were aliquoted and consequently stored at −80° until analysis.

In order to investigate NMJ damage, serum CAF concentration was evaluated. Serum CAF concentration was measured using a commercially available enzyme-linked immunosorbent assay (ELISA) kit (Human Agrin SimpleStep ELISA, Ab216945, Abcam, Cambridge, United Kingdom) following the manufacturer's instructions. A microplate ELISA reader (Infinite F50, Tecan Trading AG, Switzerland) was employed to read the absorbance at 450 nm. CAF concentrations were obtained by interpolation with a standard curve and corrected for sample dilution (Marcolin *et al.*, 2021; Monti *et al.*, 2021).

Single molecule array (SIMOA) analysis was also performed to evaluate neurofilament light chain concentration, a well-established biomarker of axonal damage, previously employed both in aging and neurological disorders scenarios (Khalil *et al.*, 2018; Pratt *et al.*, 2022). The samples were submitted to the SIMOA service offered by Wieslab AB, a Svar Life Sci company, Lundavägen MALMO (Sweden); in accordance with Good Laboratory Practice (GLP) principles. SIMOA analysis was performed on a Simoa HD-X Analyzer (PN 10041537) supplied by Quanterix in agreement with standard protocol suggested by Quanterix. In particular, serum samples were diluted 1:4 and measurements obtained in double replicates. The kit used for the reported analysis was Simoa NF-light Advantage Kit HD-1/HD-X (Item 103186; Lot 502845).

Statistical analysis

A priori power analysis was performed based on changes in CAF concentration to determine the required sample size. For an effect size calculated based on our previous work (Monti *et al.*, 2021), a required power (1-β) of 0.9 and an error α=0.05, the total required sample size was 11 subjects. Therefore, the 12 participants recruited in this work represented an appropriate sample, considering potential study drop-outs. Normality of *in vivo* muscle structure and function data, circulating biomarkers concentrations, fibre diameter variability, fibre type and markers of denervation were assessed through Shapiro–Wilk normality test and visual inspection of Q-Q plots. All the considered parameters passed normality tests. For all these variables, one-way repeated-measures ANOVA (regular or mixed-effects, depending on missing values) with Tukey's post hoc test was performed to determine whether differences among the different time points were present. For all ANOVAs, sphericity was tested with Mauchly's test and when the assumption of sphericity was violated, the correction of Greenhouse-Geisser was applied. NCAM and slow fibre type grouping datasets did not pass normality tests and was evaluated with a non-parametric Wilcoxon test and Friedman test, respectively. Gene expression analysis was performed separately on two sets of

genes identified as relevant for NMJs, based on 12 pathways extracted from the Molecular Signature Database MSigDB (v. 7.4) (Subramanian *et al.*, 2005), and skeletal muscle ion channels (Jurkat-Rott & Lehmann-Horn, 2004) (see Data S1, Data S2 and Data S3 in the Supporting Information section). For each gene set, we performed Principal Components Analysis (PCA) and differential GSEA (see details above). For the analysis of iEMG data, we performed generalized linear mixed effect models (fixed effect: time; cluster variable: subject), as multiple MUs were recorded from each participant (Yu *et al.*, 2022). The family of the distribution employed was the gamma or inverse Gaussian distribution depending on each variable, with different associated link functions (Table 1). The function used to compare the different models was the Bayesian information criterion (BIC). For models with similar minimal BIC, the canonical link function of the distribution (inverse function (1/y) and inverse squared ($1/y^2$) for gamma distribution and inverse Gaussian, respectively) was chosen. Post hoc comparisons were performed with Holm correction. Statistical significance was set at $p<0.05$. Jamovi software (version 2.2, Sydney, Australia) was used to perform statistical analysis, while GraphPad Prism (version 8.00; GraphPad Software, San Diego, CA) was employed to create all of the graphs.

RESULTS

No side effects regarding biopsy procedures, ULLS exposure or the AR phase were reported. One participant dropped out after baseline measures for personal reasons not related to the study and another one did not perform iEMG measures at 25% MVC at LS10 due to pain experienced during contractions. Two other participants decided to not undergo muscle biopsy at AR21 for personal reasons.

In-vivo muscle morphology and function

Firstly, we evaluated whether the ULLS period resulted in a significant decline in muscle size and function and whether the AR phase was effective in counteracting this loss. For quadriceps ($p<0.001$; $\eta_p^2=0.849$) and vastus lateralis ($p<0.001$; $\eta_p^2=0.839$) CSA_{mean} a main effect of time was observed (Figure1). CSA_{mean} was significantly reduced for both quadriceps ($p=0.007$) and vastus lateralis ($p=0.038$) at LS10, and subsequently increased and at AR21 they were significantly higher compared to LS10 (quadriceps: $p<0.001$; vastus lateralis: $p<0.001$). Interestingly, ~~for both muscles,~~ CSA_{mean} at AR21 was higher than LS0 and LS10 (quadriceps: $p<0.001$; vastus lateralis: $p<0.001$). All muscle function parameters were significantly influenced by time (Figure1): MVC ($p<0.001$; $\eta_p^2=0.842$),

specific force (p<0.001; η_p^2=0.724); TTP63% (p<0.001; η_p^2=0.645) and activation capacity (p=0.004; η_p^2=0.514). A significant decline in MVC was observed at LS10 (p<0.001), followed by full recovery at AR21 (p<0.001) but not at AR10 which was still reduced compared to LS0 (p=0.004). The specific force (LS0 vs LS10: p<0.001; LS10 vs AR21: p=0.002) and activation capacity (LS0 vs LS10: p=0.02; LS10 vs AR21: p<0.001) followed the same pattern, with a difference also between LS0 and AR21 for specific force (p=0.033). The TTP63% was significantly increased at LS10 (p= 0.004) and returned to baseline levels at AR21 (p= 0.003).

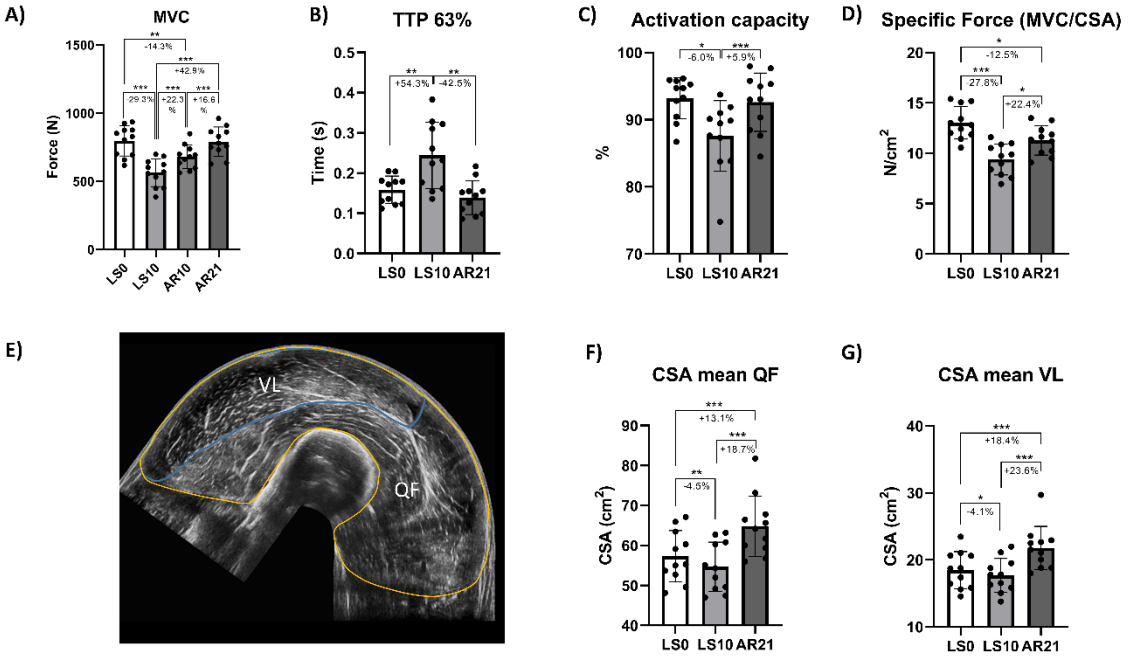

Figure 1: *Changes in the in vivo muscle morphology and function following 10 days of unilateral lower limb suspension (LS10) and 10 days (AR10) and 21 days of active recovery (AR21). Statistical analysis was performed using regular repeated-measures one-way ANOVAs. Results are shown as mean and standard deviation. Maximum voluntary contraction (A); time needed to reach the 63% of the MVC (TTP 63%) (B); activation capacity (C); specific force (D); representative quadriceps femoris (QF) and vastus lateralis (VL) panoramic ultrasound image (E); mean cross-sectional area (CSA) for QF (F) and VL (G). LS0: baseline data collection; *p<0.05; **p<0.01; ***p<0.001*

MUP properties and NMJ transmission stability

To investigate whether changes in muscle morphology and function were accompanied by electrophysiological changes, MUP properties and NMJ transmission stability were assessed with iEMG. MUPs from 814 (24.77 (12.8) on average per participant at each time point) and 1212 MUs (21.5 (11.96) on average), sampled at 10% and 25% MVC, respectively, were analysed. NF MUPs from 495 and 709 MUs, sampled at 10% (15.0 (10.26) on average) and 25% (36.73 (16.0) on average)

MVC, respectively, were analysed. MUP and NF MUP characteristics results are shown in Figures 2 and 3, respectively. No spontaneous activity (i.e., fibrillation or fasciculation potentials) was observed at any of the time points (data not shown). An increased IDI_{mean}, reflecting a lower MU firing rate, was observed at LS10 for both 10% ($p<0.001$) and 25% ($p=0.03$) MVC, while IDI_{mean} was decreased at 10% at AR21 compared to LS0 ($p=0.008$) and LS10 ($p<0.001$). MUP size (MUP area) was not affected by suspension but it was reduced at AR21 with respect to LS0 (10% MVC: $p<0.001$; 25% MVC: $p<0.001$) and LS10 (10% MVC: $p=0.008$). MUP duration followed the same pattern (LS0 vs AR21, 10% MVC: $p<0.001$, 25% MVC: $p<0.001$; LS10 vs AR21, 10% MVC: $p<0.001$, 25% MVC: $p<0.001$). At 25% MVC, MUP complexity (evaluated as the number of turns) was found to be increased at LS10 ($p<0.001$) and restored at AR21 ($p<0.001$). NF count was lower at LS0 compared to LS10 and AR21 both at 10% (LS0 vs LS10: $p=0.007$; LS0 vs AR21: $p=0.014$) and 25% MVC (LS0 vs LS10: $p=0.001$; LS0 vs AR21: $p=0.001$). NF MUP duration was greater at LS10 compared to LS0 at 25% MVC (25% MVC: $p=0.032$), with a trend also at 10% ($p=0.06$); and had a further increase at AR21 (LS0 vs AR21, 10% MVC: $p<0.001$, 25% MVC: $p<0.001$; LS10 vs AR21, 10% MVC: $p<0.001$, 25% MVC: $p=0.032$). Regarding NMJ transmission stability, NF MUP jiggle was unmodified at LS10 compared to LS0 but decreased at 10% MVC at AR21 compared to the other two time points (LS0 vs AR21: $p=0.002$; LS10 vs AR21: $p=0.001$). Finally, NF MUP segment jitter was not influenced by the interventions. Additional information on the iEMG data analysis is shown in Table 1.

Parameter	Distribution	Link function	Estimate	95% confidence intervals	P value
MUP area 10% (μV · ms)	Inverse gaussian	Identity	734.4	662 to 807.3	<0.001
MUP area 25% (μV · ms)	Inverse gaussian	Identity	949	869 to 1028.8	<0.001
MUP duration 10% (ms)	Gamma	Inverse	0.10213	0.09545 to 0.10188	<0.001
MUP duration 25% (ms)	Gamma	Inverse	0.10171	0.094 to 0.10942	<0.001
MUP turns 10% (number of turns)	Inverse gaussian	Inverse squared	0.08971	0.07874 to 0.10068	0.142
MUP turns 25% (number of turns)	Inverse gaussian	Inverse squared	0.09821	0.0874 to 0.10907	<0.001
IDI_{mean} 10% (ms)	Inverse gaussian	Identity	135.86	127.05 to 144.67	<0.001
IDI_{mean} 25% (ms)	Inverse gaussian	Identity	133.78	123.13 to 144.4	0.033
NF MUP duration 10% (ms)	Gamma	Inverse	0.4405	0.3871 to 0.49394	<0.001
NF MUP duration 25% (ms)	Gamma	Inverse	0.4482	0.4004 to 0.49497	<0.001
NF count 10% (number)	Inverse gaussian	Inverse	0.8546	0.792 to 0.9142	0.005
NF count 25% (number)	Inverse gaussian	Inverse	0.8198	0.763 to 0.8767	<0.001
NF MUP jiggle 10% (%)	Inverse gaussian	Inverse squared	9.132	8.175 to 10.088	<0.001
NF MUP jiggle 25% (%)	Inverse gaussian	Inverse squared	13.5902	11.661 to 15.52	0.948
NF MUP jitter 10% (μs)	Gamma	Inverse	0.03635	0.03254 to 0.04016	0.152
NF MUP jitter 25% (μs)	Gamma	Inverse	0.028	0.02504 to 0.03102	0.409

Table 1: *Details of the generalized linear mixed effect models performed for each variable. The overall estimate and p value of the model are reported in this table, while p values of the time-point comparison are presented in the text. MUP: motor unit potential; NF MUP: near fibre motor unit potential; IDImean: mean inter-discharge interval*

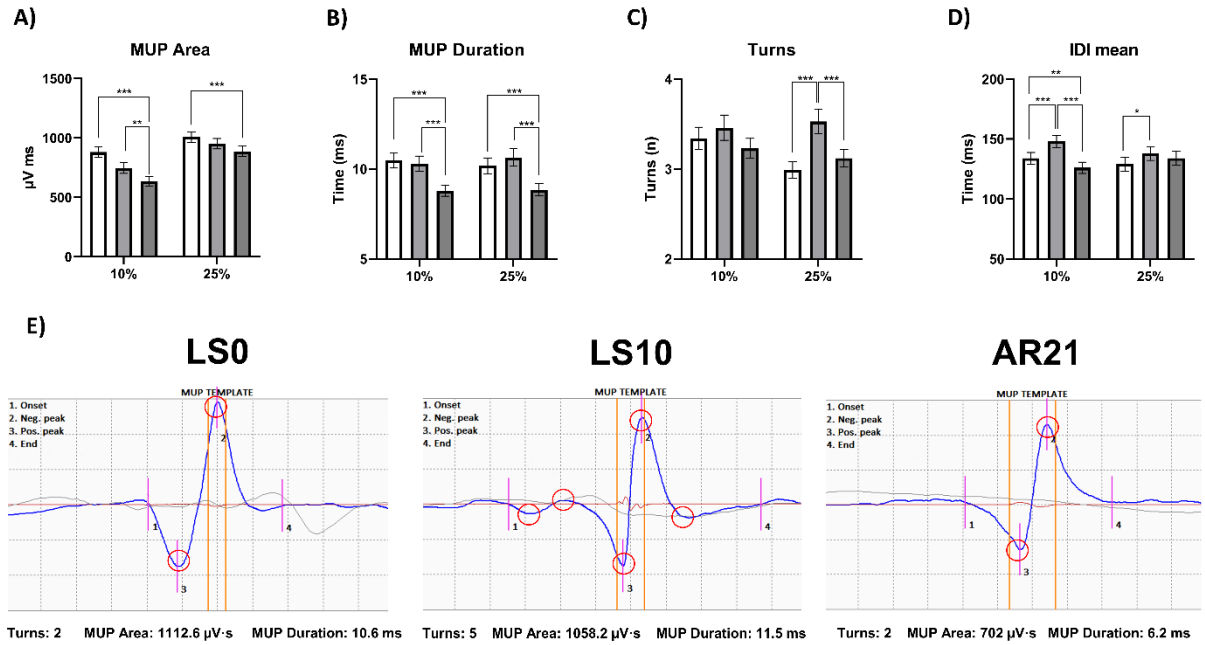

Figure 2: *Changes in MUP properties obtained using intramuscular electromyography after 10 days of unilateral lower limb suspension (LS10) and 21 days of active recovery (AR21). Statistical analysis was performed using generalized linear mixed effect models. Results are shown as estimated marginal mean and standard error. Motor unit potential (MUP) area (A); MUP duration (C); MUP turns (C) mean inter-discharge interval (IDI_{mean}) (D) and representative MUP templates at each time point (E). MUP area represents the area under the MUP waveform displayed in blue; MUP Duration was computed as the time between markers 1 and 4; each turn is highlighted by red circles. LS0: baseline data collection; *p<0.05; **p<0.01; ***p<0.001*

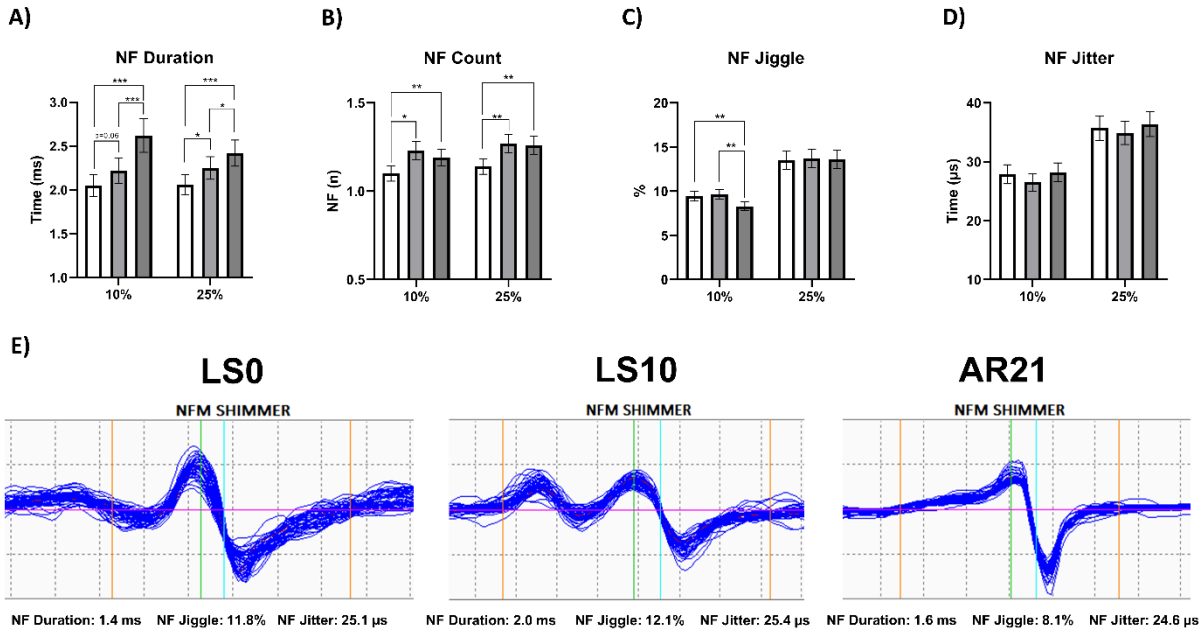

Figure 3: *Changes in near fibre (NF) electromyography outcomes following 10 days of unilateral lower limb suspension (LS10) and 21 days of active recovery (AR21). Statistical analysis was performed using generalized linear mixed effect models. Results are shown as estimated marginal mean and standard error. Near fibre motor unit potential (NFM) duration (A); NF count (B); NFM jiggle (C) NFM segment jitter (D) and representative NFM shimmers at each time point (E). LS0: baseline data collection; *p<0.05; **p<0.01; ***p<0.001*

NMJ and ion channels transcriptomic profile

In view of the observed changes in iEMG parameters, we investigated molecular events potentially connected with changes in synaptic transmission and electrical activity. In particular, we performed RNA-Seq and found a significant shift in the overall NMJ transcriptomic profile (across 290 NMJ-associated genes) comparing LS0 and LS10, with these changes restored at AR21, as evidenced by PCA (Figure 4A). Interestingly, PCA showed greater variance at LS10, indicating a heterogeneous adaptive response between participants to ULLS. The volcano plots illustrate those 290 NMJ genes compared pairwise between time points (Figure 4, panels B-D). In each of these volcano plots, the y-axis shows -log10(p-value); reference lines display the false-discovery rate (FDR) q-values 0.05 and 0.01. All the volcano plots for NMJ genes were fairly symmetrical, suggesting both upregulation and downregulation of NMJ genes in response to the interventions. With unloading, 95 NMJ genes were differently regulated at q<0.05 (70 genes at q<0.01) (Figure 4B), including some encoding for ACh receptor subunits, neurotrophins (such as *NT4* and *GDNF*), Homer proteins and other key regulators of the NMJ (neuregulins, the epidermal growth factor receptor (ErbB) and Wnts family). Most of these differently expressed genes (a total of 114 genes at q<0.05 and 81 genes at q<0.01) showed an opposite trend at AR21 (Figure 4C). Comparing LS0 and AR21, differences were much less

pronounced: only 24 genes were significantly differentially expressed at q<0.05 (7 genes at q<0.01) with also more limited log fold changes (Figure 4D). NMJ RNA-Seq dataset is available in the Supporting Information section (Data S1).

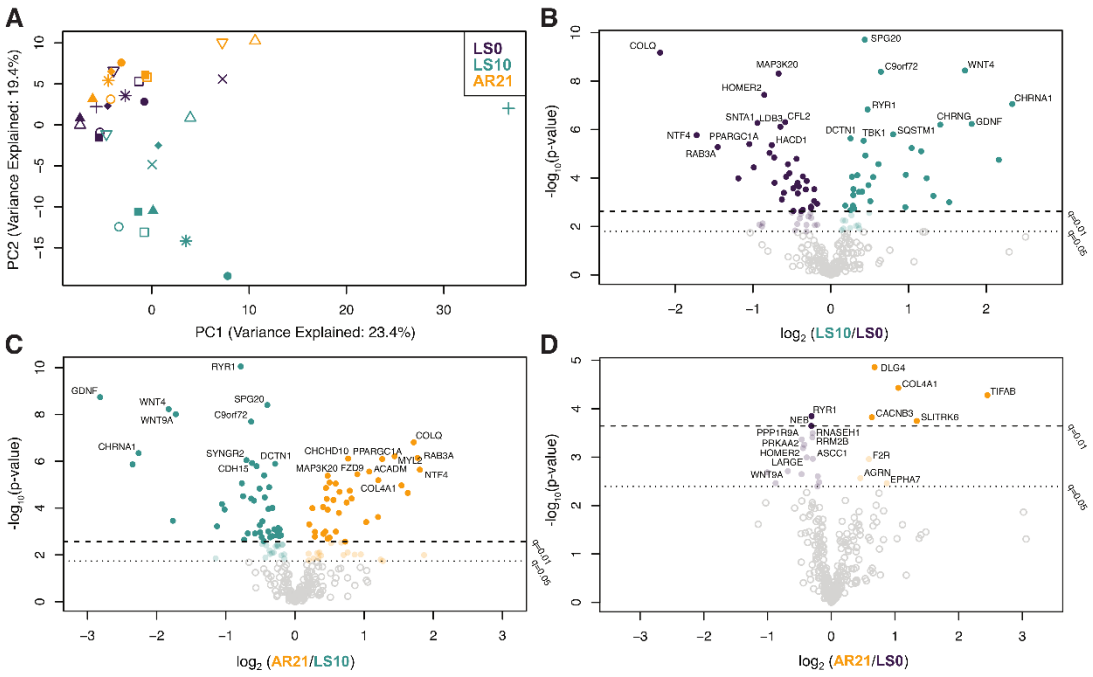

Figure 4: *Changes in the expression of 290 genes related to NMJ during unloading and active recovery as determined by RNA-Seq. Principal component analysis plot showing a shift in the overall expression of genes involved in neuromuscular junction (NMJ) regulation with 10 days of unilateral lower limb suspension (LS10) and 21 days of active recovery (AR21) (A). Volcano plots displaying differentially expressed NMJ coding genes in baseline (LS0) vs LS10 (B), LS10 vs AR21 (C) and LS0 vs AR21 (D). Samples are coloured based on time points.*

GSEA showed changes in some NMJ-related gene sets at LS10 and AR21, but not comparing LS0 and AR21 values (see Data S3 in the Supporting Information section). Differences in NMJ leading-edge genes based on GSEA are presented in Figure 5. In the top quadrant of the figure, a group of genes that were downregulated following unloading and upregulated after the AR period is shown, with *COLQ* (a collagen-tail subunit of acetylcholinesterase) being the most responsive gene. In contrast, in the bottom right quadrant, genes that increased their expression with ULLS and decreased it at AR21 are presented, including two ACh receptor subunits (*CHRNA1* and *CHRND*).

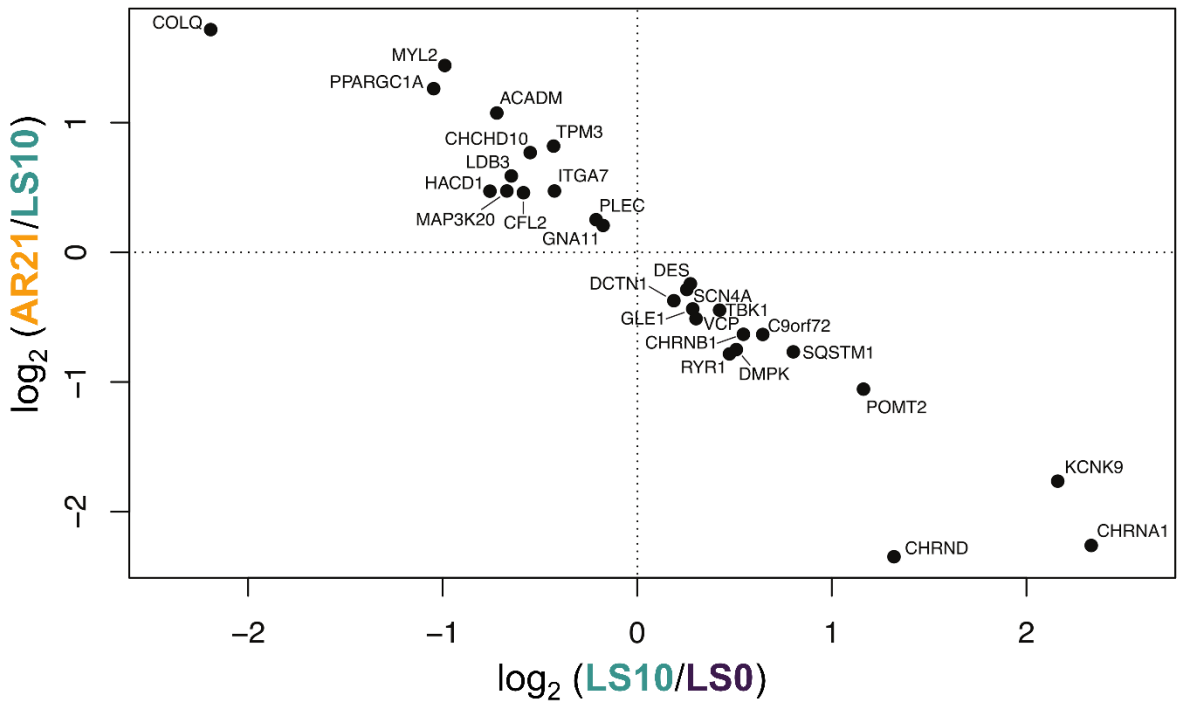

Figure 5: *Leading-edge NMJ genes from RNA-Seq in response to 10 days of unilateral lower limb suspension (LS10) and 21 days of active recovery (AR21) based on gene set enrichment analysis. In the top left quadrant of the figure, genes that were downregulated at LS10 and upregulated at AR21 are shown. In the bottom right quadrant, genes that increased their expression with ULLS and decreased it at AR21 are presented. LS0: baseline data collection*

In addition, we analysed 33 genes associated with skeletal muscle ion channels due to their key role in the maintenance of membrane resting conductance and potential and in the propagation of electrical impulses along the sarcolemma (Jurkat-Rott & Lehmann-Horn, 2004). Analogously to NMJ genes, PCA analysis showed similar overall gene expression at LS0 and AR21, while at LS10 it showed a separated and heterogeneous cluster (Figure 6A). As illustrated in the volcano plot, differences at LS10 appeared asymmetrical and biased towards LS0 (Figure 6B), suggesting an overall downregulation of the ion channels gene set, with voltage-gated potassium channels genes that seem particularly affected by unloading. Differently, the volcano plot comparing LS10 and AR21 was symmetrical: expression of different potassium channels genes was restored at AR21 but other genes encoding for instance some chloride and calcium channels subunits reduced their expression (Figure 6C). Only very small differences were observed in the comparison between LS0 and AR21 results, with few genes that remained downregulated (Figure 6D). Ion channels RNA-Seq dataset is available in the Supporting Information section (Data S2). Overall, these findings suggest that genes of NMJs and skeletal muscle ion channels underwent adaptive changes between LS0 and LS10, which are mostly reversed at AR21.

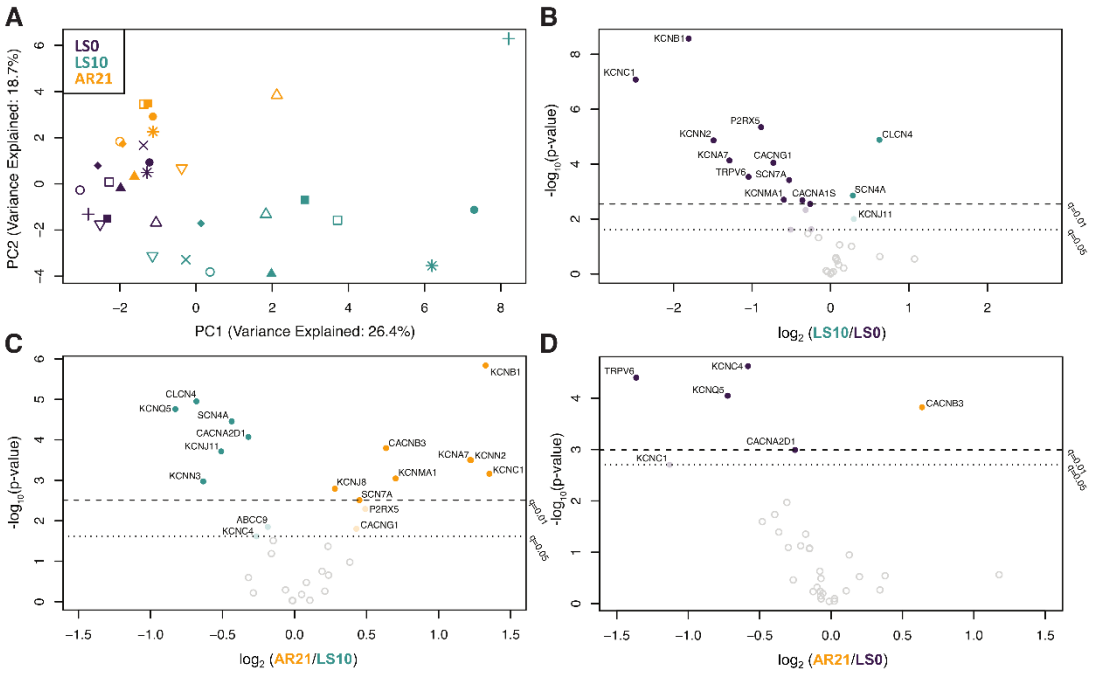

Figure 6: *Changes in expression of 33 genes related to skeletal muscle ion channels during unloading and active recovery as determined by RNA-Seq. Principal component analysis plot showing a shift in the overall expression of genes regulating ion channels with 10 days of unilateral lower limb suspension (LS10) and 21 days of active recovery (AR21) (A). Volcano plots displaying differentially expressed ion channels coding genes in baseline (LS0) vs LS10 (B), LS10 vs AR21 (C) and LS0 vs AR21 (D). Samples are coloured based on time points.*

Muscle fibre diameter variability, type and markers of regeneration/denervation

Further investigating potential mechanisms underpinning the alterations in MUP properties observed with ULLS, we evaluated several parameters derived from the immunohistochemical and ATPase staining analysis (Figure 7) and some circulating biomarkers (Figure 8). No differences were detected for fibre diameter variability for both slow and fast fibres during the interventions. Fibre type was not affected by ULLS, but slow fibre percentage increased (and consequently, fast decreased) with AR (LS0 vs AR21: p=0.004; LS10 vs AR21: p<0.001). Regarding changes of denervation markers with unloading, no flat-shaped/angulated fibres were observed at any time point (data not shown) and no changes were shown in the percentage of fibre type grouping both for slow and fast fibres. However, as a reflection of the shift towards a slow phenotype in fibre type at AR21, the percentage of fibre type grouping for fast fibre decreased (LS0 vs AR21: p=0.034; LS10 vs AR21: p=0.021). In addition, no regenerating neonatal myosin-positive fibres were found (data not shown), while the percentage of NCAM-positive fibres increased at LS10 (p=0.031; Figure 8). Evidence of initial axonal damage with unloading was shown by increased neurofilament light chain level at LS10 (p=0.001), subsequently restored at AR21 (p=0.001). Finally, we evaluated serum CAF

concentration, a well-established biomarker of NMJ molecular stability. CAF is released in the circulation upon neurotrypsin-induced cleavage of agrin, a proteoglycan that stabilizes the synaptic structures (Stephan *et al.*, 2008). Therefore, a higher concentration of this circulating biomarker reflects an increased NMJ molecular instability (Drey *et al.*, 2013; Marcolin *et al.*, 2021; Monti *et al.*, 2021). Importantly, our results showed increased CAF concentration increased at LS10 compared to LS0 (p=0.038), with no differences between the other time points.

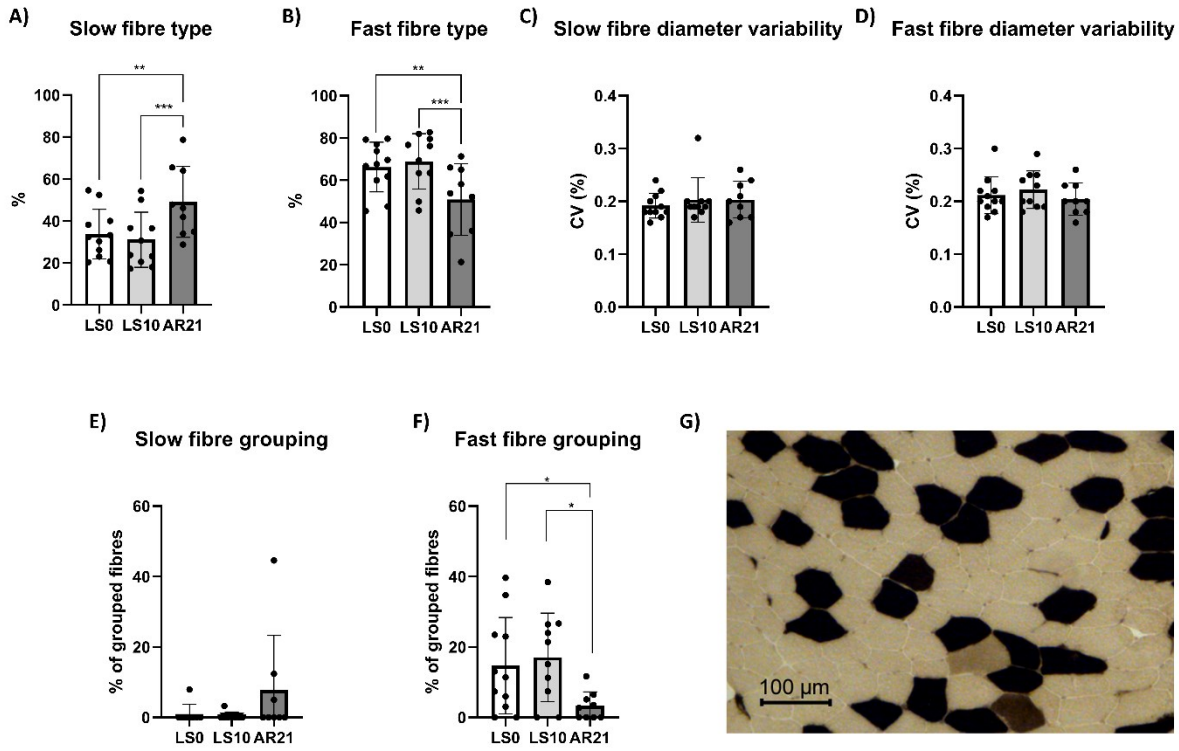

Figure 7: *Changes in parameters obtained by ATPase staining following 10 days of unilateral lower limb suspension (LS10) and 21 days of active recovery (AR21). Statistical analysis was performed using mixed-effects repeated-measures one-way ANOVAs (A-E) and Friedman test (F). Results are shown as mean and standard deviation. Percentage of slow fibre (A); percentage of fast fibre (B); fibre diameter variability in slow fibre (C); fibre diameter variability in fast fibre (D); percentage of grouped slow fibre (E); percentage of grouped fast fibre (F) and a representative ATPase staining (G). We performed ph 4.35 ATPase, hence fibres possessing a high ATPase activity (oxidative) are dark, while fibres possessing a low ATPase activity (glycolytic) are clear. Fibres possessing an intermediate metabolism are brown. LS0: baseline data collection; *p<0.05; **p<0.01*

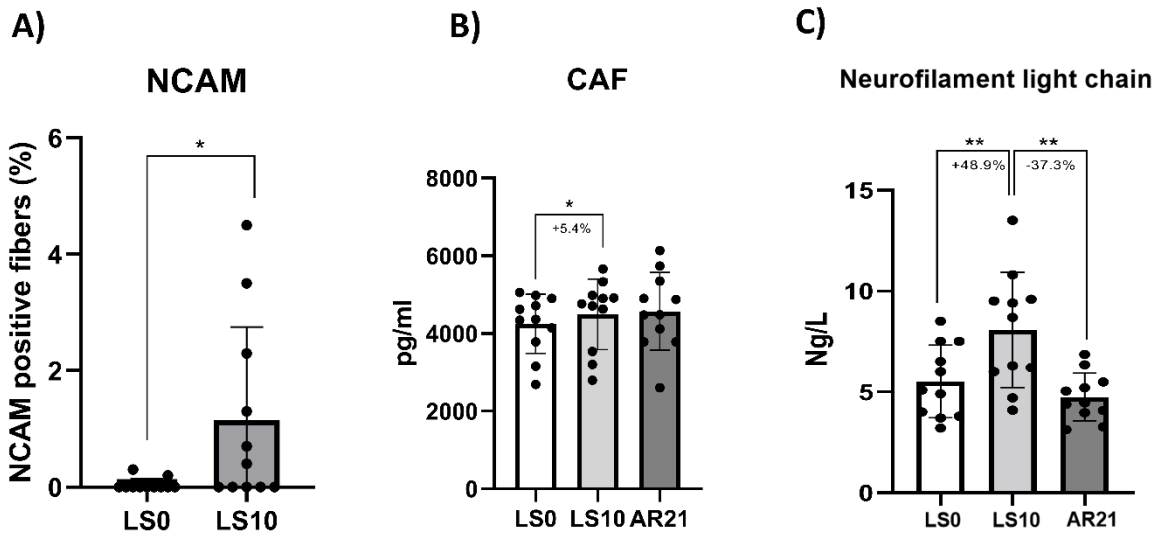

Figure 8: *Changes in neural cell adhesion molecule (NCAM) positive fibre and circulating biomarker following 10 days of unilateral lower limb suspension (LS10) and 21 days of active recovery (AR21). Statistical analysis was performed using Wilcoxon test (A) and regular repeated-measures one-way ANOVAs (B-C). Results are shown as mean and standard deviation. Neural cell adhesion molecule (NCAM) positive fibre (A); C-terminal agrin fragment concentration (CAF) (B) and neurofilament light chain concentration (C). LS0: baseline data collection; *p<0.05; **p<0.01*

DISCUSSION

The aim of this study was to investigate the neuromuscular changes induced by a short period of lower limb unloading (10 days of ULLS) followed by active recovery (21 days of resistance exercise), with a particular focus on changes in NMJ transmission stability, motor unit potential (MUP) characteristics and underlying molecular mechanisms. The main findings of this study are: (i) human NMJs are functionally resilient despite molecular destabilisation induced by a short period of unloading, at least at relatively low contraction intensity (activity of low-threshold, slow-type MUs); (ii) unloading causes alterations in MUP and near fibre (NF) MUP characteristics and (iii) the AR period reversed most of these neuromuscular changes.

Muscle structure and function and NMJ alterations with unloading

The 10-day ULLS intervention resulted in marked impairments of quadriceps muscle isometric force and capacity for rapid force production (TTP63%). These functional impairments were accompanied by a 4.5% loss in quadriceps size, in line with a previous study reporting a ∼5% decrease in quadriceps CSA after 14 days of ULLS (de Boer *et al.*, 2007).

Our results show a modest but significant increase in CAF concentration at the end of the unloading period suggesting that 10 days of unilateral limb unloading was sufficient to induce initial NMJ

molecular instability. The increase in CAF concentration in the present study appears less pronounced than that observed after 10-day bed rest (5.4% vs 19.2%, respectively) (Monti *et al.*, 2021), most likely due to the lower muscle mass undergoing unloading (one leg in ULLS versus whole body in bed rest). NMJ molecular alterations with unloading were further suggested by our RNA-Seq results, showing changes in the expression of many genes known to be involved in NMJ regulation. Among these, *CHRNA1*, *CHRNB1, CHRND* and *CHRNG*, coding for the α1, β, δ (all normally expressed in adult skeletal muscle) and ϒ (a fetal form) subunits of the ACh receptor, were found to be upregulated between baseline and after ULLS. In normal conditions, ACh receptor expression is limited to the synaptic region and the ϒ subunit is maintained only at very low expression levels. However, it is well-established that with denervation and motoneuron dysfunction muscle fibres re-express the fetal ϒ subunit and in addition, ACh receptors are re-expressed over their whole surface (Hughes *et al.*, 2006; Soendenbroe *et al.*, 2021). Thus, the upregulation of these genes may represent the onset of these processes and a first sign of an altered innervation pattern. In addition, downregulation of the gene encoding for acetylcholinesterase (*ACHE*) and its noncatalytic subunit (*COLQ*) suggests an impairment in the process of ACh elimination from the synaptic cleft, potentially leading to excessive sodium influx through ACh receptor channels which could in turn damage the post-synaptic membrane (Hughes *et al.*, 2006; Tintignac *et al.*, 2015). Interestingly, our findings are in agreement with a recent meta-analysis based on previously published transcriptomics datasets, detecting *CHRNA1, CHRND* and *COLQ* among the top inactivity-responsive genes (Pillon *et al.*, 2020). In addition, genes regulating Homer proteins, which are known to be involved in the expression of synaptic genes via the calcineurin-nuclear factor of activated T-cells (NFATc1) signalling pathway (Nishimune *et al.*, 2014), were downregulated, as previously reported with both short-term (10 days) (Monti *et al.*, 2021) and long-term (60 days) bed rest (Salanova *et al.*, 2011). Changes in the expression of some genes regulating neuregulins (*NRG2*), neurotrophins (*NT4* and *GDNF*) and the ErbB (*ERBB2* and *ERBB3*) and Wnts (*WNT4* and *WNT9A*) family, which can contribute to NMJ maintenance in different ways (Gonzalez-Freire *et al.*, 2014; Nishimune *et al.*, 2014; Bloch-Gallego, 2015; Tintignac *et al.*, 2015), further confirm initial NMJ molecular instability. Although we did not investigate changes in NMJ morphology, overall our findings highlighted initial and early NMJ instability at the molecular level with unloading, in agreement with previous research conducted in animal models (Pachter & Eberstein, 1984; Fahim & Robbins, 1986; Fahim, 1989; Deschenes & Wilson, 2003). The present study did not aim to investigate the causes of NMJ damage with ULLS, however, possible players could be (i) oxidative damage due to mitochondrial dysfunction (Rygiel *et*

al., 2016), (ii) inflammation (Gonzalez-Freire *et al.*, 2014) and (iii) altered calcium transients pattern due to decreased nerve activity (Schiaffino & Serrano, 2002).

However, contrary to our hypothesis, NMJ transmission stability, assessed through the electrophysiological evaluation of NF MUP jiggle and segment jitter, was unchanged after ULLS. This finding supports the body of literature highlighting that the NMJ is a functionally robust structure able to compensate for different insults and stresses (Robbins, 1992; Wood & Slater, 2001; Plomp, 2017). The safeguarding of NMJ transmission is regulated by its safety factor (Wood & Slater, 2001). This term is based on the concept that the amount of quanta of ACh released and the induced depolarisation of the postsynaptic membrane (endplate potential) per nerve impulse are much greater than that required to generate an action potential in the muscle fibre (Wood & Slater, 2001). This phenomenon makes NMJ transmission an extremely reliable process under various physiological and pathophysiological conditions. Our CAF concentration and transcriptomic profile results indicate an initial NMJ molecular instability after the ULLS intervention that could potentially have functional implications, affecting quantal release and/or the endplate potential. However, these stresses were probably insufficient for reducing the NMJ safety factor, and thus unlikely to impair NMJ transmission stability. Moreover, it is worth noting that the NMJ is known to exhibit remarkable compensatory plasticity that can counterbalance the safety factor reduction in aging and disease scenarios (Robbins, 1992; Plomp, 2017), with similar positive remodelling that may occur also with unloading. In support of this concept, in animal studies investigating neurotransmitter handling with disuse/unloading, unchanged or increased release of quanta of ACh was previously found (Robbins & Fischbach, 1971; Snider & Harris, 1979; Tsujimoto & Kuno, 1988). Although we showed no differences in NMJ function after 10-day ULLS, we cannot exclude that different results may be observed with longer periods and/or more extreme forms of disuse/unloading, such as casting or dry-immersion. In fact, the only study that investigated these aspects in humans based on 28-day cast immobilization found increased jitter in the soleus of healthy subjects (n = 6; aged 21 to 48 years) (Grana *et al.*, 1996). These observations prompt us to hypothesise that human NMJs are only transiently resilient from a functional perspective to muscle unloading and that NMJ functional impairment is likely to occur beyond 10 days of unloading. Finally, contraction intensity should also be considered. In our study, participants were asked to perform contractions up to 25% MVC and, therefore, we acknowledge that our findings might be limited to relatively low-intensity contractions. Indeed, we recorded the activity only of low-

threshold, slow-type MUs and these may have been differently affected by unloading compared to high-threshold, fast-type MUs.

Changes in MUP characteristics with unloading and underlying mechanisms

We report that MU electrophysiological properties were altered following ULLS. To the best of our knowledge, only few pioneering studies investigated the effects of immobilisation on human MUs and MUP characteristics, showing reduced MU firing rates in small hand muscles (specifically, the adductor pollicis and the first dorsal interosseous) following disuse during submaximal (Seki *et al.*, 2001) and maximal contractions (Duchateau & Hainaut, 1990; Seki *et al.*, 2007). Similarly, in our study we observed increased IDI_{mean} values, reflecting decreases in mean MU firing rates, potentially explained by reduced ability to activate MUs, as suggested by declines in the activation capacity (evaluated using the interpolated twitch technique) after ULLS. Moreover, our observation of an increase in neurofilament light chain levels after 10 days of ULLS, indicating axonal damage, seems consistent with the observed decrease in MU firing rates. These findings suggest an early impairment upstream to the NMJ (central nervous system and/or motoneuron) that could potentially contribute to the marked loss of muscle function observed.

In addition, our results showed increased MUP turns, NF MUP duration and NF count, overall indicating a more complex MUP and NF MUP shape. Interestingly, employing iEMG, similar changes in MUP and NF MUP properties were previously observed with ageing (Piasecki *et al.*, 2016*c*, 2016*a*; Kirk *et al.*, 2019) and neuromuscular diseases such as neuropathies (Allen *et al.*, 2015; Estruch *et al.*, 2019; Gilmore *et al.*, 2020). MUP and NF MUP features are the result of the summation of MFPs generated by the fibres of its MU. Thus, alterations in MUP and NF MUP properties are a reflection of the temporal dispersion of propagating muscle fibre action potentials (MFAPs) at the recording point (i.e., needle axial location) (Piasecki *et al.*, 2021). Additionally, declines in both axonal (due to demyelination of axonal twigs) and muscle fibres conduction velocities could contribute to magnify previously undetectable differences in temporal dispersion of propagating MFAPs at the recording point. A potential mechanism that could explain these differences in conduction times along axonal branches and/or muscle fibres are denervation/reinnervation processes (Piasecki *et al.*, 2021). We showed that unloading may have caused some initial and partial processes of denervation, as suggested for instance by upregulation of genes regulating ACh receptor subunits (see above) and increased percentage of NCAM-positive fibres, previously reported also by other studies (Arentson-Lantz *et al.*, 2016; Demangel *et al.*, 2017; Monti *et al.*, 2021). However, we did not find any evidence

of an increase in the percentage of fibre type grouping (both for slow and fast fibres) or the presence of flat-shaped/angulated and regenerating neonatal myosin-positive fibres following ULLS. In addition, using iEMG, we observed no spontaneous activity (i.e., no fibrillation potentials of denervated muscle fibres or fasciculation potentials of spontaneously active MUs). Overall these findings suggest initial and partial alterations in muscle innervation status occurring during short-term (10-day) unloading, potentially contributing to the changes in MUP characteristics observed, but in absence of marked denervation/reinnervation processes. Since the propagation velocity of an MFAP increases with increasing muscle fibre diameter (Nandedkar & Stalberg, 1983; Methenitis *et al.*, 2016), fibre diameter variability could also contribute to less synchronous MFAPs propagation (Piasecki *et al.*, 2021). However, this parameter was unchanged after ULLS. Changes in the ion channels dynamics, involved in resting membrane conductance and MFAPs propagation along the sarcolemma (Jurkat-Rott & Lehmann-Horn, 2004) and previously reported to be altered with unloading in animal models (Desaphy *et al.*, 2001; Pierno *et al.*, 2002; Tricarico *et al.*, 2010), could represent a possible mechanism underpinning the observed alterations in MUP and NF MUP characteristics. In support of this hypothesis, overall skeletal muscle ion channels gene expression was downregulated following ULLS, highlighting a possible ongoing remodelling of ion channels pool. Since unloading conditions are commonly experienced after injury, surgery and illness, these novel findings of electrophysiological alterations and underlying molecular mechanisms have considerable physiological and clinical relevance.

Neuromuscular effects of the active recovery period

The last aim of our study was to investigate the effects of an AR intervention based on resistance exercise carried out following ULLS. While it is well established that an AR period can reverse the reduction in muscle mass and function following unloading (Hortobagyi *et al.*, 2000; Suetta *et al.*, 2009; Campbell *et al.*, 2013), whether it could be effective also in counteracting NMJ molecular alterations and changes in electrophysiological properties was currently unknown. Our results demonstrate that total recovery in muscle function (i.e., MVC) was achieved after 21 days of AR, while after 10 days, muscle strength was not yet restored. Similarly, muscle size, NMJ molecular stability and iEMG outcomes were largely restored within 21 days of AR. CAF concentration at AR21 was no longer significantly different from LS0. Overall, the NMJ and ion channels gene expression seem mostly restored at the end of the AR period. In fact, gene expression at AR21 reached values similar to baseline, with only a limited number of genes that were differently regulated comparing

LS0 and AR21. The strong anti-correlation of GSEA leading-edge genes (Figure 5) represents an additional robust manifestation of unloading reversal on transcriptomic profile.

Regarding electrophysiological properties, IDI_{mean} (10% MVC only) and MUP complexity were restored at AR21, while NF count and NF MUP duration remained elevated. We also observed a reduction in MUP size (MUP area and duration) at AR21 compared to both LS0 and LS10. Since MUP size is related to the recruitment threshold of a MU (Pope *et al.*, 2016; Del Vecchio *et al.*, 2017), a possible explanation for this finding may be the fibre type shift towards a slower phenotype (increased percentage of type I fibres) observed after the end of AR, which could have led to a higher contribution from low-threshold MUs during the isometric tasks. A second explanation could be that the AR protocol improved overall neuromuscular control during submaximal isometric contractions investigated in this study, so it became more efficient, achieving the target force output with a pool of relatively smaller, lower threshold MUs. Finally, NF MUP jiggle decreased at 10% MVC post-AR. This could suggest that NMJ transmission stability may be improved by resistance training in humans, although it should be considered that smaller MUPs have generally lower NF MUP jiggle. The reasons behind these differences not observed at 25% MVC should be further investigated in future studies.

In conclusion, with this study, we show that human NMJs are destabilized at the molecular level but not functionally impaired by short-term (10 days) unloading, suggesting that NMJ transmission stability is a particularly robust process, at least at relatively low contraction intensities, at which slow-type MUs are recruited. Moreover, our findings highlight that changes in MUP and NF MUP characteristics occur following ULLS, possibly due to alterations in the dynamics of skeletal muscle ion channels, initial signs of axonal damage and partial denervation. Finally, 21 days of resistance training seems sufficient to restore neuromuscular integrity and function to baseline levels.

ADDITIONAL INFORMATION

Data Availability Statement

RNA-Seq datasets are available at the Gene Expression Omnibus repository: https://www.ncbi.nlm.nih.gov/geo/query/acc.cgi?acc=GSE211204. The other data that support the findings of this study will be made available from the corresponding author upon reasonable request.

Competing interests

The authors have no conflict of interest to declare.

Author contributions:

FS, GV, MVF, GDV, CR and MVN conceptualised and designed the study. MVN obtained the funding. FS, GV, GS and MP performed data collection. FS performed iEMG analysis, with the supervision of DWS and JSMP. FS analysed in vivo muscle morphology and function data. EM and SZ cut cryosections and carried out immunochemistry and ATPase analysis. GS performed ELISA to obtain CAF results. LMH performed RNA extraction, while JC and LG carried out RNA-Seq analysis. FS drafted the manuscript and all the authors revised it. All the authors approved the final version of the manuscript and agreed to be accountable for all aspects of the work, ensuring that questions related to the accuracy or integrity of any part of the work are appropriately investigated and resolved.

Funding

The present study was funded by the Italian Space Agency (ASI), MARS-PRE, Project, n. DC-VUM-2017-006. The authors are grateful to ASI for granting these funds to allow all the experiments to be performed.

Acknowledgements

The authors would like to thank Mr. Enrico Roma for the precious suggestions on statistical analysis, Dr. Leonardo Nogara and Dr. Luana Toniolo for helping during part of the muscle biopsy collection, Dr. Tommaso Giacon and Dr. Nicola Borasio for helping during iEMG and clinical procedures, Mr. Paul Ritsche, Mr. Lorenzo Pavan and Mr. Leonardo Cavaggioni for helping during the training sessions and Dr. Marco Pirazzini and Dr. Giulia Zanetti for the suggestions in the revision of the manuscript.

Supporting information

Additional supporting information can be found online in the Supporting Information section at the end of the HTML view of the article

(https://physoc.onlinelibrary.wiley.com/doi/full/10.1113/JP283381). Supporting information files available:

Peer Review History

Statistical Summary Document

Data S1

Data S2

Data S3

4. Pathophysiological mechanisms of reduced physical activity: insights from the human step reduction model and animal analogues

Fabio Sarto[1], Roberto Bottinelli[2,3], Martino V. Franchi[1,4], Simone Porcelli[2], Bostjan Simunič[5], Rado Pišot[5] and Marco V. Narici[1,4,5]

[1] Department of Biomedical Sciences, University of Padova, Padova, Italy

[2] Department of Molecular Medicine, Institute of Physiology, University of Pavia, Pavia, Italy

[3] IRCCS Mondino Foundation, Pavia, Italy

[4] CIR-MYO Myology Center, University of Padova, Padova, Italy

[5] Science and Research Center Koper, Institute for Kinesiology Research, Koper, Slovenia

Running title: Mechanisms of reduced physical activity

Correspondence:

Mr. Fabio Sarto: Department of Biomedical Sciences, University of Padova, Padova, Italy, 35131, Italy - Email: fabio.sarto.2@phd.unipd.it – ORCID: https://orcid.org/0000-0001-8572-5147

Prof. Marco V. Narici: Department of Biomedical Sciences, CIR-MYO Myology Centre, University of Padova, Padova, 35131, Italy - Email: marco.narici@unipd.it - ORCID: https://orcid.org/0000-0003-0167-1845

Acknowledgements: The present study was funded by the Italian Ministry of Education, Universities and Research (MIUR) (PRIN project ''InactivAge" n. 2020EM9A8X, to RB and MVN) and the Slovenian Research Agency (project J5-4593, to BS and RP). The authors would like to thank Dr. Elena Monti for her precious comments and suggestions regarding our manuscript.

Conflict of interest: The authors have no conflict of interest to declare.

The article has been published in *Acta Physiologica* and can be found at https://doi.org/10.1111/apha.13986

Abstract

Physical inactivity represents a heavy burden for modern societies and is spreading worldwide, it is a recognised pandemic and is the fourth cause of global mortality. Not surprisingly, there is an increasing interest in longitudinal studies on the impact of reduced physical activity on different physiological systems. This narrative review focuses on the pathophysiological mechanisms of step reduction (SR), an experimental paradigm that involves a sudden decrease in participants' habitual daily steps to a lower level, mimicking the effects of a sedentary lifestyle. Analogous animal models of reduced physical activity, namely the "wheel-lock" and the "cage reduction" models, which can provide the foundation for human studies, are also discussed. The empirical evidence obtained thus far shows that even brief periods of reduced physical activity can lead to substantial alterations in skeletal muscle health and metabolic function. In particular, decrements in lean/muscle mass, muscle function, muscle protein synthesis, cardiorespiratory fitness, endothelial function and insulin sensitivity, together with an increased fat mass and inflammation, have been observed. Exercise interventions seem particularly effective for counteracting these pathophysiological alterations induced by periods of reduced physical activity. A direct comparison of SR with other human models of unloading, such as bed rest and lower limb suspension/immobilisation, is presented. In addition, we propose a conceptual framework aiming to unravel the mechanisms of muscle atrophy and insulin resistance in the specific context of reduced ambulatory activity. Finally, methodological considerations, knowledge gaps and future directions for both animal and human models are also discussed in the review.

Keywords

Cage reduction; disuse; inactivity; insulin sensitivity; muscle atrophy; wheel-lock

1. Introduction

Physical inactivity is a major cause of chronic diseases (Booth *et al.*, 2017) and has been recognised as the fourth cause of global death (WHO, 2015), representing a heavy economic burden for modern society (Ding *et al.*, 2016; Costa Santos *et al.*, 2022). Physical inactivity is considered a pandemic (Kohl *et al.*, 2012; Andersen *et al.*, 2016), requiring global action for public health (World Health Organization, 2018). About 30% of the population is estimated to be physically inactive, a trend growing considerably in high-income countries (Guthold *et al.*, 2018). From an evolutionary perspective, physical inactivity represents a strategy for energy-saving and reducing the risk of predation, snake bites and musculoskeletal injury (Speakman, 2020). However, our hunter-gatherer ancestors, due to the dominant urge to collect food to eat, never experienced low levels of physical activity that could be harmful to their health. Thus, no corresponding mechanism for avoidance of physical inactivity evolved (Speakman, 2020).

Since the seminal work of Morris et al. in the 1950s (Morris *et al.*, 1953), showing a higher occurrence of coronary disease in bus drivers (a sedentary work) compared to bus conductors (a physically active work), most indirect evidence examining the detrimental effects of physical inactivity has derived from epidemiological (mainly cross-sectional) studies. However, there is mounting interest in inactivity experimental (longitudinal) studies to investigate the mechanisms by which physical inactivity impacts different physiological systems. Most of the previous studies investigating these aspects have been conducted in laboratory settings employing extreme models of disuse/unloading (e.g. bed rest, dry-immersion, unilateral limb suspension, knee bracing) (de Boer *et al.*, 2007; Brocca *et al.*, 2012; Wall *et al.*, 2014; Demangel *et al.*, 2017; Monti *et al.*, 2021; Zuccarelli *et al.*, 2021; Sarto *et al.*, 2022*b*). Such unloading models have provided essential knowledge in the understanding of the remarkable skeletal muscle plasticity and how physical inactivity leads to muscle wasting and metabolic dysfunction in different populations (de Boer *et al.*, 2007; Brocca *et al.*, 2012; Wall *et al.*, 2014; Demangel *et al.*, 2017; Monti *et al.*, 2021; Zuccarelli *et al.*, 2021; Sarto *et al.*, 2022*b*). Bed rest and dry immersion, by forcing volunteers to lay down for days or weeks, represent excellent models for comprehending the systemic effects of unloading (Zuccarelli *et al.*, 2021; Murgia *et al.*, 2022), while single limb disuse models (i.e. unilateral limb suspension, knee bracing) affords the opportunity for investigating unloading mostly at a local muscle level, although some effects at systemic level are still observed (Sarto *et al.*, 2022*b*).

More recently, an additional physical inactivity systemic model, termed step reduction (SR), has been proposed (Olsen *et al.*, 2008; Krogh-Madsen *et al.*, 2010). SR consists in inducing a sudden

reduction in participants' habitual daily steps (generally assessed by a pedometer and/or an accelerometer) to a lower maximal steps limit, ranging from ∼750 to ∼4500 steps/day (Oikawa *et al.*, 2019*b*). When compared to the traditional disuse models, SR is considered a less extreme form of physical inactivity, since participants are still exposed to loading stimuli (Bell *et al.*, 2016; Bowden Davies *et al.*, 2019; Oikawa *et al.*, 2019*b*). However, SR represents an attractive model as it is closer to real-life conditions and more appropriate to mimic the deleterious effects of a sedentary lifestyle (Thyfault & Krogh-Madsen, 2011; Perkin *et al.*, 2016; Bowden Davies *et al.*, 2019; Oikawa *et al.*, 2019*b*). In fact, SR appears well suited for mimicking a decrease in everyday life activities which supports most daily energy consumption and has been shown to increase health risk (Speakman & Selman, 2003; Frühbeck, 2005). In addition, it is important to consider that periods of reduced physical activity occur more frequently than events of prolonged bed rest or limb immobilization (Oikawa *et al.*, 2019*b*), as for instance occurred during the COVID-19 pandemic (Desine *et al.*, 2023). Low number of daily steps is also strongly associated with an increased risk of all-cause mortality (Jayedi *et al.*, 2021; Sheng *et al.*, 2021; Paluch *et al.*, 2022).

This narrative review aims to examine the impact of SR, focusing on skeletal muscle physiology and metabolic impairment. As analogous models of reduced physical activity used in rodents can provide the foundation for human investigations, they are also discussed first. In addition, methodological considerations, knowledge gaps and future directions for both animal and human models are described.

2. Reduced physical activity models in rodents

Physical inactivity is a serious threat to animals' health and in particular to the skeletal muscle. Several models have been proposed to study its effects in rodents, including hindlimb unloading (also known as "tail suspension") and cast immobilisation (Morey-Holton & Globus, 2002; Cho *et al.*, 2016). These models are considered severe forms of unloading, therefore comparable to human best rest, unilateral limb suspension and immobilisation. In contrast, there are relatively few studies on the effects of reduced daily ambulatory activity in animal models. These studies have typically used either the "wheel-lock" model or the cage reduction model.

2.1. Wheel-lock model

2.1.1. Impact of wheel-lock on insulin sensitivity

The wheel-lock model, sometimes also reported as cessation of voluntary wheel running, was the first attempt in the literature to mimic a sedentary lifestyle. Originally developed by Rhodes et al. (Rhodes *et al.*, 2000, 2003), the wheel-lock model was then employed extensively to study the effects of acute physical inactivity on metabolic dysfunction (Kump & Booth, 2005*b*, 2005*a*). In this model, rodents are provided with running wheels and allowed to voluntarily run for several weeks (3-6 weeks), after which the wheels are locked, causing the cessation of animals' normal activity and thus promoting physical inactivity. Voluntary wheel running is an intermittent activity, performed under non-stressed conditions and does not require the direct intervention of the researcher (Manzanares *et al.*, 2019). Therefore, wheel locking prevents animals' primary source of physical activity, determining the transition from the habitual level of locomotion to a lower daily amount, simulating SR studies in humans.

Wheel-lock studies produced several novel findings related to metabolic maladaptation to physical inactivity. In these studies, rats whose wheels were locked for only 5 h (WL5) constituted the control group, while rats whose wheels were locked for longer periods, including 29 h (WL29), 53 h (WL53), and in some studies also 173 h (WL173), represented the groups were inactivity was induced. Rats who never had access to voluntary wheel running constituted the sedentary group. In their first WL study (Kump & Booth, 2005*b*), insulin-stimulated 2-deoxyglucose uptake into the epitrochlearis muscle was lower in WL53 and the sedentary rats compared to WL5, indicating a rapid reduction in insulin sensitivity induced by the intervention. In addition, muscle insulin receptor ligation and signalling alterations, associated with reduced GLUT4 protein levels, were observed (Kump & Booth, 2005*b*). Noteworthy, another study showed higher plasma insulin and triglyceride concentrations in WL53 rats when compared with animals that had continuous running wheel access (Kump *et al.*, 2006). A recent investigation excluded the hypothesis that changes in muscle ceramides, a family of waxy lipid molecules considered involved in insulin sensitivity, are involved in this inactivity-induced insulin resistance (Appriou *et al.*, 2019). Differently, a decreased gene expression of two key mechanical stretch sensors (Ankrd2 and Csrp3) that play a role in skeletal muscle metabolism and hypertrophy was reported (Roberts *et al.*, 2012).

2.1.2. Impact of wheel-lock on fat mass and inflammation

Adipose mass changes rapidly in response to wheel-lock (Kump & Booth, 2005*a*; Laye *et al.*, 2007, 2009; Rector *et al.*, 2008; Company *et al.*, 2013). Fifty-three hours of wheel-lock increased relative omental and epididymal fat masses as well as triacylglycerol synthesis rates (Kump & Booth, 2005*a*), independently from food intake/energy balance (Laye *et al.*, 2007). Rector et al. (Rector *et al.*, 2008),

employing a rat model of obesity, after 16 weeks of voluntary wheel running with subsequent wheel-lock, observed increased omental and retroperitoneal fat pad masses, hepatic triglycerides and protein markers of fatty acid synthesis in the sedentary group with respect to WL5-, WL53-, and WL173-hour animals. Another study carried out in obese rats observed higher lipid peroxidation levels in epitrochlearis muscles of the sedentary group than WL5, WL53, and WL173 rats (Morris *et al.*, 2008). An additional investigation from the same group reported that the transition from high to low physical activity levels caused a reduction in fatty acid oxidative capacity in skeletal muscle, liver, and adipocytes, accompanied by fat pad mass increase, attenuated growth of lean body mass and reduced PGC1-α mRNA in both skeletal muscle and liver (Laye *et al.*, 2009). Company et al. examined the role of age (49–56 vs. 70–77 days of age) on the growth of adipose tissue mass and adipocyte size following 7 days of wheel-lock (Company *et al.*, 2013). Compared with rats that always had wheel access, 70- to 77-day-old animals had increased rates of gain in fat mass, greater adipocyte number, more small adipocytes and greater cyclin A1 mRNA in epididymal and perirenal adipose tissue.

Alterations in mRNA and protein expression in the iliac artery tissue of genes associated with inflammation (TNFR1 and ET-1) and oxidative stress (LOX-1) in the WL173 group were also observed (Padilla *et al.*, 2013). Another study, besides reporting increases in fat mass and body fat percentage, observed 646 differentially expressed transcripts in perirenal adipose tissue comparing rats with continued wheel access and wheel-lock rats (Ruegsegger *et al.*, 2015). These findings suggest that reduced mobility promotes alterations of multiple pathways related to extracellular matrix remodelling, macrophage infiltration, immunity, and pro-inflammatory function, some of which may exacerbate the development of obesity.

2.1.3. Impact of wheel-lock on brain and neural function

The wheel-lock model and other very similar models have been employed by other research groups to study the effects of physical inactivity on other factors of animal health, including the brain and neural function. For instance, differential short-term changes in brain activity (evaluated through Fos-positive cells) in numerous brain regions were detected in mice blocked from reaching their wheel compared with those always having access to the wheel (Rhodes *et al.*, 2003). Mice housed in a running wheel cage for 8 weeks and subsequently moved to a standard cage were more anxious and exhibited impaired hippocampal neurogenesis (Nishijima *et al.*, 2013). Similarly, another report suggested that forced cessation of voluntary wheel running increases anxiety-like behaviours in

rodents and exercise-induced stress resistance endured following wheel-lock (Greenwood *et al.*, 2012). Furthermore, a study reported a rapid decrease in BDNF mRNA in the hippocampus of hypertensive rats after the cessation of long-term voluntary wheel running (Widenfalk *et al.*, 1999), while conversely, a second study reported an increase in BDNF protein in the hippocampus (Berchtold *et al.*, 2010).

2.2. Cage reduction models

The cage reduction model represents an alternative approach for reducing physical activity in rodents. This model is based on the modification of rodents' home cage size and features, thereby reducing their voluntary ambulatory activity. Indeed, despite locomotor behaviour being already limited in captivity, rodents do walk around and lid climb in their cages (Bains *et al.*, 2018). Although the use of small cages is not new in rats (Barański *et al.*, 1971; Mondon *et al.*, 1983; Suvorava *et al.*, 2004; Takemura *et al.*, 2016; Marmonti *et al.*, 2017; Belova *et al.*, 2021), this approach has been re-adapted also in a few recent investigations in mice in the context of muscle adaptations and insulin resistance (Roemers *et al.*, 2019; Mahmassani *et al.*, 2020). Employing this model, reducing the living space by varying degrees, muscle atrophy (Barański *et al.*, 1971; Fushiki *et al.*, 1991; Takemura *et al.*, 2016; Belova *et al.*, 2021), reduced muscle protein synthesis (Belova *et al.*, 2021) and reduction in local (Fushiki *et al.*, 1991; Mahmassani *et al.*, 2020) and whole-body (Barański *et al.*, 1971; Mahmassani *et al.*, 2020) insulin sensibility have been shown to occur.

In a recent study conducted (Roemers *et al.*, 2019), the authors placed a plexiglass spacer in the middle of a standard type 2 macrolon cage, thus reducing the available cage volume (Roemers *et al.*, 2019). To prevent lid climbing, a sheet of plastic having small holes was positioned under the standard wire lid and fixed using cable ties (Roemers *et al.*, 2019). In addition, drinking bottles were placed so that the nozzle did not stick out and a piece of plastic was placed in all other wire lids to prevent possible licking or gnawing on the plastic. In this study, mice were allocated in six conditions: one for each of three different cage sizes with lids that either allowed or prevented lid climbing. Employing this model, the authors found that preventing climbing reduced motor coordination, muscle strength and muscle stamina after 5 and 10 weeks of intervention (Roemers *et al.*, 2019). In addition, a further reduction in cage size affected motor coordination but not grip strength or muscle stamina. Moreover, preventing climbing increased visceral fat mass but did not induce muscle atrophy over 19 weeks.

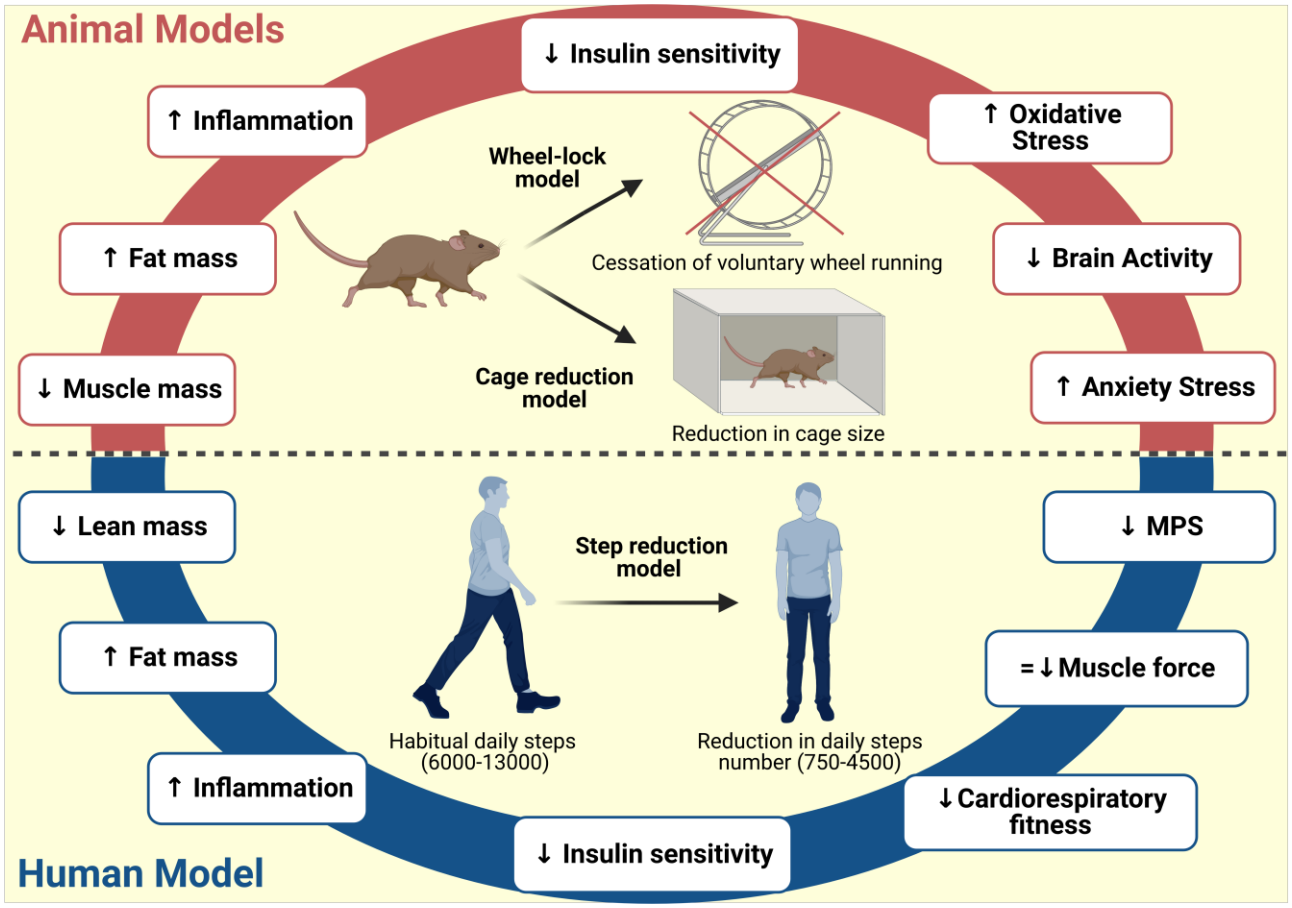

Figure 1: *Deleterious effects of step reduction and analogous animal models (wheel- lock and cage reduction). Created with BioRender.com. MPS, muscle protein synthesis.*

2.3. Methodological considerations and future directions for animal studies

In summary, both the wheel-lock and cage reduction seem appropriate models for studying the mechanisms by which reduced physical activity impacts the function of different physiological systems in animals (Figure 1). Blocking wheel access or changing cage type (i.e. from a cage equipped with a running wheel to a standard cage) should be preferred to conventional wheel-lock because mice do climb in their wheels also when they are locked (Rhodes *et al.*, 2000). Cage reduction volume should be selected carefully based on the study aim, as an excessive reduction could almost abolish animals movements, making this model more akin to an animal physiological analogue for bed rest (Marmonti *et al.*, 2017). A possible approach for future studies to further exacerbate inactivity-induced effects may be to apply both models in the same study design, reducing cage size after the cessation of daily voluntary wheel running (Reidy *et al.*, 2021). This has only been implemented in a limited number of studies thus far (Mondon *et al.*, 1983; Mahmassani *et al.*, 2020). Individual housing could represent a more severe physical inactivity model compared to partner or

social housing (Cole *et al.*, 2021; Funabashi *et al.*, 2022). For a better quantification of ambulatory activity reduction, future studies should evaluate in-cage habitual physical activity levels. Individual voluntary wheel running activity can be monitored via running wheels' number of revolutions or different commercially available systems (Bains *et al.*, 2018; Mayr *et al.*, 2020). Moreover, in-cage spontaneous physical activity can be recorded through video-tracking or other wireless procedures (Redfern *et al.*, 2017; Poffé *et al.*, 2018). Finally, using these models, very little attention has been paid to the impact of reduced physical activity on neuromuscular and cardiovascular systems; these aspects should be further investigated. Methodological considerations for animal models are summarised in Figure 2.

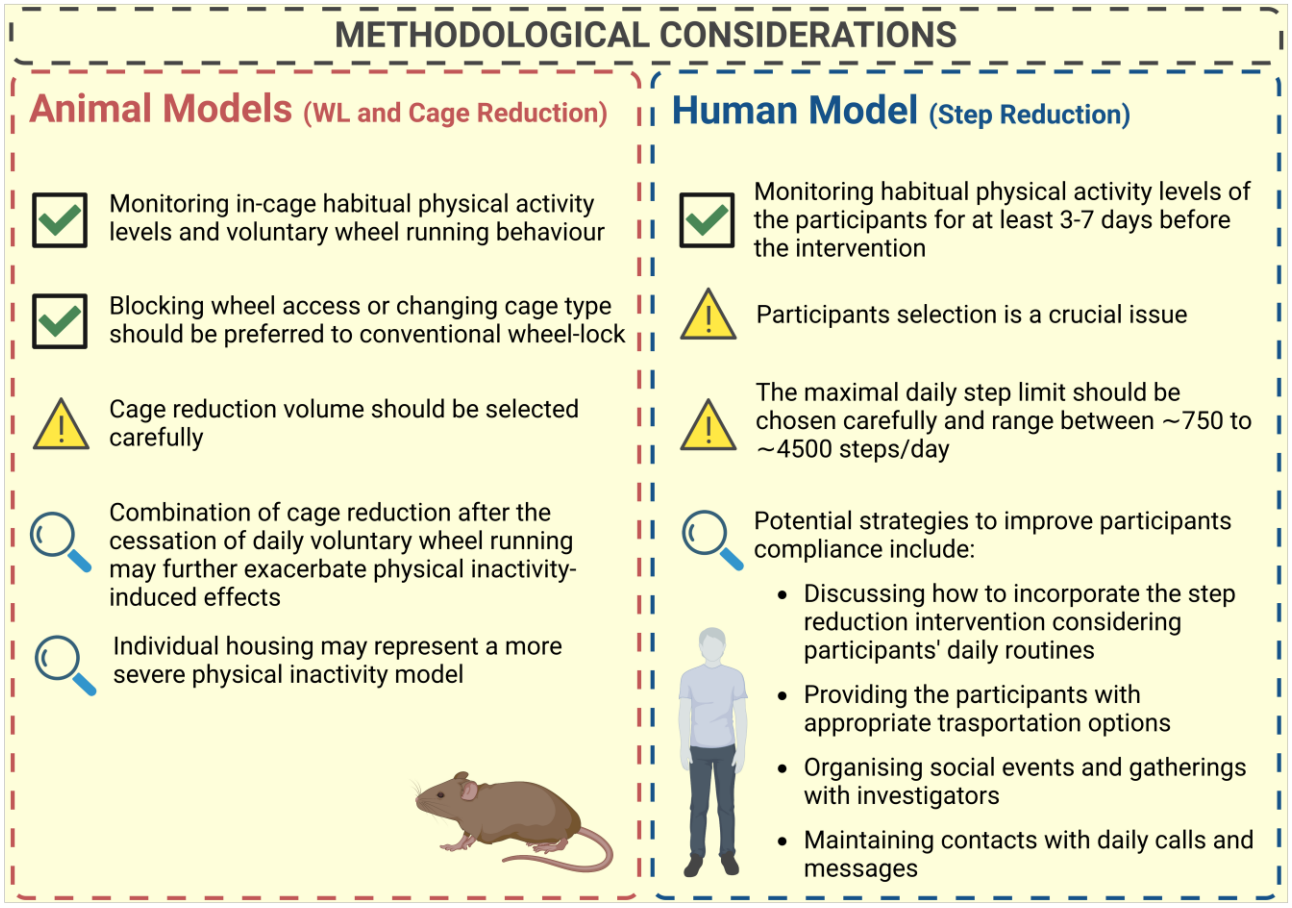

Figure 2: *Summary of the methodological considerations for animals and human models of reduced physical activity. Created with BioRender.com. WL, wheel- lock.*

3. Step reduction model in humans

In 2008, the SR model was originally designed to study changes in insulin sensitivity and adiposity in response to reduced physical activity in humans (Olsen *et al.*, 2008; Krogh-Madsen *et al.*, 2010). Ever

since this model has been employed to investigate the impact of reduced physical activity also on other physiological systems (Table 1 and Figure 1).

3.1. Impact of SR on metabolic function, body composition and inflammation

The seminal study by Olsen et al. was the first one to show the pathophysiological consequences of SR(Olsen *et al.*, 2008). Young healthy participants reduced their habitual daily steps from ∼10000 steps/day to ∼1300 steps/day, simply through a change in lifestyle behaviour (e.g. taking the elevator instead of stairs and using cars instead of walking or cycling). After 3 weeks, participants underwent metabolic changes indicative of decreased insulin sensitivity (assessed with the oral glucose tolerance test) and attenuation of postprandial lipid metabolism (evaluated with oral fat tolerance test), accompanied by increased intra-abdominal fat and decreased total fat-free mass (Olsen *et al.*, 2008). Alterations in insulin sensitivity and body composition following periods of SR (ranging from 3 days to 2 weeks) were confirmed also by later studies in young subjects (Krogh-Madsen *et al.*, 2010, 2014; Knudsen *et al.*, 2012; Mikus *et al.*, 2012; Walhin *et al.*, 2013; Reynolds *et al.*, 2015; Bowden Davies *et al.*, 2018, 2021; Shad *et al.*, 2019), middle-aged men(Dixon *et al.*, 2013) and older adults(Breen *et al.*, 2013; McGlory *et al.*, 2018; Reidy *et al.*, 2018), independently from whether the SR interventions were carried out in combination with overfeeding or not.

Investigating possible mechanisms behind these alterations, a recent study found a decline in maximal citrate synthase activity (a marker of mitochondrial content) and an increase in the protein content of p-glycogen synthase (P-GS^{S641}; a marker of reduced glycogen synthase activation) following 7 days of SR (<1500 steps/day) in the skeletal muscle (Edwards *et al.*, 2021). Differently, these authors reported no changes in total protein or phosphorylation content of markers of insulin-mediated signalling, mitochondrial function (e.g. oxidative phosphorylation complex I-V), oxidative metabolism (e.g. PGC1-α, AMPKa), or mitochondrial dynamics (e.g. FIS1, DRP1, and MFN2), possibly due to the short duration of the intervention. In addition, another study reported only modest changes in ceramides content following reduced activity and recovery (Reidy *et al.*, 2018). In studies conducted in older adults, a rise in inflammatory cytokines (levels of TNF-α, IL-6 and CRP) (Breen *et al.*, 2013; McGlory *et al.*, 2018), associated with changes in muscle inflammation cell signalling (JNK (Thr183/Tyr185), IκBα, AKT (Ser473), TLR4 and SPT2)(Reidy *et al.*, 2018) and increase in muscle macrophages (Reidy *et al.*, 2019), were detected in response to SR, contrary to what was observed in young (Krogh-Madsen *et al.*, 2010, 2014; Knudsen *et al.*, 2012) and middle-aged (Dixon *et al.*, 2013) adults. It has been hypothesized (Oikawa *et al.*, 2019*b*) that this difference in the

inflammatory response could lead to an impaired regenerative capacity that may explain why younger individuals recover from SR (Knudsen *et al.*, 2012; Bowden Davies *et al.*, 2018), while older individuals not always (McGlory *et al.*, 2018).

Investigating potential countermeasures, one study examined the effects of 45min of daily treadmill aerobic training on young healthy subjects undergoing a week of step reduction combined with overfeeding (Walhin *et al.*, 2013). The exercise intervention was effective in counteracting most of the alterations in metabolic function and adipose tissue metabolism that were observed in the control group (Walhin *et al.*, 2013). Despite this interesting finding, it should be considered that background inactivity (i.e. a low number of daily steps) can blunt metabolic benefits in response to both acute (Kim *et al.*, 2016; Akins *et al.*, 2019; Burton & Coyle, 2021) and chronic (Burton *et al.*, 2021) exercise (for a recent review on this topic we refer the reader to Coyle et al. (Coyle *et al.*, 2022)). An additional countermeasure that could be potentially interesting for limiting the metabolic impact of SR without actually increasing the number of the daily steps would be to increase the non-exercise activity thermogenesis (NEAT) (Frühbeck, 2005), employing standing workstations and gymnastic balls (Rizzato *et al.*, 2022).

3.2. Impact of SR on muscle protein turnover

Skeletal muscle is highly malleable tissue that is very sensitive to changes in mechanical loading. Loss of lean/muscle mass is evident and consistent both in young (Krogh-Madsen *et al.*, 2010; Bowden Davies *et al.*, 2018) and older adults (Breen *et al.*, 2013; Devries *et al.*, 2015; McGlory *et al.*, 2018; Oikawa *et al.*, 2018; Reidy *et al.*, 2018) already with the mild unloading stimulus induced from SR. Since declines in muscle protein synthesis (MPS) are considered one of the predominant mechanisms underpinning the loss of muscle mass in human models of disuse/unloading (Phillips & Mcglory, 2014; McKendry *et al.*, 2021; Brook *et al.*, 2022), leading experts in protein metabolism have extensively investigated the changes in integrated rates of MPS in response to SR in older populations (Breen *et al.*, 2013; Devries *et al.*, 2015; McGlory *et al.*, 2018; Oikawa *et al.*, 2018). After 2 weeks of SR (750-1500 steps/day), several studies found reductions in MPS (Breen *et al.*, 2013; McGlory *et al.*, 2018; Oikawa *et al.*, 2018), supporting the concept of muscle disuse-induced "anabolic resistance" (Glover *et al.*, 2008; McKendry *et al.*, 2021). Notably, one of these investigations observed a failed recovery in MPS rates after 2 weeks of resumption to habitual activity in overweight pre-diabetic older adults (McGlory *et al.*, 2018). In the same cohort, the non-targeted metabolite profile assessed from multisegment injection-capillary electrophoresis-mass

spectrometry on fasting plasma samples highlighted changes in circulatory metabolites associated with a decline in muscle energy metabolism and protein degradation (Saoi *et al.*, 2019). This altered metabolite profile was not fully restored after resuming normal ambulatory activity (Saoi *et al.*, 2019). Another recent SR study with ∼80% reduction in daily step number for 2 weeks, leveraging an innovative combined RNA sequencing and ribosomal profiling approach, showed decreased baseline and leucine-stimulated translation of mRNAs encoding for ribosomal proteins and alterations of circadian regulators which may precede adaptations to muscle size and metabolic function (Mahmassani *et al.*, 2021). The rapid dysregulation of MPS in response to reduced ambulatory activity has also been confirmed by a recent study on young healthy adults following one-week SR (<1500 steps/day) (Shad *et al.*, 2019). In this investigation, changes in MPS were accompanied by altered insulin sensitivity and expression of mRNA genes involved in muscle mass regulation and oxidative metabolism. Indeed, myostatin and MAFbx were upregulated after the intervention, whereas mTOR, p53 and PDK4 were downregulated (Shad *et al.*, 2019).

A series of studies investigated the effects of exercise and nutritional countermeasures on these aspects during periods of SR. In two different studies from the same SR campaign conducted on older adults (Devries *et al.*, 2015; Moore *et al.*, 2018), unilateral low-load resistance exercise training (three sessions/week) has been employed to counteract SR-induced muscle alterations. This intervention increased leg lean mass, and muscle function and maintained feeding-induced MPS rates in the exercised vs unexercised leg (Devries *et al.*, 2015). In addition, the training protocol preserved type I and II fibre cross-sectional area, Pax7+ positive cells content and capillarization(Moore *et al.*, 2018). The study by Devries et al. (Devries *et al.*, 2015) was the first one to examine whether different nutritional strategies (20 g whey protein isolate plus 15 g glycine or micellar-whey with 5 g citrulline or 15 g glycin) could attenuate the SR-induced anabolic resistance. However, the authors concluded that none of the proposed supplements attenuated the reduction in MPS following SR (Devries *et al.*, 2015). More recently, older participants were kept in energy balance for one week, then underwent one week of energy restriction, followed by a 2-week combination of energy restriction and step reduction (<750 steps/day), before a recovery period (Oikawa *et al.*, 2018). A supplementation of whey protein or collagen peptides was provided during the intervention. Despite these nutritional strategies did not protect participants against muscle mass loss, whey protein supplementation increased leg lean mass and MPS rates during the recovery phase (Oikawa *et al.*, 2018).

3.3. Impact of SR on muscle function and physical performance

While changes in metabolic function, body composition, muscle mass and MPS rates have been consistently observed in response to SR, evidence regarding muscle and physical function alterations is more controversial. Indeed, in older adults, decreases in knee extensors maximum isometric strength was found in some (Reidy *et al.*, 2018; Oikawa *et al.*, 2019*a*), but not all (Breen *et al.*, 2013; Devries *et al.*, 2015; McGlory *et al.*, 2018) SR studies, despite all having the same duration (2 weeks). Inconsistencies among studies might be due to differences in familiarisation procedures (Oikawa *et al.*, 2019*b*), knee angle set during maximum voluntary contraction and rest between trials. Following 2 weeks of combined energy restriction and SR, another investigation (Oikawa *et al.*, 2019*a*) observed an unexpected increase in maximum isometric tension in type IIA muscle fibres accompanied by augmented maximum power production in type I and IIA vastus lateralis fibres, despite a reduction in knee extensor maximum isometric strength at whole muscle level. To date, no studies have examined changes in muscle strength following SR periods in younger populations. In addition, older adults generally presented unchanged outcomes in physical performance tests (e.g. short physical performance battery, time up and go, six-meter walking test, thirty seconds chair-to-stand) after 2 weeks of reduced ambulatory activity (Breen *et al.*, 2013; Reidy *et al.*, 2018; Oikawa *et al.*, 2019*a*). Differently, as presented above, young adults showed considerable decreases in cardiorespiratory fitness in different studies (Krogh-Madsen *et al.*, 2010, 2014; Knudsen *et al.*, 2012; Bowden Davies *et al.*, 2018, 2021). This finding may be at least partially due to endothelial dysfunction, reported in different SR studies (Boyle *et al.*, 2013; Teixeira *et al.*, 2017; Bowden Davies *et al.*, 2021), similarly to what was observed with short-term bed rest (Zuccarelli *et al.*, 2021), and changes in mitochondrial content (Edwards *et al.*, 2021).

Table 1: Summary of human step reduction studies. 1RM: one-repetition maximum; 6MWT: six minutes walking test; CGM: continuous glucose monitoring; CSA: cross-sectional area; CST: chair to stand; CT: computed tomography; DEXA: Dual-energy X-ray absorptiometry; F: females; FMD: Flow Mediated Dilation; FFA: free fatty acids; H-E clamp: hyperinsulinemic clamp; HFTT: high-fat tolerance test; IL-6: Interleukin 6; OGTT: oral glucose tolerance test; OFTT: oral fat tolerance test; LDL: Low-density lipoprotein; M: males; MPS: muscle protein synthesis; MRI: magnetic resonance imaging; MVC: maximum voluntary contraction; RT: resistance training; SPPB: short physical performance battery; VL: vastus lateralis; VO_2 Max: maximal oxygen consumption; TNF-α: tumor necrosis factor alfa; TUG: timed up and go

Reference	Participants	Reduction in daily steps	Intervention duration	Effects of SR on:			
				Physical and muscle function	Muscle morphology and body composition	Muscle protein turnover / signalling pathway	Metabolism / Vascular function
Bowen-Davies et al 2018[71]	Young adults n=45 (18 M and 27 F)	12780 to 2495 steps/day	2 weeks + 2 weeks resuming activity	↓ treadmill VO_2 Max	DEXA: ↑fat mass, central and liver ↓leg lean mass = arms and trunk lean mass	Not measured	OGTT: ↑ insulin ↑ glucose ↓ Matsuda index = hepatic insulin resistance
Bowen-Davies et al 2021[73]	Young adults n=28 (18F and 10M)	12624 to <1500 steps/day	2 weeks + 2 weeks resuming activity	↓ treadmill VO_2 Max	DEXA: ↑fat mass, central and liver ↓leg lean mass = arms and trunk lean mass	Not measured	OGTT: ↓ Matsuda index Endothelial function: ↓ brachial artery FMD
Boyle et al 2013[99]	Recreationally active young adults n=11 M	12550 to <5000 steps/day	5 days	Not measured	Not measured	Not measured	Endothelial function: = brachial artery FMD ↓ popliteal artery FMD ↑ $CD31^+/CD42b^-$ endothelial microparticles

Breen et al 2013[78]	Older adults n=10 (5 M and 5 F)	5962 to 1413 steps/day	2 weeks	= isometric MVC = Physical function (SPPB)	DEXA: = total body and fat mass ↑ trunk fat mass ↓ leg lean mass	VL biopsy: ↓ MPS = basal MPS ↑inflammatory markers (TNF-α and C-reactive protein) = intramuscular signaling proteins (mTor; 4E-BP1; Akt; p70S6K)	OGTT: ↑ insulin and glucose ↓ Matsuda index
Burton & Coyle 2021[85]	Recreationally active young adults n=10 (7 M and 3 F)	10648 to a different number of daily steps based on the experimental conditions NORMAL: 2675 LIMITED: 4759 LOW: 8481	2 days for each condition 1-h bout of running on the evening of the second day	Not measured	Not measured	Not measured	HFTT: ↑postprandial plasma triglyceride (in LIMITED and LOW vs NORMAL) ↓whole body fat oxidation (in LIMITED and LOW vs NORMAL)
Devries et al 2015[89]	Older adults n=30 M SR+ unilateral retraining	~6200-7700 to ~1160-1280 steps/day	2 weeks	= isometric MVC = 1RM (↑ in the leg with RT)	DEXA: = lean mass, fat mass, appendicular lean mass ↓leg lean mass (↑ in the leg with RT)	MPS assessed but not compared with baseline measures ↓MPS in the leg with no retraining	Assessed but not compared with baseline measures

	3 groups based on supplements						
Dixon et al 2013[77]	Middle-aged adults Group 1 (lean) = 9 M Group 2 (overweight) = 9 M	~13000 to ~4000 steps/day	1 week	Only baseline measures reported	Only baseline measures reported	=TNFα, IL6, CPR, ALT	OGTT: ↑ insulin and glucose = fasting triglyceride
Edwards et al 2021[81]	Recreationally active young adults N=11 M	13054to 1192 steps/day	1 week	Not measured	Not measured	Not measured	↓ maximal citrate synthase activity ↑ protein content of p-glycogen synthase
Knudsen et al 2012[74]	Young adults n=9 M	10028 to 1521 steps/day + overfeeding	2 weeks + 2 weeks resuming activity (alterations already after 3 days)	↓ Cycle VO_2 Max	DEXA: ↑ total body fat ↑ total fat mass = total lean mass MRI: ↑visceral fat	Not measured	OGTT: ↑ insulin = glucose ↓ Matsuda index (at 3 and 7 days) ↑ leptin and adiponectin H-E clamp: ↓ Peripheral insulin sensitivity = hepatic glucose prod.
Krogh-Madsen et al 2010[20]	Young adults n=10 M	10501 to 1344 steps/day	2 weeks	↓ Cycle VO_2 Max	DEXA: ↓ leg lean mass	= inflammation (TNF-α, IL-6, IL-15, leptin, and adiponectin)	H-E clamp: ↓ Peripheral insulin sensitivity = hepatic glucose prod.

					= arm and trunk lean mass = fat mass	VL biopsy: ↓ insulin-stimulated Akt phosphorylation = IR beta and AS160	= fasting bloods
Krogh-Madsen et al 2014[75]	Young adults Group 1: step reduction + overfeeding n=10 M Group 2: control + overfeeding n=10 M	10948 to 1796 steps/day	2 weeks	↓ Cycle VO_2 Max	DEXA: ↑ fat mass = lean mass MRI: ↑ visceral adipose tissue ↑ abdominal subcutaneous adipose tissue	Not measured	OGTT: ↑insulin ↑glucose CGM: ↑ mean 24-h glucose ↑ maximum glucose ↑ FFA = TNF-α and IL6
Mahmassani et al 2021[96]	Older adults N=8 (2 M and 6 F)	10909 to 2258	2 weeks	= leg lean mass ↓(trend) type I fibre CSA	Not measured	= Plasma leucine at baseline and in response to leucine ingestion Alterations in leucine-stimulated mRNA translation (protein synthesis)	OGTT: = Glucose tolerance = Insulin Sensitivity Index
McGlory et al 2018[79]	Overweight, pre-diabetic older adults n=22 (12 M and 10 F)	7362 to 991 steps/day	2 weeks + 2 weeks resuming activity	= isometric MVC	DEXA: = total body fat and lean mass VL Biopsy:	VL Biopsy: ↓ MPS	OGTT: ↑insulin ↑glucose ↓Matsuda index

					= fibers CSA and distribution	Altered expression of mitochondrial-related genes	↑TNF-α, CRP and IL6
Mikus et al 2012[69]	Young adults n=12 (8 M and 4 F)	12956 to 4319 steps/day	3 days	Not measured	Not measured	Not measured	OGTT: ↑insulin = glucose ↓ Matsuda index CMG: ↑ post prandial glucose
Moore et al 2018[97]	Older adults n=14 M	7011 to <1500 steps/day SR+ unilateral retraining	2 weeks	Not measured	Muscle fiber CSA was assessed but not compared with baseline measures ↑CSA in the leg with RT	↑satellite content and capillarization in the leg with RT = compared with baseline measures	Not measured
Oikawa et al 2018[90]	Older adults n=32 (16 M and 16 F) SR + energy restriction + supplements	Group 1: 6237 to <750 steps/day Group 2: 8392 to <750 steps/day	2 weeks + 2 weeks resuming activity	Not measured	DEXA: ↓lean body mass ↓ leg lean mass VL Biopsy: = fibers CSA and distribution	VL Biopsy: ↓ MPS ↑TNF-α, CRP and IL6	↑ fasted blood glucose

	2 groups based on supplements						
Oikawa et al 2019[98]	Older adults n=30 (15 M and 15 F) SR + energy restriction	7315 to 920 steps/day	2 weeks + 2 weeks resuming activity	↓ isometric MVC = time to peak torque ↓ gait power = 30s CST, TUG, and 6MWT VL Biopsy (n=9): ↑ maximum isometric tension ↑ maximum power production	Not measured	Not measured	Not measured
Olsen et al 2008[19]	Young adults Study 1: n=8 M Study 2:	Study 1: 6203 to 1394 steps/day Study 2:	Study 1: 2 weeks Study 2: 3 weeks	Not measured	DEXA: ↓ lean mass = fat mass MRI:	Not measured	OGTT and OFTT: ↑ insuline ↑ C-peptide ↑ triglyceride

	Study 2: n=10 M	10501 to 1344 steps/day			↑Intraabdominal fat		
Reynolds et al 2015[70]	Young adults n=14 M	~12000 to~4000 steps/day	5 days + 1 day resuming activity	Not measured	Not measured	Not measured	OGTT: ↑ insulin = glucose ↓ Matsuda index CGM: ↑ peak postprandial glucose ↑ blood glucose variability
Reidy et al 2018[80]	Older adults n=12 (7 M and 5 F)	9004 to 2994 steps/day	2 weeks + 2 weeks resuming activity	↓isometric knee extension MVC = knee extension power = 6MWT	DEXA: ↓leg lean mass = trunk lean mass and fat mass CT: ↓ Mid-plantar flexor CSA VL biopsy: = fibers CSA and distribution	↑muscle inflammation cell signalling (JNK, IκBα, TLR4, Ser^{473}, SPT2) ↑Serum and intramuscular ceramides	H-E clamp: = resting and clamp insulin ↓insulin sensitivity
Reidy et al 2019[82]	Older adults n=12 (7 M and 5 F)	9004 to 2994 steps/day	2 weeks + 2 weeks resuming activity	Not measured	Not measured	↑ muscle macrophages ↑ satellite cells (slow fibre) = capillariation	↓H-E clamp (insulin sensitivity)

Saoi et al 2019[95]	Overweight, pre-diabetic older adults n=17 (10 M and 7 F)	7550 to 980 steps/day	2 weeks + 2 weeks resuming activity	Not measured	Not measured	Changes in circulatory metabolites involved in muscle energy metabolism, protein degradation and inflammation	OGTT: ↓ post OGTT glucose (p=0.07)
Shad et al 2019[72]	Young adults n=11 M	13054 ± 1192 steps/day	1 week	Not measured	Not measured	VL biopsy: ↓MPS Alterations in mRNA genes: ↑myostatin ↓mTor = p70S6K = MuRF1 ↑MAFbx = p53, PDK4 and PCG-1α	OGTT: ↑ insulin = glucose ↓ Matsuda index
Teixeira et al 2017[100]	Recreationally active young adults n=13 M Condition: one foot exposed to hot water immersions	13103 steps/day	5 days	Not measured	Not measured	Not measured	Endothelial function: ↓ popliteal artery FMD (nonheated leg only)
Walhin et al 2013[76]	Young adults	Group 1: 12562 to 3520 steps/day	1 week	Only baseline measures reported	DEXA: ↑total body mass ↑lean mass = fat mass	Adipose tissue biopsy: Altered expression of genes and proteins in	OGTT: Group1: ↑ insulin ↑ C-peptide

	Group 1: SR + overfeeding; n=14 M Group 2: SR + overfeeding + exercise; n=12 M	Group 2: 10544 to 3690 steps/day		adipose tissue remodelling	↓Matsuda Group 2: ↑ insulin Blood sample: ↑ adiponectin, total cholesterol, LDL cholesterol and whole blood white blood cell

3.4. Unexplored topic I: Does SR impact neuromuscular function?

Integrity of the neuromuscular system represents a pillar for muscle force production and motor control. However, to date, no studies have investigated these aspects in SR experiments. Recent evidence from severe models of unloading (bed rest, unilateral limb suspension) suggests that disuse is associated with initial signs of myofibre denervation (Demangel *et al.*, 2017; Monti *et al.*, 2021; Sarto *et al.*, 2022*b*), impairment of excitation-contraction coupling (Monti *et al.*, 2021), neuromuscular junction instability (Monti *et al.*, 2021; Sarto *et al.*, 2022*b*) and downregulation of skeletal muscle ion channels genes(Sarto *et al.*, 2022*b*). From an electrophysiological perspective, changes in neural drive (Campbell *et al.*, 2019), corticospinal excitability (Buoite Stella *et al.*, 2021) and motor unit potential properties (Sarto *et al.*, 2022*b*, 2022*c*) are considerably affected by disuse. Overall these findings highlight remarkable plasticity of the neuromuscular system in conditions of disuse. Future SR studies are warranted in order to determine whether these adaptations of the neuromuscular integrity and function could also be detected with a less severe form of inactivity, such as SR.

3.5. Unexplored topic II: Does SR impact brain activity, neurogenesis and cognitive function?

A sedentary lifestyle has been associated with decreased brain activity, cognitive function and brain structural remodelling, being also considered a risk factor for several neurological disorders, including dementia (Trejo *et al.*, 2002; Falck *et al.*, 2017; Buoite Stella *et al.*, 2021; Maasakkers *et al.*, 2022). This may be due, in part, to a blunted release of myokines involved in muscle–brain crosstalk (e.g. BDNF and IGF-1) (Pedersen, 2019) and impaired cerebrovascular perfusion (Maasakkers *et al.*, 2022) with physical inactivity. The brain's adaptations in function and structure, as well as the physiological factors that contribute to these changes, are largely unexplored in SR studies. Thus, specific attention should be placed on these aspects, especially after long-term SR. This seems particularly relevant in light of the reductions in brain function and neurogenesis observed in mice undergoing wheel-lock (Widenfalk *et al.*, 1999; Rhodes *et al.*, 2003; Nishijima *et al.*, 2013) (see paragraph 2.1.3).

3.6. Comparison of SR with other human physical inactivity models

In order to fully appreciate the potential applications, pros and cons of the SR model, we propose here a direct comparison with other traditional complete disuse models with regards to both pathophysiological impact and technical/practical aspects.

3.6.1. Pathophysiological effects

As presented above, SR is accompanied by decreases in lean and muscle mass. When compared to changes in leg lean mass reported after two weeks of bed rest in a recent meta-analysis (-8.5%) (Di Girolamo *et al.*, 2021), the reduction observed in SR studies is about one-fourth: on average -2.1%, ranging from -1.2% (Bowden Davies *et al.*, 2018) to -3.7% (Breen *et al.*, 2013). In the only SR study that evaluated muscle mass instead of lean mass, plantar flexors cross-sectional area was reduced by 2.4% in two weeks (Reidy *et al.*, 2018). This is considerably lower than the 5.6−8.4% plantar flexors cross-sectional area loss that could be expected with unilateral lower limb suspension or immobilisation after two weeks based on estimated median daily change (unilateral lower limb suspension: -0.4%·day^{-1}; unilateral lower limb immobilisation: -0.6%·day^{-1}) (Campbell *et al.*, 2019) and the 12% observed with longer 20-day bed rest studies (Narici & De Boer, 2011). Accordingly, MPS declines with SR are relevant (young adults: -27% (Shad *et al.*, 2019); older adults: -12−26% (Breen *et al.*, 2013; McGlory *et al.*, 2018; Oikawa *et al.*, 2018)) but appear of lower magnitude compared to the ones induced by traditional disuse models (∼40−60%) (Bell *et al.*, 2016; Nunes *et al.*, 2022). Changes in knee extensors isometric muscle force with 2-week SR are trivial, ranging from +2.8% (non-significant increase) (McGlory *et al.*, 2018) to -7.1% (Reidy *et al.*, 2018). These conflicting results contrast with the well-established marked loss of muscle strength with disuse, which is estimated, following a 2-week intervention, to be 13% for bed rest (Di Girolamo *et al.*, 2021), 14% for unilateral lower limb suspension (Campbell *et al.*, 2019), and 23% for unilateral lower limb immobilisation (Preobrazenski *et al.*, 2023). Cardiorespiratory fitness declines with 2-week SR are 3.4−6.4% in young adults (Krogh-Madsen *et al.*, 2010, 2014; Knudsen *et al.*, 2012) and 6.5% in older adults (Bowden Davies *et al.*, 2018) and are contained compared to what was observed in a bed rest study of the same duration (young adults: -7.6%; older adults: -15.3%) (Pišot *et al.*, 2016). Differently, declines in insulin sensitivity assessed with the Matsuda index seem similar between SR (-17.6−22%) (Breen *et al.*, 2013; Bowden Davies *et al.*, 2021) and bed rest (-19.8%) (Pišot *et al.*, 2016) in healthy older adults over 2 weeks of intervention. Similarly, a ∼30% reduction in the same parameter was observed in shorter SR (3−7 days) in young adults (Mikus *et al.*, 2012; Reynolds *et al.*, 2015; Shad *et al.*, 2019), which is comparable with the impact of bed rest of similar durations (-24−31%) (Montero *et al.*, 2018; Petrocelli *et al.*, 2020).

The comparison between SR and other disuse models confirmed that SR is a mild physical inactivity model. However, SR-induced alterations are consistent and should not be neglected, particularly concerning insulin sensitivity in which surprisingly SR might have an impact similar to bed rest.

3.6.2. Technical and practical aspects

The first relevant difference between SR and more extreme models of physical inactivity resides in the context of application. These latter are indeed often employed in the context of microgravity, as analogues of spaceflight (Narici & De Boer, 2011; Tesch *et al.*, 2016*b*). Despite differences between the effects of spaceflight and ground-based models exist, these are useful to unravel the mechanisms of muscle loss during mechanical unloading (Qaisar *et al.*, 2020). While the SR model represents probably a too mild inactivity stimulus for being applied in this scenario, it is instead very appealing for researchers interested in studying the effects of sedentarism.

One clear advantage of SR is a relatively inexpensive model compared for instance to bed rest. Moreover, SR has a limited impact on volunteers' private/social life with no particular health risks. Differently, during bed rest, symptoms such as musculoskeletal complaints (low back pain in particular), signs of anxiety and depression, vertigo, nausea, reduced appetite and gastroesophageal reflux can be occasionally experienced. It should also be considered that participants in BR studies are potentially exposed to an increased risk of renal calculi, urinary tract infections and deep vein thrombosis, this latter also reported in unilateral lower limb disuse models (Tesch *et al.*, 2016*b*). One of the most evident issues of the SR interventions is that compliance cannot be completely monitored, a limitation that is shared also with the unilateral lower limb suspension and immobilisation models, differently from full-time supervised bed rest campaigns. Procedures to ensure and assess compliance are hence needed (see paragraph 3.9).

3.7. Conceptual framework of the mechanisms involved in SR-induced muscle atrophy and insulin resistance

Despite some mechanisms remain poorly understood, we developed a conceptual framework in order to unravel the drivers leading to inactivity-induced muscle atrophy and insulin resistance, based on the evidence specifically obtained from SR studies and animals analogues (Figure 3). It is well known that the maintenance of muscle mass is regulated by the balance between rates of MPS and muscle protein breakdown (Crossland *et al.*, 2019; Nunes *et al.*, 2022). Differently from what originally believed (Bowden Davies *et al.*, 2019; Qaisar *et al.*, 2020), recent evidence suggests that muscle protein breakdown has no or little influence in the context of "uncomplicated" disuse (i.e. inactivity in absence of diseases or other catabolic processes) (Crossland *et al.*, 2019; Nunes *et al.*,

2022). Thus, it seems very unlikely to play a role in models with lower atrophic stimulus, as in the context of SR. Declines in MPS are therefore considered the primary driver of skeletal muscle disuse atrophy (Crossland *et al.*, 2019; Nunes *et al.*, 2022) and are indeed observed in several SR studies (Breen *et al.*, 2013; Devries *et al.*, 2015; McGlory *et al.*, 2018; Oikawa *et al.*, 2018) (see paragraph 3.2). However, molecular mechanisms regulating this process are still partially unknown in this scenario. Some alterations of the Akt/mTOR/p70S6K signalling cascade were found with SR in young adults(Shad *et al.*, 2019), but another study reported opposite results in older adults (Breen *et al.*, 2013), as also observed in more extreme models of disuse (Crossland *et al.*, 2019). Molecular pathways such as TNFα-IKK-NFkB and IL6-JAK-Stat3 may be involved in SR-induced muscle atrophy as inflammation is commonly observed in SR studies (Breen *et al.*, 2013; McGlory *et al.*, 2018; Reidy *et al.*, 2018, 2019), at least in older adults (see paragraph 3.1). Changes in mitochondrial content (Edwards *et al.*, 2021) and gene expression (e.g. COX7A2, ATP5E and MRPS36) (McGlory *et al.*, 2018) occur quickly with reduced ambulatory activity and could contribute to the atrophic program via increased oxidative stress, inducing calpain and caspase-3 activation and increasing expression of the ubiquitin-proteasome system (Powers *et al.*, 2012). MPS decreases could be also partially attributed to altered ribosome biogenesis and increased ribosome degradation that have been observed to regulate translational capacity in skeletal muscle during periods of disuse (Figueiredo *et al.*, 2021). This hypothesis seems supported by recent evidence showing SR-induced deficits in ribosome production (Mahmassani *et al.*, 2021). While it is still unknown whether initial signs of neuromuscular junction instability and denervation occur with SR (see paragraph 3.4), they could ultimately have an influence on reducing MPS (Crossland *et al.*, 2019), affecting the expression of a group of atrophy-related genes, such as Runx1, Trim63, Fbxo32 and Elk4 (Lin *et al.*, 2022) and causing expansion of the fibro-adipogenic precursor cells which induce an inflammatory response via the IL6-JAK-Stat3 pathway (Sartori *et al.*, 2021).

Inflammation, mitochondrial alterations, oxidative stress and denervation could also trigger impairments in insulin sensitivity with SR(Petersen & Shulman, 2018). In addition, endothelial dysfunction, reported in different cage reduction (Suvorava *et al.*, 2004) and SR (Boyle *et al.*, 2013; Teixeira *et al.*, 2017; Bowden Davies *et al.*, 2021) studies, may also contribute in part to peripheral insulin resistance due to reduced blood flow (Bowden Davies *et al.*, 2021). Differently, ceramides accumulation seems to not have a great influence on early changes in insulin sensitivity caused by reduced physical activity (Reidy *et al.*, 2018; Appriou *et al.*, 2019). Intramyocellular lipids, another well-established player in insulin resistance (Petersen & Shulman, 2018), seem also unaffected by

wheel-lock (Morris *et al.*, 2008) and SR (Bowden Davies *et al.*, 2021) interventions. It is well established that the two main molecular mechanisms that regulate glucose transport in skeletal muscle are the insulin signal transduction cascade and GLUT4 translocation (Petersen & Shulman, 2018). Pooling together evidence from animal and human studies, it seems overall supported that skeletal muscle GLUT4 content and/or translocation may be affected by reduced ambulatory activity (Kump & Booth, 2005*b*; Walhin *et al.*, 2013; Appriou *et al.*, 2019; Mahmassani *et al.*, 2020), although not all studies are in agreement (Teich *et al.*, 2017; Edwards *et al.*, 2021). Findings regarding insulin signalling are more complex to interpret. Two weeks of SR decreased insulin-simulated skeletal muscle Akt phosphorylation (Krogh-Madsen *et al.*, 2010), while 7 days of SR were sufficient to increase the protein content of P-GS^{S641}, a marker of reduced glycogen synthase (Edwards *et al.*, 2021). Wheel-lock studies seem also to support this finding showing reductions in the protein level of insulin receptor β-subunit (Kump & Booth, 2005*b*) and increase in 4-hydroxynonenal, known to induce Akt nitrosylation (Morris *et al.*, 2008). However, other evidence points towards the absence of a marked involvement of the insulin signalling, highlighting unchanged protein content and/or phosphorylation state of insulin receptor (Edwards *et al.*, 2021), IRS1 (Appriou *et al.*, 2019; Edwards *et al.*, 2021), PI3K (Edwards *et al.*, 2021) and Akt (Teich *et al.*, 2017; Appriou *et al.*, 2019; Edwards *et al.*, 2021).

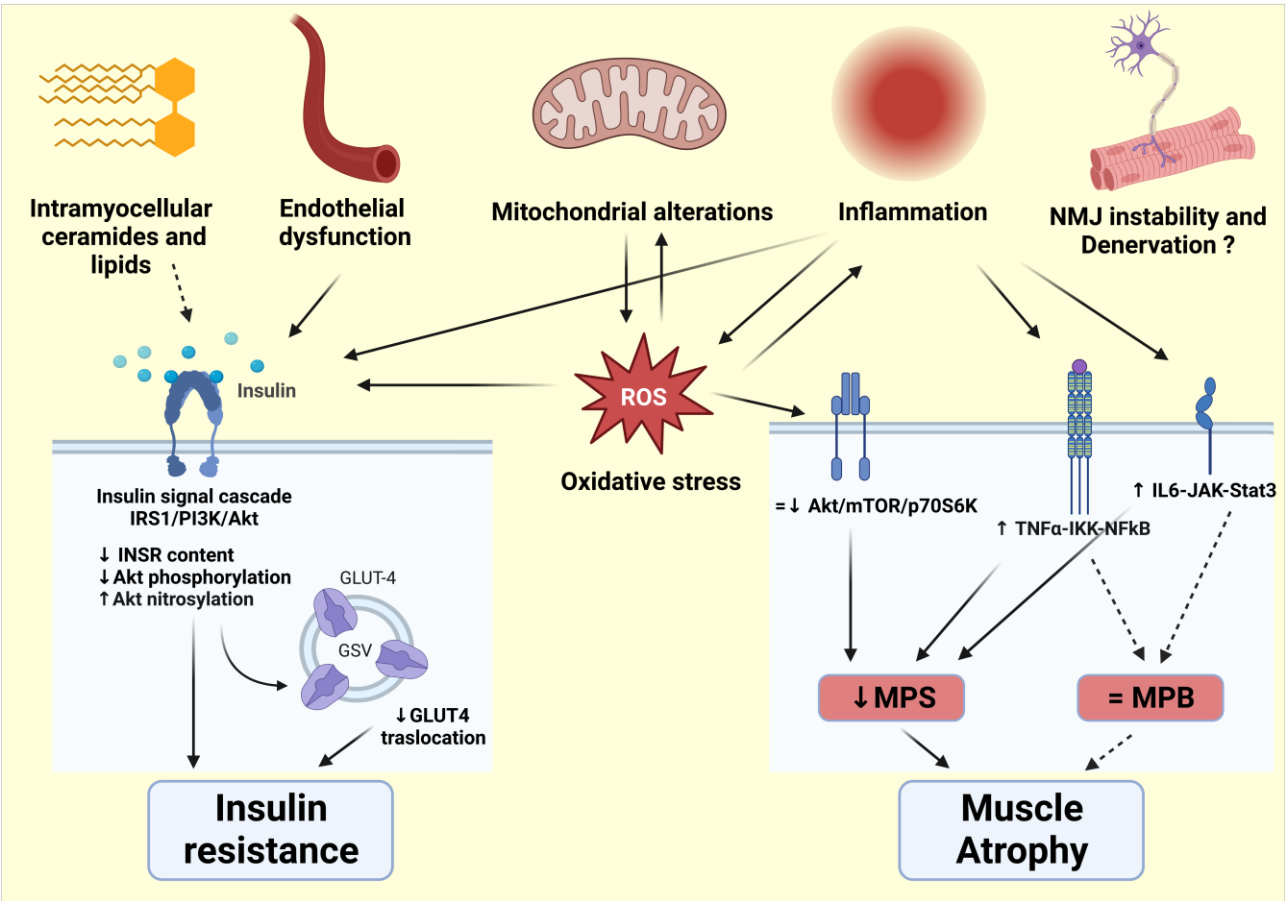

Figure 3: *Conceptual framework of the mechanisms leading to muscle atrophy and insulin resistance with reduced ambulatory activity. Dotted lines express mechanisms that theoretically have an impact, but seem to not occur in the specific context of step reduction. Denervation could play a role both in the development of muscle atrophy and insulin resistance, but it is still unknown whether initial signs of denervation are induced by step reduction. Created with BioRe nder.com. GSV, GLUT4 storage vesicles; INSR, insulin receptor; MPB: muscle protein breakdown; MPS: muscle protein synthesis; ROS: reactive oxygen species.*

3. 8. Do the SR studies support the findings of 'theoretical' epidemiological studies?

Population-based epidemiological research is essential for investigating the associations between physical activity/inactivity and health-related outcomes. A rapidly emerging area of in this field, called time-use research (Bauman *et al.*, 2019), has been recently applied in the context of physical activity/inactivity. These studies employ novel statistical approaches such as compositional data analysis and isotemporal modeling to study the impact of reallocation of a movement behaviour (e.g. sedentary behaviours, sitting, stepping, low and moderate intensity physical activity) to another one (Grgic *et al.*, 2018; Janssen *et al.*, 2020). SR model essentially follows the same principle (i.e. reallocating stepping with sedentary behaviours) but tests this relationship experimentally.

Thus, time-use research provides estimates that could theoretically align with the findings from SR experimental studies (and vice versa).

A recent interesting study used a compositional data analysis approach to model the association between physical behaviour and markers of metabolic health (including fasting glucose, two-hour glucose, Matsuda index and HOMA index) in individuals at high risk of developing diabetes, as well as evaluating the impact of time reallocation (Biddle *et al.*, 2018). Interestingly, a SR study conducted in a similar population of prediabetic older adults (HBA1c: 5.90±0.30 vs 5.7±0.5 %) with comparable age (69±4 vs 66±7.4 years old) investigated the same outcomes measures (McGlory *et al.*, 2018). Considering that in this study a reduction on average of ∼6400 steps/day was induced and assuming a stepping cadence in this population of 70 steps/min (Yates *et al.*, 2023), we can estimate that the SR intervention reduced daily stepping by approximately 1h and 30min in favour of sedentary behaviours. In the same study (McGlory *et al.*, 2018), the alterations reported in circulating metabolic biomarkers were as follow: glucose fasting: 4.5% difference, two-hour glucose: 7.5%, Matsuda index: 35% and HOMA index: 23%. Interestingly, based on the study leveraging the compositional data analysis approach (Biddle *et al.*, 2018), reallocating stepping with sitting for 1 h and 30 min would result in comparable changes of 3%, 19%, 44% and 20% for glucose fasting, two-hour glucose, Matsuda index and HOMA index, respectively.

Direct comparison of other SR and epidemiological studies is complex because most of the time-use investigations in the literature report only the reallocation from sedentary behaviours to stepping but not the opposite (e.g. (Healy *et al.*, 2015; Henson *et al.*, 2017)). This is a relevant issue as the reallocation from one behaviour to another does not necessarily result in the same association as the inverse reallocation (Chastin *et al.*, 2015; Biddle *et al.*, 2018). However, some further insights can be obtained from time-use studies using accelerometers to measure physical activity levels, assuming that most of the low-intensity physical activity levels derive from stepping. In these epidemiological studies, replacing low-intensity physical activity with sedentary time leads to increases in fat mass (Janssen *et al.*, 2020), in agreement with SR experimental observations (Bowden Davies *et al.*, 2018). Conversely, this reallocation seems to not impact lean mass (Powell *et al.*, 2020) and cardiorespiratory fitness (Dumuid *et al.*, 2018), differently from what reported in SR literature. However, it has to be considered that during SR interventions, participants are generally asked to refrain also from structured physical activities. Thus, SR studies are likely to induce a reduction also in moderate-to-vigorous physical activity levels, which reallocation to

sedentary behaviours is instead associated with alterations of the aforementioned parameters in epidemiological studies (Dumuid *et al.*, 2018; Powell *et al.*, 2020).

To the best of the authors' knowledge, this is the first article to link time-use epidemiological research with experimental SR studies. Overall, similarities in the findings of these two closely related topics are observed. Our article may pave the way for future studies leveraging this multidisciplinary epidemiological and physiological approach to further investigate associations between physical inactivity and health markers.

3.9. Methodological considerations and future directions for SR studies

In summary, the SR model has been successfully employed to study the effects of reduced physical activity on various physiological systems. Habitual physical activity levels of the participants should be monitored for at least 3-7 days before the intervention via pedometers and accelerometers; in addition, a detailed description of their habitual exercise routine should be recorded. The maximal daily step limit (ranging from ∼750 to ∼4500 steps/day) in these interventions should be chosen carefully based on the population and research outcomes of interest. Interestingly, daily steps performed by hospitalised patients are on average ∼740 (Fisher *et al.*, 2011), thus in line with the lower end of daily step count (∼750 steps/day) used in steps SR studies (Oikawa *et al.*, 2018, 2019*a*). An alternative approach may be to ask participants to reduce their daily step counts by a predetermined percentage of their baseline habitual steps activity level, ranging from 65% to 90%[9,81,95]. Selection of the participants and monitoring their compliance are other crucial issues that should not be underestimated. Volunteers should be recruited only after a careful evaluation regarding their ability to incorporate a SR intervention considering their daily routines and responsibilities. Strategies for reducing daily steps should be planned and discussed with the investigators before the beginning of the SR study. In order to facilitate adherence to the selected daily steps limit, investigators should consider providing participants with public transportation tickets, transport assistance or other appropriate transportation options, such as electric scooters. In addition, in order to promote compliance, it is advisable to foster a sense of camaraderie and collaboration among participants and investigators through the organization of social events and gatherings, as previously proposed for other physical inactivity models (Tesch *et al.*, 2016*b*). Daily calls and messages to maintain contact with the participants are also encouraged. One potential strategy to evaluate retrospectively participants' compliance could be to instruct the participants to

wear continuously the accelerometers and then, at the end of the intervention, apply algorithms (e.g. (Syed *et al.*, 2021)) to differentiate non-wear time and inactivity time from the data obtained from the accelerometers. Methodological considerations for the step reduction model are summarised in Figure 2.

Future studies should focus on the effects of SR on other aspects that to date are largely unexplored, such as the neuromuscular (see paragraph 3.4) and brain/cognitive (see paragraph 3.5) function. Molecular mechanisms regulating declines in muscle mass and insulin sensitivity with SR are only partially understood (see paragraph 3.7). Most of the SR studies lasted 1 to 2 weeks; studies of longer duration would be more relevant for deeper insights into the effects of sedentarism, given its chronic nature (Bowden Davies *et al.*, 2019). In addition, the time course of alterations is still poorly investigated. Some populations are significantly underrepresented as yet using this model. Females represent only ∼24% of the participants included in SR studies (Table 1), despite a strong rationale for potential sex differences in the context of disuses-related muscle metabolism impairment and atrophy exists (Rosa-Caldwell & Greene, 2019; Qaisar *et al.*, 2020). Moreover, only one SR study (Dixon *et al.*, 2013) was conducted in middle-aged adults, a population of particular interest as commonly subjected to periods of sedentarism due to work and family responsibilities peculiar to this period of life. The effects of different types of countermeasures (e.g. comparison of different types of training, NEAT and diet interventions) should be further investigated. Lastly, all the exercise countermeasures studies were performed exclusively during periods of SR, but none have investigated the effects of training programs following SR (i.e. during recovery from such inactivity periods). This is an important gap in this research field.

4. Conclusions

Human body quickly develops adaptive responses to altered environmental conditions, such as physical inactivity. The SR model represents a unique opportunity to mimic the effects of a sedentary lifestyle and to study the pathophysiological mechanisms by which reduced physical activity impacts different physiological systems. Analogous models in rodents, which can provide the foundation for human studies, have been developed (Figure 1). Despite SR represents a less severe form of disuse compared with traditional severe unloading models, brief periods of reduced ambulatory activity have been shown to induce marked alterations in skeletal muscle health and

metabolic function. These include reductions in lean mass, muscle function and protein synthesis, impairments in cardiorespiratory fitness, endothelial function and insulin sensitivity, accompanied by increased fat mass and inflammation (Table 1 and Figure 1). Exercise, NEAT-increasing and nutritional interventions ought to be developed for counteracting the deleterious alterations induced by periods of reduced physical activity.

5. Motor units properties impairment, axonal damage, innervation profile alterations and neuromuscular junction instability with different stages of sarcopenia

Fabio Sarto[1], Martino V. Franchi[1,2], Jamie S. McPhee[3], Daniel Stashuk[4], Matteo Paganini[1], Elena Monti[5], Maira Rossi[6], Giuseppe Sirago[1,7], Sandra Zampieri[1,2,8], Evgeniia S. Motanova[1], Giacomo Valli[1], Tatiana Moro[1], Antonio Paoli[1], Roberto Bottinelli[6,9], Maria A. Pellegrino[6], Giuseppe De Vito[1,2], Helen M. Blau[5] and Marco V. Narici[1,3]

[1] Department of Biomedical Sciences, University of Padova, Padova, Italy

[2] CIR-MYO Myology Center, University of Padova, Padova, Italy

[3] Department of Systems Design Engineering, University of Waterloo, Ontario, Canada

[4] Department of Sport and Exercise Sciences, Manchester Metropolitan University Institute of Sport, Manchester M1 7EL, United Kingdom

[5] Baxter Laboratory for Stem Cell Biology, Department of Microbiology and Immunology, Stanford University School of Medicine, Stanford, CA, USA

[6] Institute of Physiology, Department of Molecular Medicine, University of Pavia, Pavia, Italy

[7] Institute of Sport Sciences and Department of Biomedical Sciences, University of Lausanne, Lausanne, Switzerland

[8] Department of Surgery, Oncology, and Gastroenterology, University of Padova, Padova, Italy

[9] IRCCS Mondino Foundation, Pavia, Italy

Corresponding authors

Mr. Fabio Sarto, Department of Biomedical Sciences, University of Padova, Padova, Italy, 35131, Italy - Email: fabio.sarto.2@phd.unipd.it – ORCID: https://orcid.org/0000-0001-8572-5147

Prof. Marco V. Narici: Department of Biomedical Sciences, CIR-MYO Myology Centre, University of Padova, Padova, 35131, Italy - Email: marco.narici@unipd.it - ORCID: https://orcid.org/0000-0003-0167-1845

Abstract

Background: Evidence suggests that motoneuron and neuromuscular junction (NMJ) degeneration and loss of motor units (MUs) contribute to age-related muscle wasting and weakness, resulting in sarcopenia insurgence. However, these aspects are poorly investigated in humans. This study aimed to compare the neuromuscular system integrity and function across different stages of sarcopenia, with a particular focus on NMJ stability and MU potential (MUP) properties.

Methods: We recruited 42 healthy young individuals (Y) (aged 25.98±4.6 yr; 57% females) and 88 older individuals (aged 75.9±4.7 yr; 55% females). The older group underwent a sarcopenia screening according to the revised guidelines of the European Working Group on Sarcopenia in Older People (EWGSOP2). In all groups, knee extensors muscle force was evaluated by isometric dynamometry, muscle morphology by ultrasound and MUP properties by intramuscular electromyography (iEMG). MU number estimate (iMUNE) was obtained. Blood samples and muscle biopsies were collected to evaluate biomarkers of NMJ instability and neuromuscular degeneration.

Results: 39 older individuals were non-sarcopenic (NS), 31 pre-sarcopenic (PS) and 18 sarcopenic (S). A progressive decrease in quadriceps force, cross-sectional area and appendicular lean mass was observed across the different stages of sarcopenia. Handgrip force and short physical performance battery (SPPB) score were also progressively impaired. iEMG analyses revealed elevated near fiber segment jitter in NS, PS and S compared to the Y group, suggestive of decreased NMJ transmission in-vivo. Increased concentration of serum C-terminal agrin fragment and altered Cav3 protein expression were consistent with the finding of age-related NMJ instability in all the older groups. The iMUNE was lower in all older groups, confirming age-related MUs loss. Motoneuron firing rate was decreased in S vs Y. Age-related changes in MUP complexity were also observed. These observations were coupled by the detection of increased muscle denervation and axonal damage, respectively evidenced by the increase in NCAM-positive fibres and by serum concentration of neurofilament light chain. Most of these parameters in relation to MU and NMJ degeneration did not differ comparing older individuals with or without sarcopenia.

Conclusions: MU properties impairment, axonal damage, altered innervation profile and NMJ instability are prominent features of ageing of the neuromuscular system. These neuromuscular alterations are accompanied by muscle wasting and weakness but seem to precede clinically diagnosed sarcopenia, as they are already present in NS older individuals. These are important parameters to monitor and to counteract these maladaptations, slowing down sarcopenia insurgence/progression.

Keywords:

Electromyography; fibre denervation; neuromuscular system; motoneuron; muscle wasting; muscle atrophy

INTRODUCTION

Sarcopenia, characterised by the progressive loss in skeletal muscle mass and function with ageing (Cruz-Jentoft *et al.*, 2019; Larsson *et al.*, 2019), is clinically recognised as a disorder that significantly affects individuals' quality of life and leads to an increased risk of falls, functional decline, frailty and mortality (Cruz-Jentoft *et al.*, 2019). Sarcopenia is increasingly common in older populations, with ranges between 10% and 27% depending on the classification employed (Petermann-Rocha *et al.*, 2022) and represents an enormous burden on the healthcare system (Cruz-Jentoft *et al.*, 2019). The pathophysiology of sarcopenia is complex, multifactorial and not yet fully elucidated. Evidence suggests that this disorder has a key neurogenic component (Hepple & Rice, 2016; Larsson *et al.*, 2019). A reduced MUs number with ageing due to motoneuron death is a consistent finding both in anatomical and electrophysiological studies (Piasecki *et al.*, 2016*b*). This process is accompanied by recurring cycles of denervation-reinnervation inducing remodelling of the MU, fibre atrophy and fibre type grouping(Hepple & Rice, 2016). The neuromuscular junction (NMJ), a specialised synapse connecting a motoneuron with a muscle fibre (Tintignac *et al.*, 2015), also exhibits considerable remodelling with ageing. NMJ morphological adaptations include increased dimensions and complexity of nerve terminal branching, decreased number of acetylcholine (ACh)-containing vesicles, active zones, ACh receptors and junctional folds, NMJ denervation and increased endplate fragmentation (Tintignac *et al.*, 2015; Hepple & Rice, 2016; Pratt *et al.*, 2020*b*). Besides this anatomical remodelling, ageing triggers adaptations also to the NMJ physiological function, leading to a decreased safety factor and increased incidence of neurotransmission failure (Arnold & Clark, 2023). Whilst these findings imply that degeneration of motoneurons and NMJs and MUs loss, may underlie observed muscle wasting and weakness in sarcopenia, these observations have been mostly drawn from animal models. Furthermore, the scant evidence available from human studies is generally limited to the comparison between young and older individuals, without diagnosing sarcopenia using official guidelines that consider both muscle mass and function.

In this study, we aimed to comprehensively investigate muscle morphological, functional, electrophysiological and molecular alterations across different stages of primary sarcopenia, when no other discernible cause is apparent (Cruz-Jentoft *et al.*, 2019), in older humans. A particular focus was devoted to NMJ alterations and MU potential (MUP) properties. We hypothesised that an overall progressive impairment of the neuromuscular system would occur with the progression of sarcopenia.

MATERIAL AND METHODS

Participants

Forty-two healthy young individuals (Y) (57% females) and 88 older individuals (55% females) volunteered for this study. Inclusion criteria were 18 to 35 years of age for Y and >70 years for older adults. Exclusion criteria for both groups were very active individuals (>4 sessions/week) and, as we focused on primary sarcopenia, the presence of neurological disorders, diabetes with complications, stroke, late-stage cancer, chronic kidney disease (stage IV-V), severe liver insufficiency, severe cardiac disorder and serious lower limb musculoskeletal injuries in the last 12 months and implantable cardioverter-defibrillator. This study was carried out following the guidelines of the most recent version of the Declaration of Helsinki and received approval from the Ethics Committee of the Department of Biomedical Sciences, University of Padova (Italy) (reference number: HEC-DSB/03-20). Before data collection, volunteers were informed about all the experimental procedures and provided written consent.

Experimental protocol

In this cross-sectional study, volunteers were asked to visit the laboratory two to three times. On the first visit (only for older adults), participants underwent a full sarcopenia screening including the handgrip test, the Short Physical Performance Battery (SPPB) and a whole-body dual-energy X-ray absorptiometry (DEXA) scan. On the second visit, the Global Physical Activity Questionnaire (GPAQ), a blood sample, ultrasound scans, *in vivo* muscle function assessment and intramuscular electromyography (iEMG) recordings were collected in both groups. In a sub-group of participants, vastus lateralis muscle biopsies were obtained during the third visit. Participants were asked to refrain from any vigorous form of exercise during the 24 hours preceding each visit.

Sarcopenia screening and classification

Handgrip strength was evaluated following the recommendations of the European Working Group on Sarcopenia in Older Persons 2 (EWGSOP2) (Cruz-Jentoft *et al.*, 2019) using a hand-held dynamometer (Jamar Plus+, JLW Instruments, Chicago, IL, USA). The measurement was obtained with the participants sitting in a chair with their elbows close to the trunk and flexed at 90°, their forearms resting on the arms of the chair and their wrists in a neutral position with their thumbs facing upward. The measure was collected three times for both hands and the highest value was

used for the analysis. A normalised index was also obtained dividing this value by the lean mass of the respective arm assessed by DEXA.

Physical performance was assessed employing the SPPB which includes three subtests for the evaluation of static balance, gait speed over a 4-m walk, and the ability to stand repetitively 5 times from a chair as fast as possible (chair to stand test; CST) (Guralnik *et al.*, 1994). Further details can be found in Data S1.

Whole body and regional body composition were measured by DEXA (Hologic Horizon TM QDR RSeries Bedford, Massachusetts, USA). Appendicular lean mass (ALM) was computed as the sum of arms and legs lean mass.

Sarcopenia classification

Older participants were classified according to the guidelines of the EWGSOP2 (Cruz-Jentoft *et al.*, 2019), with the modified thresholds for handgrip strength recently proposed by Westbury and colleagues (Westbury *et al.*, 2023). The co-existence of both reduced muscle strength and decreased lean mass was considered indicative of sarcopenia, while the presence of either reduced muscle strength or decreased lean mass was classified as pre-sarcopenia. For males, low muscle strength was defined as handgrip strength <35.5 kg and/or CTS time >15 s, while low lean mass was defined as ALM <20 kg and/or ALM/h^2 <7.0 kg/m^2. For females, low muscle strength was defined as handgrip strength <20 kg for males and/or CTS time >15 s, while low lean mass was defined as ALM <15 kg and/or ALM/h^2 <5.5 kg/m^2. Each participant was assigned to the corresponding group with a custom Python (v.3.9) script.

***In vivo* muscle morphology and function**

Muscle size measurements

Quadriceps femoris cross-sectional area (CSA) was assessed at three different muscle regions (30%, 50% and 70% of femur length) using panoramic ultrasound imaging (Mylab70, Esaote, Genoa, Italy) (Sarto *et al.*, 2022*b*). CSA was determined by tracing their contours using ImageJ software (1.52v; National Institutes of Health, Bethesda, MD, USA). The CSA_{mean} of the quadriceps and vastus lateralis was computed by averaging the CSA values at the three different muscle regions. Vastus lateralis muscle architecture was evaluated by B-mode longitudinal ultrasound scans at 50% of femur length (Franchi *et al.*, 2019). Fascicle length (Lf) and pennation angle (PA) were obtained using ImageJ. Further details regarding image acquisition and analysis can be found in Data S1.

Quadriceps force, rapid force production and activation capacity

Quadriceps force was evaluated by isometric dynamometry at 90° of knee flexion. Three trials were recorded and the highest value reached was considered the maximum voluntary contraction (MVC). This was then divided for quadriceps CSA_{mean} to evaluate the specific force. The time required to reach 63% of MVC (TTP63%) was used as an index of rapid force production. Finally, activation capacity was evaluated using the interpolated twitch technique. For further information regarding these procedures, we refer the reader to Monti et al. (Monti *et al.*, 2021) and Data S1.

Intramuscular electromyography

The vastus lateralis central motor point was detected with low-intensity percutaneous electrical stimulations, as previously described (Sarto *et al.*, 2022*b*). iEMG recordings were obtained during submaximal isometric contractions at 10% and 25% MVC using a concentric needle electrode of 25 or 37 mm of length, depending on muscle and subcutaneous fat thickness, inserted at the motor point (S53155 or S53155, Teca Elite, Natus Medical Inc., Middleton, WI, USA). Twelve 20-second contractions were collected (six at 10% and six at 25% MVC), adjusting needle position for each pair of contractions. An experienced operator employed DQEMG software to extract MUP trains and carry out all the analyses (Stashuk, 1999*a*). The markers, relative to MUP onset, end, positive peak and negative peaks were manually adjusted, where appropriate. The following parameters were evaluated (Piasecki *et al.*, 2021; Sarto *et al.*, 2022*b*): (i) MUP area, (ii) MUP duration, (iii) number of turns (i.e. a change in MUP waveform of at least 20 µV), indicative of the complexity of the MUP and (iv) MUs firing rate pattern.

Near fibre MUPs (NF MUPs) trains were obtained after bandpass filtering MUPs using a second-order low-pass differentiator (Stashuk, 1999*b*) and were visually inspected, manually excluding NF MUPs containing contaminating activity generated by other MUs. The NF MUP properties analysed were NF MUP duration and NF Count, a measure of fibre density contributing to the NF MUP trains. NMJ transmission was evaluated by the NF MUP segment jitter, which represents temporal variability (i.e. mean absolute consecutive temporal differences) in consecutive NF MUPs and is considered an estimate of the NMJ safety factor (Juel, 2012). Motor unit number estimate (iMUNE) was also computed as the ratio between the mean MUP area and vastus lateralis CSA_{mean} (Piasecki *et al.*, 2018*a*). For further details regarding these procedures, we refer the reader to Sarto et al. (Sarto *et al.*, 2022*b*) and Data S1.

Blood sampling and circulating biomarkers assessment

Blood samples were collected from the medial cubital vein and serum was obtained by centrifugation at 3000 rpm for 10 min. Circulating biomarkers involved in neuromuscular degeneration were measured, including C-terminal agrin fragment (CAF), neurofilament light chain, BDNF and NT-4. In addition, we evaluated inflammation levels dosing IL-6. All the analyses were performed using enzyme-linked immunosorbent assay (ELISA) kits, apart from neurofilament light chain concentration that was obtained employing the single molecule array (SIMOA) technology. Further details can be found in Data S1.

Muscle Biopsy

In a sub-group of participants (Y: n=16; older adults: n=52), a vastus lateralis muscle biopsy was obtained with a Weil-Blakesley conchotome (Gebrüder Zepf Medizintechnik GmbH & Co. KG, Dürbheim, Germany) under local anaesthesia (five ml of lidocaine at 2%). Each sample was collected at ∼2 cm from the motor point. The sample was divided into a part for western blot analysis and another one for immunofluorescence analysis. We assessed protein levels of selected downstream components of the agrin pathway, expression of neural cell adhesion molecule (NCAM) positive fibres and the variability of muscle fibres diameters. Further details can be found in Data S1.

Statistical analysis

Normality of data was assessed by the Shapiro-Wilk normality test and visual inspection of the Q-Q plot. Two-way ANOVA (group x sex) with Holm post hoc was performed to determine differences with different stages of sarcopenia. Variables not normally distributed were analysed employing Kruskal-Wallis test with Dunn's multiple comparisons tests. Since multiple MUs were recorded from each participant, iEMG data were analysed using generalised linear mixed models (fixed effects: group and sex; cluster variable: subject). For a full description of the statistical analyses performed, we refer the reader to Data S1. Statistical significance was accepted at $P \leq 0.05$. Statistical analysis was performed using Jamovi software (version 2.3.21, Sydney, Australia), while GraphPad Prism (version 8.00; GraphPad Software, San Diego, CA, USA) was employed to create the graphs.

RESULTS

According to the sarcopenia screening, 39 older individuals were non-sarcopenic (NS), 31 pre-sarcopenic (PS) and 18 sarcopenic (S). Participants' characteristics for each group are reported in Table 1. All participants were included in the analysis unless otherwise reported. Figure captions report whether any data point was not collected or removed due to technical issues. Statistical tests showed that, for most of the parameters considered, no interaction between group and sex existed. Thus, males and females are pooled together in the main text results. Full results regarding the sex effect can be found in Data S1.

In vivo muscle function and physical performance

We characterised the functional impairment across human sarcopenia stages (Table 1 and Figure 1). Handgrip strength ($P < 0.0001$; $\eta p^2 = 0.49$) and MVC ($P < 0.0001$; $\eta p^2 = 0.47$) were progressively lower from NS to S. Differences between old groups disappeared when these values were normalised for arm lean mass and quadriceps $CSA_{mean,}$ respectively (Figure S1). Activation capacity, reflective of the ability to recruit MUs under a maximal effort, did not differ across groups. Older groups showed impaired rapid force production capacity ($P < 0.0001$; $\eta p^2 = 0.2$), as suggested by lower TTP63%, but no differences were observed comparing NS, PS and S. NS presented a superior performance in the overall SPPB score ($P = 0.009$) and the CTS time ($P = 0.048$) compared to S. Balance score and gait speed did not differ between groups.

	GROUP				P-value (Group)						P-value (Sex)
	Young (Y)	Non-Sarcopenic (NS)	Pre-sarcopenic (PS)	Sarcopenic (S)	Y—NS	Y—PS	Y—SAR	NS—PS	NS—SAR	PS—SAR	M—F
N TOT	42	39	31	18	/	/	/	/	/	/	/
N F/M	24/18	17/22	19/12	12/6	/	/	/	/	/	/	/
Age (yrs)	25.98 (4.52)	74.8 (3.76)	74.97 (4.21)	79.83 (5.14)	***<0.0001***	***<0.0001***	***<0.0001***	0.865	***0.001***	***0.001***	0.500
Height (m)	1.71 (0.08)	1.69 (0.08)	1.60 (0.09)	1.55 (0.08)	***0.019***	***<0.0001***	***<0.0001***	***0.001***	***<0.0001***	***0.019***	***<0.0001***
Weight (kg)	66.1 (9.85)	78.66 (12.6)	67.98 (11.13)	65.11 (8.96)	***<0.0001***	0.192	0.640	0.017	***0.0001***	0.192	***<0.0001***
GPAQ score (MET-minutes/week)	3330 (2100)	1526 (1200)	1370 (1200)	1517 (1440)	***<0.0001***	***<0.0001***	***<0.0001***	0.986	0.976	0.882	0.415
Body fat (%)	/	35.31 (7.44)	37.31 (6.82)	37.01 (8.63)	/	/	/	0.999	0.999	0.999	***<0.0001***
ALM/h^2 (kg/m^2)	/	7.34 (1.00)	6.65 (1.04)	6.41 (0.65)	/	/	/	***0.029***	***0.009***	0.999	***<0.0001***
Balance score SPPB	/	3.61 (0.78)	3.62 (0.76)	3.11 (1.08)	/	/	/	0.991	0.135	0.189	0.935

Gait speed (m/s)	/	1.12 (0.17)	1.05 (0.19)	1.06 (0.21)	/	/	/	0.387	0.744	0.744	0.249
CST time (s)	/	10.46 (2.19)	11.06 (2.56)	12.71 (3.71)	/	/	/	0.296	***0.048***	0.392	0.652

Table 1: *Participants characteristics, body composition and components of the short physical performance battery (SPPB). Data are reported as mean and standard deviation. ALM: appendicular lean mass; CST: chair to stand; GPAQ: Global Physical Activity Questionnaire*

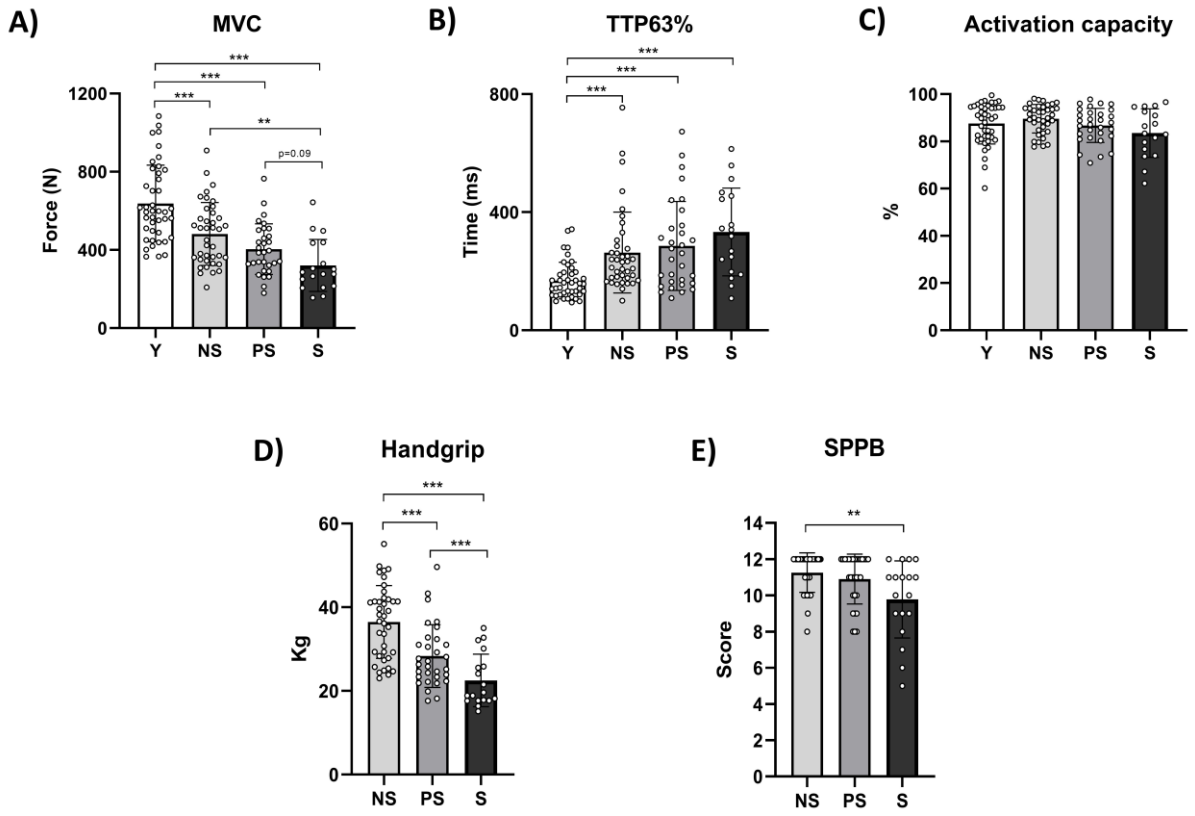

Figure 1: *Muscle function and physical performance parameters across different stages of human sarcopenia. Statistical analysis was performed using two-way ANOVAs (A-D) and Kruskal-Wallis test (E). Results are shown as mean and standard deviation. Knee extensors maximum voluntary contraction (MVC) (A); time needed to reach the 63% of the MVC (TTP 63%) (B); activation capacity (C); handgrip strength (D); and short physical performance battery (SPPB) score (E). Y: young individuals; NS: non-sarcopenic; PS: pre-sarcopenic; S: sarcopenic. Three missing values for activation capacity (1 NS, 1 PS and 1 S). **P < 0.01; *** P < 0.001*

In vivo muscle morphology

We assessed the age-related changes in lean mass and muscle morphology by DEXA and ultrasound, respectively (Table 1 and Figure 2). ALM ($P < 0.0001$; $\eta p^2 = 0.44$), ALM/h^2 ($P < 0.0046$; $\eta p^2 = 0.44$) and leg lean mass ($P < 0.0001$; $\eta p^2 = 0.39$) progressively declined across the different stages of sarcopenia. Muscle atrophy was observed also in the gradual decreases of the whole quadriceps CSA_{mean} ($P < 0.0001$; $\eta p^2 = 0.48$) and vastus lateralis CSA_{mean} ($P < 0.0001$; $\eta p^2 = 0.45$) with sarcopenia progression. Lf did not differ between groups, PA was lower in older groups compared to Y ($P = 0.0002$; $\eta p^2 = 0.44$), confirming age-related alterations in muscle architecture.

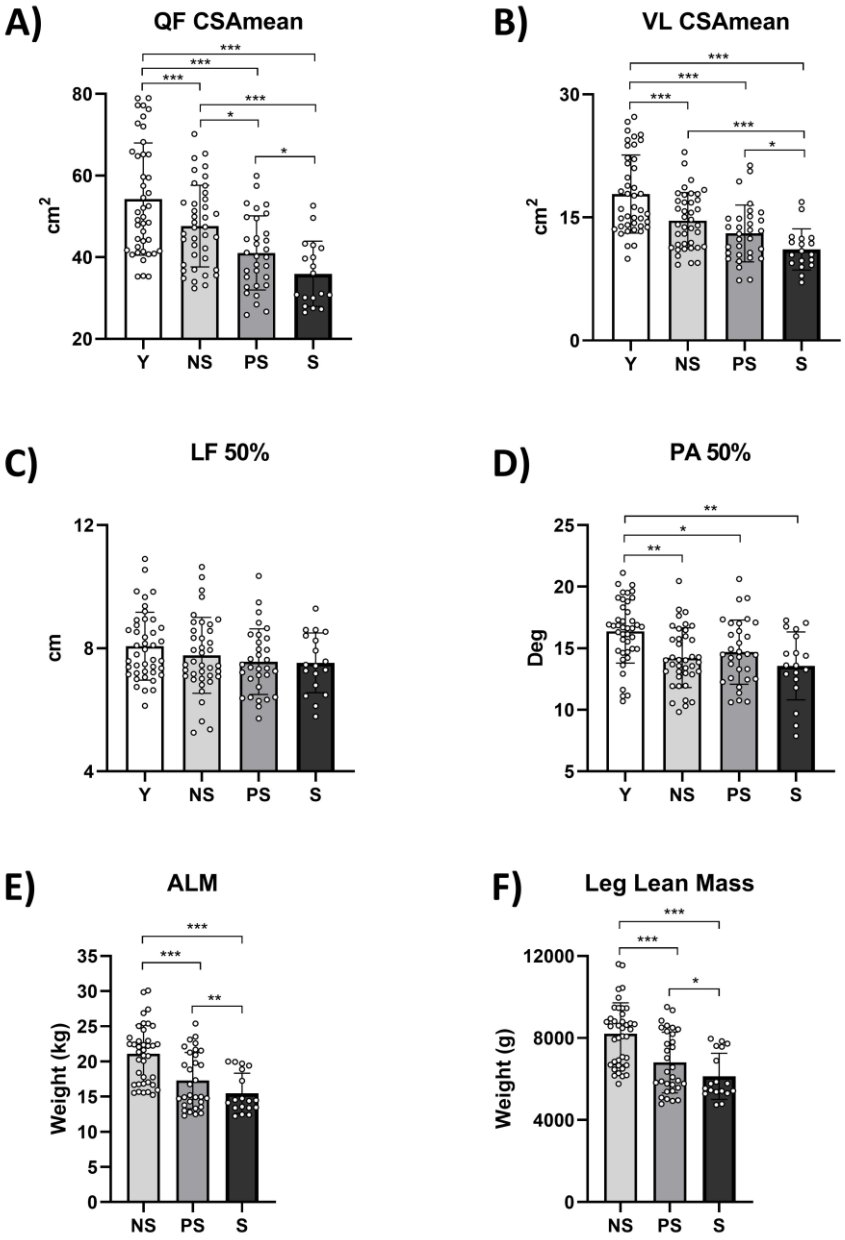

Figure 2: *Muscle morphology parameters and lean mass quantification across different stages of human sarcopenia. Statistical analysis was performed using two-way ANOVAs. Results are shown as mean and standard deviation. Quadriceps femoris (QF) cross-sectional area (CSA_{mean}): mean of the values at 30%, 50% and 70% of femur length (A); vastus lateralis (VL) CSA_{mean} (B); VL fascicle length (Lf) at 50% femur length (C); VL pennation angle (PA) at 50% femur length (D); appendicular lean mass (ALM) (E); and leg lean mass (F). Y: young individuals; NS: non-sarcopenic; PS: pre-sarcopenic; S: sarcopenic. *P < 0.05; **P < 0.01; ***P < 0.001*

iMUNE, MUP properties and NMJ transmission *in vivo*

We tested whether alterations in muscle morphology and function with sarcopenia were accompanied by MUs loss (Figure 6) and impairment in MUP properties and NMJ transmission (Figure 3 and 4). The iMUNE was decreased in all the older groups compared to Y ($P < 0.0001$; ηp^2 =

0.11). MU firing rate was lower in S compared to Y at 25% MVC (P = 0.039). MUP area and duration showed no effect of group for both contraction intensities. MUP complexity, evaluated by the number of turns, was elevated in NS compared to Y at 25% MVC (P = 0.0278). Similar behaviour was observed for NF duration (P = 0.003), while NF count was increased in NS and PS compared to Y (10% MVC: Y vs NS = 0.0045; Y vs PS: 0.0276; 25% MVC: Y vs NS = 0.0004; Y vs PS: 0.0245). Age-related NMJ transmission impairment was evaluated via the NF MUP segment jitter that was elevated in older groups with respect to Y at 25% MVC (Y vs NS and SAR: P < 0.0001; Y vs PS: P = 0.0169). Differences were detected also comparing PS with NS (P = 0.008) and S (P = 0.0072). Additional information on the iEMG data analysis is shown in Table S1.

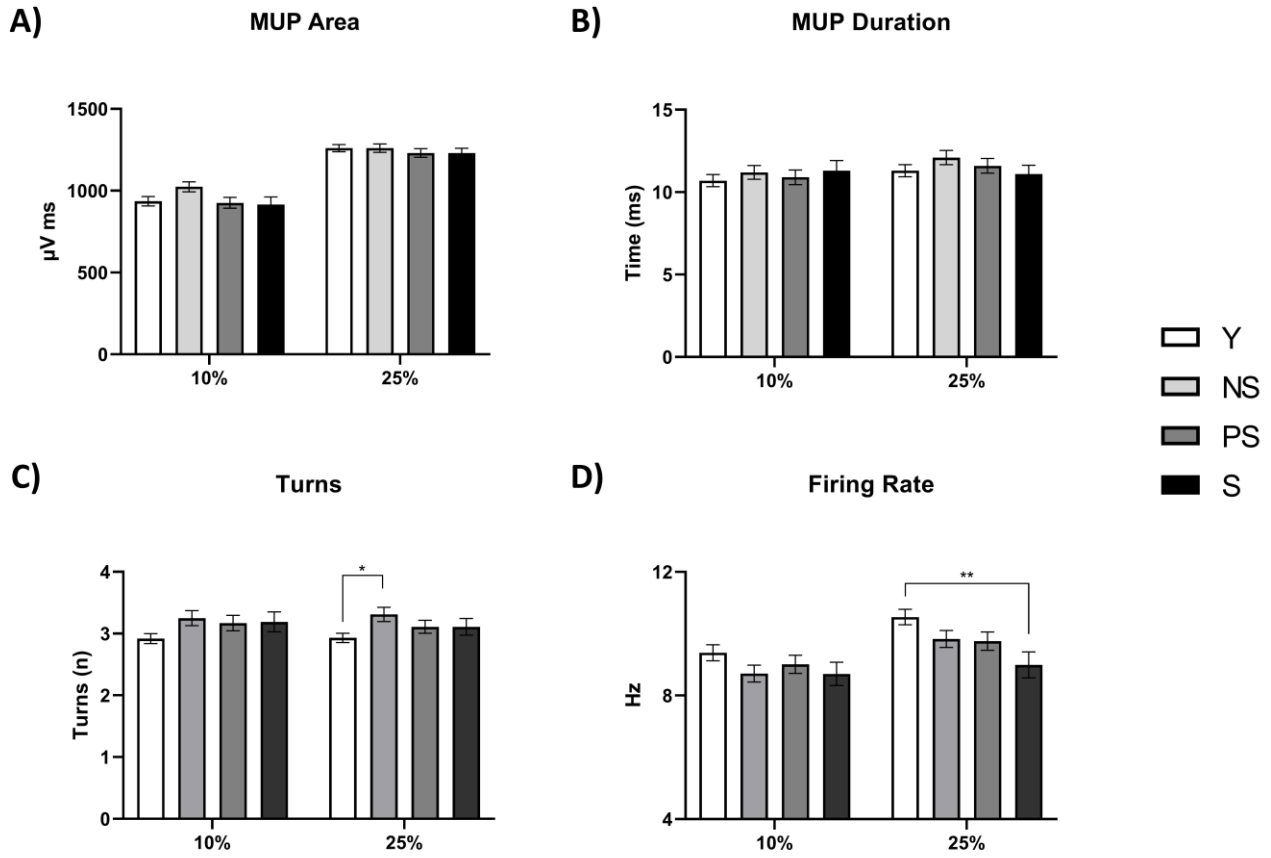

Figure 3: *Motor unit potential (MUP) parameters across different stages of human sarcopenia. Statistical analysis was performed using generalised linear mixed effect models. Results are shown as estimated marginal mean and standard error. MUP area (A); MUP duration (B); MUP turns (C); motor unit firing rate (D). Y: young individuals; NS: non-sarcopenic; PS: pre-sarcopenic; S: sarcopenic. *P < 0.05; **P < 0.01*

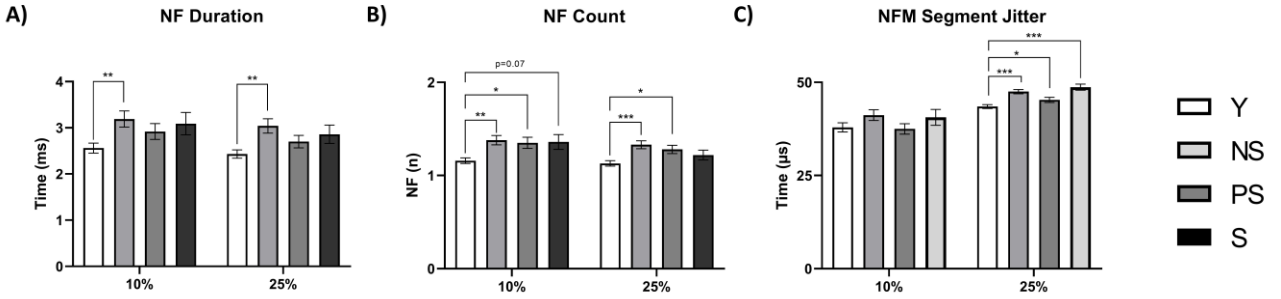

Figure 4: *Near fibre (NF) electromyography outcomes across different stages of human sarcopenia. Statistical analysis was performed using generalised linear mixed effect models. Results are shown as estimated marginal mean and standard error. NF motor unit potential duration (A); NF count (B); NF segment jitter (C). Y: young individuals; NS: non-sarcopenic; PS: pre-sarcopenic; S: sarcopenic. *P < 0.05; **P < 0.01; ***P < 0.001*

Circulating biomarkers of neurodegeneration

Considering the observed changes in muscle electrophysiological properties, we assessed circulating biomarkers of neurodegeneration (Figure 5). The cleavage of agrin induced by the enzyme neurotrypsin leads to the release of the soluble CAF into circulation, with higher concentrations of the latter considered indicative of NMJ instability (Monti *et al.*, 2023*a*). Increased CAF concentration ($P < 0.0001$; $\varepsilon^2 = 0.178$), was observed with ageing, with no differences between older groups. Neurofilament light chain concentration, a biomarker of axonal damage (Pratt *et al.*, 2022), was significantly elevated in older groups compared to Y ($P < 0.0001$; $\varepsilon^2 = 0.621$). No differences were observed comparing the four groups for circulating neurotrophins (BDNF and NT-4) and systemic inflammation (IL-6).

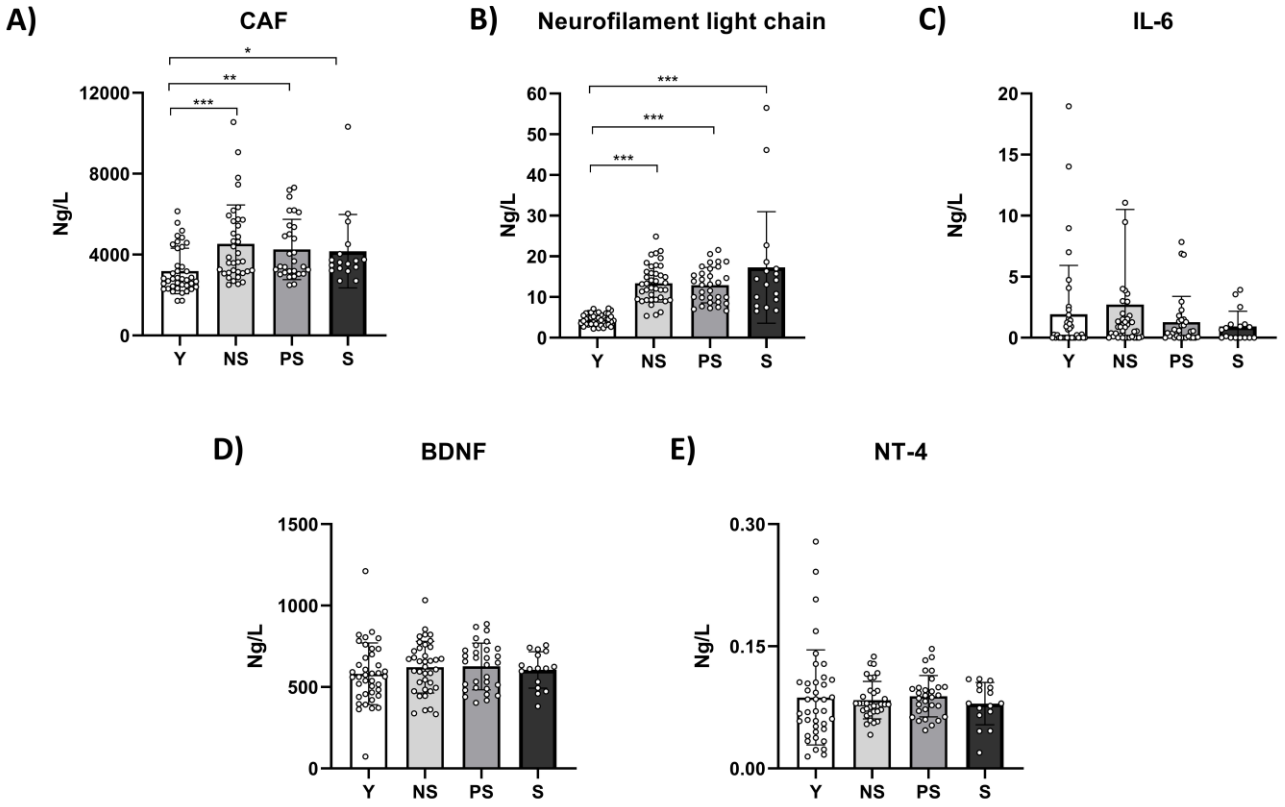

Figure 5: *Circulating biomarkers parameters across different stages of human sarcopenia. Statistical analysis was performed using Kruskal-Wallis tests (A-C) and two-way ANOVAs (D-E). Results are shown as mean and standard deviation. Blood concentration of C-terminal agrin fragment (CAF) (A); neurofilament light chain (B); interleukin-6 (IL-6) (C); brain-derived neurotrophic factor (BDNF) (D); neurotrophin-4 (E). Y: young individuals; NS: non-sarcopenic; PS: pre-sarcopenic; S: sarcopenic. For all parameters, data missing for 3 Y, 1 NS and 1 S. Additional missing values are 1 NS for CAF, 1 S for BDNF and 4 NS and 1 S for NT-4. One value is out of scale for IL-6.*P < 0.05; **P < 0.01; ***P < 0.001*

Muscle biomarkers of NMJ instability and denervation

We evaluated skeletal muscle biopsies to gain insights into the potential mechanisms driving NMJ degeneration and MUP properties alterations in ageing (Figure 6, 7 and S3). First, we assessed the principal downstream proteins of the agrin pathway, the predominant molecular mechanisms regulating ACh receptors clustering and NMJ endplate fragmentation (Tintignac *et al.*, 2015). We did not observe differences between groups in the protein levels of Lrp4, total MuSK, phosphorylated $MuSK_{(Tyr755)}$ ratio between phosphorylated and total MuSK (p-$MuSK_{(Tyr755)}$/MuSK) and Dok7. Similarly, we did not find differences in protein levels of the ACh receptors δ, γ and ε subunits (Figure S2 and S3). However, Cav3 was increased in NS (P = 0.0337) and PS (P = 0.0145) compared to Y, with a trend also for S (P = 0.09). Cav3 is a structural protein component of caveolae in muscle cells involved in agrin-induced ACh receptors phosphorylation and MuSK activation

(Henzel *et al.*, 2010). In addition, an increased percentage of NCAM-positive fibres was observed in Y vs NS ($P < 0.0001$) and Y vs S ($P = 0.02$), highlighting remodelling of the innervation pattern with ageing (Soendenbroe *et al.*, 2021). NS exhibited higher NCAM+ fibre than PS ($P = 0.0477$). Finally, the variability of muscle fibres diameter was increased in all old groups compared to Y ($P < 0.0001$; $\varepsilon^2 = 0.326$).

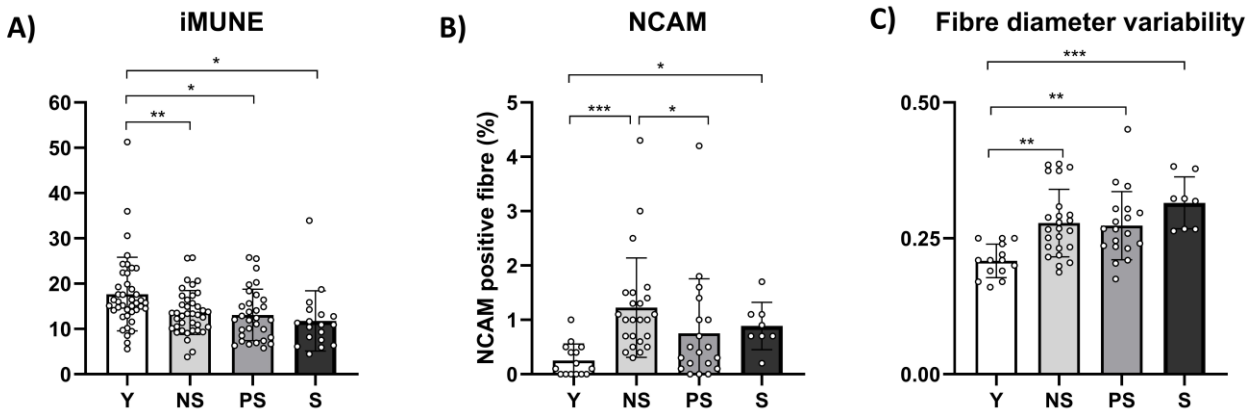

Figure 6: *Motor units loss and immunohistochemistry outcomes across different stages of human sarcopenia. Statistical analysis was performed using two-way ANOVAs (A) and Kruskal-Wallis tests (B-C). Results are shown as mean and standard deviation. Motor unit number estimate (iMUNE) (A); neural-cell adhesion molecule (NCAM) positive fibre percentage (B); fibre diameter variability, expressed as coefficient of variation (C). Y: young individuals; NS: non-sarcopenic; PS: pre-sarcopenic; S: sarcopenic. Two missing values for NCAM and fibre diameter variability (1 Y and 1 PS). *P < 0.05; **P < 0.01; ***P < 0.001*

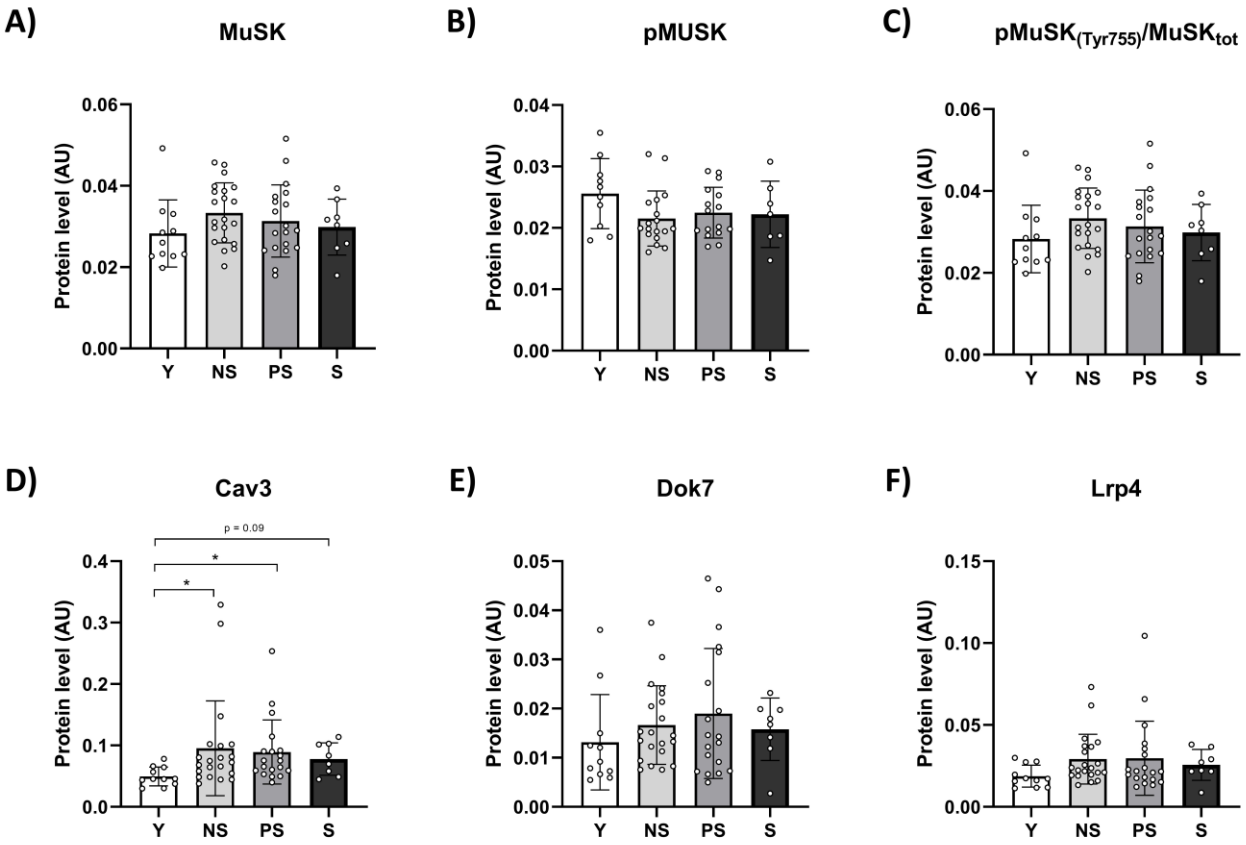

Figure 7: *Protein levels of the principal downstream elements of the agrin pathway across different stages of human sarcopenia. Statistical analysis was performed using Kruskal-Wallis tests. Results are shown as mean and standard deviation. Muscle-Specific Kinase total (MuSK) (A); phosphorylated MuSK (p-MuSK$_{(Tyr755)}$) (B); ratio between phosphorylated and total MuSK (p-MuSK$_{(Tyr755)}$/MuSK) (C); caveolin 3 (Cav3); docking protein 7 (Dok7); low-density lipoprotein receptor-related protein 4 (Lrp4). Y: young individuals; NS: non-sarcopenic; PS: pre-sarcopenic; S: sarcopenic. Data presented for 11 Y, 21 NS, 19 PS and 8 S in MuSK, Cav3, Dok7 and Lrp4 and for 10 Y, 18 NS, 16 PS and 7 S in pMuSK and pMuSK/tot.*P < 0.05*

DISCUSSION

This study provides new insights into the neuromuscular pathophysiological alterations occurring with different stages of sarcopenia in older humans. The main findings are that: (i) loss of MUs, NMJ instability, NMJ transmission impairment, myofibre denervation and axonal damage are prominent features of ageing of the neuromuscular system in older individuals; (ii) these neuromuscular alterations are accompanied by strength and size declines and they were present in all the older groups, including the non-sarcopenic participants.

Alterations in NMJ transmission and stability

As expected, S displayed an overall greater impairment in different domains of muscle function and physical performance in comparison to PS and NS. This refers not only to the parameters included in the sarcopenia definition but also to knee extensors MVC and to the ability to produce explosive force contractions (TTP63%). Males and females were similarly affected. Alteration in NMJ function is increasingly recognised as a driver of muscle weakness in the context of ageing and sarcopenia (Arnold & Clark, 2023). Our findings support this view, demonstrating an increased NMJ segment jitter, indicative of a reduced NMJ transmission (Juel, 2012; Piasecki *et al.*, 2021), in all old cohorts compared to Y. However, S did not exhibit a greater impairment compared to NS. While there is convincing evidence showing age-related alterations in jitter values both in rodents (Padilla *et al.*, 2021) and humans (Gilchrist, 1992), data in older humans clinically diagnosed with sarcopenia are scant. Only one published study was performed on this topic. This study is based on a small sample (total n=19) of pre-sarcopenic, sarcopenic and severely sarcopenic older individuals and found elevated NF jitter in individuals with severe sarcopenia compared to those with pre-sarcopenia (Gilmore *et al.*, 2017). Importantly, the present iEMG results of altered NMJ function are in line with our molecular data of NMJ integrity. Indeed, we found an age-related increase in serum CAF concentration, a well-established biomarker of NMJ instability (Monti *et al.*, 2023*a*), common to all the older groups. Ageing per se is known to result in an increased CAF concentration, although this biomarker has generally been reported to be further elevated in sarcopenic compared to non-sarcopenic older adults (Monti *et al.*, 2023*a*). A possible explanation for these contradictory results is that our study has focused on primary sarcopenia, while in most previous CAF investigations, sarcopenic individuals presented other diseases, such as chronic heart failure, chronic obstructive pulmonary disease and hip fracture (Monti *et al.*, 2023*a*). Furthermore, we excluded individuals with renal diseases, as this could affect CAF concentration (Monti *et al.*, 2023*a*). We found no differences in protein expression of selected downstream components of the agrin pathway. However, we observed an increased expression of Cav3 in the older cohorts compared to the Y controls. Cav3 is also localised at the NMJ (Carlson *et al.*, 2003) and among its functions, may contribute to the clustering of ACh receptors (Henzel *et al.*, 2010). An increased Cav3 expression in skeletal muscle might suggest an active process of NMJ remodelling in these older individuals, potentially a compensatory response as observed in muscle pathologies (Repetto *et al.*, 1999). However, due to the relatively small sample size and the obstacle of evaluating these proteins specifically at the NMJ using regular western blot analysis, these interpretations remain speculative.

Overall, altered Cav3 expression and increased agrin degradation suggested by increased CAF, point toward a NMJ structural destabilisation that may result in an impaired NMJ transmission with ageing, which precede the onset of clinically diagnosed sarcopenia. This latter observation is consistent with recent data showing that gene sets involved in NMJ regulation were not altered in sarcopenic compared to non-sarcopenic individuals across different ethnicities (Migliavacca *et al.*, 2019), although this study used bulk RNA-Seq and could not focus specifically on the signalling of NMJ nuclei.

MUs loss, alterations in MUP properties and underlying mechanisms

In agreement with the literature (Piasecki *et al.*, 2016*b*), we observed MUs loss in the older cohorts compared to the young controls, as inferred from the iMUNE data. Differently from our finding, a previous investigation using similar techniques, observed fewer MUs in sarcopenic compared to non-sarcopenic individuals in the vastus lateralis (Piasecki *et al.*, 2018*b*). However, this study included only male participants and employed a definition of sarcopenia different from that of the EWGSOP2 criteria and solely based on the assessment of muscle mass. Thus, a comparison with these previous findings seems difficult and should be made with caution.

Alterations in motoneuron and MUP properties were also observed in the present study. While age-related declines in motoneuron firing rate have been reported in different muscle groups, they have not been consistently observed in the quadriceps muscles, possibly due to their anti-gravity role (Orssatto *et al.*, 2022). In our study, firing rate assessed from the vastus lateralis was reduced only in sarcopenic compared to Y. This finding could be explained by motoneuron structural alterations(Larsson *et al.*, 2019), as supported by the observed age-related increased neurofilament light chain concentration, a circulating biomarker of axonal damage (Pratt *et al.*, 2022), although not specific for motoneurons. Reduced persistent inward current, regulating motoneuron excitability, may also play a role (Orssatto *et al.*, 2023) but its contribution to diagnosed sarcopenia has still to be determined. Reduced synaptic input onto the MU might contribute to decreased firing rates in females but not males, as sex differences were noted in the activation capacity assessed by the interpolated twitch technique (see Data S1). Nevertheless, S did not exhibit significantly lower firing rates compared to NS and PS, thus this mechanism is unlikely to explain their greater muscle weakness, which is instead probably largely explained by their smaller muscle mass. In fact, normalising handgrip and knee extensors strength for muscle/lean mass eliminated the differences between the three old groups (Figure S1).

In addition, our results showed some age-related changes in MUP turns, NF MUP duration and NF count, overall suggesting a MUP and NF MUP shape of increased complexity. Contrary to our hypothesis, this electrophysiological profile was particularly worsened in NS. This is not driven by an increased fibre diameter variability, as we observed no changes in this parameter comparing the three old groups. Recurring denervation and reinnervation cycles could also explain changes in MUP and NF MUP complexity (Piasecki *et al.*, 2021). Interestingly, the percentage of NCAM-positive fibres was particularly elevated in NS, similarly to our electrophysiological data. NCAM is an accepted muscle biomarker of denervation, reported to be re-expressed in ∼1% of aged muscle fibres in different human investigations (Soendenbroe *et al.*, 2021). More recently, it has been shown that NCAM is re-expressed (∼1.2-3.4% of positive fibres) also in conditions of short-term muscle disuse (i.e. 10-day bed rest or unilateral lower limb suspension) (Monti *et al.*, 2021; Sarto *et al.*, 2022*b*), suggesting that this biomarker is also sensitive to initial stages of neuromuscular destabilisation and altered innervation pattern. This is supported also by the fact that NCAM staining can be present also in large and round fibers (Soendenbroe *et al.*, 2021) and that its re-expression plays a role in guiding axon reinnervation, creating a large area of attraction that promotes synaptogenesis and improves the connectivity of the existing NMJs (Covault & Sanes, 1985). It is thus tempting to speculate that in NS a more "acute" and dynamic state of neuromuscular remodelling is captured by our electrophysiological and molecular assessments. In PS and S denervation processes may become more chronic and characterised by a lower reinnervation potential (Hepple & Rice, 2016; Piasecki *et al.*, 2018*b*), leading to a more limited increase in MUP complexity and NCAM expression.

Perspectives & methodological considerations

Considerations on sarcopenia definition and other influential factors

Our findings show that neuromuscular alterations (MUs loss, NMJ instability, impaired NMJ transmission, myofibre denervation and axonal damage) are present both in S and in NS individuals, in which sarcopenia was diagnosed according to the EWGSOP2 definition that considers sarcopenia as the coexistence of a condition of low muscle strength and mass (Cruz-Jentoft *et al.*, 2019). However, several studies expressed concerns regarding this definition, considered too strict and leading to a risk of underdiagnosis (Van Ancum *et al.*, 2020; Petermann-Rocha *et al.*, 2022). To solve this issue, in this study, we employed the EWGSOP2 definition with threshold modification for handgrip strength recently proposed by Westbury and colleagues, leading to higher prevalence rates while preserving the capacity to predict key health outcomes (Westbury *et al.*, 2023). Despite

the solid approach employed, we acknowledge that different sarcopenia definitions could lead to different results. Secondly, volunteers' physical activity levels could have influenced our results. According to the GPAQ score (Table 1), older groups were inactive compared to Y and this is likely to mediate at least in part their impaired neuromuscular function and integrity. Indeed, periods of muscle disuse are known to impact the neuromuscular system (Monti *et al.*, 2021; Sarto *et al.*, 2022*b*; Valli *et al.*, 2023), although, evidence in models mimicking a sedentary lifestyle is yet scant (Sarto *et al.*, 2023). Moreover, as S were not less physically active than NS and S, this could partially explain the absence of differences in the parameters regarding MU and NMJ degeneration. Thirdly, contractions up to 25% MVC were investigated, thus we acknowledge that our iEMG findings may be limited mainly to lower threshold and slower type MUs, generally considered more atrophy-resistant to neuromuscular ageing (Larsson *et al.*, 2019). However, glycogen depletion experiments (Gollnick *et al.*, 1974) showed that a switch from slow twitch to fast twitch fibres occurs at levels of about 20% of maximal exercise intensity in vastus lateralis. The choice of these intensities allows direct comparison with previous studies in the literature and is due to technical constraints of iEMG. Alternative techniques allowing decomposition at higher contraction intensities, such as high-density electromyography, do not enable the specific investigation of NMJ-related parameters and are affected in their accuracy by subcutaneous fat thickness, rendering challenging their application in the context of ageing, particularly in females.

Do MUs loss and NMJ degeneration precede sarcopenia?

Our results appear to indicate that MU loss and NMJ degeneration precede clinically diagnosed sarcopenia, as they can already be detected in non-sarcopenic older adults. This concept is supported by investigations in rodents, showing that morphological signs of NMJ denervation (Deschenes *et al.*, 2010), alterations in NMJ transcriptional and proteomic profiling (Ibebunjo *et al.*, 2013) and impaired recruitment of MUs and NMJ transmission (Tamaki *et al.*, 2014) were already evident before the overt loss of muscle mass and/or function with ageing. A plausible determinant of sarcopenia insurgence may be the time exposure to these neurodegenerative processes. While this finding has never been proven so far in humans, our study suggests there may be a need for early preventive measures, including exercise, nutritional and pharmaceutical interventions to combat this age-related neuromuscular impairment. Moreover, the electrophysiological and molecular parameters assessed in this study may serve as useful biomarkers of neuromuscular impairment with ageing. We acknowledge that the cross-sectional nature of this study represents a

limitation to our ability to definitively address this research question. Future longitudinal studies are warranted to confirm these observations.

Conclusions

This study has shown that neuromuscular alterations (MUs loss, NMJ instability, impaired NMJ transmission, myofibre denervation and axonal damage) are present in sarcopenic, pre-sarcopenic and non-sarcopenic individuals aged >70 years. This may suggest that neuromuscular alterations precede the onset of sarcopenia, as clinically defined. There is a need to combat these neuromuscular maladaptations through exercise, nutrition and pharmaceutical approaches in order to prevent the insurgence and progression of sarcopenia.

Acknowledgements

The authors thank sincerely the Municipality of Padova and "Auser Territoriale Padova APS" for the help with the recruitment of the participants and Mr. Eris Goldin and Mr. Alessandro Sampieri for the help in data collection and analysis. The authors would like to thank also all the volunteers for their priceless effort and time, as well as for the generous and most appreciated gifts.

Conflicts of interest

The authors have no conflict of interest to declare.

Funding

The present work was funded by the PRIN project 'NeuAge' (2017CBF8NJ_001) to MVN and the Milky Way Foundation, the Baxter Foundation, and the Li Ka Shing Foundation to HMB. EM was supported by the Stanford Wu Tsai Human Performance Institute fellowship and Marie Skłodowska-Curie Actions postdoctoral fellowship. We also acknowledge co-funding from Next Generation EU to MVN, in the context of the National Recovery and Resilience Plan, Investment PE8 – Project Age-It: "Ageing Well in an Ageing Society". This resource was co-financed by the Next Generation EU [DM 1557 11.10.2022]. The views and opinions expressed are only those of the authors and do not necessarily reflect those of the European Union or the European Commission. Neither the European Union nor the European Commission can be held responsible for them.

Ethics statement

The authors of this manuscript certify that they comply with the ethical guidelines for authorship and publishing in the Journal of Cachexia, Sarcopenia and Muscle(von Haehling *et al.*, 2021). As reported in the 'Methods' section, this study has been approved by the local ethics committee and performed in accordance with the ethical standards laid down in the 1964 Declaration of Helsinki and its later amendments. All the participants gave their informed consent prior to their inclusion in the study.

Data S1: Supplementary Materials

Supplementary methods

Short Physical Performance Battery (SPPB) and CTS power

Each component was graded on a scale of 0 (worst performance, inability to complete the test) to 4 (best performance). To evaluate balance, participants were asked to stand with their feet together, followed by semi-tandem and tandem positions for 10 seconds each. Gait speed was assessed through a 4-meter walk at the participant's habitual pace, with time recorded. Lastly, participants were instructed to stand up and sit down from a chair five times as quickly as possible, with their arms folded across their chests. A standard 46 cm chair was employed. The back of the chair was secured against a wall.

Muscle size measurements

A 47 mm, 7.5MHz linear array transducer was employed to collect all the ultrasound images. Transmission gel was generously applied to improve the acoustic contact for all images. Two CSA scans and three longitudinal scans were obtained at each site, and the image with the best quality was selected for the analysis. Femur length was measured as the distance between the greater trochanter and the mid-patellar point, with 0% representing the mid-patellar point (distal part) and 100% the greater trochanter (proximal part). To obtain the CSA images, the transducer was moved slowly in a transverse plane from the medial border of the vastus medialis to the lateral borders of the vastus lateralis, while maintaining consistent pressure on the skin. Lf was obtained with the manual linear extrapolation method using the segmented line tool of ImageJ (1.52v; National Institutes of Health, Bethesda, MD, USA). Briefly, the visible part of the fascicle was marked and then extrapolated with a straight line until the extension of the superficial aponeurosis. PA was defined as the angle of intersection between the fascicles and the deep aponeurosis.

Quadriceps force, rapid force production and activation capacity

During the MVC evaluation, participants were asked to push as strongly and as fast as they could for about 4s. They received visual feedback and verbal encouragement. The three trials were separated by a 1-minute rest. The force signal was recorded at 1000 Hz using LabChart software (v.8.13, ADInstrument, Dunedin, NewZealand). During the MVC testing, the participants received electrical stimulations via a stimulator device (Digitimer DS7AH), which were applied through two pads placed

on the thigh, one proximally and the other distally. One doublet stimulation was applied when the contraction reached a plateau, while the second pulse was applied one second after the contraction. The intensity of the electrical current required for each participant's supra-maximal stimulation was determined before the testing by monitoring the force output during a series of stimuli with increasing current. The current at which no further increase in force output was observed was recorded and used during the assessment. The muscle activation was calculated using the following equation:

$$Activation\ capacity = (1 - \frac{A}{B})\ x\ 100$$

where A represents the superimposed twitch torque and B represents the resting control twitch torque.

All the analyses were performed with a custom Python (v.3.9) script.

Intramuscular electromyography

The iEMG signal was recorded at 40 kHz with the LabChart software (v.8.13, ADInstruments). Visual feedback was provided during the contractions to allow participants to achieve the target constant force (10% or 25% MVC) for the required 20 seconds each. 30 s of rest was provided between contractions. The needle position was adjusted between contractions through a combination of twisting it by 180° or extracting it by 2-3 mm, so that motor units were sampled from at least 3 different muscle depths. The needle was carefully maintained in a constant position during recordings.

MUP trains with fewer than 35 MUPs, or with signal-to-noise ratios <15 and/or non-physiological shapes were excluded. The motor unit discharge pattern was considered only for MUP trains of the inter-discharge intervals akin to a Gaussian distribution. Regarding NF MUPs analysis, only trains with signal-to-noise ratios >15, >34 NF MUPs and with NF count >1 were included.

Circulating biomarkers assessment

CAF

Serum CAF concentration was obtained using a commercially available enzyme-linked immunosorbent assay (ELISA) kit (Human Agrin SimpleStep ELISA, Ab216945, Abcam, Cambridge, UK) following the manufacturer’s instructions. Samples were diluted 1:4 and run in duplicate.

Neurofilament light chain

The neurofilament light chain analysis was carried out at the facility 'Centro Piattaforme Tecnologiche' of the University of Verona (Verona, Italy) employing the single molecule array (SIMOA) Bead Technology (Quanterix Corporation 900 Middlesex Turnpike, Billerica, MA 10821) on a Quanterix SR-x (#1913QP0444) platform with Simoa® Nf-light Advantage Kit (SR-x). Samples were diluted 1:4 and analysed in duplicate.

BDNF

Serum BDNF concentration was obtained using a commercially available enzyme-linked immunosorbent assay (ELISA) kit (Brain-derived neurotrophic factor ELISA, ab212166, Abcam, Cambridge, UK) following the manufacturer's instructions. Samples were diluted 1:20 and run in duplicate.

NT-4

Serum NT-4 concentration was obtained using a commercially available enzyme-linked immunosorbent assay (ELISA) kit (Glial Derived Neurotrophic Factor ELISA, ELH-NT4, Raybiotech, US) following the manufacturer's instructions. Samples were diluted 1:1 and run in duplicate.

IL-6

Serum IL-6 concentration was obtained using a commercially available enzyme-linked immunosorbent assay (ELISA) kit (Interleukin-6 ELISA, Ab178013, Abcam, Cambridge, UK) following the manufacturer's instructions. Samples were diluted 1:1 and run in duplicate.

Muscle Biopsy

The biopsy part for western blot analysis was frozen in liquid nitrogen and stored at −80°C, while the part for immunohistochemical analysis was included in optimal cutting temperature (OCT), frozen in isopentane and stored at −80°C. Cryosections were cut with a manual cryostat (Leica CM3050 S), producing 10 µm-thick sections.

Immunofluorescence analyses

Detection and quantification of denervated myofibres were performed by NCAM immunofluorescent staining as described: serial cryosections were fixed in 4% PFA for 5 minutes, washed in PBS, permeabilised in 1% triton in PBS (PBS-T) and then blocked in 5% GS+1%BSA in PBS-T. The same cryosections were then labelled (overnight, 4C) using mouse IgG1 antibody directed against human CD56/NCAM (clone HCD56, BioLegend, cat. 318302) and rabbit antibody directed against laminin (Abcam, cat. ab11575) 1:200 and 1:500 diluted, respectively, in 5% GS+1%BSA in PBS-T. Sections were rinsed PBS-T (3x5 min) and then incubated with Cy3-affinity pure goat anti-

mouse IgG1 and Alexa Fluor 488 affinity pure goat anti-rabbit (Jackson Immunoresearch, cat. 115-165-205 and 111-546-045, respectively) 1:200 and Oechst (Thermo Scientific, cat. H3570) 1:1000 diluted in 5% GS+1%BSA in PBS-T. (1 hour at room temperature). Sections were washed in PBS-T (3x5 min) and incubated for 1 minute in 1:20 True Black Lipofuscin Autofluorescence Quencher (Biotium, cat. 23007) diluted in 70% ethanol. After washing in PBS, sections were coverslipped. Negative controls were performed by omitting the primary antibodies from sample incubations. All sections were imaged using a Keyence fluorescent microscope (Keyence, BZ-X810) at 20x magnification. Collages were generated through a semi-automated algorithm to reconstruct the whole tissue section image. NCAM-positive fibres were counted on captured collages, using ImageJ software (1.52v; National Institutes of Health, Bethesda, MD) and expressed as the number of positive myofibres per total number of myofibres detected in the biopsy area by laminin staining (400-2000 muscle fibres). The variability of muscle fibres diameters was expressed as the coefficient of variation (CV; standard deviation/mean of all the muscle fibres visible on the biopsy section).

Western Blot Analysis

Frozen muscle samples were pulverized and immediately re-suspended in a lysis buffer (20 mM Tris-HCl, 1% Triton X100, 10% Glycerol, 150 mM NaCl, 5 mM EDTA, 100 mM NaF and 2 mM NaPPi supplemented with 5× Protease Inhibitor (Protease Inhibitor Cocktail, Sigma-Aldrich, St. Louis MO), 1× phosphatase inhibitors (Phosphatase Inhibitor Cocktail, Sigma-Aldrich) and 1mM PMSF). The homogenate obtained was incubated on ice for 40 min and then centrifuged at 18000 × g for 20 min at 4°C. Total protein concentration was determined for each sample using an RC DC™ Protein Assay kit (Bio-Rad Laboratories, Inc., Hercules, CA, USA). Equal amounts of muscle samples (40 µg) were denatured and separated on 4-20% gradient precast gels (Bio-Rad Laboratories, Inc.). Due to the elevated number of samples under investigation, a reference sample was prepared and loaded in every gel during the same experimental session to make the comparison possible among the samples. After the gel run, proteins were electro-transferred to PVDF membranes at 35 mA overnight. The membranes were blocked using 5% nonfat dried milk in TBST (0.02 M Tris, 0.05 M NaCl, 0.1% Tween-20) for 2 hours at room temperature, rinsed with TBST and subsequently probed with specific primary antibodies (see below), in blocking solution overnight at 4°C. Thereafter, the membranes were incubated for 1 hour at room temperature with corresponding horseradish peroxidase (HRP)-conjugated secondary antibodies. Protein bands were visualized by an enhanced chemiluminescence method (Amersham ECL Select™, GE Healthcare, Little Chalfont, UK). The content of each protein investigated was assessed by determining the Brightness–Area Product of

the protein band normalized to total protein content, obtained by Ponceau S staining (0.2% Ponceau Red in 3% acetic acid) or evaluated between phosphorylated and unphosphorylated total forms of the same protein (expressed as arbitrary units, AU). Antibodies used were: anti-mouse AChRδ (1:1000, MA3-043; Thermo Fisher Scientific, Waltham, MA, US), anti-rabbit AChRε (1:1000, PA5-87600; Thermo Fisher Scientific), anti-rabbit AChRγ (1:1000, PA5-103556; Thermo Fisher Scientific), anti-rabbit Cav3 (1:1000, GTX109650; GeneTex Inc., Irvine, CA, US), anti-rabbit Dok7 (1:1000, ab75049; Abcam, Cambridge, UK), anti-rabbit Lrp4 (1:1000, ab230188; Abcam), anti-rabbit MuSK (1:1000, ab92950; Abcam), anti-rabbit *p*-MuSK$_{(Tyr755)}$ (1:1000, ab192583; Abcam); rabbit anti-mouse IgG (1:5000, P0161; Dako North America Inc., Carpinteria, CA, US); goat anti-rabbit IgG (1:10000, #7074; Cell Signalling Technology, Inc., Danvers, MA, USA).

Statistical analysis

The following is the list of variables not normally distributed, in which non-parametric statistics was applied: CAF, neurofilament light chain concentration, IL-6 and the biomarkers derived from muscle biopsies (NCAM, variability of muscle fibres diameter and all the proteins assessed from the Agrin-Lrp4-MuSK-Dok7 pathway). Non-parametric statistics was also employed for GPAQ, SPPB and balance scores, representing categorical variables. As explained in the main text, iEMG data were analysed using generalised linear mixed models (fixed effects: group and sex; cluster variable: subject). The family of distribution used in the analysis varied depending on each variable, with the gamma or inverse Gaussian distribution being employed. Different link functions were associated with each distribution (Table S1). The Bayesian information criterion (BIC) was used to compare the models. When multiple models had similar minimal BIC values, the canonical link function for the respective distribution was selected (i.e. inverse function (1/y) for gamma distribution and inverse squared ($1/y^2$) for inverse Gaussian distribution). Post hoc comparisons were carried out using the Holm correction.

Supplementary results

Sex differences in muscle function and physical performance

Handgrip strength ($P < 0.0001$, $\eta p^2 = 0.65$) and MVC showed a large effect of sex ($P < 0.0001$; $\eta p^2 = 0.41$), with females (F) exhibiting lower isometric forces than males (M). However, no group*sex interaction was found for both variables. The knee extensors specific force (MVC/CSA) was slightly superior in M ($P = 0.0114$; $\eta p^2 = 0.05$), with no interaction. No sex differences were observed for

handgrip strength normalised for arm lean mass. TTP63% did not display any effect of sex or interaction. Activation capacity showed a small effect of sex ($P = 0.0432$; $\eta p^2 = 0.03$) and a significant interaction ($P = 0.0423$; $\eta p^2 = 0.07$). Indeed, M have slightly higher activation capacity values; while in F, differently to M, the comparison between Y and S was significant ($P = 0.0161$). No significant effect of sex was found for SPPB and its components: CST time, balance score and gait speed.

Sex differences in muscle morphology

All DEXA parameters showed an effect of sex: ALM ($P < 0.0001$; $\eta p^2 = 0.72$), ALM/h^2 ($P < 0.0001$; $\eta p^2 = 0.51$), leg lean mass ($P < 0.0001$; $\eta p^2 = 0.69$); with F presenting lower lean mass values. These were observed without significant group*sex interaction. Quadriceps and vastus lateralis CSA_{mean} presented a large effect of sex (quadriceps: $P < 0.0001$; $\eta p^2 = 0.56$; vastus lateralis: $P < 0.0001$; $\eta p^2 = 0.41$) and a significant interaction (quadriceps: $P = 0.0099$; $\eta p^2 = 0.09$; vastus lateralis: $P = 0.0103$; $\eta p^2 = 0.09$). Specifically, F presented a smaller CSA_{mean}. Moreover, for VL in F, no differences were found in S compared to NS and PS, differently from M (NS vs S: 0.0096; PS vs S: 0.0357). Regarding muscle architecture parameters, Lf showed no group*sex interaction but an effect of sex ($P = 0.0006$; $\eta p^2 = 0.09$) was observed, pointing toward longer fascicles in M. Similar trend was observed for PA, with larger angles observed in M ($P = 0.0105$; $\eta p^2 = 0.05$).

Sex differences in iMUNE, MUP properties and NMJ transmission

The iMUNE showed an effect of sex ($P < 0.0001$; $\eta p^2 = 0.14$), indicating higher values in M, with no group*sex interaction. No effect of sex and interaction were detected in all the iEMG parameters considered. Thus, this variable was excluded from the final generalised linear mixed models presented in the main manuscript.

Sex differences in circulating biomarkers of neurodegeneration

No effect of sex was noticed for CAF, neurofilament light chain and IL-6 concentration. Similarly, no significant effect of sex and group*sex interaction was observed for BDNF and NT-4.

Sex differences in muscle biomarkers of NMJ instability and denervation

Due to the more limited sample size, as muscle biopsies were collected only in a subgroup of participants, sex differences were not investigated for muscle biomarkers of NMJ instability and denervation.

Supplementary tables and figures

Parameter	Distribution	Link function	Estimate	95% CI	P value Group
MUP area 10% (µV · ms)	Inverse gaussian	Identity	950	915.21 to 985.1	0.075
MUP area 25% (µV · ms)	Inverse gaussian	Identity	1245.448	1208.3 to 1282.64	0.1674
MUP duration 10% (ms)	Gamma	Inverse	0.0908	0.087 to 0.0946	0.8784
MUP duration 25% (ms)	Gamma	Inverse	0.0868	0.0834 to 0.0901	0.4675
MUP turns 10% (number of turns)	Inverse gaussian	Inverse squared	0.1025	0.0945 to 0.1104	***0.0798***
MUP turns 25% (number of turns)	Inverse gaussian	Inverse squared	0.1037	0.0965 to 0.1108	***0.0345***
Firing Rate 10% (Hz)	Inverse gaussian	Identity	8.954	8.65 to 9.2557	0.2694
Firing Rate 25% (Hz)	Inverse gaussian	Identity	9.782	9.47 to 10.0955	***0.0091***
NF MUP duration 10% (ms)	Gamma	Inverse	0.3425	0.3223 to 0.3627	***0.0093***
NF MUP duration 25% (ms)	Gamma	Inverse	0.3652	0.3462 to 0.3842	***0.0037***
NF count 10%	Inverse gaussian	Inverse	0.766	0.733 to 0.799	***0.0027***

(number)					
NF count 25% (number)	Inverse gaussian	Inverse	0.8099	0.782 to 0.8376	***0.0008***
NF MUP segment jitter 10% (µs)	Gamma	Inverse	0.0255	0.0245 to 0.0246	0.1905
NF MUP segment jitter 25% (µs)	Gamma	Inverse	0.0216	0.0214 to 0.0219	***<0.0001***

Table S1: *Details of the generalised linear mixed effect models performed for each iEMG variable. The overall estimate and p value of the model are reported in this table, while p values of the time-point comparison are presented in the text. Motor unit potentials (MUPs) from 4160 (32.25 (13.8) on average per participant) and 6340 MUPs (49.15 (14.24) on average), sampled at 10% and 25% MVC, respectively, were analysed. Near fibre MUPs from 1724 and 2644 MUPs, sampled at 10% (13.36 (8.62) on average) and 25% (20.5 (10.05) on average) MVC, respectively, were analysed.*

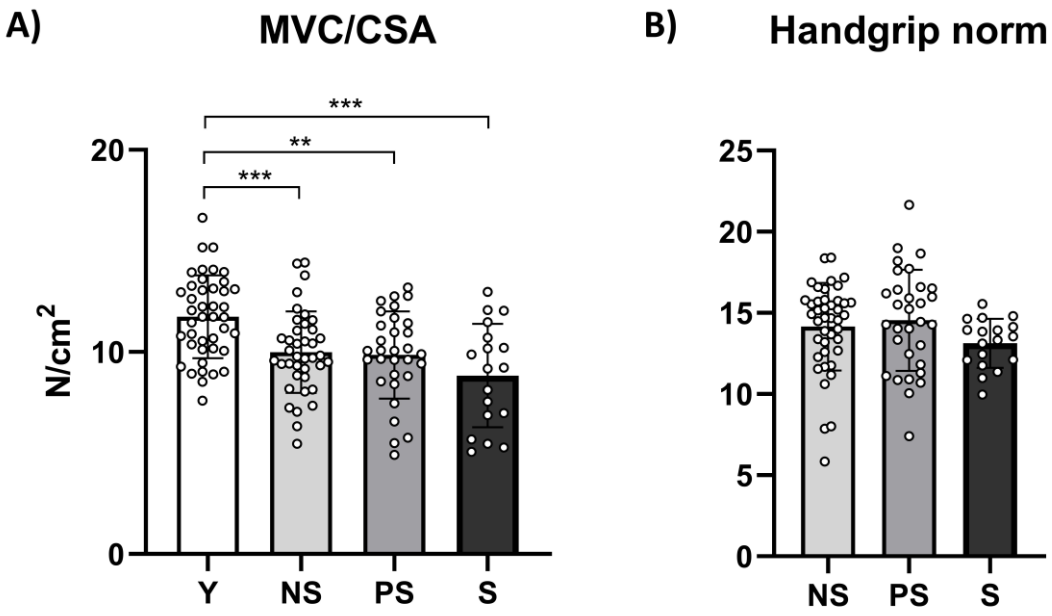

Figure S1: *Knee extensors and handgrip specific force across different stages of human sarcopenia. Statistical analysis was performed using and two-way ANOVAs. Results are shown as mean and standard deviation. Knee extensors maximum voluntary isometric force (MVC) normalised for the mean quadriceps cross-sectional area (CSA; mean of the values at 30%, 50% and 70% of femur length) (A); handgrip strength normalised for arm lean mass (B). Y: young individuals; NS: non-sarcopenic; PS: pre-sarcopenic; S: sarcopenic. **P < 0.01; ***P < 0.001*

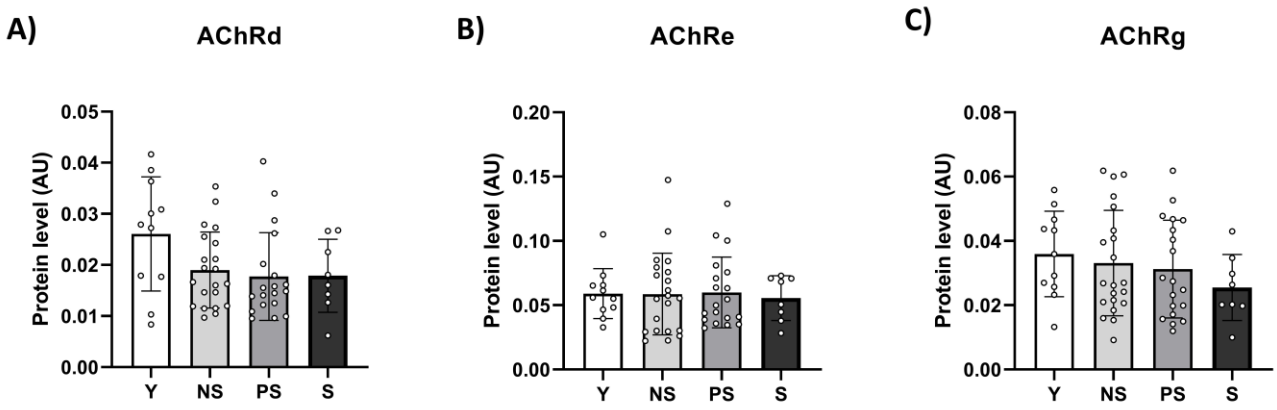

Figure S2: *Proteins levels of different acetylcholine receptors (AChR) subunits across different stages of human sarcopenia. Statistical analysis was performed using Kruskal-Wallis tests. Results are shown as mean and standard deviation. AChR δ subunit (A); AChR ε subunit (B); AChR γ subunit (C). Y: young individuals; NS: non-sarcopenic; PS: pre-sarcopenic; S: sarcopenic. Data presented for 11 Y, 21 NS, 19 PS and 8 S. **P < 0.01; ***P < 0.001*

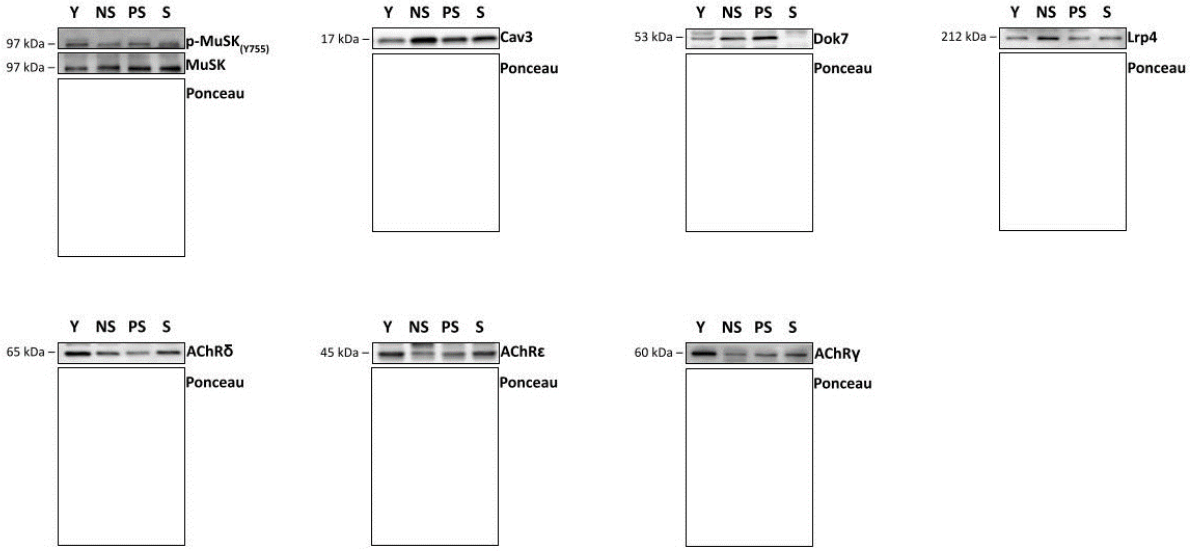

Single blots from each membrane

Figure S3: *Representative western blot of muscle-specific kinase total (MuSK), phosphorylated MuSK (p-MuSK(Tyr755)), caveolin 3 (Cav3), docking protein 7 (Dok7), low-density lipoprotein receptor-related protein 4 (Lrp4) and acetylcholine receptors (AChR) subunits δ, ε and γ. Y: young individuals; NS: non-sarcopenic; PS: pre-sarcopenic; S: sarcopenic.*

6. CONCLUSIONS

Throughout my PhD, I contributed to 16 papers in the field of neuromuscular physiology, of which 7 as first author, as presented in Chapter 2. The present dissertation focused on two original research articles and one review article, investigating the impact of muscle disuse, reduced physical activity and sarcopenia on human health. The two experimental studies delved into the exploration of neuromuscular system plasticity, with a specific emphasis on MU remodelling and NMJ instability, leveraging an integrative physiological approach that combined in vivo imaging, functional and electrophysiological measurements with ex vivo molecular analysis. Each paper contains an extensive discussion specifically related to the topic investigated. The following are some concluding thoughts that interconnect the various studies of my PhD, as summarized in Table 2.

Parameter	Step Reduction	Muscle Disuse	Ageing	Sarcopenia (vs Ageing)
Muscle mass	↓	↓	↓	↓
Muscle function	=	↓	↓	↓
Activation capacity	?	=↓	=	=
CAF concentration	?	↑	↑	=
NCAM-positive fibre	?	↑	↑	=
Neurofilament light concentration	?	↑	↑	=
NMJ transmission	?	=	↓	=
MUP complexity	?	↑	↑	=
Firing rate	?	↓	=↓	=

Table 2: *Summary of the changes in different neuromuscular parameters with reduced physical activity (step reduction, (Sarto et al., 2023)), muscle disuse (bed rest* (Monti *et al.*, 2021) *and unilateral lower limb suspension (Sarto et al., 2022b)), ageing (non-sarcopenic older individuals (Sarto et al; Chapter 5)) and sarcopenia (diagnosed according to the EWGSOP2; Sarto et al; Chapter 5). CAF: C-terminal agrin fragment; NCAM: neural cell adhesion molecule; NMJ: neuromuscular junction; MUP: motor unit potential.*

During the early days of my PhD I was involved in the data collection and analysis of the MARSPRE2019 campaign, a 10-day bed rest study in young healthy individuals. Despite disuse is known to induce rapid and marked decreases in muscle mass and force (Narici & De Boer, 2011;

Campbell *et al.*, 2019; Di Girolamo *et al.*, 2021; Hardy *et al.*, 2022; Preobrazenski *et al.*, 2023), alterations in some muscle groups remain poorly investigated. We showed that short-term bed rest impact not only postural muscles, such as the quadriceps (Monti *et al.*, 2021), but also, induces morphological and contractile properties alterations in a nonpostural muscle group, the hamstrings (Sarto *et al.*, 2021*a*; Franchi *et al.*, 2022*a*). The main article of the bed rest campaign showed that unloading is associated with impairment in calcium dynamics and initial signs of myofibre denervation and NMJ molecular instability (Monti *et al.*, 2021). **My first PhD study** (Sarto *et al.*, 2022*b*) aimed to expand these previous findings testing whether NMJ function and MU potential properties could also be affected by disuse and studying the reversibility of these alterations to a subsequent retraining period. We employed a different model of disuse, the ULLS, for the same duration (10 days) and confirmed the previous observations concerning the alterations of the neuromuscular system reported following bed rest (Monti *et al.*, 2021). Additionally, we observed alterations in MU potential properties (increased MU potential complexity and reduced firing rate), accompanied by signs of axonal damage and downregulation of skeletal muscle ion channels genes. NMJ transmission was unchanged, in line with another study of similar duration published a few weeks after our work (Inns *et al.*, 2022).

These detrimental alterations were observed to complete disuse (ULLS and bed rest). It is still to be ascertained whether analogous impairments can be observed in milder experimental models of physical inactivity, such as step reduction, which more accurately mimics a sedentary lifestyle. This matter was highlighted in my **second PhD study** (Sarto *et al.*, 2023)**,** where I performed a comprehensive literature review on this topic. We also planned a step reduction study, which started during the final months of my PhD. This experiment will contribute to filling this knowledge gap.

The findings from our ULLS campaign also suggest that a retraining period based on a traditional resistance training protocol (3 sets at 70% 1RM) seems effective in reversing the neuromuscular changes induced by short-term disuse (Sarto *et al.*, 2022*b*; Valli *et al.*, 2023). However, this restoration may require about twice the duration of the disuse period, similarly to what previously reported (Suetta *et al.*, 2009). This further highlights the remarkable plasticity of the neuromuscular system.

According to **my third PhD study** (Sarto et al; Chapter 5), ageing (i.e. non-sarcopenic older individuals without major diseases) seems accompanied by electrophysiological and molecular

alterations of MU and NMJ similar to those induced by muscle disuse. Indeed, besides the well-established age-related loss of muscle mass, function and specific force (muscle force divided for muscle size), we observed increased CAF and neurofilament light chain concentration and NCAM-positive fibre percentage and MUP complexity. Although ageing is well known to be accompanied by a reductions in physical activity levels and certainly shares similar effects on the neuromuscular system, it can also induce differential adaptations. For instance, ageing is known to promote a shift towards the slow phenotype (i.e. increased type I fibre percentage) (Schiaffino & Reggiani, 2011), while disuse to a fast phenotype (i.e. increased type II fibre percentage) (Blaauw *et al.*, 2013; Vikne *et al.*, 2020). Additionally, our study showed that the chronic nature of ageing seems to trigger NMJ transmission impairment, which conversely showed resilience in disuse conditions, at least during short-term ULLS. MUs loss, evaluated with the iMUNE method, was also observed with ageing, differently from ULLS (unpublished data). Thus, ageing and disuse, despite interconnected, should be considered two distinct phenomena.

Contrary to our hypothesis, sarcopenic individuals did not exhibit an exacerbated MU and NMJ degeneration compared to non-sarcopenic older adults, although they displayed greater muscle loss and more profound impairments in muscle function and physical performance. These results suggest that the observed alterations are already present in normal ageing, likely driving at least in part age-related muscle weakness, and thus seem to precede sarcopenia. At the same time, the traditional view, considering MU and NMJ degeneration as crucial differentiators between non-sarcopenic and sarcopenic individuals, is questioned by our observations, prompting the need for further investigations.

In conclusion, the findings of this dissertation contributed to advancing the present knowledge on the neuromuscular system plasticity with disuse and sarcopenia. By elucidating the mechanisms underlying MUs and NMJs alterations in humans, this dissertation established a solid foundation for the development of targeted interventions in these scenarios, opening new avenues for enhancing health and quality of life.

7. REFERENCES

Akins JD, Crawford CK, Burton HM, Wolfe AS, Vardarli E & Coyle EF (2019). Inactivity induces resistance to the metabolic benefits following acute exercise. *J Appl Physiol* **126,** 1088–1094.

Alcazar J, Ara I, García-García FJ & Alegre LM (2022). Number of Chair Stands Should Not Be Considered a Muscle Function Measure, But a Physical Performance Measure. What Can We Do Then? *J Frailty Aging* **11,** 245–246.

Allen MD, Dalton BH, Gilmore KJ, Mcneil CJ, Doherty TJ, Rice CL & Power GA (2021). Neuroprotective effects of exercise on the aging human neuromuscular system. *Exp Gerontol* **152,** 111465.

Allen MD, Stashuk DW, Kimpinski K, Doherty TJ, Hourigan ML & Rice CL (2015). Increased neuromuscular transmission instability and motor unit remodelling with diabetic neuropathy as assessed using novel near fibre motor unit potential parameters. *Clin Neurophysiol* **126,** 794–802.

Alway S, Mohamed J & Myers M (2017). Mitochondria Initiate and Regulate Sarcopenia. *Exerc Sport Sci Rev* **45,** 34–40.

Anagnostou ME & Hepple RT (2020). Mitochondrial Mechanisms of Neuromuscular Junction Degeneration with Aging. *Cells*.

Van Ancum JM, Alcazar J, Meskers CGM, Nielsen BR, Suetta C & Maier AB (2020). Impact of using the updated EWGSOP2 definition in diagnosing sarcopenia: A clinical perspective. *Arch Gerontol Geriatr* **90,** 104125.

Andersen LB, Mota J & Di Pietro L (2016). Update on the global pandemic of physical inactivity. *Lancet* **388,** 1255–1256.

Anker SD, Morley JE & von Haehling S (2016). Welcome to the ICD-10 code for sarcopenia. *J Cachexia Sarcopenia Muscle* **7,** 512–514.

Appriou Z, Nay K, Pierre N, Saligaut D, Lefeuvre-Orfila L, Martin B, Cavey T, Ropert M, Loréal O, Rannou-Bekono F & Derbré F (2019). Skeletal muscle ceramides do not contribute to physical-inactivity-induced insulin resistance. *Appl Physiol Nutr Metab* **44,** 1180–1188.

Arentson-Lantz EJ, English KL, Paddon-Jones D & Fry CS (2016). Fourteen days of bed rest induces a decline in satellite cell content and robust atrophy of skeletal muscle fibers in middle-aged adults. *J Appl Physiol* **120,** 965–975.

Arizono N, Koreto O, Iway Y, Hidaka K & Takeoka O (1984). Morphometric analysis of human

neuromuscular junction in different ages. *Pathol Int* **34,** 1243–1249.

Arnold WD & Clark BC (2023). Neuromuscular junction transmission failure in aging and sarcopenia: The nexus of the neurological and muscular systems. *Ageing Res Rev* **89,** 101966.

Atkov O & Bednenko V (1992). Hypokinesia and weightlessness: clinical and physiologic aspects. In *International University Press, Madison*, p. 506.

Attias J, Grassi A, Bosutti A, Ganse B, Degens H & Drey M (2020). Head-down tilt bed rest with or without artificial gravity is not associated with motor unit remodeling. *Eur J Appl Physiol* **120,** 2407–2415.

Aubertin-Leheudre M, Pion CH, Vallée J, Marchand S, Morais JA, Bélanger M & Robitaille R (2019). Improved Human Muscle Biopsy Method To Study Neuromuscular Junction Structure and Functions with Aging. *Journals Gerontol Ser A* **75,** 2098–2102.

Badawi Y & Nishimune H (2020). Impairment Mechanisms and Intervention Approaches for Aged Human Neuromuscular Junctions. *Front Mol Neurosci* **13,** 1–16.

Baehr LM, West DWD, Marcotte G, Marshall AG, De Sousa LG, Baar K & Bodine SC (2016). Age-related deficits in skeletal muscle recovery following disuse are associated with neuromuscular junction instability and ER stress, not impaired protein synthesis. *Aging (Albany NY)* **8,** 127–146.

Bains RS, Wells S, Sillito RR, Armstrong JD, Cater HL, Banks G & Nolan PM (2018). Assessing mouse behaviour throughout the light/dark cycle using automated in-cage analysis tools. *J Neurosci Methods* **300,** 37–47.

Banzrai C, Nodera H, Kawarai T, Higashi S, Okada R, Mori A, Shimatani Y, Osaki Y & Kaji R (2016). Impaired axonal Na+ current by hindlimb unloading: Implication for disuse neuromuscular atrophy. *Front Physiol* **7,** 1–11.

Barański S, Kwarecki K, Szmigielski S & Rozyński J (1971). Histochemistry of skeletal muscle fibres in rats undergoing long-term experimental hypokinesia. *Folia Histochem Cytochem* **9,** 381–386.

Barazzoni R, Cederholm T, Zanetti M & Gortan Cappellari G (2023). Defining and diagnosing sarcopenia: Is the glass now half full? *Metabolism* **143,** 155558.

Barbosa-Silva TG, Menezes AMB, Bielemann RM, Malmstrom TK & Gonzalez MC (2016). Enhancing SARC-F: Improving Sarcopenia Screening in the Clinical Practice. *J Am Med Dir Assoc* **17,** 1136–1141.

Bauman A, Bittman M & Gershuny J (2019). A short history of time use research; implications for

public health. *BMC Public Health*.

Baumgartner RN, Koehler KM, Gallagher D, Romero L, Heymsfield SB, Ross RR, Garry PJ & Lindeman RD (1998). Epidemiology of sarcopenia among the elderly in New Mexico. *Am J Epidemiol* **147,** 755–763.

Beachle TR & Earle R (1994). *Essentials of Strength Training and Conditioning*. NSCA, Human Kinetics, USA.

Beckman EL, Coburn KR, Chambers RM, Deforest RE, Benson VG & Augerson WS (1961). Some physiological changes observed in human subjects during zero G simulation by immersion in water up to neck level. *Aerosp Med* **32,** 1031–1041.

Bell KE, von Allmen MT, Devries MC & Phillips SM (2016). Muscle Disuse as a Pivotal Problem in Sarcopenia-related Muscle Loss and Dysfunction. *J Frailty Aging* **5,** 33–41.

Belova SP, Tyganov SA, Mochalova EP & Shenkman BS (2021). Restricted Activity and Protein Synthesis in Postural and Locomotor Muscles. *J Evol Biochem Physiol* **57,** 720–729.

Berchtold NC, Castello N & Cotman CW (2010). Exercise and time-dependent benefits to learning and memory. *Neuroscience* **167,** 588–597.

Berg HE, Dudley GA, Haggmark T, Ohlsen H & Tesch PA (1991). Effects of lower limb unloading on skeletal muscle mass and function in humans. *J Appl Physiol* **70,** 1882–1885.

Bhasin S et al. (2020). Sarcopenia Definition: The Position Statements of the Sarcopenia Definition and Outcomes Consortium. *J Am Geriatr Soc* **68,** 1410–1418.

Biddle GJH, Edwardson CL, Henson J, Davies MJ, Khunti K, Rowlands A V & Yates T (2018). Associations of Physical Behaviours and Behavioural Reallocations with Markers of Metabolic Health: A Compositional Data Analysis. *Int J Environ Res Public Health* **15,** 1–14.

Blaauw B, Schiaffino S & Reggiani C (2013). Mechanisms modulating skeletal muscle phenotype. *Compr Physiol* **3,** 1645–1687.

Bleeker MWP, Hopman MTE, Rongen GA & Smits P (2004). Unilateral lower limb suspension can cause deep venous thrombosis. *Am J Physiol - Regul Integr Comp Physiol* **286,** R1176–R1177.

Bloch-Gallego E (2015). Mechanisms controlling neuromuscular junction stability. *Cell Mol Life Sci* **72,** 1029–1043.

Blottner D, Trautmann G, Furlan S, Gambara G, Block K, Gutsmann M, Sun LW, Worley PF, Gorza L, Scano M, Lorenzon P, Vida I, Volpe P & Salanova M (2022). Reciprocal homer1a and homer2 isoform expression is a key mechanism for muscle soleus atrophy in spaceflown mice. *Int J Mol Sci* **23,** 1–20.

Bodine SC (2013). Disuse-induced muscle wasting. *Int J Biochem Cell Biol* **45,** 1–17.

de Boer MD, Maganaris CN, Seynnes OR, Rennie MJ & Narici MV (2007). Time course of muscular, neural and tendinous adaptations to 23 day unilateral lower-limb suspension in young men. *J Physiol* **583,** 1079–1091.

Booth FW (1982). Effect of limb immobilization on skeletal muscle. *J Appl Physiol Respir Environ Exerc Physiol* **52,** 1113–1118.

Booth FW & Kelso JR (1973). Production of rat muscle atrophy by cast fixation. *J Appl Physiol* **34,** 404–406.

Booth FW, Roberts CK, Thyfault JP, Ruegsegger GN & Toedebusch RG (2017). Role of inactivity in chronic diseases: Evolutionary insight and pathophysiological mechanisms. *Physiol Rev* **97,** 1351–1402.

Botter A, Oprandi G, Lanfranco F, Allasia S, Maffiuletti NA & Minetto MA (2011). Atlas of the muscle motor points for the lower limb: Implications for electrical stimulation procedures and electrode positioning. *Eur J Appl Physiol* **111,** 2461–2471.

Bottinelli R, Canepari M, Pellegrino MA & Reggiani C (1996). Force-velocity properties of human skeletal muscle fibres: Myosin heavy chain isoform and temperature dependence. *J Physiol* **495,** 573–586.

Bowden Davies K, Pickles S, Sprung V, Kemp G, Alam U, Moore D, Tahrani A & Cuthbertson D (2019). Reduced physical activity in young and older adults: metabolic and musculoskeletal implications. *Ther Adv Endocrinol Metab* **10,** 1–15.

Bowden Davies KA, Norman JA, Thompson A, Mitchell KL, Harrold JA, Halford JCG, Wilding JPH, Kemp GJ, Cuthbertson DJ & Sprung VS (2021). Short-Term Physical Inactivity Induces Endothelial Dysfunction. *Front Physiol* **12,** 1–9.

Bowden Davies KA, Sprung VS, Norman JA, Thompson A, Mitchell KL, Halford JCG, Harrold JA, Wilding JPH, Kemp GJ & Cuthbertson DJ (2018). Short-term decreased physical activity with increased sedentary behaviour causes metabolic derangements and altered body composition: effects in individuals with and without a first-degree relative with type 2 diabetes. *Diabetologia* **61,** 1282–1294.

Boyle LJ, Credeur DP, Jenkins NT, Padilla J, Leidy HJ, Thyfault JP & Fadel PJ (2013). Impact of reduced daily physical activity on conduit artery flow-mediated dilation and circulating endothelial microparticles. *J Appl Physiol* **115,** 1519–1525.

Breen L, Stokes KA, Churchward-Venne TA, Moore DR, Baker SK, Smith K, Atherton PJ & Phillips SM

(2013). Two weeks of reduced activity decreases leg lean mass and induces “anabolic resistance” of myofibrillar protein synthesis in healthy elderly. *J Clin Endocrinol Metab* **98,** 2604–2612.

Brocca L, Cannavino J, Coletto L, Biolo G, Sandri M, Bottinelli R & Pellegrino MA (2012). The time course of the adaptations of human muscle proteome to bed rest and the underlying mechanisms. *J Physiol* **590,** 5211–5230.

Brocca L, Longa E, Cannavino J, Seynnes O, de Vito G, Mcphee J, Narici M, Pellegrino MA & Bottinelli R (2015). Human skeletal muscle fibre contractile properties and proteomic profile: Adaptations to 3 weeks of unilateral lower limb suspension and active recovery. *J Physiol* **593,** 5361–5385.

Brook MS, Stokes T, Gorissen SHM, Bass JJ, McGlory C, Cegielski J, Wilkinson DJ, Phillips BE, Smith K, Phillips SM & Atherton PJ (2022). Declines in muscle protein synthesis account for short-term muscle disuse atrophy in humans in the absence of increased muscle protein breakdown. *J Cachexia Sarcopenia Muscle*; DOI: 10.1002/jcsm.13005.

Brooks NE & Myburgh KH (2014). Skeletal muscle wasting with disuse atrophy is multi-dimensional: The response and interaction of myonuclei, satellite cells and signaling pathways. *Front Physiol* **5 MAR,** 1–14.

Brown MC & Ironton R (1977). Motor neurone sprouting induced by prolonged tetrodotoxin block of nerve action potentials. *Nature* **265,** 459–461.

Brzycki M (1993). Strength Testing—Predicting a One-Rep Max from Reps-to-Fatigue. *J Phys Educ Recreat Danc* **64,** 88–90.

Buller BYAJ, Eccles JC & Eccles RM (1960). Interactions between motoneurones and muscles in respect of the characteristic speeds of their responses. *J Physiol* **150,** 417–439.

Buoite Stella A, Ajčević M, Furlanis G & Manganotti P (2021). Neurophysiological adaptations to spaceflight and simulated microgravity. *Clin Neurophysiol* **132,** 498–504.

Burke R, Levine D, Tsairis P & Zajac F (1973). Physiological types and histochemical profiles in motor units of the cat gastrocnemius. *J Physiol* **234,** 723–748.

Burton HM & Coyle EF (2021). Daily Step Count and Postprandial Fat Metabolism. *Med Sci Sports Exerc* **53,** 333–340.

Burton HM, Wolfe AS, Vardarli E, Satiroglu R & Coyle EF (2021). Background Inactivity Blunts Metabolic Adaptations to Intense Short-Term Training. *Med Sci Sports Exerc* **53,** 1937–1944.

Bütikofer L, Zurlinden A, Bolliger MF, Kunz B & Sonderegger P (2011). Destabilization of the

neuromuscular junction by proteolytic cleavage of agrin results in precocious sarcopenia. *FASEB J* **25,** 4378–4393.

Campbell EL, Seynnes OR, Bottinelli R, McPhee JS, Atherton PJ, Jones DA, Butler-Browne G & Narici M V. (2013). Skeletal muscle adaptations to physical inactivity and subsequent retraining in young men. *Biogerontology* **14,** 247–259.

Campbell M, Varley-Campbell J, Fulford J, Taylor B, Mileva KN & Bowtell JL (2019). Effect of Immobilisation on Neuromuscular Function In Vivo in Humans: A Systematic Review. *Sport Med* **49,** 931–950.

Canu MH, Carnaud M, Picquet F & Goutebroze L (2009). Activity-dependent regulation of myelin maintenance in the adult rat. *Brain Res* **1252,** 45–51.

Canu MH, Langlet C, Dupont E & Falempin M (2003). Effects of hypodynamia-hypokinesia on somatosensory evoked potentials in the rat. *Brain Res* **978,** 162–168.

Carlson BM, Carlson JA, Dedkov EI & McLennan IS (2003). Concentration of caveolin-3 at the neuromuscular junction in young and old rat skeletal muscle fibers. *J Histochem Cytochem* **51,** 1113–1118.

Carraro U, Morale D, Mussini I, Lucke S, Cantini M, Betto R, Catani C, Dalla Libera L, Danieli Betto D & Noventa D (1985). Chronic denervation of rat hemidiaphragm: Maintenance of fiber heterogeneity with associated increasing uniformity of myosin isoforms. *J Cell Biol* **100,** 161–174.

Castro RW, Lopes MC, Settlage RE & Valdez G (2023). Aging alters mechanisms underlying voluntary movements in spinal motor neurons of mice, primates, and humans. *JCI insight*. Available at: http://www.ncbi.nlm.nih.gov/pubmed/37154159.

Chastin SFM, Palarea-albaladejo J & Dontje ML (2015). Combined Effects of Time Spent in Physical Activity , Sedentary Behaviors and Sleep on Obesity and Cardio-Metabolic Health Markers: A Novel Compositional Data Analysis Approach. *PLoS One* **10,** e0139984.

Chen LK et al. (2014). Sarcopenia in Asia: Consensus report of the Asian working group for sarcopenia. *J Am Med Dir Assoc* **15,** 95–101.

Chen LK et al. (2020). Asian Working Group for Sarcopenia: 2019 Consensus Update on Sarcopenia Diagnosis and Treatment. *J Am Med Dir Assoc* **21,** 300-307.e2.

Chibalin A V., Benziane B, Zakyrjanova GF, Kravtsova V V. & Krivoi II (2018). Early endplate remodeling and skeletal muscle signaling events following rat hindlimb suspension. *J Cell Physiol* **233,** 6329–6336.

Cho SH, Kim JH & Song W (2016). In Vivo Rodent Models of Skeletal Muscle Adaptation to Decreased Use. *Endocrinol Metab* **31,** 31.

Christensen K, McGue M, Yashin A, Iachine I, Holm N V. & Vaupel JW (2000). Genetic and environmental influences on functional abilities in Danish twins aged 75 years and older. *Journals Gerontol - Ser A Biol Sci Med Sci* **55,** 446–452.

Christian CJ & Benian GM (2020). Animal models of sarcopenia. *Aging Cell* **19,** 1–11.

Chugh D, Iyer CC, Wang X, Bobbili P, Rich MM & Arnold WD (2020). Neuromuscular junction transmission failure is a late phenotype in aging mice. *Neurobiol Aging* **86,** 182–190.

Chung T, Tian Y, Walston J & Hoke A (2018). Increased Single-Fiber Jitter Level Is Associated with Reduction in Motor Function with Aging. *Am J Phys Med Rehabil* **97,** 551–556.

Clark BC (2023). Neural Mechanisms of Age-related Loss of Muscle Performance and Physical Function. *J Gerontoloy Ser A*.

Coelho-Júnior HJ, Picca A, Calvani R & Marzetti E (2022). Prescription of resistance training for sarcopenic older adults: Does it require specific attention? *Ageing Res Rev*; DOI: 10.1016/j.arr.2022.101720.

Cole SW, Cacioppo JT, Cacioppo S, Bone K, Del Rosso LA, Spinner A, Arevalo JMG, Dizon TP & Capitanio JP (2021). The Type I interferon antiviral gene program is impaired by lockdown and preserved by caregiving. *Proc Natl Acad Sci U S A* **118,** 6–11.

Coletta G & Phillips SM (2023). An elusive consensus definition of sarcopenia impedes research and clinical treatment: A narrative review. *Ageing Res Rev* **86,** 101883.

Company JM, Roberts MD, Toedebusch RG, Cruthirds CL & Booth FW (2013). Sudden decrease in physical activity evokes adipocyte hyperplasia in 70- to 77-day-old rats but not 49- to 56-day-old rats. *Am J Physiol - Regul Integr Comp Physiol*; DOI: 10.1152/ajpregu.00139.2013.

Cormery B, Beaumont E, Csukly K & Gardiner P (2005). Hindlimb unweighting for 2 weeks alters physiological properties of rat hindlimb motoneurones. *J Physiol* **568,** 841–850.

Costa Santos A, Willumsen J, Meheus F, Ilbaw A & Bull FC (2022). The Cost of Inaction on Physical Inactivity to Healthcare Systems. *Lancet Glob Heal*1–8.

Covault J & Sanes JR (1985). Neural cell adhesion molecule (N-CAM) accumulates in denervated and paralyzed skeletal muscles. *Proc Natl Acad Sci U S A* **82,** 4544–4548.

Coyle EF, Burton HM & Satiroglu R (2022). Inactivity Causes Resistance to Improvements in Metabolism After Exercise. *Exerc Sport Sci Rev*; DOI: 10.1249/jes.0000000000000280.

Crossland H, Skirrow S, Puthucheary ZA, Constantin-Teodosiu D & Greenhaff PL (2019). The impact

of immobilisation and inflammation on the regulation of muscle mass and insulin resistance: different routes to similar end-points. *J Physiol* **597,** 1259–1270.

Cruz-Jentoft AJ et al. (2019). Sarcopenia: Revised European consensus on definition and diagnosis. *Age Ageing* **48,** 16–31.

Cruz-Jentoft AJ, Baeyens JP, Bauer JM, Boirie Y, Cederholm T, Landi F, Martin FC, Michel JP, Rolland Y, Schneider SM, Topinková E, Vandewoude M & Zamboni M (2010). Sarcopenia: European consensus on definition and diagnosis. *Age Ageing* **39,** 412–423.

Cruz-Jentoft AJ, Landi F, Schneider SM, Zúñiga C, Arai H, Boirie Y, Chen LK, Fielding RA, Martin FC, Michel J, Sieber C, Stout JR, Studenski SA, Vellas B, Woo J, Zamboni M & Cederholm T (2014). Prevalence of and interventions for sarcopenia in ageing adults: A systematic review. Report of the International Sarcopenia Initiative (EWGSOP and IWGS). *Age Ageing* **43,** 48–759.

Cruz-Jentoft AJ & Sayer AA (2019). Sarcopenia. *Lancet* **393,** 2636–2646.

Cuthbertson DP (1929). The influence of prolonged muscular rest on metabolism. *Biochem J* **23,** 1328–1345.

Dahl R, Larsen S, Dohlmann TL, Qvortrup K, Helge JW, Dela F & Prats C (2015). Three-dimensional reconstruction of the human skeletal muscle mitochondrial network as a tool to assess mitochondrial content and structural organization. *Acta Physiol* **213,** 145–155.

Daley T & Smith AD (2013). Predicting the molecular complexity of sequencing libraries. *Nat Methods* **10,** 325.

Darabid H, Perez-Gonzalez AP & Robitaille R (2014). Neuromuscular synaptogenesis: Coordinating partners with multiple functions. *Nat Rev Neurosci* **15,** 703–718.

Davies CTM, Rutherford IC & Thomas DO (1987). Electrically evoked contractions of the triceps surae during and following 21 days of voluntary leg immobilization. *Eur J Appl Physiol Occup Physiol* **56,** 306–312.

Davis LA, Fogarty MJ, Brown A & Sieck GC (2022). Structure and Function of the Mammalian Neuromuscular Junction. *Compr Physiol* **12,** 1–36.

De-Doncker L, Kasri M & Falempin M (2006). Soleus motoneuron excitability after rat hindlimb unloading using histology and a new electrophysiological approach to record a neurographic analogue of the H-reflex. *Exp Neurol* **201,** 368–374.

Delbono O, Rodrigues ACZ, Bonilla HJ & Messi ML (2021). The emerging role of the sympathetic nervous system in skeletal muscle motor innervation and sarcopenia. *Ageing Res Rev* **67,** 101305.

Delmonico MJ, Harris TB, Lee JS, Visser M, Nevitt M, Kritchevsky SB, Tylavsky FA & Newman AB (2007). Alternative definitions of sarcopenia, lower extremity performance, and functional impairment with aging in older men and women. *J Am Geriatr Soc* **55,** 769–774.

Demangel R, Treffel L, Py G, Brioche T, Pagano AF, Bareille MP, Beck A, Pessemesse L, Candau R, Gharib C, Chopard A & Millet C (2017). Early structural and functional signature of 3-day human skeletal muscle disuse using the dry immersion model. *J Physiol* **595,** 4301–4315.

Dennison EM, Sayer AA & Cooper C (2017). Epidemiology of sarcopenia and insight into possible therapeutic targets. *Nat Rev Rheumatol* **13,** 340–347.

Dent E et al. (2018). International Clinical Practice Guidelines for Sarcopenia (ICFSR): Screening, Diagnosis and Management. *J Nutr Heal Aging* **22,** 1148–1161.

Dent E, Woo J, Scott D & Hoogendijk EO (2021). Toward the recognition and management of sarcopenia in routine clinical care. *Nat Aging* **1,** 982–990.

Desaphy JF, Pierno S, Léoty C, George AL, De Luca A & Camerino DC (2001). Skeletal muscle disuse induces fibre type-dependent enhancement of Na+ channel expression. *Brain* **124,** 1100–1113.

Deschenes M, Matthew AA, Kapral MC, Kressin KA, Leathrum CM, Seo A, Li S & Schaffrey EC (2018). Neuromuscular Adaptability of Male and Female Rats to Muscle Unloading. *J Neurosci Res* **96,** 284–296.

Deschenes MR, Flannery R, Hawbaker A, Patek L & Mifsud M (2022). Adaptive Remodeling of the Neuromuscular Junction with Aging. *Cells*.

Deschenes MR, Roby MA, Eason MK & Harris MB (2010). Remodeling of the neuromuscular junction precedes sarcopenia related alterations in myofibers. *Exp Gerontol* **45,** 389–393.

Deschenes MR, Tenny KA & Wilson MH (2006). Increased and decreased activity elicits specific morphological adaptations of the neuromuscular junction. *Neuroscience* **137,** 1277–1283.

Deschenes MR, Trebelhorn AM, High MC, Tufts HL & Oh J (2021). Sensitivity of subcellular components of neuromuscular junctions to decreased neuromuscular activity. *Synapse* **75,** 1–13.

Deschenes MR & Wilson MH (2003). Age-Related Differences in Synaptic Plasticity following Muscle Unloading. *J Neurobiol* **57,** 246–256.

Desine S, Master H, Annis J, Hughes A, Roden DM, Harris PA & Brittain EL (2023). Daily Step Counts Before and After the COVID-19 Pandemic Among All of Us Research Participants. *JAMA Netw Open* **6,** 1–5.

Devries MC, Breen L, Von Allmen M, MacDonald MJ, Moore DR, Offord EA, Horcajada MN, Breuillé D & Phillips SM (2015). Low-load resistance training during step-reduction attenuates declines in muscle mass and strength and enhances anabolic sensitivity in older men. *Physiol Rep* **3,** 1–13.

Ding D, Lawson KD, Kolbe-Alexander TL, Finkelstein EA, Katzmarzyk PT, van Mechelen W & Pratt M (2016). The economic burden of physical inactivity: a global analysis of major non-communicable diseases. *Lancet* **388,** 1311–1324.

Divjak M, Sedej G, Murks N, Gerževič M, Marusic U, Pišot R, Šimunič B & Holobar A (2022). Inter-Person Differences in Isometric Coactivations of Triceps Surae and Tibialis Anterior Decrease in Young, but Not in Older Adults After 14 Days of Bed Rest. *Front Physiol* **12,** 1–14.

Dixon NC, Hurst TL, Talbot DCS, Tyrrell RM & Thompson D (2013). Effect of short-term reduced physical activity on cardiovascular risk factors in active lean and overweight middle-aged men. *Metabolism* **62,** 361–368.

Dobin A, Davis CA, Schlesinger F, Drenkow J, Zaleski C, Jha S, Batut P, Chaisson M & Gingeras TR (2013). STAR: ultrafast universal RNA-seq aligner. *Bioinformatics* **29,** 15–21.

Dodds R, Denison HJ, Ntani G, Cooper R, Cooper C, Sayer AA & Baird J (2012). Birth weight and muscle strength: A systematic review and meta-analysis. *J Nutr Heal Aging* **16,** 609–615.

Dominguez R (2011). Tropomyosin: The gatekeeper's view of the actin filament revealed. *Biophys J* **100,** 797–798.

Drey M, Sieber CC, Bauer JM, Uter W, Dahinden P, Fariello RG & Vrijbloed JW (2013). C-terminal Agrin Fragment as a potential marker for sarcopenia caused by degeneration of the neuromuscular junction. *Exp Gerontol* **48,** 76–80.

van Dronkelaar C, van Velzen A, Abdelrazek M, van der Steen A, Weijs PJM & Tieland M (2018). Minerals and Sarcopenia; The Role of Calcium, Iron, Magnesium, Phosphorus, Potassium, Selenium, Sodium, and Zinc on Muscle Mass, Muscle Strength, and Physical Performance in Older Adults: A Systematic Review. *J Am Med Dir Assoc* **19,** 6-11.e3.

Duchateau J (1995). Bed rest induces neural and contractile adaptations in triceps surae. *Med Sci Sports Exerc* **27,** 1581–1589.

Duchateau J & Hainaut K (1990). Effects of immobilization on contractile properties, recruitment and firing rates of human motor units. *J Physiol* **422,** 55–65.

Dumuid D, Lewis LK, Olds TS, Maher C, Bondarenko C & Norton L (2018). Relationships between older adults ' use of time and cardio-respiratory fi tness , obesity and cardio-metabolic risk : A

compositional isotemporal substitution analysis. *Maturitas* **110,** 104–110.

Dzik KP & Kaczor JJ (2019). Mechanisms of vitamin D on skeletal muscle function: oxidative stress, energy metabolism and anabolic state. *Eur J Appl Physiol* **119,** 825–839.

Eccles JC (1958). Problems of plasticity and organization at simplest levels of mammalian central nervous system. *Perspect Biol Med* **1,** 379–396.

Eccles JC, Eccles RM & Lundberg A (1957). Durations of After-hyperpolarization of Motoneurones supplying Fast and Slow Muscles. *Nature* **179,** 866–868.

Edgerton VR, Barnard RJ, Peter JB, Maier A & Simpson DR (1975). Properties of immobilized hind-limb muscles of the Galago senegalensis. *Exp Neurol* **46,** 115–131.

Edwards SJ, Shad BJ, Marshall RN, Morgan PT, Wallis GA & Breen L (2021). Short-term step reduction reduces citrate synthase activity without altering skeletal muscle markers of oxidative metabolism or insulin-mediated signaling in young males. *J Appl Physiol* **131,** 1653–1662.

Eldridge L, Liebholdt M & Steinbach J (1981). Alterations in cat skeletal neuromuscular junction following prolonged inactivity. *J Physiol* **313,** 529–545.

Essomba MJN, Atsa D, Noah DZ, Zingui-Ottou M, Paula G, Nkeck JR, Noubiap JJ & Ashuntantang G (2020). Geriatric syndromes in an urban elderly population in Cameroon: A focus on disability, sarcopenia and cognitive impairment. *Pan Afr Med J* **37,** 1–14.

Estruch OGC, Cano GD & Stashuk D (2019). P32-S Application of decomposition based quantitative EMG (DQEMG) to focal neuropathies. *Clin Neurophysiol* **130,** e104.

Fahim MA (1989). Rapid neuromuscular remodeling following limb immobilization. *Anat Rec* **224,** 102–109.

Fahim MA & Robbins N (1986). Remodelling of the neuromuscular junction after subtotal disuse. *Brain Res* **383,** 353–356.

Falck RS, Davis JC & Liu-Ambrose T (2017). What is the association between sedentary behaviour and cognitive function? A systematic review. *Br J Sports Med* **51,** 800–811.

Fernandes LV, Paiva AEG, Silva ACB, de Castro IC, Santiago AF, de Oliveira EP & Porto LCJ (2022). Prevalence of sarcopenia according to EWGSOP1 and EWGSOP2 in older adults and their associations with unfavorable health outcomes: a systematic review. *Aging Clin Exp Res* **34,** 505–514.

Fielding RA et al. (2011). Sarcopenia: An Undiagnosed Condition in Older Adults. Current Consensus Definition: Prevalence, Etiology, and Consequences. International Working Group

on Sarcopenia. *J Am Med Dir Assoc* **12,** 249–256.

Figueiredo VC, D'Souza RF, Van Pelt DW, Lawrence MM, Zeng N, Markworth JF, Poppitt SD, Miller BF, Mitchell CJ, McCarthy JJ, Dupont-Versteegden EE & Cameron-Smith D (2021). Ribosome biogenesis and degradation regulate translational capacity during muscle disuse and reloading. *J Cachexia Sarcopenia Muscle* **12,** 130–143.

Fischbach BYGD & Robbins N (1969). Changes in contractile properties of disused soleus muscles. *J Physiol* **201,** 305–320.

Fischbach GD & Robbins N (1971). Effect of chronic disuse of rat soleus neuromuscular junctions on postsynaptic membrane. *J Neurophysiol* **34,** 562–569.

Fisher SR, Goodwin JS, Protas EJ, Kuo Y-F, Graham JE, Ottenbacher KJ & Ostir G V. (2011). Ambulatory Activity of Older Adults Hospitalized with Acute Medical Illness. *J Am Geriatr Soc* **59,** 91–95.

Fitts RH, Romatowski JG, Peters JR, Paddon-Jones D, Wolfe RR & Ferrando AA (2007). The deleterious effects of bed rest on human skeletal muscle fibers are exacerbated by hypercortisolemia and ameliorated by dietary supplementation. *Am J Physiol - Cell Physiol* **293,** 313–320.

Franchi M V., Monti E, Carter A, Quinlan JI, Herrod PJJ, Reeves ND & Narici M V. (2019). Bouncing back! Counteracting muscle aging with plyometric muscle loading. *Front Physiol* **10,** 1–11.

Franchi M V., Sarto F, Simunič B, Pišot R & Narici M V. (2022*a*). Early Changes of Hamstrings Morphology and Contractile Properties During 10 Days of Complete Inactivity. *Med Sci Sport Exerc* **54,** 1346–1354.

Franchi M V, Badiali F, Sarto F, Mueller P, Mueller N, Rehfeld K, Monti E, Rankin D, Longo S, Hokelmann A & Narici M V. (2022*b*). Neuromuscular Aging: A Case for the Neuroprotective Effects of Dancing. *Gerontology* **69,** 73–81.

Frontera WR & Ochala J (2015). Skeletal Muscle: A Brief Review of Structure and Function. *Calcif Tissue Int* **96,** 183–195.

Frühbeck G (2005). Does a NEAT difference in energy expenditure lead to obesity? *Lancet* **366,** 615–616.

Fuchs CJ, Kuipers R, Rombouts JA, Brouwers K, Schrauwen-Hinderling VB, Wildberger JE, Verdijk LB & van Loon LJC (2023). Thigh muscles are more susceptible to age-related muscle loss when compared to lower leg and pelvic muscles. *Exp Gerontol* **175,** 112159.

Funabashi D, Wakiyama Y, Muto N, Kita I & Nishijima T (2022). Social isolation is a direct

determinant of decreased home-cage activity in mice: A within-subjects study using a body-implantable actimeter. *Exp Physiol* **107,** 133–146.

Fushiki T, Kano T, Inoue K & Sugimoto E (1991). Decrease in muscle glucose transporter number in chronic physical inactivity in rats. *Am J Physiol - Endocrinol Metab* **260,** E403–E410.

Garcia M, Fernandez A & Solas M (2013). Mitochondria, motor neurons and aging. *J Neurol Sci* **330,** 18–26.

Gardiner PF (2006). Changes in α-motoneuron properties with altered physical activity levels. *Exerc Sport Sci Rev* **34,** 54–58.

Gilchrist JM (1992). Single fiber EMG reference values: A collaborative effort. *Muscle Nerve* **15,** 151–161.

Gilmore KJ, Kirk EA, Doherty TJ, Kimpinski K & Rice CL (2020). Abnormal motor unit firing rates in chronic inflammatory demyelinating polyneuropathy. *J Neurol Sci* **414,** 116859.

Gilmore KJ, Morat T, Doherty TJ & Rice CL (2017). Motor unit number estimation and neuromuscular fidelity in 3 stages of sarcopenia. *Muscle and Nerve* **55,** 676–684.

Di Girolamo FG, Fiotti N, Milanović Z, Situlin R, Mearelli F, Vinci P, Šimunič B, Pišot R, Narici M & Biolo G (2021). The Aging Muscle in Experimental Bed Rest: A Systematic Review and Meta-Analysis. *Front Nutr* **8,** 1–13.

Glover EI, Phillips SM, Oates BR, Tang JE, Tarnopolsky MA, Selby A, Smith K & Rennie MJ (2008). Immobilization induces anabolic resistance in human myofibrillar protein synthesis with low and high dose amino acid infusion. *J Physiol* **586,** 6049–6061.

Goldspink G (1985). Malleability of the motor system: A comparative approach. *J Exp Biol* **VOL. 115,** 375–391.

Gollnick P, Piehl K & Saltin B (1974). Selective glycogen depletion pattern in human muscle fibres after exercise of varying intensity and at varying pedalling rates. *J Physiol* **241,** 45–57.

Gonzalez-Freire M, de Cabo R, Studenski SA & Ferrucci L (2014). The neuromuscular junction: Aging at the crossroad between nerves and muscle. *Front Aging Neurosci* **6,** 1–11.

Grana EA, Chiou-Tan F & Jaweed MM (1996). Endplate dysfunction in healthy muscle following a period of disuse. *Muscle and Nerve* **19,** 989–993.

Graveline DE, Balke B, McKenzie RE & Hartman B (1961). Psychobiologic effects of water-immersion-induced hypodynamics. *Aerosp Med* **32,** 387–400.

Greenwood BN, Loughridge AB, Sadaoui N, Christianson JP & Fleshner M (2012). The protective effects of voluntary exercise against the behavioral consequences of uncontrollable stress

persist despite an increase in anxiety following forced cessation of exercise. *Behav Brain Res* **233,** 314–321.

Grgic J, Dumuid D, Bengoechea EG, Shrestha N, Bauman A, Olds T & Pedisic Z (2018). Health outcomes associated with reallocations of time between sleep , sedentary behaviour , and physical activity : a systematic scoping review of isotemporal substitution studies. *Int J Behav Nutr Phys Act*.

Grosicki GJ, Zepeda CS & Sundberg CW (2022). Single muscle fibre contractile function with ageing. *J Physiol* **600,** 5005–5026.

Guralnik JM, Simonsick EM, Ferrucci L, Glynn RJ, Berkman LF, Blazer DG, Scherr PA & Wallace RB (1994). A Short Physical Performance Battery Assessing Lower Extremity Function: Association With Self-Reported Disability and Prediction of Mortality and Nursing Home Admission. *J Gerontol* **49,** 85–94.

Guthold R, Stevens GA, Riley LM & Bull FC (2018). Worldwide trends in insufficient physical activity from 2001 to 2016: a pooled analysis of 358 population-based surveys with 1·9 million participants. *Lancet Glob Heal* **6,** e1077–e1086.

Haase CB, Brodersen JB & Bulow J (2022). Sarcopenia: Early prevention or overdiagnosis? *BMJ* **376,** 1–5.

Hackney KJ & Ploutz-Snyder LL (2012). Unilateral lower limb suspension: Integrative physiological knowledge from the past 20 years (1991-2011). *Eur J Appl Physiol* **112,** 9–22.

von Haehling S, Coats AJS & Anker SD (2021). Ethical guidelines for publishing in the Journal of Cachexia, Sarcopenia and Muscle: update 2021. *J Cachexia Sarcopenia Muscle* **12,** 2259–2261.

Hardy EJO, Inns TB, Hatt J, Doleman B, Bass JJ, Atherton PJ, Lund JN & Phillips BE (2022). The time course of disuse muscle atrophy of the lower limb in health and disease. *J Cachexia Sarcopenia Muscle* **13,** 2616–2629.

Hargens A, Steskal J, Johansson C & Tipton C (1984). Tissue fluid shift, forelimb loading, and tail tension in tail-suspended rats. *Physiologist* **27,** S37–S38.

Harrow J et al. (2012). GENCODE: The reference human genome annotation for The ENCODE Project. *Genome Res* **22,** 1760.

Hassan AS, Fajardo ME, Cummings M, McPherson LM, Negro F, Dewald JPA, Heckman CJ & Pearcey GEP (2021). Estimates of persistent inward currents are reduced in upper limb motor units of older adults. *J Physiol* **599,** 4865–4882.

Healy GN, Winkler EAH, Owen N, Anuradha S & Dunstan DW (2015). Replacing sitting time with

standing or stepping: associations with cardio-metabolic risk biomarkers. *Eur Heart J* **36,** 2643–2649.

Heckman CJ & Enoka RM (2004). *Physiology of the motor neuron and the motor unit*. Elsevier B.V. Available at: http://dx.doi.org/10.1016/S1567-4231(04)04006-7.

Heckman CJ & Enoka RM (2012). Motor unit. *Compr Physiol* **2,** 2629–2682.

Heckman CJ, Johnson M, Mottram C & Schuster J (2008). Persistent inward currents in spinal motoneurons and their influence on human motoneuron firing patterns. *Neuroscientist* **14,** 264–275.

Henderson CA, Gomez CG, Novak SM, Mi-Mi L & Gregorio CC (2017). Overview of the muscle cytoskeleton. *Compr Physiol* **7,** 891–944.

Henson J, Edwardson CL, Bodicoat DH, Davies MJ, Khunti K, Talbot DCS, Henson J, Edwardson CL, Bodicoat DH, Davies MJ, Khunti K, Talbot DCS & Yates T (2017). Reallocating sitting time to standing or stepping through isotemporal analysis: associations with markers of chronic low-grade inflammation. *J Sports Sci* **36,** 1586–1593.

Henzel M, de Groat WC & Galbiati F (2010). Caveolin-3 Promotes Nicotinic Acetylcholine Receptor Clustering and Regulates Neuromuscular Junction Activity. *Mol Biol Cell* **21,** 302–310.

Hepple RT & Rice CL (2016). Innervation and neuromuscular control in ageing skeletal muscle. *J Physiol* **594,** 1965–1978.

Herbert RD & Balnave RJ (1993). The effect of position of immobilisation on resting length, resting stiffness, and weight of the soleus muscle of the rabbit. *J Orthop Res* **11,** 358–366.

Herzog W, Leonard TR, Renaud JM, Wallace J, Chaki G & Bornemisza S (1992). Force-length properties and functional demands of cat gastrocnemius, soleus and plantaris muscles. *J Biomech* **25,** 1329–1335.

Hesser BA, Henschel O & Witzemann V (2006). Synapse disassembly and formation of new synapses in postnatal muscle upon conditional inactivation of MuSK. *Mol Cell Neurosci* **31,** 470–480.

Hettwer S, Lin S, Kucsera S, Haubitz M, Oliveri F, Fariello RG, Ruegg MA & Vrijbloed JW (2014). Injection of a soluble fragment of neural agrin (NT-1654) considerably improves the muscle pathology caused by the disassembly of the neuromuscular junction. *PLoS One* **9,** 1–9.

Hortobagyi T, Dempsey L, Fraser D, Zheng D, Hamilton G, Lambert J & Dohm L (2000). Changes in muscle strength, muscle fibre size and myofibrillar gene expression after immobilization and retraining in humans. *J Physiol* **524,** 293–304.

Hourigan ML, McKinnon NB, Johnson M, Rice CL, Stashuk DW & Doherty TJ (2015). Increased motor unit potential shape variability across consecutive motor unit discharges in the tibialis anterior and vastus medialis muscles of healthy older subjects. *Clin Neurophysiol* **126,** 2381–2389.

Hughes BW, Kusner LL & Kaminski HJ (2006). Molecular architecture of the neuromuscular junction. *Muscle and Nerve* **33,** 445–461.

Hunter SK, Pereira XHM & Keenan KG (2016). The aging neuromuscular system and motor performance. *J Appl Physiol* **121,** 982–995.

Huxley AF & Hanson J (1954). Changes in the Cross-Striations of Muscle during Contraction and Stretch and their Structural Interpretation. *Nature* **173,** 973–976.

Huxley AF & Niedergerke R (1954). Structural changes in muscle during contraction. *Nature* **4412,** 971–973.

Hvid L, Aagaard P, Justesen L, Bayer ML, Andersen JL, Ørtenblad N, Kjaer M & Suetta C (2010). Effects of aging on muscle mechanical function and muscle fiber morphology during short-term immobilization and subsequent retraining. *J Appl Physiol* **109,** 1628–1634.

Hvid LG, Ørtenblad N, Aagaard P, Kjaer M & Suetta C (2011). Effects of ageing on single muscle fibre contractile function following short-term immobilisation. *J Physiol* **589,** 4745–4757.

Ibebunjo C et al. (2013). Genomic and Proteomic Profiling Reveals Reduced Mitochondrial Function and Disruption of the Neuromuscular Junction Driving Rat Sarcopenia. *Mol Cell Biol* **33,** 194–212.

Inns TB, Bass JJ, Edward JOH, Wilkinson DJ, Stashuk DW, Atherton PJ, Phillips BE & Piasecki M (2022). Motor unit dysregulation following 15 days of unilateral lower limb immobilisation. *J Physiol* **600,** 4753–4769.

Ishihara A, Oishi Y, Roy RR & Edgerton VR (1997). Influence of two weeks of non-weight bearing on rat soleus motoneurons and muscle fibers. *Aviat Sp Environ Med* **68,** 421–425.

Islamov RR, Mishagina EA, Tyapkina O V., Shajmardanova GF, Eremeev AA, Kozlovskaya IB, Nikolskij EE & Grigorjev AI (2011). Mechanisms of spinal motoneurons survival in rats under simulated hypogravity on earth. *Acta Astronaut* **68,** 1469–1477.

Islamov RR, Tyapkina O V., Nikol'skii EE, Kozlovskaya IB & Grigor'ev AI (2015). The Role of Spinal Cord Motoneurons in the Mechanisms of Development of Low-Gravity Motor Syndrome. *Neurosci Behav Physiol* **45,** 96–103.

Islamov RR, Tyapkina O V., Shaimardanova GF, Kozlovskaya IB & Nikol'skii EE (2008). Apoptosis

resistance of rat spinal motoneurons under simulated microgravity. *Dokl Biol Sci* **420,** 155–157.

Iwasaka C, Yamada Y, Nishida Y, Hara M, Yasukata J, Miyoshi N, Shimanoe C, Nanri H, Furukawa T, Koga K, Horita M, Higaki Y & Tanaka K (2023). Dose-response relationship between daily step count and prevalence of sarcopenia: A cross-sectional study. *Exp Gerontol* **175,** 112135.

Janssen I, Clarke AE, Carson V, Chaput JP, Giangregorio LM, Kho ME, Poitras VJ, Ross R, Saunders TJ, Ross-White A & Chastin SFM (2020). A systematic review of compositional data analysis studies examining associations between sleep, sedentary behaviour, and physical activity with health outcomes in adults. *Appl Physiol Nutr Metab* **45,** S248–S257.

Jayedi A, Gohari A & Shab-Bidar S (2021). Daily Step Count and All-Cause Mortality: A Dose–Response Meta-analysis of Prospective Cohort Studies. *Sport Med* **52,** 89–99.

Jennekens FGI, Tomlinson BE & Walton JN (1971). Histochemical aspects of five limb muscles in old age an autopsy study. *J Neurol Sci* **14,** 259–276.

Jones EJ, Chiou SY, Atherton PJ, Phillips BE & Piasecki M (2022). Ageing and exercise-induced motor unit remodelling. *J Physiol* **600,** 1839–1849.

Jones EJ, Piasecki J, Ireland A, Stashuk DW, Atherton PJ, Bethan E, Mcphee JS & Piasecki M (2021*a*). Lifelong exercise is associated with more homogeneous motor unit potential features across deep and superficial areas of vastus lateralis. *Geroscience* **43,** 1555–1565.

Jones G et al. (2021*b*). Genome-wide meta-analysis of muscle weakness identifies 15 susceptibility loci in older men and women. *Nat Commun* **12,** 1–11.

Jones RA, Harrison C, Eaton SL, Llavero Hurtado M, Graham LC, Alkhammash L, Oladiran OA, Gale A, Lamont DJ, Simpson H, Simmen MW, Soeller C, Wishart TM & Gillingwater TH (2017). Cellular and Molecular Anatomy of the Human Neuromuscular Junction. *Cell Rep* **21,** 2348–2356.

Juel VC (2012). Evaluation of neuromuscular junction disorders in the electromyography laboratory. *Neurol Clin* **30,** 621–639.

Jurkat-Rott, K., & Lehmann-Horn, F. (2004) Chapter 10: Ion channels and electrical properties of skeletal muscle. In: A. G. Engel, & C. Franzini-Armstrong (Eds.), Myology (vol. 2. 3rd ed., pp. 203–231). McGraw-Hill, New York

Jyväkorpi SK, Urtamo A, Kivimäki M & Strandberg TE (2020). Macronutrient composition and sarcopenia in the oldest-old men: The Helsinki Businessmen Study (HBS). *Clin Nutr* **39,** 3839–3841.

Kanning KC, Kaplan A & Henderson CE (2010). Motor neuron diversity in development and disease. *Annu Rev Neurosci* **33,** 409–440.

Karlin A (2002). Ion channel structure: Emerging structure of the Nicotinic Acetylcholine receptors. *Nat Rev Neurosci* **3,** 102–114.

Katti P, Hall AS, Parry HA, Ajayi PT, Kim Y, Willingham TB, Bleck CKE, Wen H & Glancy B (2022). Mitochondrial network configuration influences sarcomere and myosin filament structure in striated muscles. *Nat Commun* **13,** 1–17.

Kawamura Y, Okazaki H, O'Brien P & Dyck P (1977). Lumbar motoneurons of man: I) number and diameter histogram of alpha and gamma axons of ventral root. *J Neuropathol Exp Neurol* **36,** 853–860.

Khalil M, Teunissen CE, Otto M, Piehl F, Sormani MP, Gattringer T, Barro C, Kappos L, Comabella M, Fazekas F, Petzold A, Blennow K, Zetterberg H & Kuhle J (2018). Neurofilaments as biomarkers in neurological disorders. *Nat Rev Neurol* **14,** 577–589.

Kim IY, Park S, Chou TH, Trombold JR & Coyle EF (2016). Prolonged sitting negatively affects the postprandial plasma triglyceride-lowering effect of acute exercise. *Am J Physiol - Endocrinol Metab* **311,** E891–E898.

Kirk EA, Gilmore KJ, Stashuk DW, Doherty TJ & Rice CL (2019). Human motor unit characteristics of the superior trapezius muscle with age-related comparisons. *J Neurophysiol* **122,** 823–832.

Knudsen SH, Hansen LS, Pedersen M, Dejgaard T, Hansen J, Van Hall G, Thomsen C, Solomon TPJ, Pedersen BK & Krogh-Madsen R (2012). Changes in insulin sensitivity precede changes in body composition during 14 days of step reduction combined with overfeeding in healthy young men. *J Appl Physiol* **113,** 7–15.

Kohl HW et al. (2012). The pandemic of physical inactivity: Global action for public health. *Lancet* **380,** 294–305.

König M, Spira D, Demuth I, Steinhagen-Thiessen E & Norman K (2018). Polypharmacy as a Risk Factor for Clinically Relevant Sarcopenia: Results From the Berlin Aging Study II. *Journals Gerontol - Ser A Biol Sci Med Sci* **73,** 117–122.

Korotkevich G, Sukhov V, Budin N, Shpak B, Artyomov MN & Sergushichev A (2021). Fast gene set enrichment analysis. *bioRxiv*060012.

Kravtsova V V., Saburova EA & Krivoi II (2019). The Structural and Functional Characteristics of Rat Soleus Endplates under Short-Term Disruption of Motor Activity. *Biophys (Russian Fed* **64,** 772–776.

Krogh-Madsen R, Pedersen M, Solomon TPJ, Knudsen SH, Hansen LS, Karstoft K, Lehrskov-Schmidt L, Pedersen KK, Thomsen C, Holst JJ & Pedersen BK (2014). Normal physical activity obliterates the deleterious effects of a high-caloric intake. *J Appl Physiol* **116,** 231–239.

Krogh-Madsen R, Thyfault JP, Broholm C, Mortensen OH, Olsen RH, Mounier R, Plomgaard P, Van Hall G, Booth FW, Pedersen BK & Harry S (2010). A 2-wk reduction of ambulatory activity attenuates peripheral insulin sensitivity. *J Appl Physiol* **108,** 1034–1040.

Kump DS & Booth FW (2005*a*). Sustained rise in triacylglycerol synthesis and increased epididymal fat mass when rats cease voluntary wheel running. *J Physiol* **565,** 911–925.

Kump DS & Booth FW (2005*b*). Alterations in insulin receptor signalling in the rat epitrochlearis muscle upon cessation of voluntary exercise. *J Physiol* **562,** 829–838.

Kump DS, Laye MJ & Booth FW (2006). Increased mitochondrial glycerol-3-phosphate acyltransferase protein and enzyme activity in rat epididymal fat upon cessation of wheel running. *Am J Physiol - Endocrinol Metab*; DOI: 10.1152/ajpendo.00321.2005.

L'in E & Novikov V (1980). Stand for modelling the physiological effects of weightlessness in laboratory experiments with rats. *Kosm Biol Aviakosm Med* **14,** 79–80.

Labovitz SS, Robbins N & Fahim MA (1984). Endplate topography of denervated and disused rat neuromuscular junctions: Comparison by scanning and light microscopy. *Neuroscience* **11,** 963–971.

Landi F, Calvani R, Martone AM, Salini S, Zazzara MB, Candeloro M, Coelho-Junior HJ, Tosato M, Picca A & Marzetti E (2020). Normative values of muscle strength across ages in a 'real world' population: results from the longevity check-up 7+ project. *J Cachexia Sarcopenia Muscle* **11,** 1562–1569.

Larsson L, Degens H, Li M, Salviati L, Lee Y Il, Thompson W, Kirkland JL & Sandri M (2019). Sarcopenia: Aging-related loss of muscle mass and function. *Physiol Rev* **99,** 427–511.

Law CW, Chen Y, Shi W & Smyth GK (2014). Voom: Precision weights unlock linear model analysis tools for RNA-seq read counts. *Genome Biol* **15,** 1–17.

Laye MJ, Scott Rector R, Borengasser SJ, Naples SP, Uptergrove GM, Ibdah JA, Booth FW & Thyfault JP (2009). Cessation of daily wheel running differentially alters fat oxidation capacity in liver, muscle, and adipose tissue. *J Appl Physiol* **106,** 161–168.

Laye MJ, Thyfault JP, Stump CS & Booth FW (2007). Inactivity induces increases in abdominal fat. *J Appl Physiol* **102,** 1341–1347.

Lexell J, Taylor CC & Sjöström M (1988). What is the cause of the ageing atrophy? Total number,

size and proportion of different fiber types studied in whole vastus lateralis muscle from 15- to 83-year-old men. *J Neurol Sci* **84,** 275–294.

Li B & Dewey CN (2011). RSEM: Accurate transcript quantification from RNA-Seq data with or without a reference genome. *BMC Bioinformatics* **12,** 1–16.

Li L, Xiong WC & Mei L (2018). Neuromuscular Junction Formation, Aging, and Disorders. *Annu Rev Physiol* **80,** 159–188.

Li X, He J & Sun Q (2023). Sleep Duration and Sarcopenia: An Updated Systematic Review and. *J Am Med Dir Assoc*; DOI: 10.1016/j.jamda.2023.04.032.

Lin H, Ma X, Sun Y, Peng H, Wang Y, Thomas SS & Hu Z (2022). Decoding the transcriptome of denervated muscle at single-nucleus resolution. *J Cachexia Sarcopenia Muscle* **13,** 2102–2117.

Liu JC, Dong SS, Shen H, Yang DY, Chen B Bin, Ma XY, Peng YR, Xiao HM & Deng HW (2022). Multi-omics research in sarcopenia: Current progress and future prospects. *Ageing Res Rev* **76,** 101576.

Lundbye-Jensen J & Nielsen JB (2008). Immobilization induces changes in presynaptic control of group Ia afferents in healthy humans. *J Physiol* **586,** 4121–4135.

Luo S, Chen X, Hou L, Yue J, Liu X, Wang Y, Xia X & Dong B (2021). The Relationship between Sarcopenia and Vitamin D Levels in Adults of Different Ethnicities: Findings from the West China Health and Aging Trend Study. *J Nutr Heal Aging* **25,** 909–913.

Maasakkers CM, Weijs RWJ, Dekkers C, Gardiner PA, Ottens R, Olde Rikkert MGM, Melis RJF, Thijssen DHJ & Claassen JAHR (2022). Sedentary behaviour and brain health in middle-aged and older adults: A systematic review. *Neurosci Biobehav Rev*; DOI: 10.1016/j.neubiorev.2022.104802.

Mahmassani ZS, McKenzie AI, Petrocelli JJ, de Hart NM, Fix DK, Kelly JJ, Baird LM, Howard MT & Drummond MJ (2021). Reduced Physical Activity Alters the Leucine-Stimulated Translatome in Aged Skeletal Muscle. *Journals Gerontol Ser A* **76,** 2112–2121.

Mahmassani ZS, Reidy PT, McKenzie AI, Petrocelli JJ, Matthews O, de Hart NM, Ferrara PJ, O'Connell RM, Funai K & Drummond MJ (2020). Absence of MyD88 from Skeletal Muscle Protects Female Mice from Inactivity-Induced Adiposity and Insulin Resistance. *Obesity* **28,** 772–782.

Malathi S & Batmanabane M (1983). Alterations in the morphology of the neuromuscular junctions following experimental immobilization in cats. *BirkMuser Verlag* **39,** 547–549.

Malmstrom TK, Miller DK, Simonsick EM, Ferrucci L & Morley JE (2016). SARC-F: A symptom score to predict persons with sarcopenia at risk for poor functional outcomes. *J Cachexia Sarcopenia Muscle* **7,** 28–36.

Manganotti P, Stella AB, Ajcevic M, di Girolamo FG, Biolo G, Franchi M V., Monti E, Sirago G, Marusic U, Simunic B, Narici M V. & Pisot R (2021). Peripheral nerve adaptations to 10 days of horizontal bed rest in healthy young adult males. *Am J Physiol - Regul Integr Comp Physiol* **321,** R495–R503.

Manzanares G, Brito-Da-Silva G & Gandra PG (2019). Voluntary wheel running: Patterns and physiological effects in mice. *Brazilian J Med Biol Res* **52,** 1–9.

Marcolin G, Franchi M V., Monti E, Pizzichemi M, Sarto F, Sirago G, Paoli A, Maggio M, Zampieri S & Narici M V. (2021). Active older dancers have lower C-terminal Agrin fragment concentration and better balance and gait performance than sedentary peers. *Exp Gerontol*.

Marmonti E, Busquets S, Toledo M, Ricci M, Beltrà M, Gudiño V, Oliva F, López-Pedrosa JM, Manzano M, Rueda R, López-Soriano FJ & Argilés JM (2017). A rat immobilization model based on cage volume reduction: A physiological model for bed rest? *Front Physiol* **8,** 1–11.

Martin M (2011). Cutadapt removes adapter sequences from high-throughput sequencing reads. *EMBnet.journal* **17,** 10–12.

Marusic U, Narici M, Simunic B, Pisot R & Ritzmann R (2021). Nonuniform loss of muscle strength and atrophy during bed rest: A systematic review. *J Appl Physiol* **131,** 194–206.

Mayhew AJ, Amog K, Phillips S, Parise G, McNicholas PD, De Souza RJ, Thabane L & Raina P (2019). The prevalence of sarcopenia in community-dwelling older adults, an exploration of differences between studies and within definitions: A systematic review and meta-analyses. *Age Ageing* **48,** 48–56.

Mayr KA, Young L, Molina LA, Tran MA & Whelan PJ (2020). An economical solution to record and control wheel-running for group-housed mice. *J Neurosci Methods* **331,** 108482.

McGlory C, Von Allmen MT, Stokes T, Morton RW, Hector AJ, Lago BA, Raphenya AR, Smith BK, McArthur AG, Steinberg GR, Baker SK & Phillips SM (2018). Failed recovery of glycemic control and myofibrillar protein synthesis with 2 wk of physical inactivity in overweight, prediabetic older adults. *Journals Gerontol - Ser A Biol Sci Med Sci* **73,** 1070–1077.

McKendry J, Stokes T, Mcleod J & Phillips SM (2021). Resistance Exercise, Aging, Disuse, and Muscle Protein Metabolism. *Compr Physiol* **11,** 2249–2278.

Mendell LM (2005). The size principle: A rule describing the recruitment of motoneurons. *J*

Neurophysiol **93,** 3024–3026.

Methenitis S, Karandreas N, Spengos K, Zaras N, Stasinaki AN & Terzis G (2016). Muscle Fiber Conduction Velocity, Muscle Fiber Composition, and Power Performance. *Med Sci Sports Exerc* **48,** 1761–1771.

Midrio M (2006). The denervated muscle: Facts and hypotheses. A historical review. *Eur J Appl Physiol* **98,** 1–21.

Migliavacca E et al. (2019). Mitochondrial oxidative capacity and NAD+ biosynthesis are reduced in human sarcopenia across ethnicities. *Nat Commun*; DOI: 10.1038/s41467-019-13694-1.

Mijnarends DM, Koster A, Schols JMGA, Meijers JMM, Halfens RJG, Gudnason V, Eiriksdottir G, Siggeirsdottir K, Sigurdsson S, Jónsson P V., Meirelles O & Harris T (2016). Physical activity and incidence of sarcopenia: The population-based AGES-Reykjavik Study. *Age Ageing* **45,** 614–621.

Mikus C, Oberlin D, Libla J, Taylor A, Booth F & Thyfault J (2012). Lowering Physical Activity Impairs Glycemic Control in Healthy Volunteers. *Med Sci Sport Exerc* **44,** 225–231.

Mitchell WK, Williams J, Atherton P, Larvin M, Lund J & Narici M (2012). Sarcopenia, dynapenia, and the impact of advancing age on human skeletal muscle size and strength; a quantitative review. *Front Physiol* **3 JUL,** 1–18.

Mitsiopoulos N, Baumgartner RN, Heymsfield SB, Lyons W, Gallagher D & Ross R (1998). Cadaver validation of skeletal muscle measurement by magnetic resonance imaging and computerized tomography. *J Appl Physiol* **85,** 115–122.

Mondon C, Dolkas C & Reaven G (1983). Effect of confinement in small space flight size cages on insulin sensitivity of exercise-trained rats. *Aviat Sp Env Med* **54,** 919–922.

Montero D, Oberholzer L, Haider T, Breenfeldt-Andersen A, Dandanell S, Meinild-Lundby AK, Maconochie H & Lundby C (2018). Increased capillary density in skeletal muscle is not associated with impaired insulin sensitivity induced by bed rest in healthy young men. *Appl Physiol Nutr Metab* **43,** 1334–1340.

Monti E, Franchi MV, Badiali F, Quinlan JI, Longo S & Narici MV (2020*a*). The time-course of changes in muscle mass, architecture and power during 6 weeks of plyometric training. *Front Physiol* **11,** 1–14.

Monti E, Reggiani C, Franchi M V, Toniolo L, Sandri M, Armani A, Zampieri S, Giacomello E, Sarto F, Sirago G, Murgia M, Nogara L, Marcucci L, Ciciliot S, Šimunic B, Pišot R & Narici M V (2021). Neuromuscular junction instability and altered intracellular calcium handling as early

determinants of force loss during unloading in humans. *J Physiol* **599,** 3037–3061.

Monti E, Sarto F, Sartori R, Zanchettin G, Lö S, Kern H, Narici MV & Zampieri S (2023*a*). C-terminal agrin fragment as a biomarker of muscle wasting and weakness: a narrative review. *J Cachexia Sarcopenia Muscle* **14,** 730–744.

Monti E, Tagliaferri S, Zampieri S, Sarto F, Sirago G, Franchi MV, Ticinesi A, Longobucco Y, Adorni E, Lauretani F, Haehling S Von, Marzetti E, Calvani R, Bernabei R, Cesari M, Maggio M & Narici MV (2023*b*). Effects of a 2-year exercise training on neuromuscular system health in older individuals with low muscle function. *J Cachexia Sarcopenia Muscle* **14,** 794–804.

Monti E, Toniolo L, Marcucci L, Bondì M, Martellato I, Šimunič B, Toninello P, Franchi MV, Narici MV & Reggiani C (2020*b*). Are muscle fibres of body builders intrinsically weaker? A comparison with single fibres of aged-matched controls. *Acta Physiol* **231,** e13557.

Moore DR, Kelly RP, Devries MC, Churchward-Venne TA, Phillips SM, Parise G & Johnston AP (2018). Low-load resistance exercise during inactivity is associated with greater fibre area and satellite cell expression in older skeletal muscle. *J Cachexia Sarcopenia Muscle* **9,** 747–754.

Moreira-Pais A, Ferreira R, Oliveira PA & Duarte JA (2022). A neuromuscular perspective of sarcopenia pathogenesis: deciphering the signaling pathways involved. *GeroScience* **44,** 1199–1213.

Morey-Holton ER & Globus RK (2002). Hindlimb unloading rodent model: Technical aspects. *J Appl Physiol* **92,** 1367–1377.

Morey ER (1979). Spaceflight and Bone Turnover: Correlation with a New Rat Model of Weightlessness. *Bioscience* **29,** 168–172.

Morley JE et al. (2011). Sarcopenia With Limited Mobility: An International Consensus. *J Am Med Dir Assoc* **12,** 403–409.

Morris JN, Heady JA, Raffle PAB, Roberts CG & Parks JW (1953). Coronary heart-disease and physical activity of work. *Lancet* **262,** 1053–1057.

Morris RT, Laye MJ, Lees SJ, Rector RS, Thyfault JP & Booth FW (2008). Exercise-induced attenuation of obesity, hyperinsulinemia, and skeletal muscle lipid peroxidation in the OLETF rat. *J Appl Physiol* **104,** 708–715.

Murgia M, Brocca L, Monti E, Franchi M V., Zwiebel M, Steigerwald S, Giacomello E, Sartori R, Zampieri S, Capovilla G, Gasparini M, Biolo G, Sandri M, Mann M & Narici M V. (2022). Plasma proteome profiling of healthy subjects undergoing bed rest reveals unloading-dependent changes linked to muscle atrophy. *J Cachexia Sarcopenia Muscle*439–451.

Murgia M, Toniolo L, Nagaraj N, Ciciliot S, Vindigni V, Schiaffino S, Reggiani C & Mann M (2017). Single Muscle Fiber Proteomics Reveals Fiber-Type-Specific Features of Human Muscle Aging. *Cell Rep* **19,** 2396–2409.

Musacchia XJ, Deavers DR, Meininger GA & Davis TP (1980). A model for hypokinesia: effects on muscle atrophy in the rat. *J Appl Physiol Respir Environ Exerc Physiol* **48,** 479–486.

Muscaritoli M, Anker SD, Argilés J, Aversa Z, Bauer JM, Biolo G, Boirie Y, Bosaeus I, Cederholm T, Costelli P, Fearon KC, Laviano A, Maggio M, Fanelli FR, Schneider SM, Schols A & Sieber CC (2010). Consensus definition of sarcopenia, cachexia and pre-cachexia: Joint document elaborated by Special Interest Groups (SIG) " cachexia-anorexia in chronic wasting diseases" and " nutrition in geriatrics." *Clin Nutr* **29,** 154–159.

Nagatomo F, Ishihara A & Ohira Y (2009). Effects of hindlimb unloading at early postnatal growth on cell body size in spinal motoneurons innervating soleus muscle of rats. *Int J Dev Neurosci* **27,** 21–26.

Nandedkar S & Stalberg E (1983). Simulation of single muscle fibre action potentials. *Med Biol, Eng Compu* **21,** 158–165.

Narici M V. & De Boer MD (2011). Disuse of the musculo-skeletal system in space and on earth. *Eur J Appl Physiol* **111,** 403–420.

Narici M V. & Maffulli N (2010). Sarcopenia: Characteristics, mechanisms and functional significance. *Br Med Bull* **95,** 139–159.

Naruse M, Trappe S & Trappe TA (2023). Human skeletal muscle-specific atrophy with aging: a comprehensive review. *J Appl Physiol*; DOI: 10.1152/JAPPLPHYSIOL.00768.2022.

Do Nascimento PRC, Bilodeau M & Poitras S (2021). How do we define and measure sarcopenia? A meta-analysis of observational studies. *Age Ageing* **50,** 1906–1913.

Navasiolava NM, Custaud MA, Tomilovskaya ES, Larina IM, Mano T, Gauquelin-Koch G, Gharib C & Kozlovskaya IB (2011). Long-term dry immersion: Review and prospects. *Eur J Appl Physiol* **111,** 1235–1260.

Nishijima T, Llorens-Martín M, Tejeda GS, Inoue K, Yamamura Y, Soya H, Trejo JL & Torres-Alemán I (2013). Cessation of voluntary wheel running increases anxiety-like behavior and impairs adult hippocampal neurogenesis in mice. *Behav Brain Res* **245,** 34–41.

Nishikawa K (2020). Titin: A tunable spring in active muscle. *Physiology* **35,** 209–217.

Nishimune H, Stanford JA & Mori Y (2014). Role of exercise in maintaining the integrity of the neuromuscular junction. *Muscle and Nerve* **49,** 315–324.

Norman K & Otten L (2019). Financial impact of sarcopenia or low muscle mass – A short review. *Clin Nutr* **38,** 1489–1495.

Nunes EA, Stokes T, McKendry J, Currier BS & Phillips SM (2022). Disuse-induced skeletal muscle atrophy in disease and non-disease states in humans: mechanisms, prevention, and recovery strategies. *Am J Physiol - Cell Physiol* **322,** C1068–C1084.

Oda K (1984). Age changes of motor innervation and acetylcholine receptor distribution on human skeletal muscle fibres. *J Neurol Sci* **66,** 327–338.

Oikawa SY, Callahan DM, Mcglory C, Toth MJ & Phillips SM (2019*a*). Maintenance of skeletal muscle function following reduced daily physical activity in healthy older adults: a pilot trial. *Appl Physiol Nutr Metab* **44,** 1052–1056.

Oikawa SY, Holloway TM & Phillips SM (2019*b*). The impact of step reduction on muscle health in aging: Protein and exercise as countermeasures. *Front Nutr* **6,** 1–11.

Oikawa SY, McGlory C, D'Souza LK, Morgan AK, Saddler NI, Baker SK, Parise G & Phillips SM (2018). A randomized controlled trial of the impact of protein supplementation on leg lean mass and integrated muscle protein synthesis during inactivity and energy restriction in older persons. *Am J Clin Nutr* **108,** 1060–1068.

Olsen RH, Krogh-Madsen R, Thomsen C, Booth F & Pedersen B (2008). Metabolic Responses to Reduced Daily Steps in Healthy Nonexercising Men. *JAMA* **299,** 4–6.

Orssatto LBR, Blazevich AJ & Trajano GS (2023). Ageing reduces persistent inward current contribution to motor neurone firing: Potential mechanisms and the role of exercise. *J Physiol* **0,** 1–12.

Orssatto LBR, Borg DN, Blazevich AJ, Sakugawa RL, Shield AJ & Trajano GS (2021). Intrinsic motoneuron excitability is reduced in soleus and tibialis anterior of older adults. *GeroScience* **43,** 2719–2735.

Orssatto LBR, Borg DN, Pendrith L, Blazevich AJ, Shield AJ & Trajano GS (2022). Do motoneuron discharge rates slow with aging? A systematic review and meta-analysis. *Mech Ageing Dev* **203,** 111647.

Ottenheijm CAC & Granzier H (2010). Lifting the nebula: Novel insights into skeletal muscle contractility. *Physiology* **25,** 304–310.

Ouanounou G, Baux G & Bal T (2016). A novel synaptic plasticity rule explains homeostasis of neuromuscular transmission. *Elife* **5,** 1–20.

Pachter BR & Eberstein A (1984). Neuromuscular plasticity following limb immobilization. *J*

Neurocytol **13,** 1013–1025.

Pachter BR & Spielholz NI (1990). Tenotomy-induced motor endplate alterations in rat soleus muscle. *Anat Rec* **228,** 104–108.

Padilla CJ, Harrigan ME, Harris H, Schwab JM, Rutkove SB, Rich MM, Clark BC & Arnold WD (2021). Profiling age-related muscle weakness and wasting: neuromuscular junction transmission as a driver of age-related physical decline (GeroScience, (2021), 43, 3, (1265-1281), 10.1007/s11357-021-00369-3). *GeroScience* **43,** 1265–1281.

Padilla J, Jenkins N, Roberts M, Arce-Esquivel A, Martin S, Laughlin MH & Booth FW (2013). Differential changes in vascular mRNA levels between rat iliac and renal arteries produced by cessation of voluntary running. *Exp Physiol* **98,** 337–347.

Paluch AE et al. (2022). Daily steps and all-cause mortality: a meta-analysis of 15 international cohorts. *Lancet Public Heal* **7,** e219–e228.

Papadopoulou SK, Tsintavis P, Potsaki G & Papandreou D (2020). Differences in the Prevalence of Sarcopenia in Community-Dwelling, Nursing Home and Hospitalized Individuals. A Systematic Review and Meta-Analysis. *J Nutr Heal Aging* **24,** 83–90.

Patel AN, Razzak ZA & Dastur DK (1969). Disuse Atrophy of Human Skeletal Muscles. *Arch Neurol* **20,** 413–421.

Patel HP, White MC, Westbury L, Syddall HE, Stephens PJ, Clough GF, Cooper C & Sayer AA (2015). Skeletal muscle morphology in sarcopenia defined using the EWGSOP criteria: Findings from the Hertfordshire Sarcopenia Study (HSS) Physical functioning, physical health and activity. *BMC Geriatr* **15,** 1–6.

Pavy-Le Traon A, Heer M, Narici M V., Rittweger J & Vernikos J (2007). From space to Earth: Advances in human physiology from 20 years of bed rest studies (1986-2006). *Eur J Appl Physiol* **101,** 143–194.

Pedersen BK (2019). Physical activity and muscle–brain crosstalk. *Nat Rev Endocrinol* **15,** 383–392.

Perkin O, McGuigan P, Thompson D & Stokes K (2016). A reduced activity model: a relevant tool for the study of ageing muscle. *Biogerontology* **17,** 435–447.

Perkisas S, Baudry S, Bauer J, Beckwée D, De Cock AM, Hobbelen H, Jager-Wittenaar H, Kasiukiewicz A, Landi F, Marco E, Merello A, Piotrowicz K, Sanchez E, Sanchez-Rodriguez D, Scafoglieri A, Cruz-Jentoft A & Vandewoude M (2018). Application of ultrasound for muscle assessment in sarcopenia: towards standardized measurements. *Eur Geriatr Med* **9,** 739–757.

Pestronk A & Drachman DB (1978). Motor nerve sprouting and acetylcholine receptors. *Science*

(80-) **199,** 1223–1225.

Pestronk A, Drachman DB & Griffin JW (1976). Effect of muscle disuse on acetylcholine receptors. *Nature* **260,** 352–353.

Petermann-Rocha F, Balntzi V, Gray SR, Lara J, Ho FK, Pell JP & Celis-Morales C (2022). Global prevalence of sarcopenia and severe sarcopenia: a systematic review and meta-analysis. *J Cachexia Sarcopenia Muscle* **13,** 86–99.

Petermann-Rocha F, Chen M, Gray SR, Ho FK, Pell JP & Celis-Morales C (2020). Factors associated with sarcopenia: A cross-sectional analysis using UK Biobank. *Maturitas* **133,** 60–67.

Petersen MC & Shulman GI (2018). Mechanisms of insulin action and insulin resistance. *Physiol Rev* **98,** 2133–2223.

Petrocelli JJ, McKenzie AI, Mahmassani ZS, Reidy PT, Stoddard GJ, Poss AM, Holland WL, Summers SA, Drummond MJ & Le Couteur D (2020). Ceramide Biomarkers Predictive of Cardiovascular Disease Risk Increase in Healthy Older Adults after Bed Rest. *Journals Gerontol - Ser A Biol Sci Med Sci* **75,** 1663–1670.

Phillips SM & Mcglory C (2014). CrossTalk proposal: The dominant mechanism causing disuse muscle atrophy is decreased protein synthesis. *J Physiol* **592,** 5341–5343.

Piasecki M, Garnés-Camarena O & Stashuk DW (2021). Near-fiber electromyography. *Clin Neurophysiol* **132,** 1089–1104.

Piasecki M, Ireland A, Coulson J, Stashuk DW, Hamilton-Wright A, Swiecicka A, Rutter MK, McPhee JS & Jones DA (2016*a*). Motor unit number estimates and neuromuscular transmission in the tibialis anterior of master athletes: evidence that athletic older people are not spared from age-related motor unit remodeling. *Physiol Rep* **4,** e12987.

Piasecki M, Ireland A, Jones DA & McPhee JS (2016*b*). Age-dependent motor unit remodelling in human limb muscles. *Biogerontology* **17,** 485–496.

Piasecki M, Ireland A, Piasecki J, Stashuk DW, McPhee JS & Jones DA (2018*a*). The reliability of methods to estimate the number and size of human motor units and their use with large limb muscles. *Eur J Appl Physiol* **118,** 767–775.

Piasecki M, Ireland A, Piasecki J, Stashuk DW, Swiecicka A, Rutter MK, Jones DA & McPhee JS (2018*b*). Failure to expand the motor unit size to compensate for declining motor unit numbers distinguishes sarcopenic from non-sarcopenic older men. *J Physiol* **596,** 1627–1637.

Piasecki M, Ireland A, Stashuk D, Hamilton-Wright A, Jones DA & McPhee JS (2016*c*). Age-related neuromuscular changes affecting human vastus lateralis. *J Physiol* **594,** 4525–4536.

Piekarz KM, Bhaskaran S, Sataranatarajan K, Street K, Premkumar P, Saunders D, Zalles M, Gulej R, Khademi S, Laurin J, Peelor R, Miller BF, Towner R & Van Remmen H (2020). Molecular changes associated with spinal cord aging. *GeroScience* **42,** 765–784.

Pierno S, Desaphy JF, Liantonio A, De Bellis M, Bianco G, De Luca A, Frigeri A, Nicchia GP, Svelto M, Léoty C, George AL & Conte Camerino D (2002). Change of chloride ion channel conductance is an early event of slow-to-fast fibre type transition during unloading-induced muscle disuse. *Brain* **125,** 1510–1521.

Pillon NJ, Gabriel BM, Dollet L, Smith JAB, Sardón Puig L, Botella J, Bishop DJ, Krook A & Zierath JR (2020). Transcriptomic profiling of skeletal muscle adaptations to exercise and inactivity. *Nat Commun*.

Pišot R, Marusic U, Biolo G, Mazzucco S, Lazzer S, Grassi B, Reggiani C, Toniolo L, Di Prampero PE, Passaro A, Narici M, Mohammed S, Rittweger J, Gasparini M, Blenkuŝ MG & Šimuniĉ B (2016). Greater loss in muscle mass and function but smaller metabolic alterations in older compared with younger men following 2 wk of bed rest and recovery. *J Appl Physiol* **120,** 922–929.

Plomp JJ (2017). Trans-synaptic homeostasis at the myasthenic neuromuscular junction. *Front Biosci* **22,** 1033–1051.

Ploutz-Snyder LL, Tesch PA, Crittenden DJ & Dudley GA (1995). Effect of unweighting on skeletal muscle use during exercise. *J Appl Physiol* **79,** 168–175.

Poffé C, Dalle S, Kainz H, Berardi E & Hespel P (2018). A noninterfering system to measure in-cage spontaneous physical activity in mice. *J Appl Physiol* **125,** 263–270.

Pope ZK, Hester GM, Benik FM & DeFreitas JM (2016). Action potential amplitude as a noninvasive indicator of motor unit-specific hypertrophy. *J Neurophysiol* **115,** 2608–2614.

Popov D V, Makhnovskii PA, Zgoda VG, Gazizova GR, Vepkhvadze TF, Lednev EM, Motanova ES, Lysenko EA, Orlov OI & Tomilovskaya ES (2023). Rapid changes in transcriptomic profile and mitochondrial function in human soleus muscle after 3-day dry immersion. *J Appl Physiol*1256–1264.

Pourmotabbed A, Ghaedi E, Babaei A, Mohammadi H, Khazaie H, Jalili C, Symonds ME, Moradi S & Miraghajani M (2020). Sleep duration and sarcopenia risk: a systematic review and dose-response meta-analysis. *Sleep Breath* **24,** 1267–1278.

Powell C, Browne LD, Carson BP, Dowd KP, Perry IJ, Kearney PM, Harrington JM & Donnelly AE (2020). Use of Compositional Data Analysis to Show Estimated Changes in Cardiometabolic Health by Reallocating Time to Light - Intensity Physical Activity in Older Adults. *Sport Med*

50, 205–217.

Powers SK, Smuder AJ & Judge AR (2012). Oxidative stress and disuse muscle atrophy: Cause or consequence? *Curr Opin Clin Nutr Metab Care* **15,** 240–245.

Pratt J, Boreham C, Ennis S, Ryan AW & De Vito G (2020*a*). Genetic associations with aging muscle: A systematic review. *Cells* **9,** 1–31.

Pratt J, De Vito G, Narici M & Boreham C (2020*b*). Neuromuscular Junction Aging: A Role for Biomarkers and Exercise. *Journals Gerontol Ser A*1–10.

Pratt J, De Vito G, Segurado R, Pessanha L, Dolan J, Narici M & Boreham C (2022). Plasma neurofilament light levels associate with muscle mass and strength in middle-aged and older adults: findings from GenoFit. *J Cachexia Sarcopenia Muscle* **13,** 1811–1820.

Preobrazenski N, Seigel J, Halliday S, Janssen I & Mcglory C (2023). Single-leg disuse decreases skeletal muscle strength, size, and power in uninjured adults: A systematic review and meta-analysis. *J Cachexia Sarcopenia Muscle*; DOI: 10.1002/jcsm.13201.

Prokopidis K, Giannos P, Reginster JY, Bruyere O, Petrovic M, Cherubini A, Triantafyllidis KK, Kechagias KS, Dionyssiotis Y, Cesari M, Ibrahim K, Scott D, Barbagallo M & Veronese N (2023). Sarcopenia is associated with a greater risk of polypharmacy and number of medications: a systematic review and meta-analysis. *J Cachexia Sarcopenia Muscle*; DOI: 10.1002/jcsm.13190.

Qaisar R, Karim A & Elmoselhi AB (2020). Muscle unloading: A comparison between spaceflight and ground-based models. *Acta Physiol* **228,** 1–22.

Rayment I, Rypniewski WR, Schmidt-Bäse K, Smith R, Tomchick DR, Benning MM, Winkelmann DA, Wesenberg G & Holden HM (1993). Three-dimensional structure of myosin subfragment-1: A molecular motor. *Science (80-)* **261,** 50–58.

Rector SR, Thyfault JP, Laye MJ, Morris TR, Borengasser SJ, Uptergrove GM, Chakravarthy M V., Booth FW & Ibdah JA (2008). Cessation of daily exercise dramatically alters precursors of hepatic steatosis in Otsuka Long-Evans Tokushima Fatty (OLETF) rats. *J Physiol* **586,** 4241–4249.

Redfern WS, Tse K, Grant C, Keerie A, Simpson DJ, Pedersen JC, Rimmer V, Leslie L, Klein SK, Karp NA, Sillito R, Chartsias A, Lukins T, Heward J, Vickers C, Chapman K & Armstrong JD (2017). Automated recording of home cage activity and temperature of individual rats housed in social groups: The Rodent Big Brother project. *PLoS One* **12,** 1–26.

Reggiani C (2015). Not all disuse protocols are equal: New insight into the signalling pathways to

muscle atrophy. *J Physiol* **593,** 5227–5228.

Reidy PT, McKenzie AI, Mahmassani Z, Morrow VR, Yonemura NM, Hopkins PN, Marcus RL, Rondina MT, Lin YK & Drummond MJ (2018). Skeletal muscle ceramides and relationship with insulin sensitivity after 2 weeks of simulated sedentary behaviour and recovery in healthy older adults. *J Physiol* **596,** 5217–5236.

Reidy PT, Monnig JM, Pickering CE, Funai K & Drummond MJ (2021). Preclinical rodent models of physical inactivity-induced muscle insulin resistance: Challenges and solutions. *J Appl Physiol* **130,** 537–544.

Reidy PT, Yonemura NM, Madsen JH, McKenzie AI, Mahmassani ZS, Rondina MT, Lin YK, Kaput K & Drummond MJ (2019). An accumulation of muscle macrophages is accompanied by altered insulin sensitivity after reduced activity and recovery. *Acta Physiol* **226,** e13251.

Rekling JC, Funk GD, Bayliss DA, Dong X-W & Feldman JL (2000). Synaptic Control of Motoneuronal Excitability. *Physiol Rev* **80,** 767–852.

Repetto S, Bado M, Broda P, Lucania G, Masetti E, Sotgia F, Carbone I, Pavan A, Bonilla E, Cordone G, Lisanti MP & Minetti C (1999). Increased number of caveolae and caveolin-3 overexpression in Duchenne muscular dystrophy. *Biochem Biophys Res Commun* **261,** 547–550.

Reynolds L, Credeur D, Holwerda S, Leidy H, Fadel P & Thyfault J (2015). Acute Inactivity Impairs Glycemic Control but Not Blood Flow to Glucose Ingestion. *Med Sci Sports Exerc* **47,** 1087–1094.

Rhodes JS, Garland T & Gammie SC (2003). Patterns of Brain Activity Associated with Variation in Voluntary Wheel-Running Behavior. *Behav Neurosci* **117,** 1243–1256.

Rhodes JS, Koteja P, Swallow JG, Carter PA & Garland T (2000). Body temperatures of house mice artificially selected for high voluntary wheel-running behavior: Repeatability and effect of genetic selection. *J Therm Biol* **25,** 391–400.

Ritsche P, Wirth P, Cronin N, Sarto F, Narici M V., Faude O & Franchi M V. (2022). DeepACSA: Automatic Segmentation of Cross-sectional Area in Ultrasound Images of Lower Limb Muscles Using Deep Learning. *Med Sci Sport Exerc* **54,** 2188–2195.

Rizzato A, Marcolin G & Paoli A (2022). Non-exercise activity thermogenesis in the workplace: The office is on fire. *Front Public Heal* **10,** 1024856.

Robbins N (1992). Compensatory plasticity of aging at the neuromuscular junction. *Exp Gerontol* **27,** 75–81.

Robbins N & Fischbach GD (1971). Effect of chronic disuse of rat soleus neuromuscular junctions on presynaptic function. *J Neurophysiol* **34,** 570–577.

Roberts HC, Denison HJ, Martin HJ, Patel HP, Syddall H, Cooper C & Sayer AA (2011). A review of the measurement of grip strength in clinical and epidemiological studies: Towards a standardised approach. *Age Ageing* **40,** 423–429.

Roberts MD, Childs TE, Brown JD, Davis JW & Booth FW (2012). Early depression of Ankrd2 and Csrp3 mRNAs in the polyribosomal and whole tissue fractions in skeletal muscle with decreased voluntary running. *J Appl Physiol* **112,** 1291–1299.

Robinson GA, Enoka RM & Stuart DG (1991). Immobilization-induced changes in motor unit force and fatigability in the cat. *Muscle Nerve*563–573.

Robinson MD, McCarthy DJ & Smyth GK (2010). edgeR: a Bioconductor package for differential expression analysis of digital gene expression data. *Bioinformatics* **26,** 139–140.

Roemers P, Hulst Y, van Heijningen S, van Dijk G, van Heuvelen MJG, De Deyn PP & van der Zee EA (2019). Inducing Physical Inactivity in Mice: Preventing Climbing and Reducing Cage Size Negatively Affect Physical Fitness and Body Composition. *Front Behav Neurosci*; DOI: 10.3389/fnbeh.2019.00221.

Rosa-Caldwell ME & Greene NP (2019). Muscle metabolism and atrophy: Let's talk about sex. *Biol Sex Differ* **10,** 1–14.

Rosenberg IH (1997). Symposium: Sarcopenia: Diagnosis and Mechanisms Sarcopenia: Origins and Clinical Relevance 1. *J Nutr* **127,** 990–991.

Rudolf R, Deschenes MR & Sandri M (2016). Neuromuscular Junction Degeneration In Muscle Wasting. *Curr Opin Clin Nutr Metab Care* **19,** 177–181.

Ruegg DG, Kakebeeke TH, Gabriel JP & Bennefeld M (2003). Conduction velocity of nerve and muscle fiber action potentials after a space mission or a bed rest. *Clin Neurophysiol* **114,** 86–93.

Ruegsegger GN, Company JM, Toedebusch RG, Roberts CK, Roberts MD & Booth FW (2015). Rapid alterations in perirenal adipose tissue transcriptomic networks with cessation of voluntary running. *PLoS One*; DOI: 10.1371/journal.pone.0145229.

Rygiel KA, Picard M & Turnbull DM (2016). The ageing neuromuscular system and sarcopenia: a mitochondrial perspective. *J Physiol* **594,** 4499–4512.

Salanova M, Bortoloso E, Schiffl G, Gutsmann M, Belavý DL, Felsenberg D, Furlan S, Volpe P & Blottner D (2011). Expression and regulation of Homer in human skeletal muscle during

neuromuscular junction adaptation to disuse and exercise. *FASEB J* **25,** 4312–4325.

Saltin B, Blomqvist G, Mitchell J, Johnson RJ, Wildenthal K & Chapman C (1968). Response to exercise after bed rest and after training. *Cirulation* **38,** VII1–VII78.

Sánchez-Sánchez JL, Mañas A, García-García FJ, Ara I, Carnicero JA, Walter S & Rodríguez-Mañas L (2019). Sedentary behaviour, physical activity, and sarcopenia among older adults in the TSHA: isotemporal substitution model. *J Cachexia Sarcopenia Muscle* **10,** 188–198.

Sanders DB, Arimura K, Cui LY, Ertaş M, Farrugia ME, Gilchrist J, Kouyoumdjian JA, Padua L, Pitt M & Stålberg E (2019). Guidelines for single fiber EMG. *Clin Neurophysiol* **130,** 1417–1439.

Sanes JR (2003). The basement membrane/basal lamina of skeletal muscle. *J Biol Chem* **278,** 12601–12604.

Saoi M, Li A, McGlory C, Stokes T, von Allmen MT, Phillips SM & Britz-Mckibbin P (2019). Metabolic perturbations from step reduction in older persons at risk for sarcopenia: Plasma biomarkers of abrupt changes in physical activity. *Metabolites* **9,** 1–19.

Sargeant AJ, Davies CTM, Edwards RHT, Maunder C & Young A (1977). Functional and structural changes after disuse of human muscle. *Clin Sci Mol Med* **52,** 337–342.

Sarto F, Bottinelli R, Franchi M V, Porcelli S, Simunič B, Pišot R & Narici M V (2023). Pathophysiological mechanisms of reduced physical activity: insights from the human step reduction model and animal analogues. *Acta Physiol*; DOI: 10.1111/apha.13986.

Sarto F, Monti E, Simunič B, Pišot R, Narici M V. & Franchi M V. (2021*a*). Changes in Biceps Femoris Long Head Fascicle Length after 10-day Bed Rest Assessed with Different Ultrasound Methods. *Med Sci Sport Exerc* **53,** 1529–1536.

Sarto F, Pizzichemi M, Chiossi F, Bisiacchi PS, Franchi M V., Narici M V., Monti E, Paoli A & Marcolin G (2022*a*). Physical active lifestyle promotes static and dynamic balance performance in young and older adults. *Front Physiol* **13,** 986881.

Sarto F, Spörri J, Fitze DP, Quinlan JI, Narici M V & Franchi M V (2021*b*). Implementing Ultrasound Imaging for the Assessment of Muscle and Tendon Properties in Elite Sports: Practical Aspects, Methodological Considerations and Future Directions. *Sport Med* **51,** 1151–1170.

Sarto F, Stashuk DW, Franchi M V, Monti E, Zampieri S, Valli G, Sirago G, Candia J, Hartnell LM, Paganini M, Mcphee J, Vito G De, Ferrucci L, Reggiani C & Narici M V (2022*b*). Effects of short-term unloading and active recovery on human motor unit properties, neuromuscular junction transmission and transcriptomic profile. *J Physiol* **600,** 4731–4751.

Sarto F, Valli G & Monti E (2022*c*). Motor units alterations with muscle disuse: what is new? *J*

Physiol **600,** 4811–4813.

Sartori R, Romanello V & Sandri M (2021). Mechanisms of muscle atrophy and hypertrophy: implications in health and disease. *Nat Commun* **12,** 1–12.

Sayer AA & Cruz-Jentoft A (2022). Sarcopenia definition, diagnosis and treatment: Consensus is growing. *Age Ageing* **51,** 1–5.

Schiaffino S & Reggiani C (2011). Fiber types in Mammalian skeletal muscles. *Physiol Rev* **91,** 1447–1531.

Schiaffino S & Serrano AL (2002). Calcineurin signaling and neural control of skeletal muscle fiber type and size. *Trends Pharmacol Sci* **23,** 569–575.

Seki K, Kizuka T & Yamada H (2007). Reduction in maximal firing rate of motoneurons after 1-week immobilization of finger muscle in human subjects. *J Electromyogr Kinesiol* **17,** 113–120.

Seki K, Taniguchi Y & Narusawa M (2001). Effects of joint immobilization on firing rate modulation of human motor units. *J Physiol* **530,** 507–519.

Seynnes OR, Maffiuletti NA, Horstman AM & Narici M V. (2010). Increased H-reflex excitability is not accompanied by changes in neural drive following 24 days of unilateral lower limb suspension. *Muscle Nerve* **42,** 749–755.

Shad BJ, Thompson JL, Holwerda AM, Stocks BEN, Elhassan YS, Philp A, Van Loon LUCJC & Wallis GA (2019). One Week of Step Reduction Lowers Myofibrillar Protein Synthesis Rates in Young Men. *Med Sci Sports Exerc* **51,** 2125–2134.

Shafiee G, Keshtkar A, Soltani A, Ahadi Z, Larijani B & Heshmat R (2017). Prevalence of sarcopenia in the world: A systematic review and meta- analysis of general population studies. *J Diabetes Metab Disord* **16,** 1–10.

Shen Y, Shi Q, Nong K, Li S, Yue J, Huang J, Dong B, Beauchamp M & Hao Q (2023). Exercise for sarcopenia in older people: A systematic review and network meta-analysis. *J Cachexia Sarcopenia Muscle* **14,** 1199–1211.

Sheng M, Yang J, Bao M, Chen T, Cai R, Zhang N, Chen H, Liu M, Wu X, Zhang B, Liu Y & Chao J (2021). The relationships between step count and all-cause mortality and cardiovascular events: A dose–response meta-analysis. *J Sport Heal Sci* **10,** 620–628.

Shenkman B, Kozlovskaya I, Nemirovskaya T & Tcheglova I (1997). Human muscle atrophy in supportlessness: effects of short-term exposure to dry immersion. *J Gravit Physiol* **4,** 137–138.

Sherrington C (1925). Remarks on some aspects of reflex inhibition. *Proc R Soc L B Biol Sci* **B97:,**

19–45.

Shi L, Fu AKY & Ip NY (2012). Molecular mechanisms underlying maturation and maintenance of the vertebrate neuromuscular junction. *Trends Neurosci* **35,** 441–453.

Shulzhenko E & Vil-Vilyams I (1975). Simulation of the human body deconditioning with the method of '"dry"' immersion. *Xth KE Tziolkovski readings*39–47.

Shulzhenko E & Vil-Vilyams I (1976). Possibility of carrying out prolonged water immersion by the method of "dry" submersion. *Kosm Biol Aviakosm Med* **10,** 82–84.

Sirago G, Candia J, Franchi M V, Sarto F, Monti E, Toniolo L, Reggiani C, Giacomello E, Zampieri S, Hartnell LM, Vito G De, Sandri M, Ferrucci L & Narici M V (2023). Upregulation of Sarcolemmal Hemichannels and Inflammatory Transcripts with Neuromuscular Junction Instability during Lower Limb Unloading in Humans. *Biology (Basel)* **12,** 431.

Slater CR (1992). Structure and function of neuromuscular junctions in the vastus lateralis of man. *Brain* **115,** 451–478.

Slater CR (2020*a*). 'Fragmentation' of NMJs: a sign of degeneration or regeneration? A long journey with many junctions. *Neuroscience* **439,** 28–40.

Slater CR (2020*b*). 'Fragmentation' of NMJs: a sign of degeneration or regeneration? A long journey with many junctions. *Neuroscience* **439,** 28–40.

Smith JAB, Murach KA, Dyar KA & Zierath JR (2023). Exercise metabolism and adaptation in skeletal muscle. *Nat Rev Mol Cell Biol*; DOI: 10.1038/s41580-023-00606-x.

Smyth GK (2004). Linear models and empirical bayes methods for assessing differential expression in microarray experiments. *Stat Appl Genet Mol Biol*.

Snider WD & Harris G (1979). A physiological correlate of disuse-induced sprouting at the neuromuscular junction. *Nature* **281,** 70–71.

Soendenbroe C, Andersen JL & Mackey AL (2021). Muscle-nerve communication and the molecular assessment of human skeletal muscle denervation with aging. *Am J Physiol Physiol* **321,** C317–C329.

Speakman JR (2020). An Evolutionary Perspective on Sedentary Behavior. *BioEssays* **42,** 42–46.

Speakman JR & Selman C (2003). Physical activity and resting metabolic rate. *Proc Nutr Soc* **62,** 621–634.

Stålberg E V. & Sonoo M (1994). Assessment of variability in the shape of the motor unit action potential, the "jiggle," at consecutive discharges. *Muscle Nerve* **17,** 1135–1144.

Stashuk DW (1999*a*). Decomposition and quantitative analysis of clinical electromyographic

signals. *Med Eng Phys* **21,** 389–404.

Stashuk DW (1999*b*). Detecting single fiber contributions to motor unit action potentials. *Muscle and Nerve* **22,** 218–229.

Steffl M, Bohannon RW, Petr M, Kohlikova E & Holmerova I (2015). Relation between cigarette smoking and sarcopenia: Meta-analysis. *Physiol Res* **64,** 419–426.

Stephan A, Mateos JM, Kozlov S V., Cinelli P, Kistler AD, Hettwer S, Rülicke T, Streit P, Kunz B & Sonderegger P (2008). Neurotrypsin cleaves agrin locally at the synapse. *FASEB J* **22,** 1861–1873.

Stuck AK, Basile G, Freystaetter G, de Godoi Rezende Costa Molino C, Lang W & Bischoff-Ferrari HA (2022). Predictive validity of current sarcopenia definitions (EWGSOP2, SDOC, and AWGS2) for clinical outcomes: A scoping review. *J Cachexia Sarcopenia Muscle* **14,** 71–83.

Studenski SA, Peters KW, Alley DE, Cawthon PM, McLean RR, Harris TB, Ferrucci L, Guralnik JM, Fragala MS, Kenny AM, Kiel DP, Kritchevsky SB, Shardell MD, Dam TTL & Vassileva MT (2014). The FNIH sarcopenia project: Rationale, study description, conference recommendations, and final estimates. *Journals Gerontol - Ser A Biol Sci Med Sci* **69 A,** 547–558.

Subramanian A, Tamayo P, Mootha VK, Mukherjee S, Ebert BL, Gillette MA, Paulovich A, Pomeroy SL, Golub TR, Lander ES & Mesirov JP (2005). Gene set enrichment analysis: A knowledge-based approach for interpreting genome-wide expression profiles. *Proc Natl Acad Sci U S A* **102,** 15545–15550.

Südhof TC (2004). The synaptic vesicle cycle. *Annu Rev Neurosci* **27,** 509–547.

Südhof TC (2012). The presynaptic active zone. *Neuron* **75,** 11–25.

Suetta C, Frandsen U, Jensen L, Jensen MM, Jespersen JG, Hvid LG, Bayer M, Petersson SJ, Schrøder HD, Andersen JL, Heinemeier KM, Aagaard P, Schjerling P & Kjaer M (2012). Aging Affects the Transcriptional Regulation of Human Skeletal Muscle Disuse Atrophy. *PLoS One*; DOI: 10.1371/journal.pone.0051238.

Suetta C, Hvid LG, Justesen L, Christensen U, Neergaard K, Simonsen L, Ortenblad N, Magnusson SP, Kjaer M & Aagaard P (2009). Effects of aging on human skeletal muscle after immobilization and retraining. *J Appl Physiol* **107,** 1172–1180.

Suvorava T, Lauer N & Kojda G (2004). Physical inactivity causes endothelial dysfunction in healthy young mice. *J Am Coll Cardiol* **44,** 1320–1327.

Syed S, Morseth B, Hopstock LA & Horsch A (2021). A novel algorithm to detect non-wear time from raw accelerometer data using deep convolutional neural networks. *Sci Rep* **11,** 1–12.

Tabary J, Tabary C, Tardieu C, Tardieu G & Goldspink G (1972). Physiological and structural changes in the cats's solecus muscle due to immobilization at different lenghts by plaster casts. *J Physiol* **224,** 231–244.

Taetzsch T, Valdez G & Tech V (2019). NMJ maintenace and reapir in aging. *Curr Opin Physiol* **4,** 57–64.

Takemura A, Roy RR, Reggie Edgerton V & Ishihara A (2016). Biochemical adaptations in a slow and a fast plantarflexor muscle of rats housed in small cages. *Aerosp Med Hum Perform* **87,** 443–448.

Tamaki T, Hirata M & Uchiyama Y (2014). Qualitative alteration of peripheral motor system begins prior to appearance of typical sarcopenia syndrome in middle-aged rats. *Front Aging Neurosci* **6,** 1–14.

Tay L, Ding YY, Leung BP, Ismail NH, Yeo A, Yew S, Tay KS, Tan CH & Chong MS (2015). Sex-specific differences in risk factors for sarcopenia amongst community-dwelling older adults. *Age (Omaha)* **37,** 1–12.

Teich T, Pivovarov JA, Porras DP, Dunford EC & Riddell MC (2017). Curcumin limits weight gain, adipose tissue growth, and glucose intolerance following the cessation of exercise and caloric restriction in rats. *J Appl Physiol* **123,** 1625–1634.

Teixeira AL, Padilla J & Vianna LC (2017). Impaired popliteal artery flow-mediated dilation caused by reduced daily physical activity is prevented by increased shear stress. *J Appl Physiol* **123,** 49–54.

Tesch PA, Lundberg TR & Fernandez-Gonzalo R (2016*a*). Unilateral lower limb suspension: From subject selection to "omic" responses. *J Appl Physiol* **120,** 1207–1214.

Tesch PA, Lundberg TR & Fernandez-Gonzalo R (2016*b*). Unilateral lower limb suspension: From subject selection to "omic" responses. *J Appl Physiol* **120,** 1207–1214.

Thome T, Miguez K, Willms AJ, Burke SK, Chandran V, de Souza AR, Fitzgerald LF, Baglole C, Anagnostou ME, Bourbeau J, Jagoe RT, Morais JA, Goddard Y, Taivassalo T, Ryan TE & Hepple RT (2022). Chronic aryl hydrocarbon receptor activity phenocopies smoking-induced skeletal muscle impairment. *J Cachexia Sarcopenia Muscle* **13,** 589–604.

Thyfault JP & Krogh-Madsen R (2011). Metabolic disruptions induced by reduced ambulatory activity in free-living humans. *J Appl Physiol* **111,** 1218–1224.

Ticinesi A, Meschi T, Narici M V., Lauretani F & Maggio M (2017). Muscle Ultrasound and Sarcopenia in Older Individuals: A Clinical Perspective. *J Am Med Dir Assoc* **18,** 290–300.

Tieland M, Trouwborst I & Clark BC (2018). Skeletal muscle performance and ageing. *J Cachexia Sarcopenia Muscle* **9,** 3–19.

Tintignac LA, Brenner HR & Rüegg MA (2015). Mechanisms regulating neuromuscular junction development and function and causes of muscle wasting. *Physiol Rev* **95,** 809–852.

Tischler ME, Henriksen EJ, Munoz KA, Stump CS, Woodman CR & Kirby CR (1993). Spaceflight on STS-48 and earth-based unweighting produce similar effects on skeletal muscle of young rats. *J Appl Physiol* **74,** 2161–2165.

Tomilovskaya E, Shigueva T, Sayenko D, Rukavishnikov I & Kozlovskaya I (2019). Dry immersion as a ground-based model of microgravity physiological effects. *Front Physiol* **10,** 1–17.

Tomlinson BE & Irving D (1977). The numbers of limb motor neurons in the human lumbosacral cord throughout life. *J Neurol Sci* **34,** 213–219.

Trappe S, Creer A, Minchev K, Slivka D, Louis E, Luden N & Trappe T (2008). Human soleus single muscle fiber function with exercise or nutrition countermeasures during 60 days of bed rest. *Am J Physiol - Regul Integr Comp Physiol* **294,** 939–947.

Trejo JL, Carro E, Nuñez A & Torres-Aleman I (2002). Sedentary life impairs self-reparative processes in the brain: The role of serum insulin-like growth factor-I. *Rev Neurosci* **13,** 365–374.

Tricarico D, Mele A, Camerino GM, Bottinelli R, Brocca L, Frigeri A, Svelto M, George AL & Camerino DC (2010). The KATP channel is a molecular sensor of atrophy in skeletal muscle. *J Physiol* **588,** 773–784.

Tsujimoto T & Kuno M (1988). Calcitonin gene-related peptide prevents disuse-induced sprouting of rat motor nerve terminals. *J Neurosci* **8,** 3951–3957.

Valli G, Sarto F, Casolo A, Vecchio A Del, Franchi M V, Narici M V & Vito G De (2023). Lower limb suspension induces threshold-specific alterations of motor units properties that are reversed by active recovery. *J Sport Heal Sci*; DOI: 10.1016/j.jshs.2023.06.004.

Del Vecchio A, Negro F, Felici F & Farina D (2017). Associations between motor unit action potential parameters and surface EMG features. *J Appl Physiol* **123,** 835–843.

Vikne H, Strøm V, Pripp AH & Gjøvaag T (2020). Human skeletal muscle fiber type percentage and area after reduced muscle use: A systematic review and meta-analysis. *Scand J Med Sci Sport* **30,** 1298–1317.

Visser M, Deeg DJH & Lips P (2003). Low Vitamin D and High Parathyroid Hormone Levels as Determinants of Loss of Muscle Strength and Muscle Mass (Sarcopenia): The Longitudinal

Aging Study Amsterdam. *J Clin Endocrinol Metab* **88,** 5766–5772.

Walhin JP, Richardson JD, Betts JA & Thompson D (2013). Exercise counteracts the effects of short-term overfeeding and reduced physical activity independent of energy imbalance in healthy young men. *J Physiol* **591,** 6231–6243.

Walker SM & Schrodt GR (1974). I segment lengths and thin filament periods in skeletal muscle fibers of the rhesus monkey and the human. *Anat Rec* **178,** 63–81.

Wall BT, Dirks ML & Van Loon LJC (2013). Skeletal muscle atrophy during short-term disuse: Implications for age-related sarcopenia. *Ageing Res Rev* **12,** 898–906.

Wall BT, Dirks ML, Snijders T, Senden JMG, Dolmans J & Van Loon LJC (2014). Substantial skeletal muscle loss occurs during only 5 days of disuse. *Acta Physiol* **210,** 600–611.

Wang L, Wang S & Li W (2012). RSeQC: quality control of RNA-seq experiments. *Bioinformatics* **28,** 2184–2185.

Watenpaugh DE (2016). Analogs of microgravity: Head-down tilt and water immersion. *J Appl Physiol* **120,** 904–914.

Wehrwein EA, Roskelley EM & Spitsbergen JM (2002). GDNF is regulated in an activity-dependent manner in rat skeletal muscle. *Muscle and Nerve* **26,** 206–211.

Westbury LD, Beaudart C, Bruyère O, Cauley JA, Cawthon P, Cruz-jentoft AJ, Curtis EM, Ensrud K, Fielding RA, Johansson H & Kanis JA (2023). Recent sarcopenia definitions — prevalence, agreement and mortality associations among men: Findings from population-based cohorts. *J Cachexia Sarcopenia Muscle*; DOI: 10.1002/jcsm.13160.

White MJ, Davies CTM & Brooksby P (1984). the Effects of Short-Term Voluntary Immobilization on the Contractile Properties of the Human Triceps Surae. *Q J Exp Physiol* **69,** 685–691.

World Health Organization. Health topics: physical activity. 2015 http://www.who.int/topic s/physi cal_activ ity/en/

Widenfalk J, Olson L & Thorén P (1999). Deprived of habitual running, rats downregulate BDNF and TrkB messages in the brain. *Neurosci Res* **34,** 125–132.

Widrick JJ, Norenberg KM, Romatowski JG, Blaser CA, Karhanek M, Sherwood J, Trappe SW, Trappe TA, Costill DL & Fitts RH (1998). Force-velocity-power and force-pCa relationships of human soleus fibers after 17 days of bed rest. *J Appl Physiol* **85,** 1949–1956.

Widrick JJ, Romatowski JG, Norenberg KM, Knuth ST, Bain JLW, Riley DA, Trappe SW, Trappe TA, Costill DL & Fitts RH (2001). Functional properties of slow and fast gastrocnemius muscle fibers after a 17-day spaceflight. *J Appl Physiol* **90,** 2203–2211.

Widrick JJ, Trappe SW, Romatowski JG, Riley DA, Costill DL & Fitts RH (2002). Unilateral lower limb suspension does not mimic bed rest or spaceflight effects on human muscle fiber function. *J Appl Physiol* **93,** 354–360.

Wilkie DR (1949). The relation between force and velocity in human muscle. *J Physiol* **110,** 249–280.

Willadt S, Nash M & Slater C (2018). Age-related changes in the structure and function of mammalian neuromuscular junctions. *Ann N Y Acad Sci* **1412,** 41–53.

Willadt S, Nash M & Slater CR (2016). Age-related fragmentation of the motor endplate is not associated with impaired neuromuscular transmission in the mouse diaphragm. *Sci Rep* **6,** 1–8.

Williams PE & Goldspink G (1971). Longitudinal growth of striated muscle fibres. *J Cell Sci* **232,** 751–756.

Willingham TB, Kim Y, Lindberg E, Bleck CKE & Glancy B (2020). The unified myofibrillar matrix for force generation in muscle. *Nat Commun* **11,** 1–10.

Wilson MH & Deschenes MR (2005). The neuromuscular junction: Anatomical features and adaptations to various forms of increased, or decreased neuromuscular activity. *Int J Neurosci* **115,** 803–828.

Wokke JHJ, Jennekens FGI, van den Oord CJM, Veldman H, Smit LME & Leppink GJ (1990). Morphological changes in the human end plate with age. *J Neurol Sci* **95,** 291–310.

Wood DE & Salzberg SL (2014). Kraken: Ultrafast metagenomic sequence classification using exact alignments. *Genome Biol* **15,** 1–12.

Wood SJ & Slater CR (2001). Safety factor at the neuromuscular junction. *Prog Neurobiol* **64,** 393–429.

World Health Organization (2018). Global action plan on physical activity 2018- 2030: more active people for a healthier world. *Geneva World Heal Organ*.

Xie W qing, He M, Yu D jie, Wu Y xiang, Wang X hua, Lv S, Xiao W feng & Li Y sheng (2021). Mouse models of sarcopenia: classification and evaluation. *J Cachexia Sarcopenia Muscle* **12,** 538–554.

Yadav A et al. (2023). A cellular taxonomy of the adult human spinal cord. *Neuron* **111,** 328-344.e7.

Yates T, Henson J, Mcbride P, Maylor B, Herring LY, Sargeant JA & Davies MJ (2023). Moderate - intensity stepping in older adults: insights from treadmill walking and daily living. *Int J Behav Nutr Phys Act*1–7.

Yeung SSY, Reijnierse EM, Trappenburg MC, Hogrel JY, McPhee JS, Piasecki M, Sipila S, Salpakoski A, Butler-Browne G, Pääsuke M, Gapeyeva H, Narici M V., Meskers CGM & Maier AB (2018). Handgrip Strength Cannot Be Assumed a Proxy for Overall Muscle Strength. *J Am Med Dir Assoc* **19,** 703–709.

Yu R, Wong M, Leung J, Lee J, Auyeung TW & Woo J (2014). Incidence, reversibility, risk factors and the protective effect of high body mass index against sarcopenia in community-dwelling older Chinese adults. *Geriatr Gerontol Int* **14,** 15–28.

Yu Z, Guindani M, Grieco SF, Chen L, Holmes TC & Xu X (2022). Beyond t test and ANOVA: applications of mixed-effects models for more rigorous statistical analysis in neuroscience research. *Neuron* **110,** 21–35.

Yuan S & Larsson SC (2023). Epidemiology of sarcopenia: Prevalence, risk factors, and consequences. *Metabolism*; DOI: 10.1016/j.metabol.2023.155533.

Zanker J et al. (2023). Consensus guidelines for sarcopenia prevention, diagnosis and management in Australia and New Zealand. *J Cachexia Sarcopenia Muscle* **14,** 142–156.

Zeppelin Z, Vaeggemose M, Witt A, Hvid LG & Tankisi H (2023). Exploring the peripheral mechanisms of lower limb immobilisation on muscle function using novel electrophysiological methods. *Clin Neurophysiol* **151,** 18–27.

Zuccarelli L, Baldassarre G, Magnesa B, Degano C, Comelli M, Gasparini M, Manferdelli G, Marzorati M, Mavelli I, Pilotto A, Porcelli S, Rasica L, Šimunič B, Pišot R, Narici M & Grassi B (2021). Peripheral impairments of oxidative metabolism after a 10-day bed rest are upstream of mitochondrial respiration. *J Physiol* **599,** 4813–4829.